PB-244 402

IDENTIFICATION OF REGENERABLE METAL OXIDE SO2 SORBENTS FOR FLUIDIZED-BED COAL COMBUSTION

P. S. Lowell, et al

Radian Corporation

Prepared for:

National Environmental Research Center

July 1975

DISTRIBUTED BY:

NTIS
National Technical Information Service
U. S. DEPARTMENT OF COMMERCE

04

246075

PB244402

EPA-650/2-75-065

July 1975

Environmental Protection Technology Series

IDENTIFICATION OF REGENERABLE METAL OXIDE SO_2 SORBENTS FOR FLUIDIZED-BED COAL COMBUSTION

Reproduced by
NATIONAL TECHNICAL
INFORMATION SERVICE
U S Department of Commerce
Springfield VA 22151

UNITED STATES ENVIRONMENTAL PROTECTION AGENCY

U.S. Environmental Protection Agency
Office of Research and Development
Washington, D.C. 20460

215

TECHNICAL REPORT DATA

(Please read Instructions on the reverse before completing)

1. REPORT NO.
EPA-650/2-75-065

2.

3.
PB 244 402

4. TITLE AND SUBTITLE
Identification of Regenerable Metal Oxide SO_2 Sorbents for Fluidized-Bed Coal Combustion

5. REPORT DATE
July 1975

6. PERFORMING ORGANIZATION CODE

7. AUTHOR(S)
P.S. Lowell and T.B. Parsons

8. PERFORMING ORGANIZATION REPORT NO.

9. PERFORMING ORGANIZATION NAME AND ADDRESS
Radian Corporation
P.O. Box 9948
Austin, Texas 78766

10. PROGRAM ELEMENT NO.
1AB013; ROAP 21ADD-042

11. CONTRACT/GRANT NO.
68-02-1319, Task 10

12. SPONSORING AGENCY NAME AND ADDRESS
EPA, Office of Research and Development
Control Systems Laboratory
Research Triangle Park, NC 27711

13. TYPE OF REPORT AND PERIOD COVERED
Task Final: 6/74 - 4/75

14. SPONSORING AGENCY CODE

15. SUPPLEMENTARY NOTES

16. ABSTRACT

The report briefly summarizes results of an analysis to identify regenerable metal oxide SO2 sorbents for fluidized-bed coal combustion. It recommends continued investigation. It discusses both the approach used for the theoretical study of sorption/regeneration processes and implications of the results. The Appendix contains two technical notes that are major products of this effort: Technical Note 200-045-10-01a, 'Thermodynamic Screening of Dry Metal Oxides for High Temperature SO2 Removal,' giving complete details of the thermodynamic analysis of the sorption process; and Technical Note 200-045-10-02a, 'The Thermodynamics of Chemical Regeneration of Metal Oxide SO2 Sorbents,' giving detailed methods and results of the identification of sorbents that can be regenerated by reductive decomposition of the sulfate.

17. KEY WORDS AND DOCUMENT ANALYSIS

a. DESCRIPTORS		b. IDENTIFIERS/OPEN ENDED TERMS	c. COSATI Field/Group
Air Pollution	Sulfur Oxides	Air Pollution Control	13B
Desulfurization	Sorption	Stationary Sources	07A, 07D
Metals	Coal	Metal Oxides	11F, 07B 21D
Oxides	Combustion		21B
Regeneration (Engineering)	Fluidized Bed Processing		13H
Thermodynamics			20M

PRICES SUBJECT TO CHANGE

18. DISTRIBUTION STATEMENT
Unlimited

19. SECURITY CLASS (This Report)
Unclassified

20. SECURITY CLASS (This page)
Unclassified

21. NO. OF PAGES
205

22. PRICE
$7.25- 9.75

EPA Form 2220-1 (9-73)

EPA-650/2-75-065

IDENTIFICATION OF REGENERABLE METAL OXIDE SO_2 SORBENTS FOR FLUIDIZED-BED COAL COMBUSTION

by

P. S. Lowell and T. B. Parsons

Radian Corporation
P. O. Box 9948
Austin, Texas 78766

Contract No. 68-02-1319, Task 10
ROAP No. 21ADD-042
Program Element No. 1AB013

EPA Project Officer: P. P. Turner

Control Systems Laboratory
National Environmental Research Center
Research Triangle Park, North Carolina 27711

Prepared for

U.S. ENVIRONMENTAL PROTECTION AGENCY
OFFICE OF RESEARCH AND DEVELOPMENT
WASHINGTON, D.C. 20460

July 1975

ia

EPA REVIEW NOTICE

This report has been reviewed by the National Environmental Research Center - Research Triangle Park, Office of Research and Development, EPA, and approved for publication. Approval does not signify that the contents necessarily reflect the views and policies of the Environmental Protection Agency, nor does mention of trade names or commercial products constitute endorsement or recommendation for use.

RESEARCH REPORTING SERIES

Research reports of the Office of Research and Development, U.S. Environmental Protection Agency, have been grouped into series. These broad categories were established to facilitate further development and application of environmental technology. Elimination of traditional grouping was consciously planned to foster technology transfer and maximum interface in related fields. These series are:

1. ENVIRONMENTAL HEALTH EFFECTS RESEARCH
2. ENVIRONMENTAL PROTECTION TECHNOLOGY
3. ECOLOGICAL RESEARCH
4. ENVIRONMENTAL MONITORING
5. SOCIOECONOMIC ENVIRONMENTAL STUDIES
6. SCIENTIFIC AND TECHNICAL ASSESSMENT REPORTS
9. MISCELLANEOUS

This report has been assigned to the ENVIRONMENTAL PROTECTION TECHNOLOGY series. This series describes research performed to develop and demonstrate instrumentation, equipment and methodology to repair or prevent environmental degradation from point and non-point sources of pollution. This work provides the new or improved technology required for the control and treatment of pollution sources to meet environmental quality standards.

This document is available to the public for sale through the National Technical Information Service, Springfield, Virginia 22161.

Publication No. EPA-650/2-75-065

TABLE OF CONTENTS

Page

1.0 INTRODUCTION 1
1.1 Background 1
1.2 Objectives 2
1.3 Contents of the Report 3

2.0 SUMMARY AND RECOMMENDATIONS 4
2.1 Summary of Results 4
2.2 Recommendations for Future Work 9

3.0 RESULTS AND CONCLUSIONS 10
3.1 Sorption 10
3.2 Regeneration 12
3.3 Other Considerations 26
3.3.1 Support Materials 26
3.3.2 Heat Transfer 28

4.0 BIBLIOGRAPHY 29

5.0 APPENDIX 30
5.1 Technical Note 200-045-10-01a "Thermodynamic Screening of Dry Metal Oxides for High Temperature SO_2 Removal" 31
5.2 Technical Note 200-045-10-02a "The Thermodynamics of Chemical Regeneration of Metal Oxide SO_2 Sorbents" 107

1.0 INTRODUCTION

This report summarizes work done by Radian Corporation under EPA Contract No. 68-02-1319, Task 10. The investigation was a theoretical study of the feasibility of using dry metal oxides as regenerable SO_2 sorbents during fluidized bed combustion. The work was performed from July through December 1974.

1.1 Background

Direct-contact fluidized bed combustion employs a granular bed material which does not undergo combustion. The bed is fluidized by air. Heat exchange surfaces are immersed in the fluidized bed where the fuel combustion rate is extremely rapid. Heat exchange occurs in the actual combustion zone between heat transfer surfaces and the fluidized particles rather than hot combustion gases. The resulting heat release rate is much greater than in conventional furnaces, and boilers utilizing fluidized bed combustion are expected to be a fraction of conventional boiler size (AN-001).

In addition to savings due to reduction in the boiler size, fluidized bed combustion offers the potential of providing efficient reduction in air pollutant emissions. The fluidized bed may be used to advantage in this respect. While particulate removal equipment is required, there may be no requirement for additional stack gas cleaning equipment. Gaseous air pollutants NO_x and SO_2 are formed during coal and oil combustion in conventional furnaces. NO_x formation from thermal fixation of atmospheric nitrogen is anticipated to be substantially reduced in fluidized bed combustion due to relatively higher heat release rates and lower combustion temperatures. NO_x formation from fuel-bound nitrogen is still possible in fluidized bed combustion processes. While formation of sulfur dioxide occurs in fluidized bed combustion, studies have shown that its emission in stack gas can be prevented by the utilization of limestone as the granular bed material. Reaction of SO_2 with the limestone produces calcium sulfate (AN-001).

There are a number of problems attendant with the use of limestone as bed material and SO_2 sorbent. While limestone is inexpensive and easily obtained in some areas, there may be other locations at which the mineral is unavailable. In addition, some limestones are known to have limited kinetic activity. Finally, the calcium sulfate product must be either discarded as solid waste in a once-through process or treated to regenerate the calcium oxide (or carbonate) sorbent. Since the sulfate is thermally quite stable, heating to decompose it requires prohibitively high temperatures. Attempts at chemical regeneration with a reducing agent have identified problems such as sulfide formation.

1.2 Objectives

The goal of the work described herein was to identify potential solid SO_2 sorbents for a fluidized bed combustion sorption - regeneration process. Candidate sorbents were to be evaluated theoretically using thermodynamic analysis of the sorption and regeneration reactions. The objective was to identify metal oxide sorbents which could be chemically regenerated by reductive decomposition to produce a gaseous product containing SO_2 (or possibly S_2). Two options were investigated. The first was regeneration directly to the oxide. The second option was a two-step regeneration process with a sulfide intermediate. The thermodynamic analysis was to employ data and computational tools developed under an earlier study done for EPA (PA-016).

Because of the screening nature of this study only a small amount of time could be spent on each potential sorbent. Point design conditions were chosen. Process assumptions were made. Situations that are based upon different assumptions can give somewhat different answers. The differences are calculable and deviations from the results presented here can usually be quantified.

1.3 Contents of the Report

A brief summary of the results of this analysis and recommendations for continued investigation are given in Section 2.0. The approach used for the theoretical study of sorption-regeneration processes and implications of the results are discussed in Section 3.0. Section 4.0 is the Bibliography. Section 5.0, the Appendix, contains the two technical notes which are the major product of this effort. Technical Note 200-045-10-01a, "Thermodynamic Screening of Dry Metal Oxides for High Temperature SO_2 Removal", gives the complete details of the thermodynamic analysis of the sorption process. Technical Note 200-045-10-02a, "The Thermodynamics of Chemical Regeneration of Metal Oxide SO_2 Sorbents", gives the detailed methods and results of the identification of sorbents which can be regenerated by reductive decomposition of the sulfate.

2.0 SUMMARY AND RECOMMENDATIONS

Calculations were made to determine the three following items:

- the temperature range in which the sorbent would pick up SO_x,
- the temperature range in which the sorbent could be regenerated by a variety of reducing gases, and
- an estimate of the sulfide forming tendencies of the sorbents.

A general framework for screening was chosen. Choices were made for screening criteria. For example, the sorbent screening basis was the thermodynamic ability to reduce SO_x to 100 ppm total SO_x at one atmosphere. Regeneration was with a gas at one atmosphere pressure containing no diluents. While different pressures, equipment arrangements, etc., will give somewhat different numbers, no gross changes are expected as a result of basis changes.

2.1 Summary of Results

Fifty three single and binary metal oxides were evaluated as candidate SO_2 sorbents for a fluidized bed combustion process. The oxides were screened on the basis of their potential to react with SO_2 to produce sulfates.

Thermodynamic calculations were made to determine metal oxides for which the total SO_x partial pressure in the flue gas would be reduced to 100 ppm. Process temperatures considered were 600 to 1400°C (1100-2550°F). Regeneration calculations were made with a reducing gas at one atmosphere total pressure (with no diluent). Sorption or regeneration conditions other than these might change the conclusions slightly. The procedures used are outlined in enough detail so that these adjustments may be made.

The sorption criteria used were that the sorbent must be stable enough to sorb SO_2 but not so stable that regeneration would be difficult. These criteria eliminated the not stable enough sulfates, e.g., ferric sulfate, and the "too stable" sulfates, e.g., potassium sulfate. It was found that sodium, calcium, strontium, and barium oxides; lithium, sodium, calcium, strontium, and barium aluminates; lithium and sodium ferrates; and lithium, strontium, and barium titanates produce sulfates with the required stability. These compounds are listed in Table 2-1.

The oxides were further evaluated to identify those which could be regenerated directly by reductive decomposition of the sulfate in the temperature range 600-1400°C. Six reducing agents were considered. They are listed in Table 2-2 in the order of their ability to react with oxygen. Note that the reducing agents vary both in type (H_2 versus C) and stoichiometry (1 to 4). The sorbents were evaluated to determine if they could be regenerated or not. Regeneration to the oxide was considered superior to regeneration to the sulfide. Therefore the oxide stability with respect to sulfide formation was also calculated. Each reducing agent - sulfate combination was evaluated from 600 to 1400°C.

As a result of this work, processes may be based on compounds listed in Table 2-3. Sorption and regeneration processes employing compounds were found to be thermodynamically favored between 600 and 1400°C. Individual temperatures depend on the particular oxide-reducing agent combinations.

TABLE 2-1
POTENTIAL SORBENTS BASED ON SORPTION CRITERIA

Na_2O
CaO
SrO
BaO

$Li_2Fe_2O_4$
$Na_2Fe_2O_4$

$Li_2Al_2O_4$
$Na_2Al_2O_4$
$CaAl_2O_4$
$SrAl_2O_4$
$BaAl_2O_4$

Li_2TiO_3
$SrTiO_3$
$BaTiO_3$

TABLE 2-2

REDUCING AGENTS CONSIDERED

Reducing Agent per mole SO_2	Gram Atoms O Reacted
H_2	1.0
CO	1.0
CO + $\frac{1}{2}H_2$	1.5
C (char)	2.0
CH (coal)	2.5
CH_4	4.0

TABLE 2-3

COMPOUNDS SUITABLE AS A BASIS FOR A HIGH TEMPERATURE SO_2 REMOVAL PROCESS

SO_2 sorption to form the sulfate and regeneration to form the oxide:

Oxides
- calcium

Aluminates
- lithium
- sodium
- calcium
- strontium
- barium

Ferrates
- lithium
- sodium

Titanates
- strontium
- barium

SO_2 sorption to form the sulfate and regeneration with sulfide intermediate:

Oxides
- calcium
- strontium

Aluminates
- calcium

Ferrates
- lithium
- sodium

Titanates
- lithium
- strontium
- barium

2.2 Recommendations for Future Work

The thermodynamic analysis identified a number of potential sorbents as well as the conditions at which regeneration to the oxide is predicted. The selection of materials and conditions on which to base a process should begin with these. Continued work should include an evaluation of published data on the physical and chemical properties of these potential sorbents. Data of interest include such things as melting and softening point, possibility of flux formation or reaction with ash constituents, piezoelectric properties, mechanical strength, etc. It is anticipated that limited data may also be available describing tests of fluidized bed combustor SO_2 removal and possibly sorbent regeneration. These data should also be collected and evaluated.

Thermodynamic predictions have provided a starting point for future work which should be primarily experimental in nature. Preliminary screening experiments to confirm the predicted sorption and regeneration potentials are suggested as a first step. The most promising candidates can then be evaluated further in experiments to define the required reaction kinetics.

3.0 RESULTS AND CONCLUSIONS

This section presents a discussion of the results of a thermodynamic analysis of high temperature SO_2 sorption by metal oxides and reductive decomposition of the resulting metal sulfate. The philosophy of this method of investigation is described, and the significance and implications of the results are assessed. Details of methods used in obtaining the results are given in the two technical notes in Section 5. The sorption step is discussed in Section 3.1, the regeneration step is assessed in Section 3.2, and other problems are considered in Section 3.3.

3.1 Sorption

The fifty three metal oxides listed in Table 3-1 were evaluated as candidate SO_2 sorbents. The candidates were selected on the basis of oxide and sulfate stability. Volatile oxides such as tungstates or molybdates and oxides whose sulfates decompose at temperatures below 600°C were not considered. Previous work had indicated that sulfate is the SO_2 sorption product in the oxidizing combustion gas atmosphere.

For an actual process to "go" a driving force must exist. The driving force can be expressed as the difference between actual conditions and equilibrium. The tendency of metal oxide sorbents to form sulfates was evaluated by considering the driving force available for SO_3 sorption. The available driving force was determined by comparing the desired partial pressure of SO_3 in the combustion gas (actual conditions) with the equilibrium SO_3 vapor pressure over the sulfate. At temperatures where the SO_3 vapor pressure of the sulfate is less than the SO_3 partial

TABLE 3-1

METAL OXIDES CONSIDERED IN THERMODYNAMIC SCREENING

Li_2O
Na_2O
K_2O
BeO
CaO
SrO
BaO
NiO
ZnO
CdO
Ce_2O_3
CeO_2

$LiAlO_2$
Li_2CrO_4
$Li_2Cr_2O_4$
$LiFeO_2$
Li_2TiO_3
$LiVO_3$

$NaAlO_2$
Na_2CrO_4
$Na_2Cr_2O_4$
$NaFeO_2$
Na_2TiO_3
$NaVO_3$

$KAlO_2$
K_2CrO_4
$K_2Cr_2O_4$
$KFeO_2$
K_2TiO_3
KVO_3

$BeAl_2O_4$
$BeCrO_4$
$BeCr_2O_4$
$BeFe_2O_4$
$BeTiO_3$
BeV_2O_6

$CaAl_2O_4$
$CaCrO_4$
$CaCr_2O_4$
$CaFe_2O_4$
CaV_2O_6

$SrAl_2O_4$
$SrCrO_4$
$SrCr_2O_4$
$SrFe_2O_4$
$SrTiO_3$
SrV_2O_6

$BaAl_2O_4$
$BaCrO_4$
$BaCr_2O_4$
$BaFe_2O_4$
$BaTiO_3$
BaV_2O_6

pressure in the combustion gas, there is a driving force for the metal oxide to remove SO_3 from the combustion gas.

The driving force concept is shown in Figure 3-1. For Sorbent 1 the sulfur oxide could not be completely removed. Either Sorbent 2 or 3 could remove sulfur oxides down to the appropriate level. Since the process is cyclical, Sorbent 2 will be thermodynamically easier to regenerate.

The vapor pressure of SO_3 over the metal sulfate may be calculated from the following equilibrium.

$$\text{Metal Sulfate} \rightarrow SO_3 + \text{Metal Oxide} \qquad (3\text{-}1a)$$

$$Me_xSO_4 \rightarrow SO_3 + Me_xO \qquad (3\text{-}1b)$$

Table 3-2 lists single and binary metal oxides for which thermodynamic data indicate sulfate formation is favored between 600 and 1400°C at combustion gas conditions. The combustion exit conditions were chosen as 100 ppm total SO_x, 5% O_2, and one atmosphere total pressure. These are conditions that are more stringent than the EPA standard of 1.2 pounds SO_2/million Btu. The conditions were purposely chosen for a screening study for a second (or third) generation process. For details see Appendix 5.1. The oxides listed in Table 3-2 were evaluated further to identify conditions at which regeneration could be accomplished.

3.2 Regeneration

While the simplicity of thermal decomposition is intriguing from a process point of view, Table 3-2 indicates that the sulfates formed are quite stable and prohibitively high temperatures would be required. The same conclusion was reached by Vogel and coworkers (VO-034) for the calcium system.

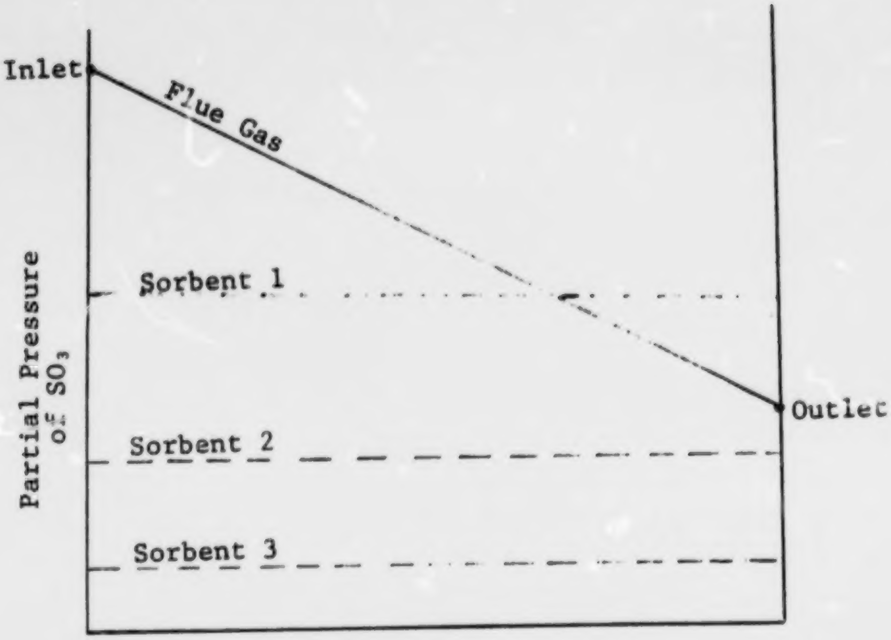

FIGURE 3-1 - SORPTION DRIVING FORCE

TABLE 3-2

POTENTIAL SORBENTS FOR SO_x REMOVAL FROM FLUE GASES

Sorbent*	Maximum Sorption** Temperature (°C)
Na_2O	1380
CaO	1090
SrO	1260
BaO	1380
$LiAlO_2$	1200
$LiFeO_2$	950
Li_2TiO_3	1200
$NaAlO_2$	820
$NaFeO_2$	1020
$CaAl_2O_4$	950
$SrAl_2O_4$	1000
$SrTiO_3$	920
$BaAl_2O_4$	1000
$BaTiO_3$	1000

---

* Potential sorbents were selected on the basis of the vapor pressure of SO_3 over the metal sulfate. If the SO_3 vapor pressure was less than the partial pressure of SO_3 in the flue gas, then a driving force for sorption was said to exist. See Technical Note 200-045-10-01a for details.

** Conditions other than one atmosphere total pressure, 5% O_2, and 100 ppm SO_x would change this maximum temperature.

Chemical regeneration as shown in reaction 3-2 was therefore investigated.

$$\text{Metal Sulfate} + \text{Reducing Agent} \rightarrow \text{Metal Oxide} + \text{Products} \qquad (3\text{-}2)$$

Since the actual mechanism of the reductive decomposition process is unknown, it is reasonable to choose some set of steps which are assumed to be at equilibrium and which can be evaluated using available thermodynamic data. The steps shown below were convenient for the purposes of this study:

$$\begin{array}{rcll} Me_xSO_4 & \rightarrow & SO_3 + Me_xO & (3\text{-}1) \\ SO_3 + \text{Reducing Agent} & \rightarrow & \text{Products} & (3\text{-}3) \\ \hline Me_xSO_4 + \text{Reducing Agent} & \rightarrow & Me_xO + \text{Products} & (3\text{-}2) \end{array}$$

The approach was to describe the individual reactions at equilibrium at various temperatures within the range of interest. Then the individual results were compared over the temperature range and the conditions at which the overall reaction was feasible were identified. Note that reaction 3-1 had been used in a similar manner for the sorption step.

The conclusions reached in the regeneration study are based upon logical but assumed process equipment arrangements and operating conditions. Furthermore, there is an error associated with the thermodynamic data used. The results, which are a list of sorbents and suggested operating temperature ranges, should be considered only as guidelines when making decisions for further investigations.

The six reducing atmospheres described in Table 2-2 were considered. The reducing atmospheres are of varying strength, as indicated in Table 2-2 by their capacity to react with oxygen.

The reducing agent must react with a very low concentration of SO_3. The most efficient use of the reducing agent occurs when it removes only one gram atom of oxygen from SO_3 (S in the +6 oxidation state) to produce SO_2 (S in +4 oxidation state). An example of this is reaction 3-4.

$$SO_3 + CO \rightarrow SO_2 + CO_2 \qquad (3\text{-}4)$$

Reduction of the SO_3 sulfur to a lower oxidation state by production of S_2 (oxidation state zero) is efficient only if elemental sulfur is the desired product. Production of H_2S (oxidation state -2) would be less efficient since that would be a greater reduction than is required. It could be more efficient to produce a concentrated SO_2 stream from the reducing agent - SO_3 reaction and to achieve any further desired change in sulfur oxidation state by treating the concentrated SO_2 stream when it is no longer in contact with the sorbent.

The products of reaction between SO_3 and the reducing agents were predicted by calculating the distribution of products at equilibrium for a number of temperatures between 600 and 1400°C. Products considered are listed in Table 3-3.

COS and CS_2 are undesirable due to their toxicity. Table 3-4 shows the major sulfur bearing and other products formed from reaction between one mole of SO_2 with each of

TABLE 3-3

GASEOUS PRODUCTS CONSIDERED

SO_2

SO_3

H_2S

COS

S_2

H_2

H_2O

O_2

CO

CO_2

CH_4

CS_2

TABLE 3-4

MAJOR PRODUCTS OF THE REACTION OF SO_3 WITH REDUCING AGENTS

	Sulfur Bearing Products		Other Products	
Reactants	600°C	1400°C	600°C	1400°C
$SO_3 + H_2$	100% SO_2	100% SO_2	100% H_2O	100% H_2O
$SO_3 + CO$	100% SO_2	100% SO_2	100% CO_2	100% CO_2
$SO_3 + CO + H$	83% SO_2 17% H_2S	100% SO_2	75% CO_2 25% H_2O	63% CO_2 24% H_2O 6% CH_4 7% CO
$SO_3 + C + H$	50% SO_2 40% H_2S 10% S_2	86% SO_2 14% S_2	88% CO_2 12% H_2O	66% CO_2 16% CH_4 9% H_2O 14% CO
$SO_3 + C$	66% SO_2 34% S_2	75% SO_2 25% S_2	100% CO_2	80% CO_2 20% CO
$SO_3 + CH_4$	100% H_2S	86% SO_2 14% H_2S	50% CO_2 50% H_2O	20% CO_2 40% CH_4 40% H_2O

the reducing agents. Note that COS and CS_2 are not predicted in significant quantities under these conditions. Variations in type and excess of reducing agent and total pressure would be expected to produce different product distributions.

As in the sorption step analysis, the feasibility of reductive decomposition of metal sulfates with each reducing agent was assessed by considering the available driving force. Reducing gas SO_3 partial pressures were compared to the SO_3 vapor pressure over the sulfate. At temperatures where the vapor pressure of SO_3 over the sulfate was greater than P_{SO_3} in the reducing gas, driving force was said to exist for the sulfate to give up SO_3 to the reducing gas, or decompose to the oxide. The regeneration concept is shown in Figure 3-2. Regeneration Gas A is not as effective as Regeneration Gas B. Sorbent 1 could be completely regenerated by either gas, Sorbent 2 by Gas B, and Sorbent 3 by neither gas.

Minimum temperatures at which such decomposition would be thermodynamically favored are given in Table 3-5. In general, Table 3-5 shows that the strongest reducing agents give the lowest sulfate decomposition temperatures.

The actual path of the reductive decomposition will depend partly on the equipment and operating conditions selected. A cocurrent gas solid reactor would be accurately described by the equilibrium calculations made. A fixed or moving bed process may be operated so that a large excess of reducing agent is present at the gas inlet. The reducing gas is consumed as it moves through the bed. At low stoichiometries, which are desirable from an economic standpoint, the gas at the outlet approaches an oxidizing atmosphere. A countercurrent gas-solid contactor would provide different reducing conditions than a cocurrent contactor and would be expected to produce different products.

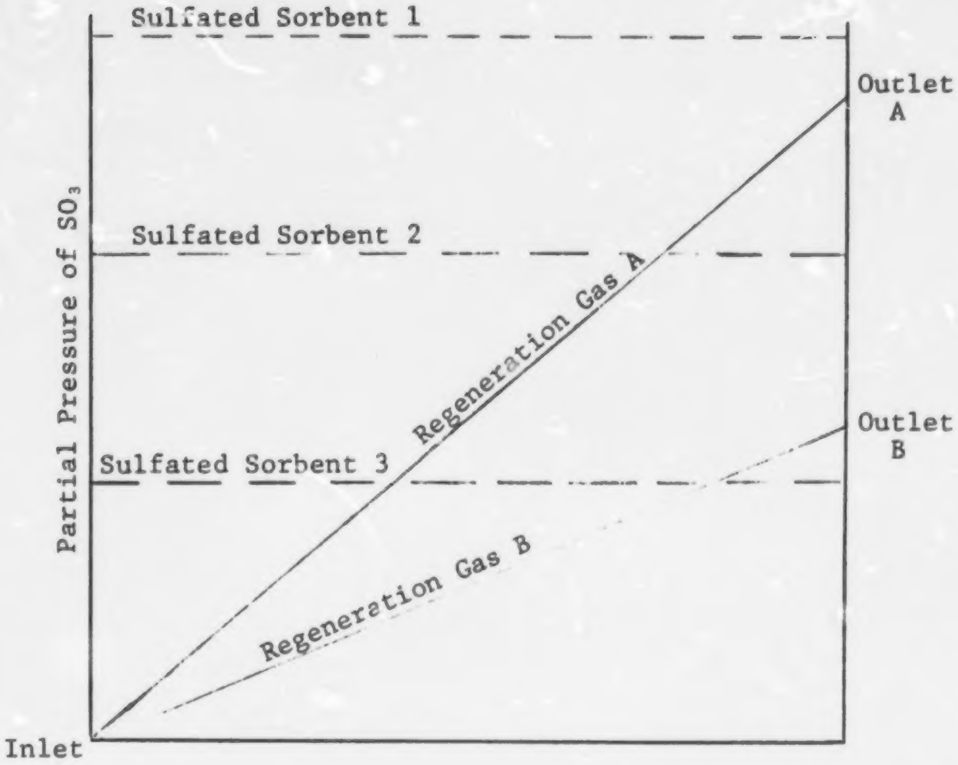

FIGURE 3-2 - REGENERATION

TABLE 3-5

MINIMUM TEMPERATURES AT WHICH METAL SULFATES ARE REDUCED BY SIX REDUCING AGENTS*

Metal Sulfates / Reducing Agents	Temperature (°C)					
	Hydrogen H_2	Carbon Monoxide CO	Synthesis Gas $CO + \frac{1}{2}H_2$	Coal C/H = 1	Char C	Methane CH_4
Na_2SO_4	>1400	>1400	>1400	>1400	>1400	>1400
$CaSO_4$	1320	1340	1025	960	960	730
$SrSO_4$	>1400	>1400	1310	1240	1210	1060
$BaSO_4$	>1400	>1400	>1400	>1400	>1400	>1400
$Li_2SO_4 + Al_2O_3$	>1400	>1400	1400	960	960	
$Li_2SO_4 + Fe_2O_3$	1110	1160	825	775	785	<600
$Li_2SO_4 + TiO_2$	>1400	>1400	1350	1140	1140	660
$Na_2SO_4 + Al_2O_3$	830	800	670	645	655	<600
$Na_2SO_4 + Fe_2O_3$	1220	1245	930	875	890	670
$CaSO_4 + Al_2O_3$	1180	1220	840	790	800	600
$SrSO_4 + Al_2O_3$	1250	1290	900	840	860	640
$SrSO_4 + TiO_2$	1020	1040	775	735	740	<600
$BaSO_4 + Al_2O_3$	1230	1290	890	840	850	630
$BaSO_4 + TiO_2$	1190	1220	910	850	860	630

---

* Minimum temperature for which the vapor pressure of SO_3 over the metal sulfate is greater than the partial pressure of SO_3 in the reducing gas.

The literature indicates the possibility of formation of metal sulfides (BO-001) and reduction to the elemental metal (PO-001) during reductive sulfate decomposition. The formation of metal sulfides would be undesirable since an additional processing step would be required to produce the oxide for recycle. Therefore, the possibility of metal sulfide formation in the reducing gases was considered. Transition between oxide and sulfide is shown in reaction 3-5.

$$Me_xO + \tfrac{1}{2}S_2 \rightarrow Me_xS + \tfrac{1}{2}O_2 \qquad (3\text{-}5)$$

Partial pressures of O_2 and S_2 over the metal oxide and sulfide at equilibrium were compared to those in the reducing gases. The temperature range where P_{O_2}/P_{S_2} is greater in the reducing gas than over the metal oxide and sulfide at equilibrium was identified. In that temperature range the oxide is predicted to be stable. Each oxide was evaluated for the temperature range for oxide stability with respect to sulfide formation in each reducing gas. Table 3-6 summarizes the predicted temperature ranges for oxide stability for each sulfate-reducing agent combination.

Conditions and reagents for oxide producing and sulfide producing regeneration processes were identified using the data from Tables 3-5 and 3-6. Table 3-7 lists sorbent-reducing agent combinations and temperature ranges for processes in which oxide formation is predicted. Table 3-8 lists sorbent-reducing agent combinations and temperature for processes in which sulfide formation is predicted.

TABLE 3-6

MINIMUM TEMPERATURE OF STABILITY OF METAL OXIDE WITH RESPECT TO FORMATION OF METAL SULFIDE IN REDUCING GAS*

Metal Oxide \ Reducing Agents	Temperature (°C)					
	Hydrogen H_2	Carbon Monoxide CO	Synthesis Gas $CO + \frac{1}{2}H_2$	Coal C/H = 1	Char C	Methane CH_4
Na_2O	970	955	>1400	>1400	>1400	>1400
CaO	<600	<600	1250	>1400	>1400	1370
SrO	<600	590	>1400	>1400	>1400	>1400
BaO	<600	700	>1400	>1400	>1400	>1400
$LiAlO_2$	<600	<600	<600	<600	<600	<600
$LiFeO_2$	<600	<600	750	1100	975	890
Al_2O_3	<600	<600	<600	<600	<600	<600
TiO_2	600-1190	880-1325	>1400	>1400	>1400	>1400
$NaAlO_2$	<600	<600	<600	<600	600	<600
$NaFeO_2$	<600	<600	820	1175	1030	980
$CaAl_2O_4$	<600	<600	740	1360	970-1350	890
$SrAl_2O_4$	<600	<600	<600	<600	<600	<600
$SrTiO_3$	<600	<600	<600	<600	<600	<600
$BaAl_2O_4$	<600	<600	<600	<600	<600	<600
$BaTiO_3$	<600	<600	<600	<600	<600	<600
Li_2TiO_3	<600	<600	<600	<600	<600	<600

---

* Minimum temperature at which the ratio of oxygen activity to sulfur activity in the reducing gas is greater than the ratio of oxygen to sulfur activities at equilibrium for the reaction $2MeO + S_2 \rightarrow 2MeS + O_2$.

TABLE 3-7

SORPTION-REGENERATION PROCESSES IN WHICH OXIDE FORMATION OCCURS

Sorbent	Maximum Sorption Temperature (°C)	Reducing Agent[1]	Temperature Range for Regeneration with Oxide Formation (°C)
CaO	1090	H_2	1320-1400
		CO	1340-1400
		$CO + \frac{1}{2}H_2$	1250-1400
		CH_4	1370-1400
$LiAlO_2$	1200	Coal and Char	960-1400
		CH_4	600-1400
$LiFeO_2$[2]	950	H_2	1110-1400
		CO	1160-1400
		$CO + \frac{1}{2}H_2$	825-1400
		Coal	1100-1400
		Char	(975?) 1020-1400
		Methane	890-1400
$NaAlO_2$	820	H_2	830-1400
		CO	800-1400
		$CO + \frac{1}{2}H_2$	670-1400
		Coal and Char	650-1400
		Methane	600-1400
$NaFeO_2$[2]	1020	H_2	1220-1400
		CO	1245-1400
		$CO + \frac{1}{2}H_2$	930-1400
		Coal	1030-1400
		Char	1175-1400
		Methane	980-1400
$CaAl_2O_4$	950	H_2	1180-1400
		CO	1220-1400
		$CO + \frac{1}{2}H_2$	840-1400
		Char	970-1350
		Coal	1360-1400
		Methane	890-1400
$SrAl_2O_4$	1000	H_2	1250-1400
		CO	1290-1400
		$CO + \frac{1}{2}H_2$	900-1400
		Coal and Char	~850-1400
		Methane	640-1400
$SrTiO_3$	920	H_2	1020-1400
		CO	1040-1320
$BaAl_2O_4$	1000	H_2	1230-1400
		$CO + \frac{1}{2}H_2$	1290-1400
		Coal and Char	850-1400
		Methane	630-1400
$BaTiO_3$	1000	H_2	1190-1400
		CO	1220-1320

---

[1]

Formula	Reducing Agent
CH_4	Methane
$C + \frac{1}{2}H_2$	Coal
C	Char
$CO + \frac{1}{2}H_2$	Synthesis Gas
CO	Carbon Monoxide
H_2	Hydrogen

One mole of reducing agent per mole of SO_2 was assumed.

[2] Possibility of iron sulfide formation no investigated due to lack of thermodynamic data.

TABLE 3-8

SORPTION-REGENERATION PROCESSES IN WHICH SULFIDE FORMATION OCCURS

Sorbent	Maximum Sorption Temperature (°C)	Reducing Agent[1]	Temperature Range for Regeneration with Sulfide Formation (°C)
CaO	1090	$CO + \frac{1}{2}H_2$	1030-1250
		Coal and Char	960-1400
		Methane	725-1370
SrO	1260	$CO + \frac{1}{2}H_2$	1310-1400
		Coal and Char	1240-1400
		Methane	1060-1400
$LiFeO_2$ [2]	950	Coal	775-1100
		Char	775-1020 (975?)
		Methane	600-890
$NaFeO_2$ [2]	1020	Coal	875-1030
		Char	875-1175
		Methane	670-980
$CaAl_2O_4$	950	Char	800-970
		Coal	800-1360
		Methane	600-890
$SrTiO_3$	920	CO	1320-1400
		$CO + \frac{1}{2}H_2$	775-1400
		Coal and Char	740-1400
		Methane	600-1400
$BaTiO_3$	1000	CO	1320-1400
		$CO + \frac{1}{2}H_2$	910-1400
		Coal and Char	850-1400
		Methane	630-1400
Li_2TiO_3	1200	$CO + \frac{1}{2}H_2$	1350-1400
		Coal and Char	1140-1400
		Methane	660-1400

---

[1]

Formula	Reducing Agent	
CH_4	Methane	One mole of reducing agent per mole of SO_2 was assumed.
$C + \frac{1}{2}H_2$	Coal	
C	Char	
$CO + \frac{1}{2}H_2$	Synthesis Gas	
CO	Carbon Monoxide	
H_2	Hydrogen	

[2] Possibility of iron sulfide formation not investigated due to lack of thermodynamic data.

3.3 Other Considerations

Although the main thrust of this program was devoted to thermodynamic screening of potential sorbent and regeneration materials, limited consideration was given to support material and heat transfer requirements. The results of those considerations are briefly discussed in the following subsections.

3.3.1 Support Materials

The majority of the potential sorbents identified by thermodynamic screening could not be used in their pure form but would have to be distributed or dispersed on some support material. Some of the reasons for supporting the sorbent materials include:

(1) to increase resistance to sintering,

(2) to increase resistance to poisoning,

(3) to improve thermal conductivity to and from the sorbent surface and in the fluidized bed,

(4) to improve the mechanical strength of the sorbent system and reduce abrasion losses, and

(5) to provide suitable framework for deposition of the sorbent resulting in a greater total surface.

One of the questions to be answered in this program was whether or not supports existed which would be suitable for use at high temperatures in a fluidized bed. To answer this question several catalyst carrier manufacturers were contacted (MC-122, FR-110, PE-105). Criteria given to the carrier manufacturers were that the support should be inert, have high thermal stability, and have high mechanical strength.

Contacts with the carrier manufacturers indicated that a wide variety of materials, shapes, sizes, porosities and structures were available. Low surface area carriers (less than $3m^2/g$) such as α-alumina and various refractories were suggested as being suitable. However, it was the general conclusion of all manufacturers contacted that definitive recommendations on support materials could not be made until more was known about the porosity and surface area requirements.

Porosity, pore structure, and pore size are extremely important factors in the selection of support materials. The pore structure of a particular support will be a controlling factor in the way a sorbent will be deposited. It will also contribute significantly to the final properties of a finished sorbent which affect residence time of reactants within the structure, rate of reaction, useful sorbent surface area, and the extent of undesirable side reactions. Clearly any future experimental work on the potential sorbents identified in this study should be devoted in part to identifying the support material porosity and surface area requirements.

3.3.2 Heat Transfer

In the development of a process it is essential to make both material and heat balances. The calculations presented thus far have addressed themselves to the temperature and pressure at which a process might proceed. It is also important to assess the heat transfer requirements.

It would be desirable to have the solid from the sorber pass to the regenerator and come back without involving a heat transfer step. Should this not be possible, the amount of heating (or cooling) required must be known. An estimate was made for the calcium system. This estimate indicated that the decomposition of the sulfated sorbent is highly endothermic (requires heat). The reaction of the evolved SO_3 with the reducing gas is moderately exothermic (gives off heat). The amount of heat given off is slightly dependent on which reducing gas is used. The net effect is a heat requirement of about 50 Kcal per mole of sulfate decomposed.

While the calculation of heat requirements is beyond the scope of this screening study, it does appear as if most regeneration processes will be endothermic. Heat balances must be considered in future work.

4.0 BIBLIOGRAPHY

AN-001 Anonymous, "Fluidized Bed Steam Generators for Utilities", Environmental Science and Technology 8(12), 968-70 (1974).

BO-001 Bowen, J. Harry and C. K. Cheng, "Regeneration of Sulfated Alkalized Alumina", Environmental Science and Technology 8(8), 747-51 (1974).

FR-110 Fritz, R. C., Private Communication, Girdler Chemical Inc., Catalysts Division, 6006 Bellaire Blvd., Suite 118-5, Houston, Texas, 77036, 18 October 1974.

MC-122 McDowell, Robert G., Private Communication, Norton Company, Chemical Process Products Division, 3701 Kirby Building, Suite 890, Houston, Texas, 77006, 10 August 1974.

PA-016 Parsons, T. B., Gary D. Schroeder, and David DeBerry, Applicability of Metal Oxides to the Development of New Processes for Removing SO_2 from Flue Gases, two volumes, Austin, Texas, Tracor, Inc., 1969.

PE-105 Perkins, J. D., Private Communication, The HarsHaw Chemical Company, P.O. Box 6813, Houston, Texas, 77005, 14 October 1974.

PO-001 Pohlenz, J. B., "The Shell Flue Gas Desulfurization Process", presented at the Environmental Protection Agency Flue Gas Desulfurization Symposium, Atlanta, Georgia, November 4-7, 1974.

VO-034 Vogel, G. J., et al., Reduction of Atmospheric Pollution by the Application of Fluidized-Bed Combustion and Regeneration of Sulfur-Containing Additives, EPA-R-2-73-253, Argonne, Ill., Argonne Nat'l Lab., 1973.

5.0 APPENDIX

5.1 Technical Note 200-045-10-01a

"Thermodynamic Screening of Dry Metal Oxides for High Temperature SO_2 Removal", prepared by N. P. Phillips, 1 May 1975.

5.2 Technical Note 200-045-10-02a

"The Thermodynamics of Chemical Regeneration of Metal Oxide SO_2 Sorbents", prepared by Philip S. Lowell and Terry B. Parsons, 25 April 1975.

RADIAN
CORPORATION

Section 5.1

TECHNICAL NOTE 200-045-10-01a

THERMODYNAMIC SCREENING OF DRY METAL OXIDES FOR HIGH TEMPERATURE SO_2 REMOVAL

1 May 1975

Prepared by:

N. P. Phillips

TABLE OF CONTENTS

		Page
1.0	INTRODUCTION	33
2.0	METHODS	34
2.1	Selection of Sorbents for Screening	34
2.2	Thermodynamic Screening	38
3.0	RESULTS	43
4.0	BIBLIOGRAPHY	48
	APPENDIX - FIGURES A-1 THROUGH A-53	49

1.0 INTRODUCTION

This technical note presents the results of the thermodynamic screening of potential metal oxide and mixed metal oxide sorbents for use as SO_2 sorbents in high temperature fluidized bed combustors. Fluidized bed combustion of fossil fuels for electrical power generation, as all combustion processes, generates sulfur oxide emissions. One approach to SO_x removal for this combustion method is injection of limestone into the combustion zone. In many cases, however, limestone has been found to be unsuitable for fluidized combustion processes. This has been due to either limestone type or process conditions. Also, there are some locations in which limestone is not readily available. Therefore, metal oxides and mixed metal oxides will be evaluated as alternate high temperature regenerable SO_2 sorbents to avoid these problems.

In a previous study, a thermodynamic approach was employed to select potential dry metal oxide sorbents for a lower temperature SO_2 removal process (PA-016). The methods developed during that study were applied to the screening task involved in the present investigation. These earlier results are extended to high temperatures, and the fact that SO_3 is not the dominant species is accounted for.

2.0 METHODS

Although the species actually sorbed during the sorption process is SO_2, the relative pressures of SO_3 in the flue gas and over the metal sulfate determine the feasibility of a metal oxide as an SO_2 sorbent. The actual mechanism of reaction is unknown. The SO_2 is probably catalytically oxidized and reacts with the metal oxide. A generalized reaction for sulfate decomposition is shown in Equation 1. While Equation 1 results in formation of the metal oxide plus SO_3, it is equivalent to the decomposition to oxygen and sulfur dioxide as discussed by Vogel, et al. (VO-034, page 35).

$$Me_xSO_4 \rightleftarrows Me_xO + SO_3 \qquad (1)$$

For a metal oxide to be an effective sorbent, the metal sulfate must be stable at the temperature at which sorption takes place. The degree of sulfate stability is indicated by the vapor pressure of SO_3 over the solid sulfate at the temperature of interest. A potential sorbent will remove SO_x at temperature T if the partial pressure of SO_3 in the flue gas is greater than the vapor pressure of SO_3 over the metal sulfate. Comparison of these two partial pressures over the temperature range of interest (750-1200°C) will be used as the basis for screening potential metal oxide SO_2 sorbents.

2.1 Selection of Sorbents for Screening

The results of an earlier investigation (PA-016) of a dry metal oxide SO_2 removal process were used as a starting point for the sorbent screening task in this study. In the earlier work, a computerized data base of thermodynamic properties was compiled for inorganic metal oxides, mixed metal oxides, sulfates, sulfur oxide gaseous species, and numerous other inorganic compounds. Decomposition behavior as reported in the literature was also reviewed. Logarithms of the equilibrium constant (which is numerically equal to the partial pressure of SO_3) for reactions of the type shown in Equation (1) were calculated and plotted as a function of temperature through 800° C for a number of metal oxides. Analysis of these earlier results was used as a preliminary screening technique for high temperature SO_2 sorbents. The following criteria were used:

1. Metal oxides whose sulfates decompose below 600° C were eliminated (PA-016, T.M. 004-009, Ch. 8 and 16).

2. The oxide itself must be stable at high temperature (PA-016, T.M. 004-009, Ch. 7).

3. For those oxides whose sulfates are stable up to at least 600° C, the SO_3 vapor pressure over the sulfate at 600° C should be low enough to allow sufficient free energy available as driving force for SO_3 sorption (PA-016, Section 8.2).

4. Potential single metal oxide sorbents were eliminated from further consideration if they were not produced in reasonable quantities (PA-016, T.M. 004-009, Ch. 6).

5. The thermodynamic data base must contain standard state heat of formation, absolute entropy, and heat capacity coefficients for each species involved in the reaction in order for log K to be calculated.

Estimation methods were used to supply some of the data. Those oxides for which the necessary information was not available and could not be estimated were excluded from further consideration.

6. Binary metal oxides of alkali and alkaline earth compounds were considered. However, because of their volatilities, molybdates and tungstates were not included in the study. In addition, silicates were not considered because thermodynamic data for this class of compounds had not been included in the data base.

Table I shows the results of this initial screening.

Heat capacity data over the temperature range of interest for the reactants (metal sulfates) and products (metal oxides plus SO_3) of the sulfate decomposition reaction are required to calculate log K. In most cases the range of validity for the heat capacity coefficients stored in the data base does not extend to 1400° C, the upper temperature limit in this investigation. The computer routine used to calculate log K automatically extends the range of the stored heat capacity coefficients; therefore, it was necessary to check the validity of such extensions. The expected behavior of heat capacity at high temperature is a gradual increase with increasing temperature. However, negative values for B, C, or D in the heat capacity equation shown below may cause a slight decrease at high temperatures.

$$C_p = A + BT + CT^2 - DT^{-2} \qquad (2)$$

TABLE I
RESULTS OF PRELIMINARY SCREENING OF METAL OXIDES

Sulfate Decomposition > 600°C

Li_2O
Na_2O
K_2O
Rb_2O***
Cs_2O***
BeO
MgO*
CaO
SrO
BaO
Sc_2O_3*

Y_2O_3*
La_2O_3*
Ce_2O_3
CeO_2
MnO*
MnO_2*
Mn_2O_3*
Fe_2O_3*
CoO*
NiO

CuO*
Cu_2O*
Ag_2O**
ZnO
CdO
Al_2O_3*
PbO**
PbO_2**
Bi_2O_3*
ThO_2*

Sulfate Decomposition < 600°C

TiO_2
ZrO_2
HfO_2
V_2O_3

VO_2
V_2O_5
Cr_2O_3

FeO
SnO_2
UO_2

Sulfate Decomposition Data Unavailable

Nb_2O_5
Ta_2O_5
MoO_3
WO_3

ReO_2
Rh_xO_y
IrO_2
PdO

Ga_2O_3
GeO_2
Sb_2O_3

---

* Indicates oxides eliminated from further consideration on the basis of SO_3 partial pressure over the sulfate.

** Oxide is very unstable in temperature range of interest, therefore not considered further.

*** No heat capacity data available.

This error would introduce inaccuracies into the log K calculation. Therefore, a short computer program was written and used to calculate heat capacity values at 100 degree intervals over the temperature range from 600 to 1400°C using the coefficients stored in the data base. This was done for SO_3 and all candidate metal oxides and corresponding sulfates. The only compound data set requiring revision was that of SO_3 . This was accomplished by correlating heat capacity versus temperature data reported in the literature using a least-squares curve fitting routine to estimate improved heat capacity coefficients.

2.2 Thermodynamic Screening

As described previously, the free energy available as driving force for SO_2 sorption is related to the difference between vapor pressure of SO_3 over the sulfate and flue gas SO_3 partial pressure. These two were calculated separately and compared in the final screening analysis.

The flue gas SO_3 partial pressure is described by the following equilibrium reaction:

$$SO_3 \rightleftarrows SO_2 + \tfrac{1}{2}O_2 \qquad (3)$$

The equilibrium constant for this reaction may be written

$$K_1 = \frac{(a_{SO_2})\ (a_{O_2})^{\frac{1}{2}}}{a_{SO_3}} \qquad (4)$$

Thus, the concentrations of SO_3 and SO_2 at a given temperature are a function of the total SO_x present (assumed to be 100 ppm or 10^{-4} atm), the oxygen partial pressure in the flue gas, and the equilibrium constant at that pressure.

The choice of the total SO_x partial pressure is somewhat arbitrary. The following rationale was followed. A pound of coal will generate 0.45 to 0.6 pound moles of flue gas. Heating values range from 9000 to 12000 Btu per pound. To meet an emission regulation of 1.2 pounds SO_2/million Btu would result in SO_2 concentrations of 200 to 500 ppm based upon the above ranges. In setting a goal for second generation processes it is advisable to look beyond today's requirements. For this reason 100 ppm was chosen as a basis with 5% O_2 in the flue gas.

Log K_1 (per mole SO_3) was calculated and plotted from 600 to 1400°C at flue gas oxygen partial pressures of 0.02, 0.03, 0.05, and 0.10 atm. The following expression was then used to calculate SO_3 partial pressures at 50 degree intervals over the temperature range of interest.

$$\text{Log } K_1 = \text{Log } \frac{(P_{SO_2})(P_{O_2})^{\frac{1}{2}}}{P_{SO_3}}$$

SO_3 concentrations derived from the log K_1 calculations agreed well with expected values. At 0.05 atm O_2 the calculated SO_3 content was 70 ppm at 600°C and 0.5 ppm at 1400°C. Table II shows the results for the case in which the oxygen standard state was 0.05 atm.

The second parameter which was calculated was the vapor pressure of SO_3 over the metal sulfate. This was determined by calculating the equilibrium constant for the sulfate decomposition reaction (Equation 1) for each potential sorbent over the temperature range of interest. The equilibrium constant for this reaction is numerically equal to the partial pressure of SO_3 if activities of the solid

TABLE II

PARTIAL PRESSURE OF SO_3 IN FLUE GAS

(Total SO_x = 100 ppm, O_2 = 5%, Total Pressure = 1 atm)

Temp. °C	$\log_{10} K_1^*$	K_1^*	$1 + K_1^*$	$P_{SO_3} = \frac{1.0\times10^{-4}}{1 + K_1^*}$	$\log P_{SO_3}$
600	-0.32680	0.47118	1.47118	6.7973×10^{-5}	-4.1677
650	-0.01807	0.95922	1.95922	5.1041×10^{-5}	-4.2921
700	0.25752	1.8093	2.8093	3.5596×10^{-5}	-4.4486
750	0.50485	3.1978	4.1978	2.3822×10^{-5}	-4.6230
800	0.72788	5.3442	6.3442	1.5762×10^{-5}	-4.8024
850	0.92987	8.5088	9.5088	1.0517×10^{-5}	-4.9781
900	1.1135	13.646	14.646	6.8278×10^{-5}	-5.1657
950	1.2810	19.098	20.098	4.9756×10^{-6}	-5.3031
1000	1.4344	27.189	28.189	3.5475×10^{-6}	-5.4501
1050	1.5752	37.601	38.601	2.5906×10^{-6}	-5.5866
1100	1.7048	50.676	51.676	1.9351×10^{-6}	-5.7133
1150	1.8243	66.727	67.727	1.4765×10^{-6}	-5.8308
1200	1.9349	86.079	87.079	1.1484×10^{-6}	-5.9399
1250	2.0374	108.99	109.99	9.0917×10^{-7}	-6.0413
1300	2.1326	135.71	136.71	7.3147×10^{-7}	-6.1358
1350	2.2212	166.42	167.42	5.9730×10^{-7}	-6.2238
1400	2.3037	201.23	202.23	4.9449×10^{-7}	-6.3058

K_1 = equilibrium constant for the reaction $SO_3 \rightleftarrows SO_2 + 0.5\ O_2$

$$K_1^* = \frac{K_1}{(0.05)^{\frac{1}{2}}}$$

species are equal to one. Log K per mole of SO_3 was calculated from thermodynamic data stored in the data base and plotted as a function of temperature for all metal oxides listed in Table III. The resulting curve was equivalent to the logarithm of the vapor pressure of SO_3 over the sulfate.

TABLE III

METAL OXIDES CONSIDERED IN THERMODYNAMIC SCREENING

Li_2O
Na_2O
K_2O
BeO
CaO
SrO
BaO
NiO
ZnO
CdO
Ce_2O_3
CeO_2

$LiAlO_2$
Li_2CrO_4
$Li_2Cr_2O_4$
$LiFeO_2$
Li_2TiO_3
$LiVO_3$

$NaAlO_2$
Na_2CrO_4
$Na_2Cr_2O_4$
$NaFeO_2$
Na_2TiO_3
$NaVO_3$

$KAlO_2$
K_2CrO_4
$K_2Cr_2O_4$
$KFeO_2$
K_2TiO_3
KVO_3

$BeAl_2O_4$
$BeCrO_4$
$BeCr_2O_4$
$BeFe_2O_4$
$BeTiO_3$
BeV_2O_6

$CaAl_2O_4$
$CaCrO_4$
$CaCr_2O_4$
$CaFe_2O_4$
CaV_2O_6

$SrAl_2O_4$
$SrCrO_4$
$SrCr_2O_4$
$SrFe_2O_4$
$SrTiO_3$
SrV_2O_6

$BaAl_2O_4$
$BaCrO_4$
$BaCr_2O_4$
$BaFe_2O_4$
$BaTiO_3$
BaV_2O_6

3.0 RESULTS

The selection of promising high temperature SO_2 sorbents was made on the basis of free energy available as driving force for sorption. The results of the calculations described in the preceding section were used for this analysis. The plots of log K per mole SO_3 versus T for the various sulfate decomposition reactions were compared to the plot of log P_{SO_3} versus T for the SO_3 - SO_2 equilibrium reaction. Comparison of the two plots provides a direct means of determining if the process is thermodynamically feasible. That is, if the partial pressure of SO_3 in the flue gas is greater than vapor pressure of SO_3 over the sulfate, sorption will occur. The plots for each sulfate decomposition are included in the appendix to this technical note. Also shown on each figure is the plot of log P_{SO_3} versus temperature representing the flue gas SO_3 partial pressure.

For temperature regions in which the curve of log K per mole SO_3 for the sulfate decomposition reaction indicated (i.e., P_{SO_3} over the sulfate) is above the curve of log P_{SO_3} (i.e., partial pressure of SO_3 in the flue gas), sorption is not thermodynamically favored. For the region below the log P_{SO_3} curve, the vapor pressure over the sulfate is less than the flue gas SO_3 partial pressure. Therefore, SO_x could be sorbed from flue gas in that temperature range. In the example shown in Figure 1, the portion of the curve above A represents the feasible sorption range and below A the unfeasible region. Using this basic criterion, the potential sorbents were screened from 750-1200° C.

Several other criteria were also employed in the screening. Very low values of log K for the sulfate decomposition reaction, say about 6 logarithmic units below the flue gas

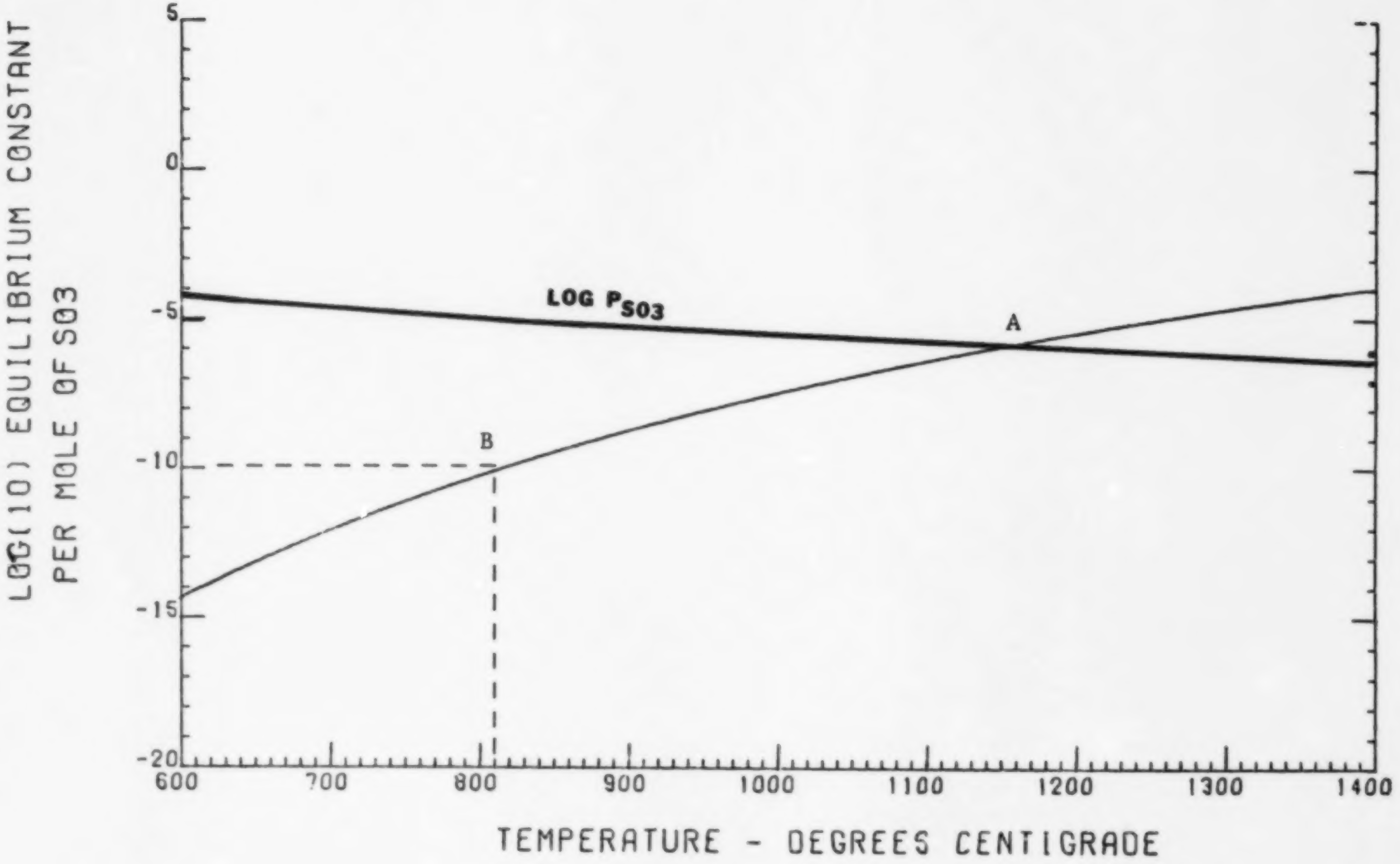

08 AUG 74

FIGURE 1

Log K Versus T for A Sulfate Decomposition Reaction

SO_3 line, indicate stable sulfates. In such cases, although sorption would occur readily, the oxide might not be suitable for an SO_2 removal process because of high energy requirements for sorbent regeneration. In Figure 1 the portion of the curve below B is less desirable. There is no sharp cutoff so judgment is required. One of the purposes of this screening study is to identify metal oxide - SO_3 reactions that form sulfate for which the free energy change is very large. Such metal oxides would be attractive as sorbents. However, the energy requirement in the regeneration step would be too great. This idea is illustrated by comparing Figures 1 and A-3. Figure 1 shows a sorbent with a relatively small free energy change (several logarithmic units) for the sulfate forming reaction. Figure A-3 shows a difference of 10 to 25 logarithmic units between the two SO_3 partial pressures. Such a metal oxide would be eliminated from further consideration for the reasons just described.

A relatively gradual increase of log K with respect to increasing temperature indicates a lower heat of reaction than a curve with a steep slope over the temperature range of interest. The sorption reaction with a lesser slope would require much less heat but a greater temperature change for thermal regeneration than would a reaction whose equilibrium constant increases rapidly with temperature. Regeneration by altering the chemical conditions, e.g., reducing atmospheres, will also be considered.

The purpose of this study is to use approximate thermodynamic calculations for identifying metal oxides for which SO_3 sorption-regeneration is favored. The approach is to eliminate some of the metal oxides from consideration as potential sorbents. If a metal oxide is "on the borderline", it is not eliminated, since the data used in screening are approximate. A factor of 10 in SO_3 partial pressure (one logarithmic unit) is not significant for this screening study, and a potential sorbent would not be screened out on that basis. In summarizing the criteria described above, the most promising candidates are those whose log K plots lie less than five logarithmic units below the log P_{SO_3} curve. The type of regeneration used will depend on the slope over the temperature range from 750 to 1200°C.

Based on the above criteria, the metal oxides having the greatest potential as SO_2 sorbents in a fluidized bed combustion system are listed in Table IV. The temperature range over which the criteria hold are included for each compound.

As seen in Table IV, the only single metal oxides having any potential are strontium oxide and calcium oxide since sodium and barium oxides are feasible only over very narrow temperature ranges. Calcium oxide appears feasible over the lower region of the temperature range of interest, while strontium oxide has potential only in the upper region of the temperature range considered. Several binary metal oxides containing aluminum, titanium, or iron(III) also appear promising. Of these $LiAlO_2$ and Li_2TiO_3 meet all criteria over the whole temperature range considered in this investigation.

TABLE IV

MOST PROMISING SORBENTS BASED ON THERMODYNAMIC SCREENING RESULTS

Sorbent	Temperature Range °C
Na_2O	1100-1200
CaO	750-1090
SrO	950-1200
BaO	1080-1200
$LiAlO_2$	750-1200
$LiFeO_2$	750-950
Li_2TiO_3	750-1200
$NaAlO_2$	750-820
$NaFeO_2$	750-1020
$CaAl_2O_4$	750-950
$SrAl_2O_4$	750-1000
$SrTiO_3$	750-920
$BaAl_2O_4$	750-1000
$BaTiO_3$	750-1000

4.0 BIBLIOGRAPHY

PA-016 Parsons, Terry, Gary D. Schroeder, and David DeBerry, *Applicability of Metal Oxides to the Development of New Processes for Removing SO_2 from Flue Gases*, Two Volumes, Austin, Texas, Tracor, Inc., 1969.

VO-034 Vogel, G. J., et al., *Reduction of Atmospheric Pollution by the Application of Fluidized-Bed Combustion and Regeneration of Sulfur-Containing Additives*, EPA-R2-73-253, Argonne, Ill., Argonne National Lab., 1973.

APPENDIX

FIGURES A-1 THROUGH A-53

LIST OF FIGURES

Figure	
A-1	Log K Versus T for the Reaction $Li_2SO_4 \rightleftarrows Li_2O + SO_3$
A-2	Log K Versus T for the Reaction $Na_2SO_4 \rightleftarrows Na_2O + SO_3$
A-3	Log K Versus T for the Reaction $K_2SO_4 \rightleftarrows K_2O + SO_3$
A-4	Log K Versus T for the Reaction $BeSO_4 \rightleftarrows BeO + SO_3$
A-5	Log K Versus T for the Reaction $CaSO_4 \rightleftarrows CaO + SO_3$
A-6	Log K Versus T for the Reaction $SrSO_4 \rightleftarrows SrO + SO_3$
A-7	Log K Versus T for the Reaction $BaSO_4 \rightleftarrows BaO + SO_3$
A-8	Log K Versus T for the Reaction $NiSO_4 \rightleftarrows NiO + SO_3$
A-9	Log K Versus T for the Reaction $ZnSO_4 \rightleftarrows ZnO + SO_3$
A-10	Log K Versus T for the Reaction $CdSO_4 \rightleftarrows CdO + SO_3$
A-11	Log K Versus T for the Reaction $1/3\ Ce_2(SO_4)_3 \rightleftarrows 1/3\ Ce_2O_3 + SO_3$
A-12	Log K Versus T for the Reaction $\frac{1}{2}Ce(SO_4)_2 \rightleftarrows \frac{1}{2}CeO_2 + SO_3$
A-13	Log K Versus T for the Reaction $Li_2SO_4 + Al_2O_3 \rightleftarrows 2LiAlO_2 + SO_3$

Figure

A-14 Log K Versus T for the Reaction $Li_2O_4 + CrO_3 \rightleftarrows Li_2CrO_4 + SO_3$

A-15 Log K Versus T for the Reaction $Li_2SO_4 + Cr_2O_3 \rightleftarrows Li_2Cr_2O_4 + SO_3$

A-16 Log K Versus T for the Reaction $Li_2SO_4 + Fe_2O_3 \rightleftarrows 2LiFeO_2 + SO_3$

A-17 Log K Versus T for the Reaction $Li_2SO_4 + TiO_2 \rightleftarrows Li_2TiO_3 + SO_3$

A-18 Log K Versus T for the Reaction $Li_2SO_4 + V_2O_5 \rightleftarrows 2LiVO_3 + SO_3$

A-19 Log K Versus T for the Reaction $Na_2SO_4 + Al_2O_3 \rightleftarrows 2NaAlO_2 + SO_3$

A-20 Log K Versus T for the Reaction $Na_2SO_4 + CrO_3 \rightleftarrows Na_2CrO_4 + SO_3$

A-21 Log K Versus T for the Reaction $Na_2SO_4 + Cr_2O_3 \rightleftarrows Na_2Cr_2O_4 + SO_3$

A-22 Log K Versus T for the Reaction $Na_2SO_4 + Fe_2O_3 \rightleftarrows 2NaFeO_2 + SO_3$

A-23 Log K Versus T for the Reaction $Na_2SO_4 + TiO_2 \rightleftarrows Na_2TiO_3 + SO_3$

A-24 Log K Versus T for the Reaction $Na_2SO_4 + V_2O_5 \rightleftarrows 2NaVO_3 + SO_3$

A-25 Log K Versus T for the Reaction $K_2SO_4 + Al_2O_3 \rightleftarrows 2KAlO_2 + SO_3$

A-26 Log K Versus T for the Reaction $K_2SO_4 + CrO_3 \rightleftarrows K_2\ CrO_4 + SO_3$

A-27 Log K Versus T for the Reaction $K_2SO_4 + Cr_2O_3 \rightleftarrows K_2Cr_2O_4 + SO_3$

Figure	
A-28	Log K Versus T for the Reaction $K_2SO_4 + Fe_2O_3 \rightleftarrows 2KFeO_2 + SO_3$
A-29	Log K Versus T for the Reaction $K_2SO_4 + TiO_2 \rightleftarrows K_2TiO_3 + SO_3$
A-30	Log K Versus T for the Reaction $K_2SO_4 + V_2O_5 \rightleftarrows 2KVO_3 + SO_3$
A-31	Log K Versus T for the Reaction $BeSO_4 + Al_2O_3 \rightleftarrows BeAl_2O_4 + SO_3$
A-32	Log K Versus T for the Reaction $BeSO_4 + CrO_3 \rightleftarrows BeCrO_4 + SO_3$
A-33	Log K Versus T for the Reaction $BeSO_4 + Cr_2O_3 \rightleftarrows BeCr_2O_4 + SO_3$
A-34	Log K Versus T for the Reaction $BeSO_4 + Fe_2O_3 \rightleftarrows BeFe_2O_4 + SO_3$
A-35	Log K Versus T for the Reaction $BeSO_4 + TiO_2 \rightleftarrows BeTiO_3 + SO_3$
A-36	Log K Versus T for the Reaction $BeSO_4 + V_2O_5 \rightleftarrows BeV_2O_6 + SO_3$
A-37	Log K Versus T for the Reaction $CaSO_4 + Al_2O_3 \rightleftarrows CaAl_2O_4 + SO_3$
A-38	Log K Versus T for the Reaction $CaSO_4 + CrO_3 \rightleftarrows CaCrO_4 + SO_3$
A-39	Log K Versus T for the Reaction $CaSO_4 + Cr_2O_3 \rightleftarrows CaCr_2O_4 + SO_3$
A-40	Log K Versus T for the Reaction $CaSO_4 + Fe_2O_3 \rightleftarrows CaFe_2O_4 + SO_3$

Figure

A-41 Log K Versus T for the Reaction $CaSO_4 + V_2O_5 \rightleftarrows CaV_2O_6 + SO_3$
A-42 Log K Versus T for the Reaction $SrSO_4 + Al_2O_3 \rightleftarrows SrAl_2O_4 + SO_3$
A-43 Log K Versus T for the Reaction $SrSO_4 + CrO_3 \rightleftarrows SrCrO_4 + SO_3$
A-44 Log K Versus T for the Reaction $SrSO_4 + Cr_2O_3 \rightleftarrows SrCr_2O_4 + SO_3$
A-45 Log K Versus T for the Reaction $SrSO_4 + Fe_2O_3 \rightleftarrows SrFe_2O_4 + SO_3$
A-46 Log K Versus T for the Reaction $SrSO_4 + TiO_2 \rightleftarrows SrTiO_3 + SO_3$
A-47 Log K Versus T for the Reaction $SrSO_4 + V_2O_5 \rightleftarrows SrV_2O_6 + SO_3$
A-48 Log K Versus T for the Reaction $BaSO_4 + Al_2O_3 \rightleftarrows BaAl_2O_4 + SO_3$
A-49 Log K Versus T for the Reaction $BaSO_4 + CrO_3 \rightleftarrows BaCrO_4 + SO_3$
A-50 Log K Versus T for the Reaction $BaSO_4 + Cr_2O_3 \rightleftarrows BaCr_2O_4 + SO_3$
A-51 Log K Versus T for the Reaction $BaSO_4 + Fe_2O_3 \rightleftarrows BaFe_2O_4 + SO_3$
A-52 Log K Versus T for the Reaction $BaSO_4 + TiO_2 \rightleftarrows BaTiO_3 + SO_3$
A-53 Log K Versus T for the Reaction $BaSO_4 + V_2O_5 \rightleftarrows BaV_2O_6 + SO_3$

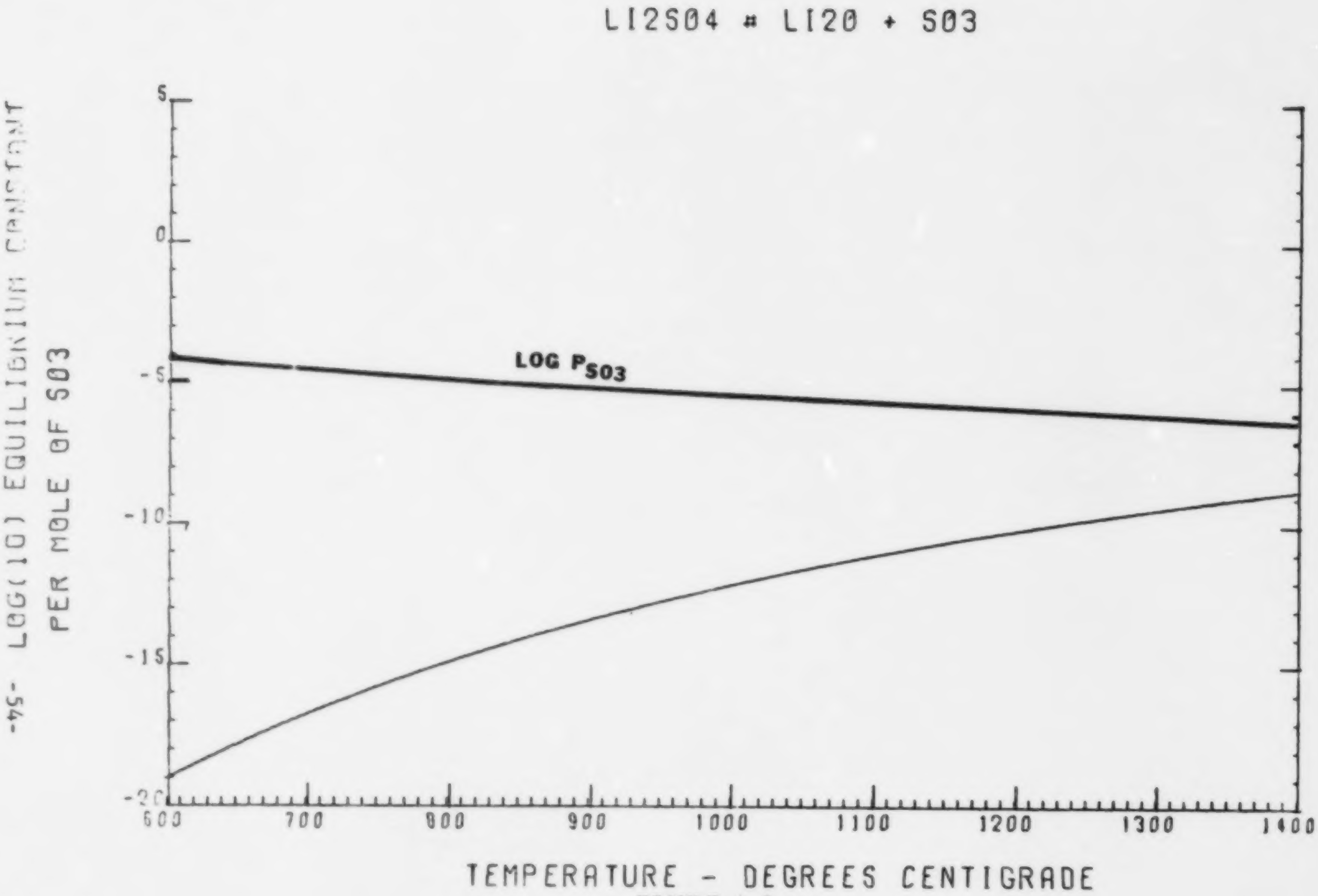

FIGURE A-1

Log K Versus T for the Reaction
$Li_2SO_4 \rightleftarrows Li_2O + SO_3$

AUG 74

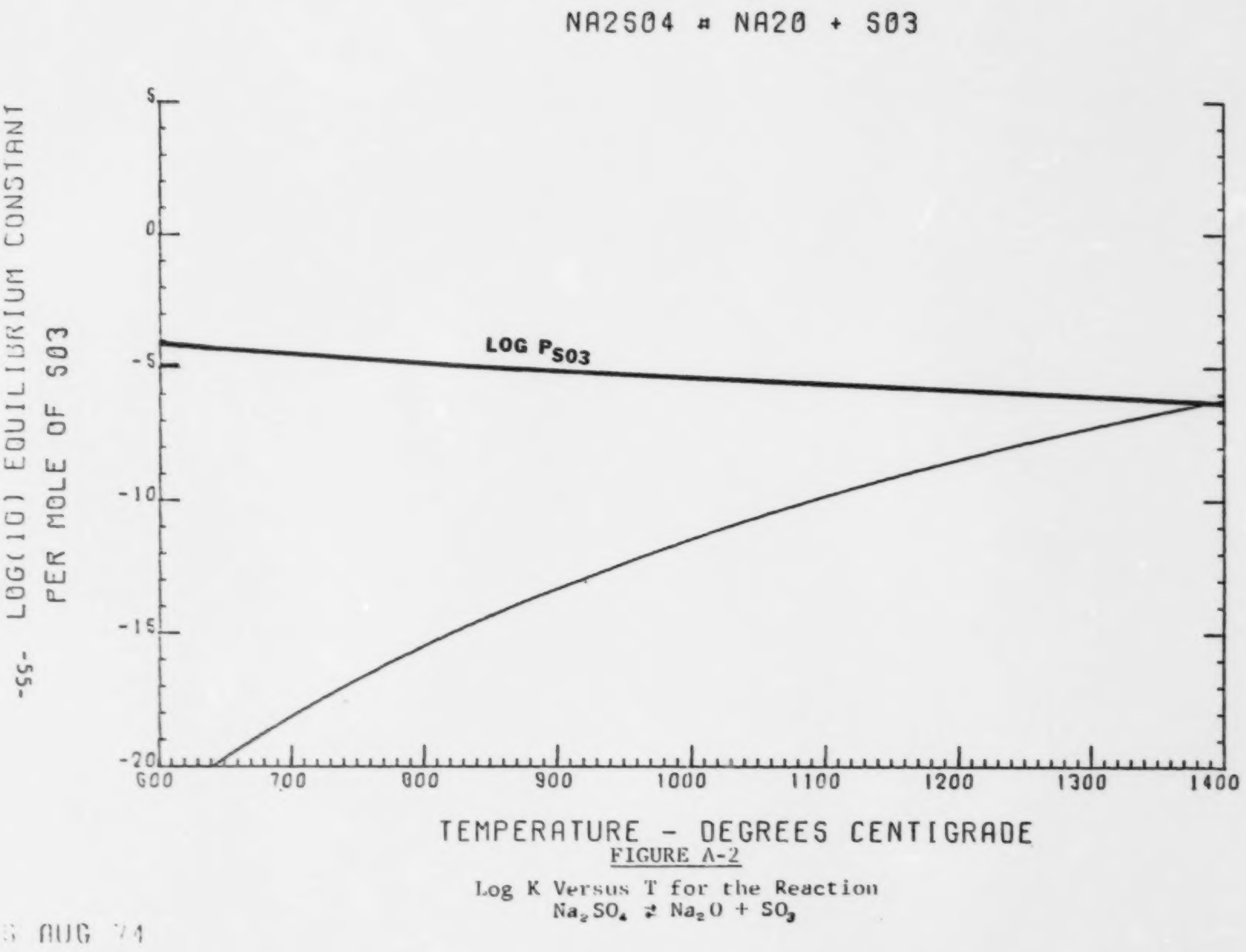

FIGURE A-2

Log K Versus T for the Reaction
$Na_2SO_4 \rightleftarrows Na_2O + SO_3$

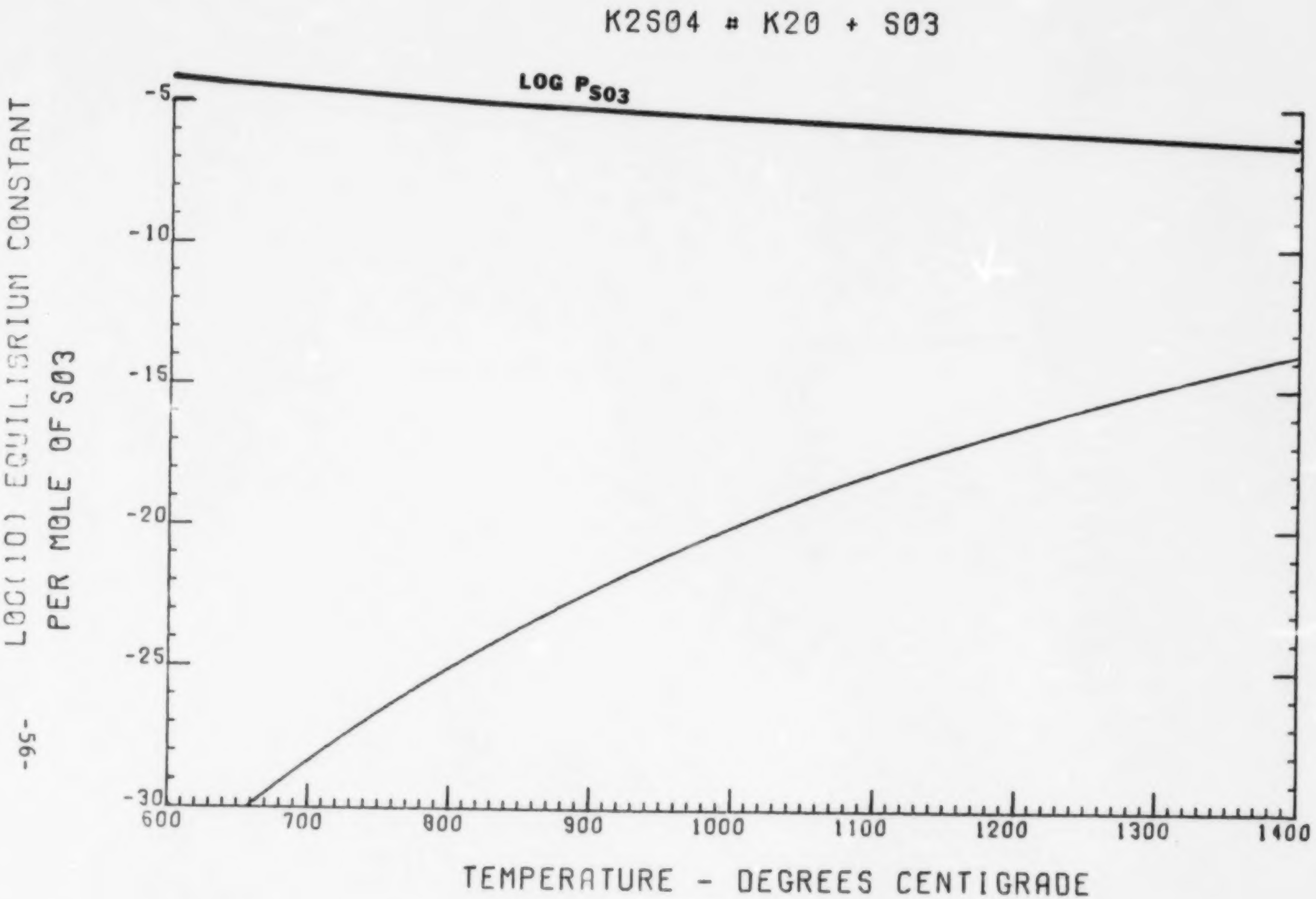

FIGURE A-3

Log K Versus T for the Reaction
$K_2SO_4 \rightleftarrows K_2O + SO_3$

06 AUG 74

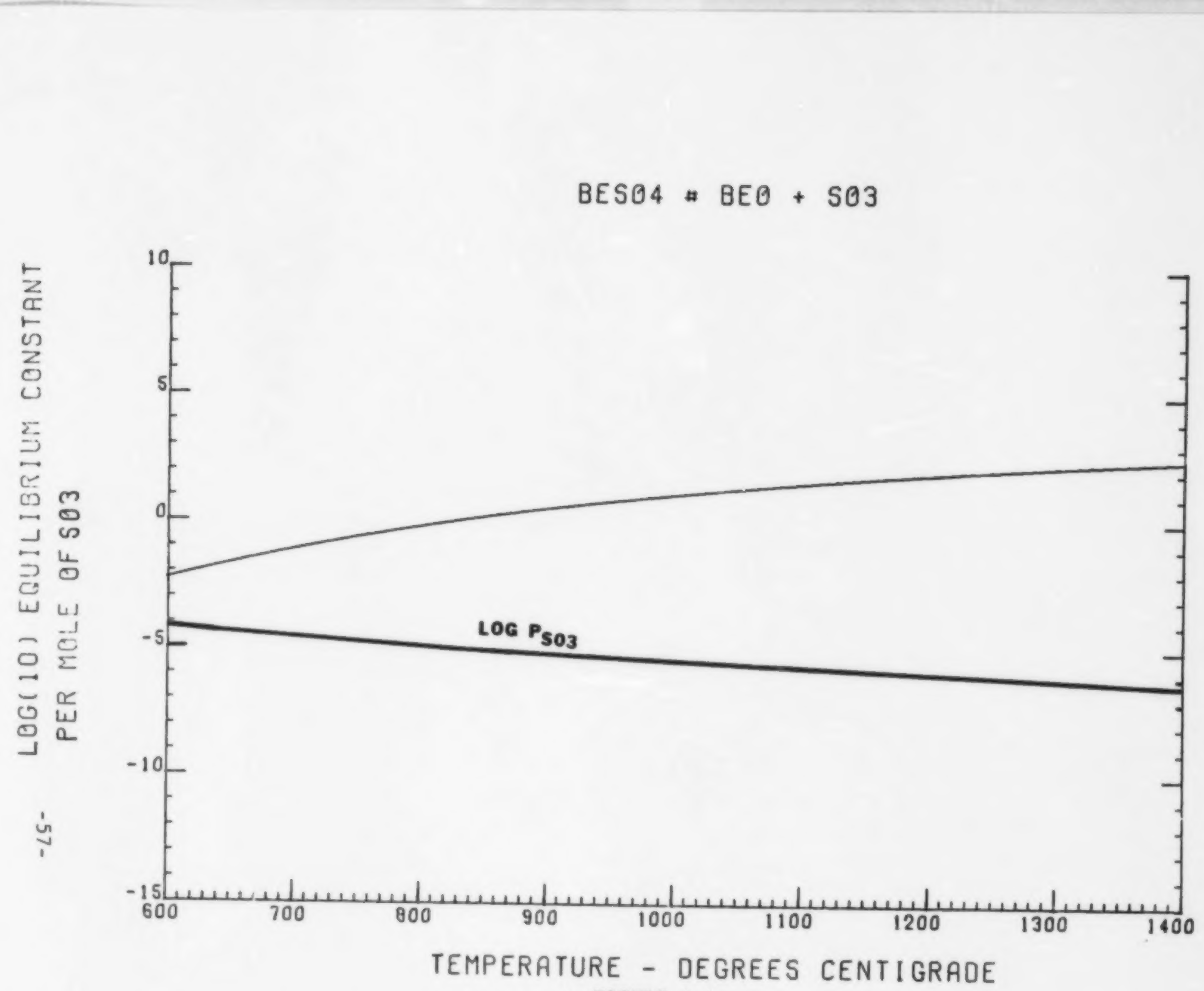

FIGURE A-4

Log K Versus T for the Reaction
$BeSO_4 \rightleftarrows BeO + SO_3$

06 AUG 74

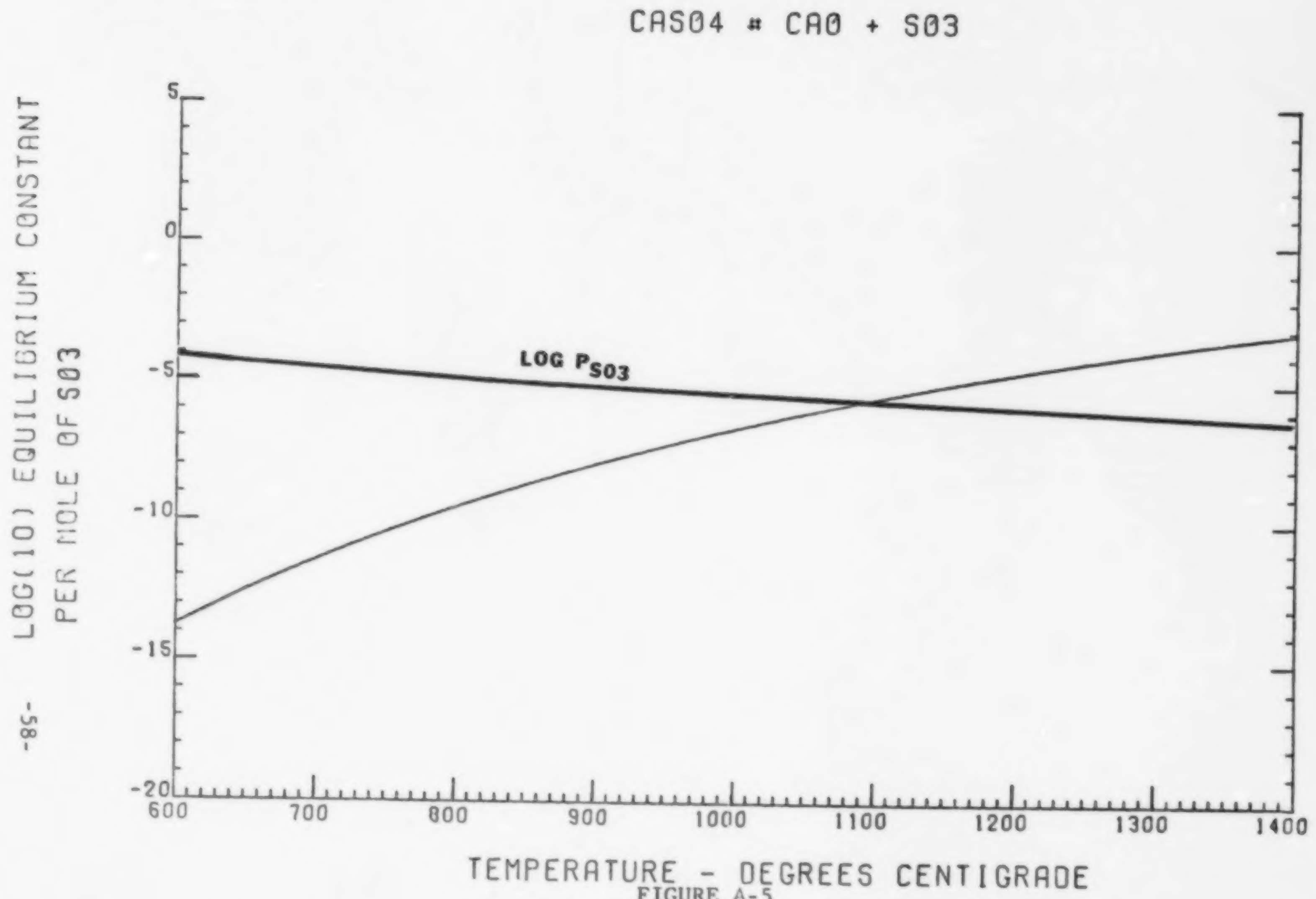

FIGURE A-5

Log K Versus T for the Reaction
$CaSO_4 \rightleftarrows CaO + SO_3$

06 AUG 74

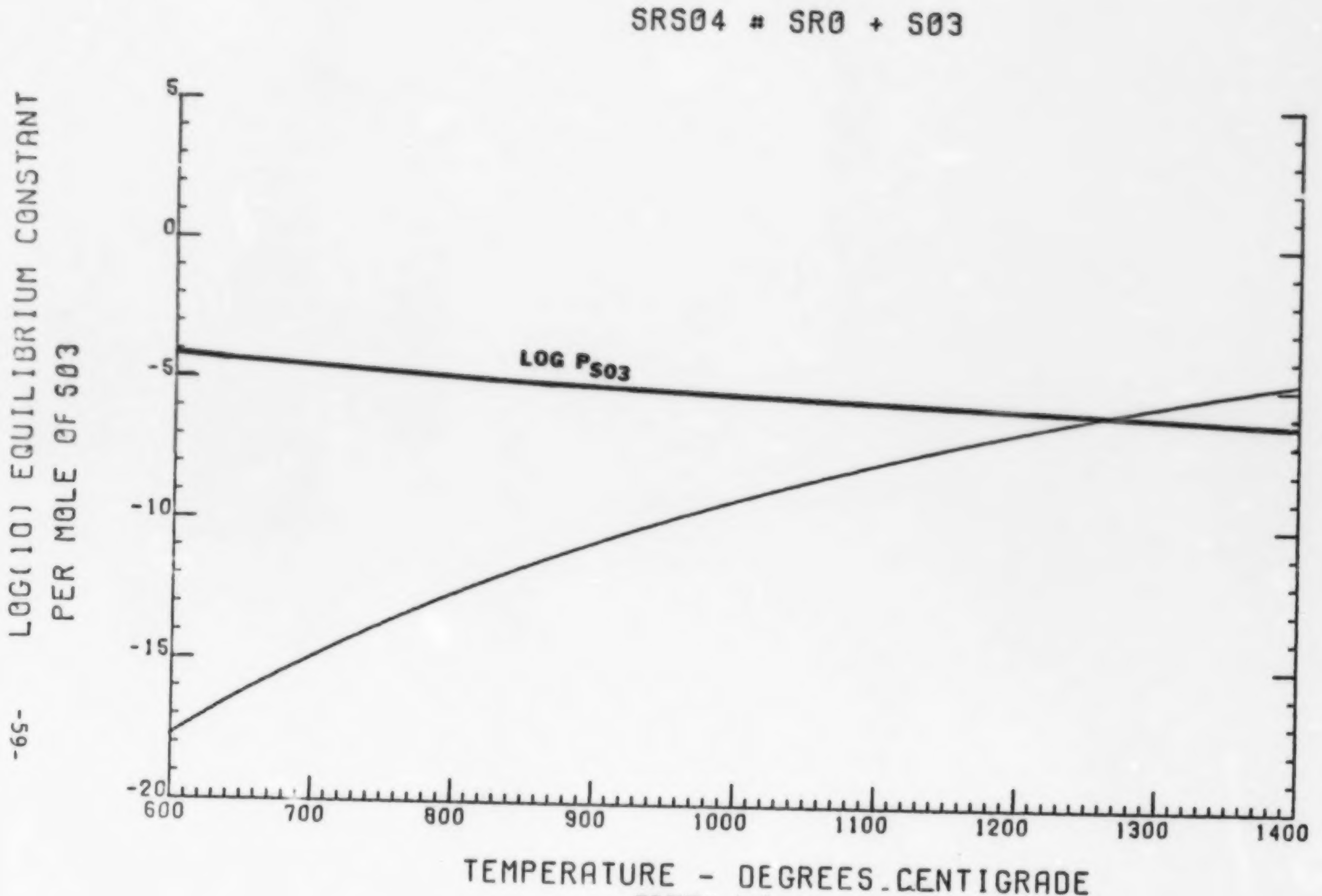

FIGURE A-6

Log K Versus T for the Reaction
$SrSO_4 \rightleftarrows SrO + SO_3$

07 AUG 74

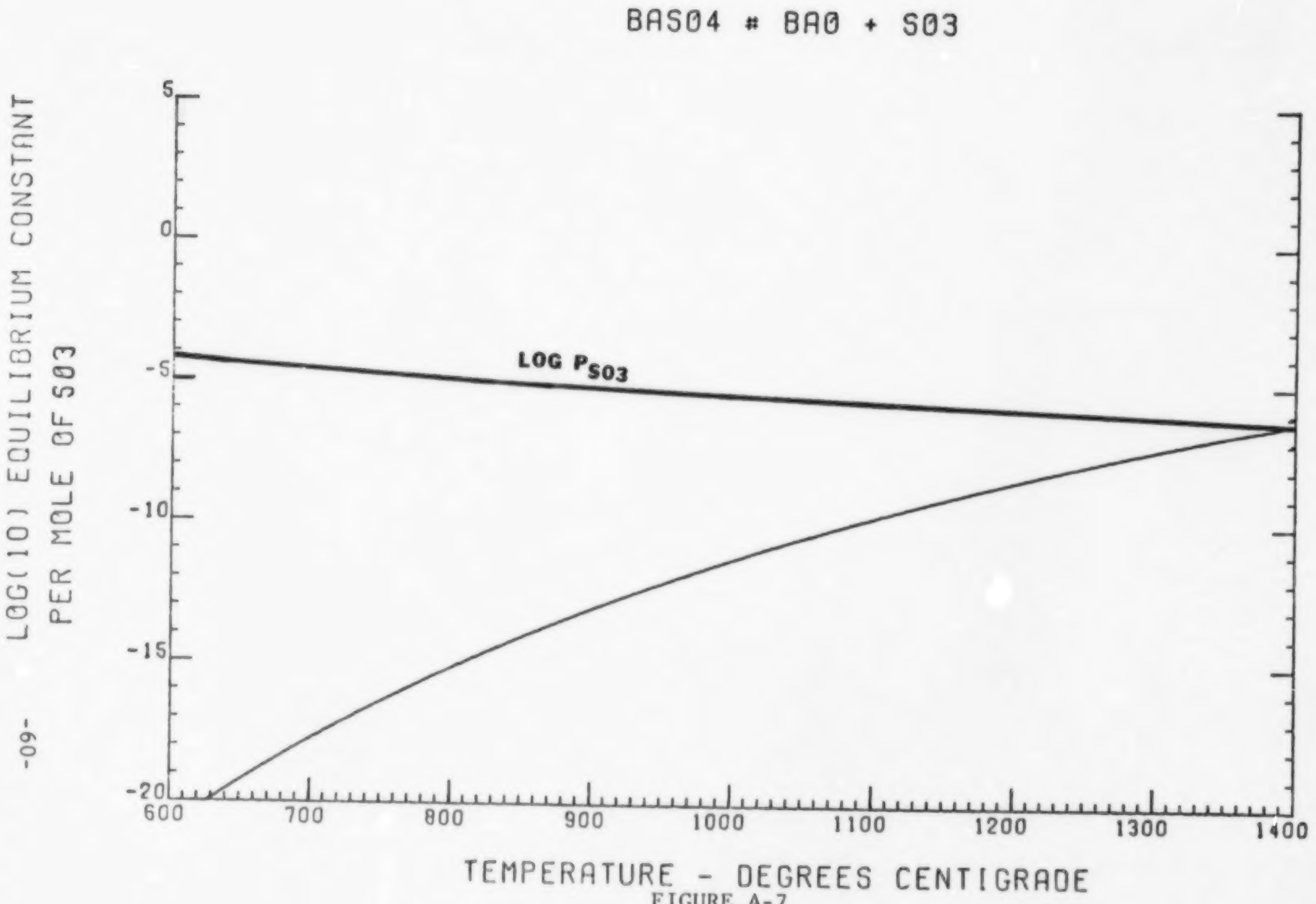

FIGURE A-7

Log K Versus T for the Reaction $BaSO_4 \rightleftarrows BaO + SO_3$

06 AUG 74

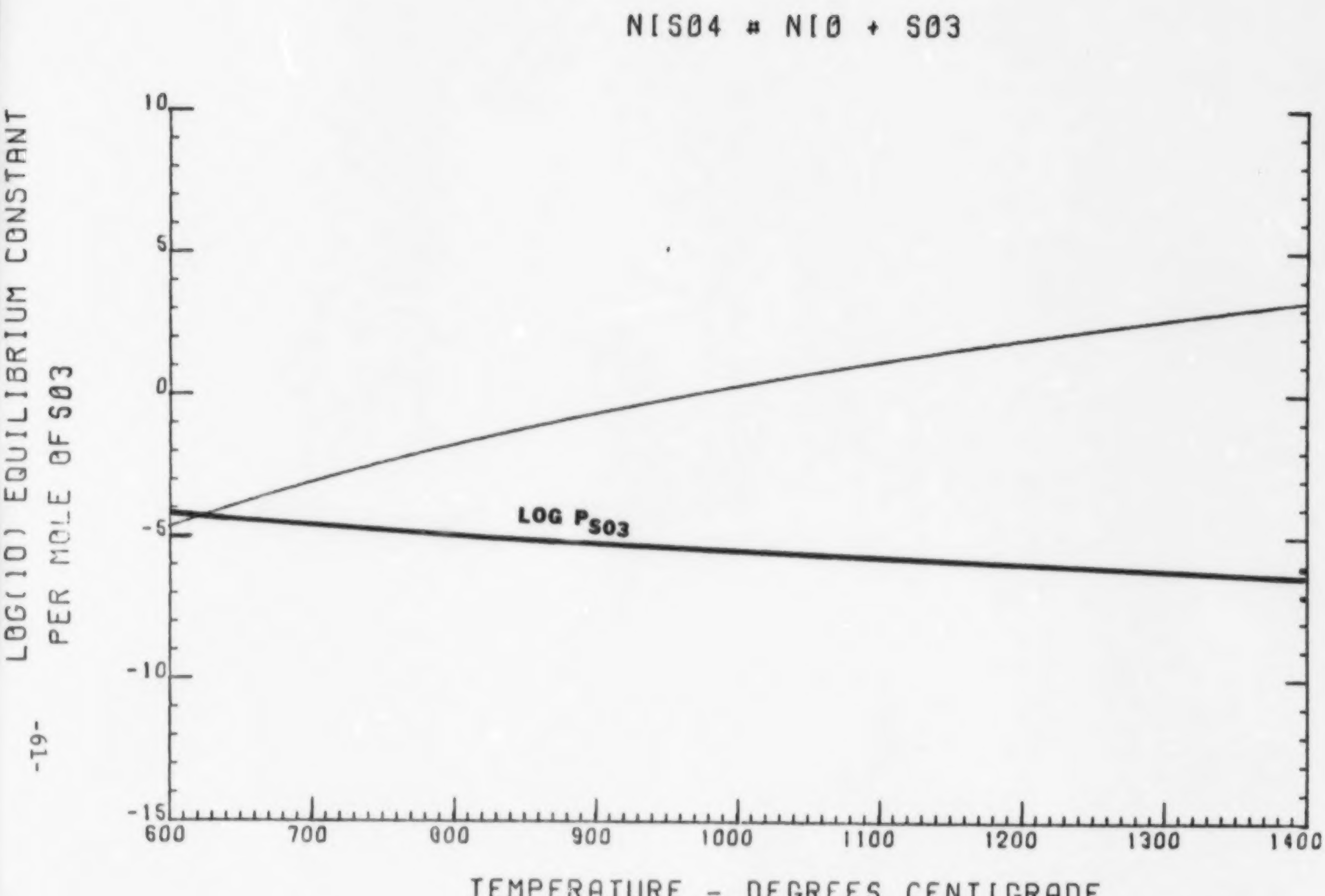

FIGURE A-8

Log K Versus T for the Reaction
$NiSO_4 \rightleftarrows NiO + SO_3$

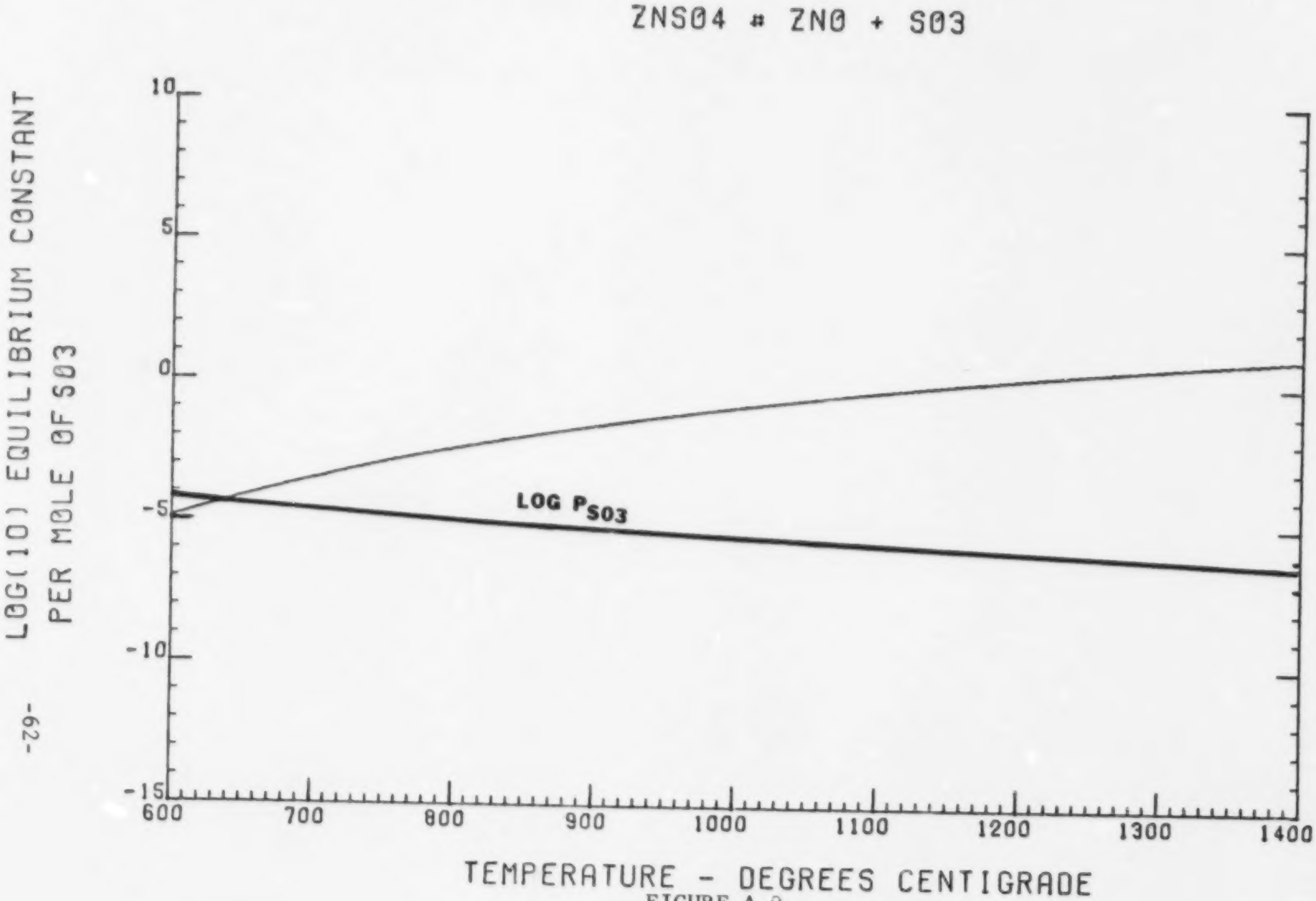

FIGURE A-9

Log K Versus T for the Reaction
$ZnSO_4 \rightleftarrows ZnO + SO_3$

07 AUG 74

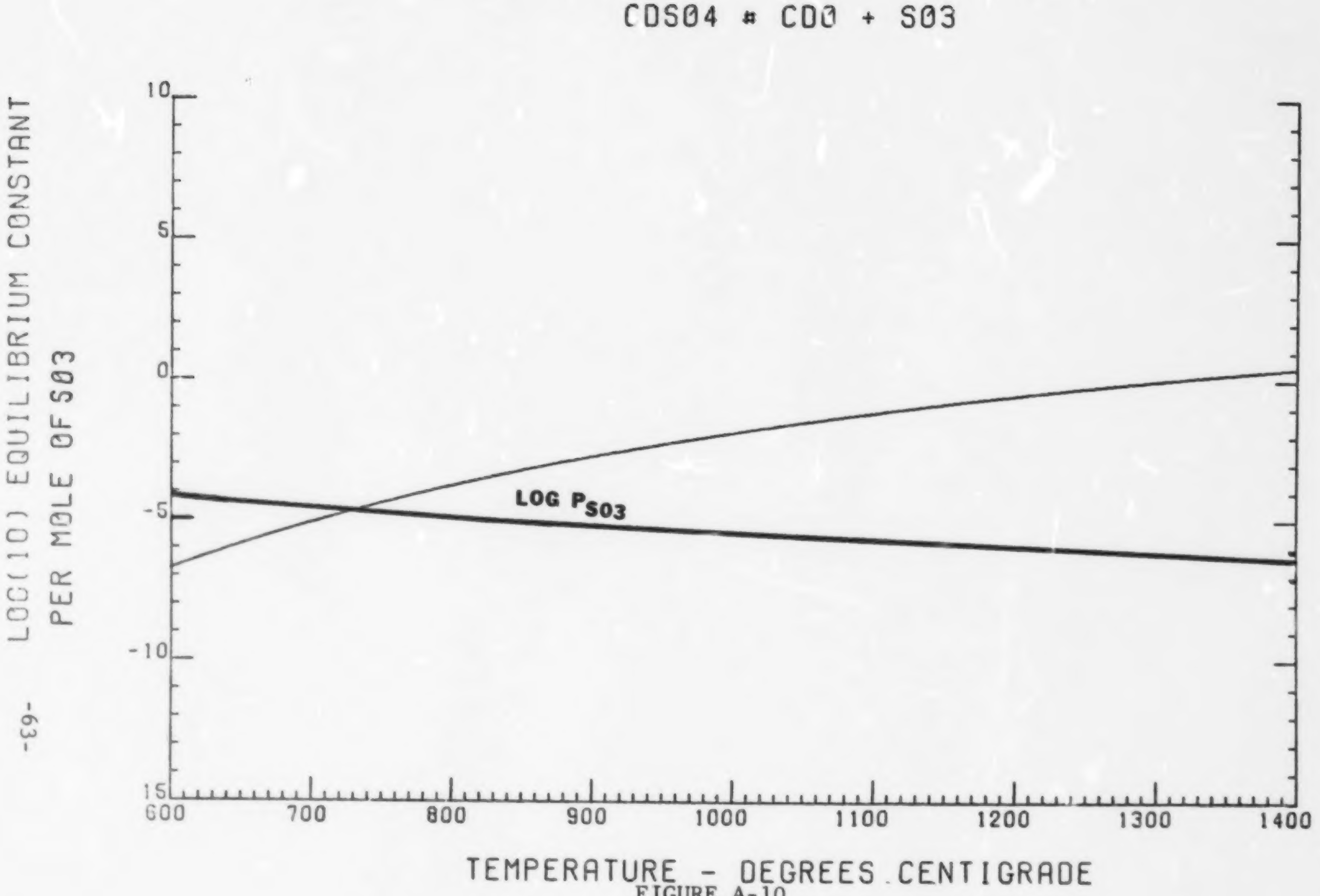

FIGURE A-10

Log K Versus T for the Reaction
$CdSO_4 \rightleftarrows CdO + SO_3$

06 AUG 74

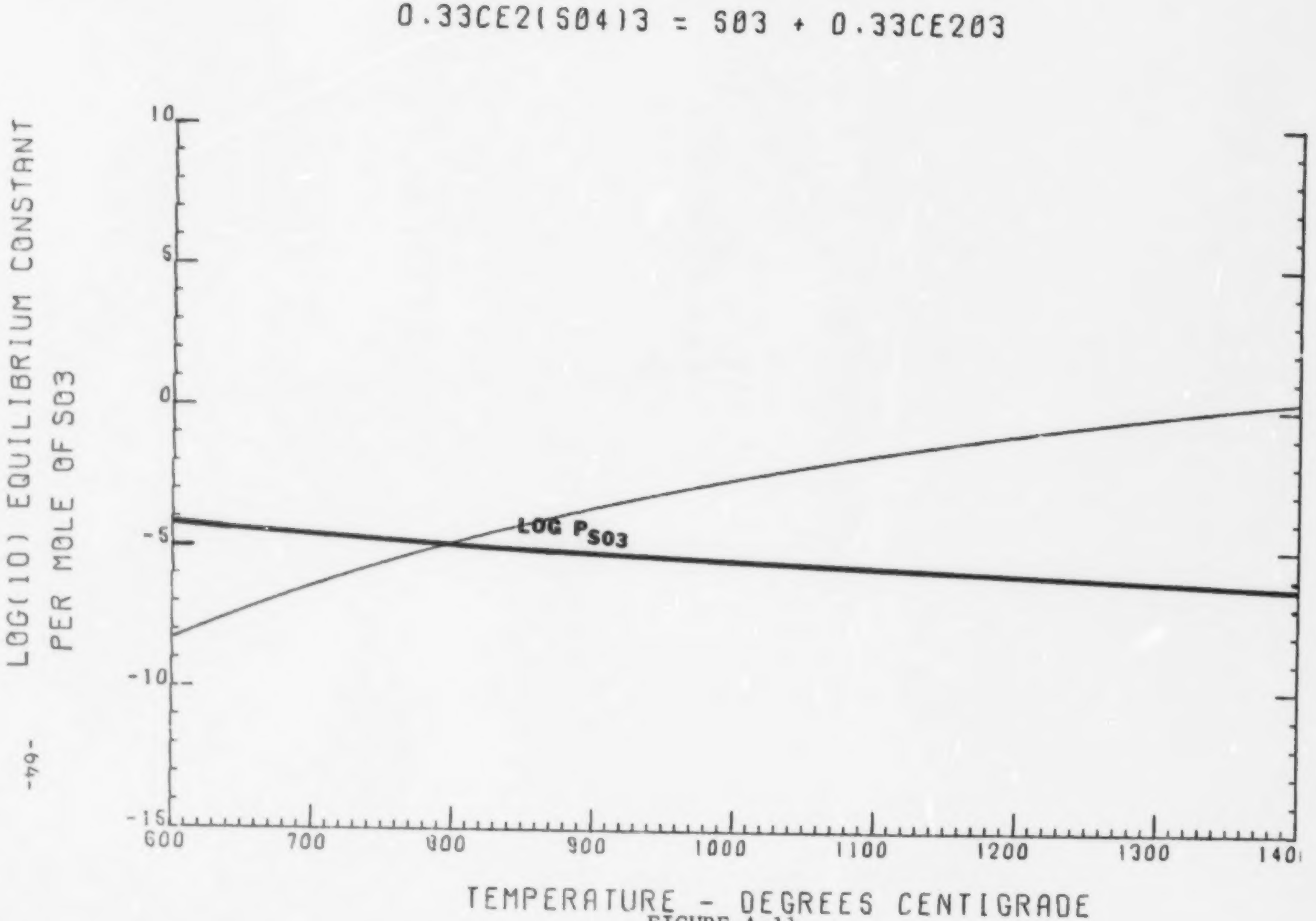

FIGURE A-11

Log K Versus T for the Reaction
1/3 $Ce_2(SO_4)_3 \rightleftarrows 1/3\ Ce_2O_3 + SO_3$

08 AUG 74

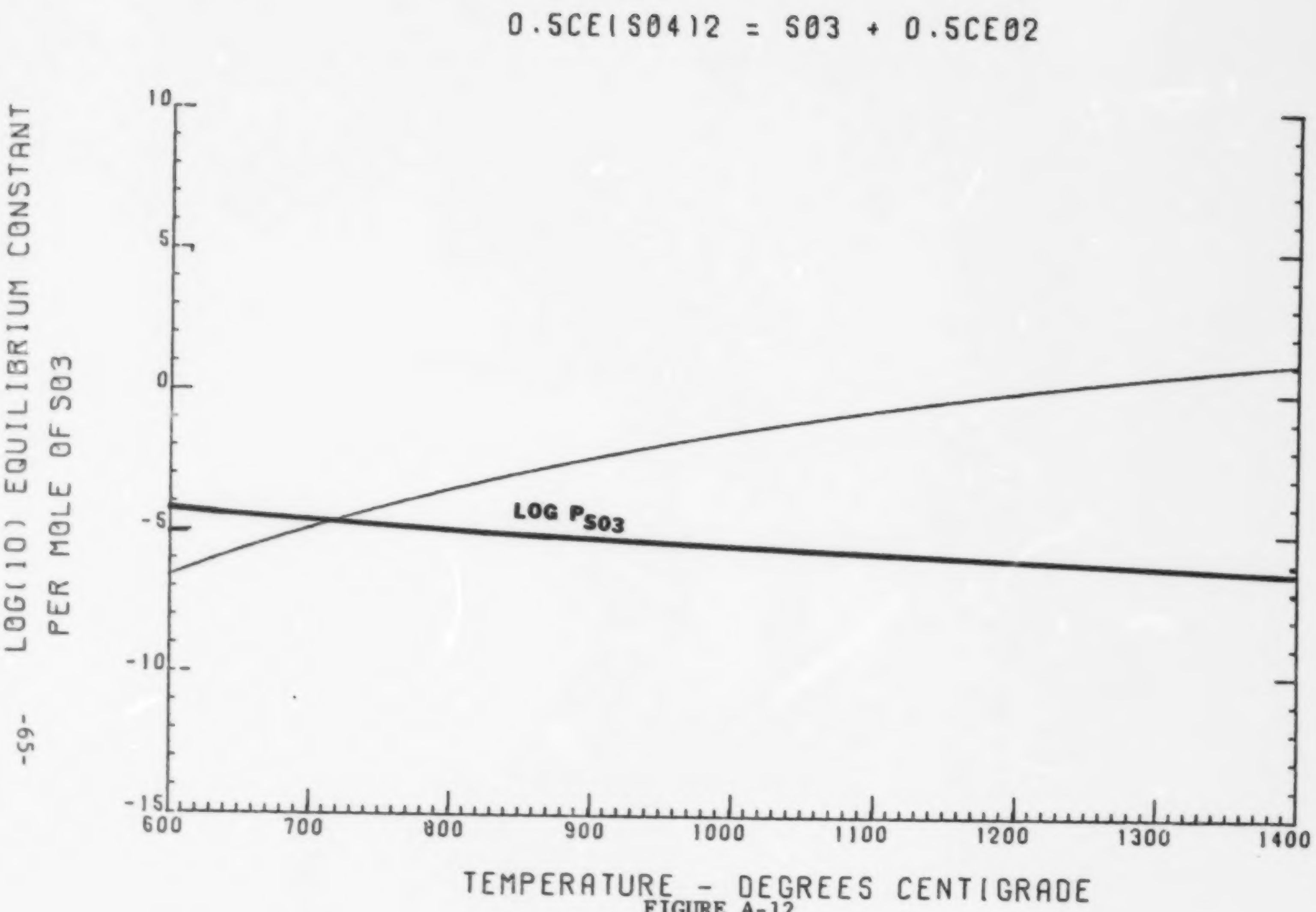

FIGURE A-12

Log K Versus T for the Reaction
$\frac{1}{2}Ce(SO_4)_2 \rightleftarrows \frac{1}{2}CeO_2 + SO_3$

08 AUG 74

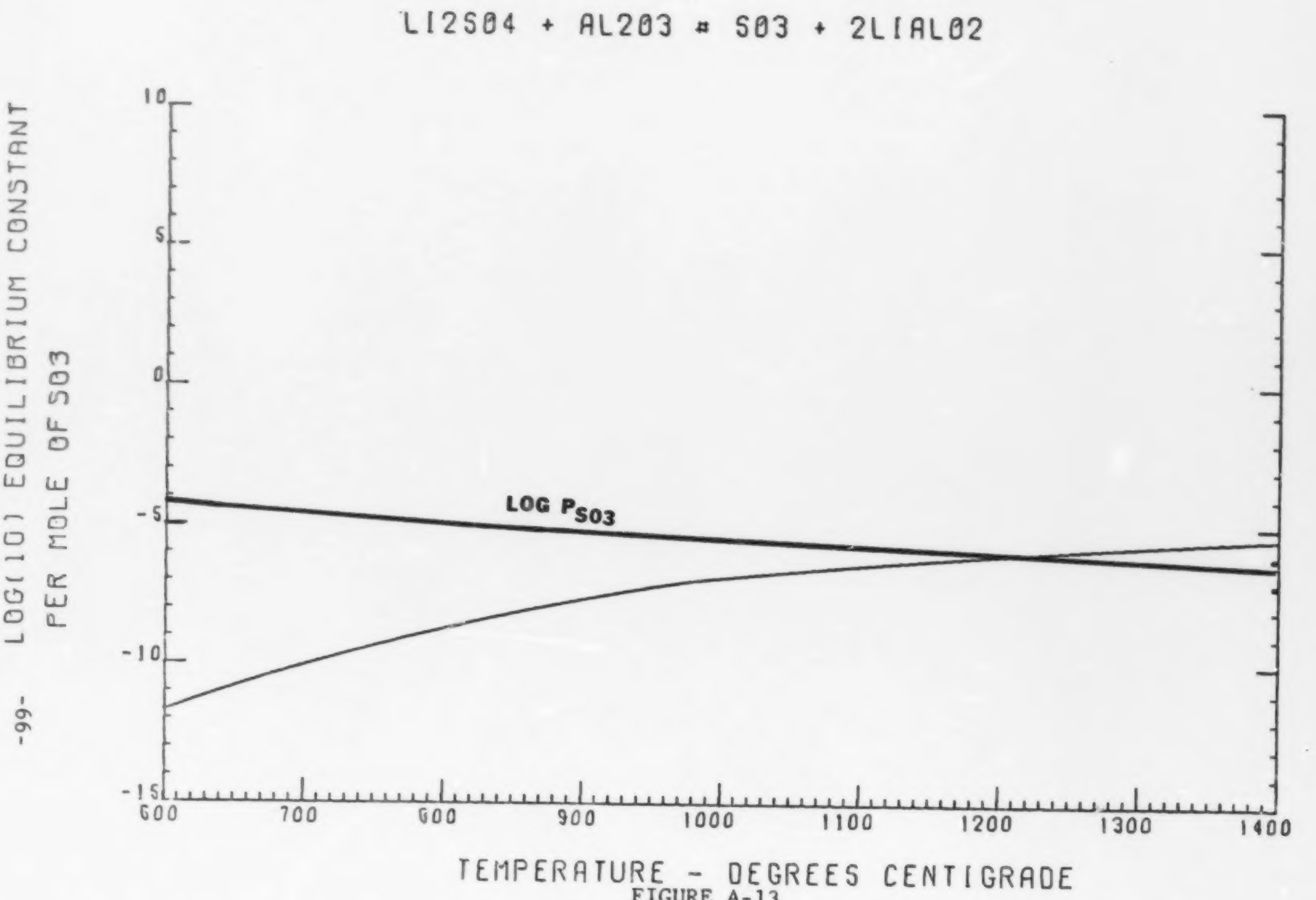

FIGURE A-13

Log K Versus T for the Reaction
$Li_2SO_4 + Al_2O_3 \rightleftarrows 2LiAlO_2 + SO_3$

18 AUG 74

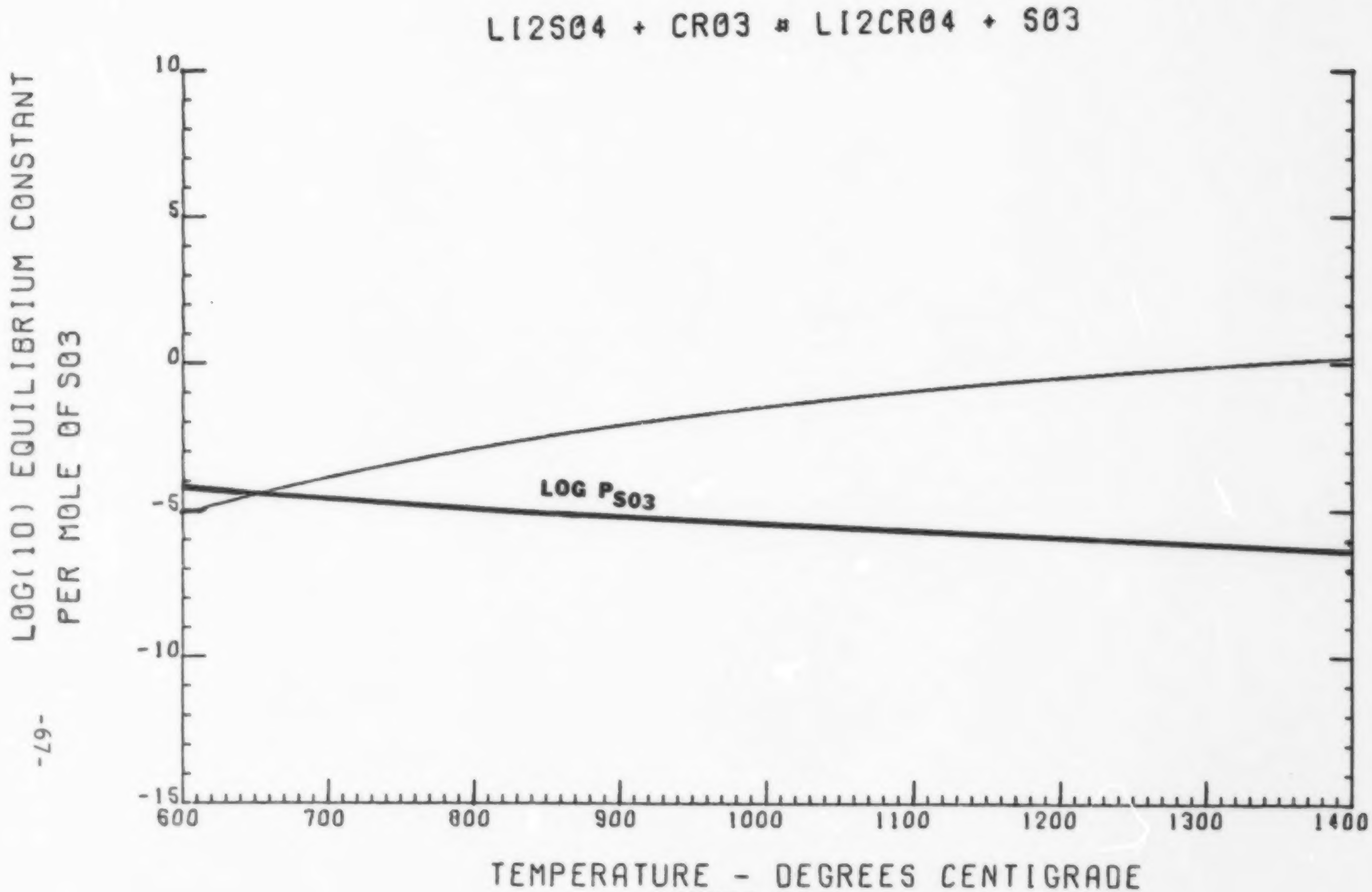

FIGURE A-14

Log K Versus T for the Reaction $Li_2SO_4 + CrO_3 \rightleftarrows Li_2CrO_4 + SO_3$

07 AUG 74

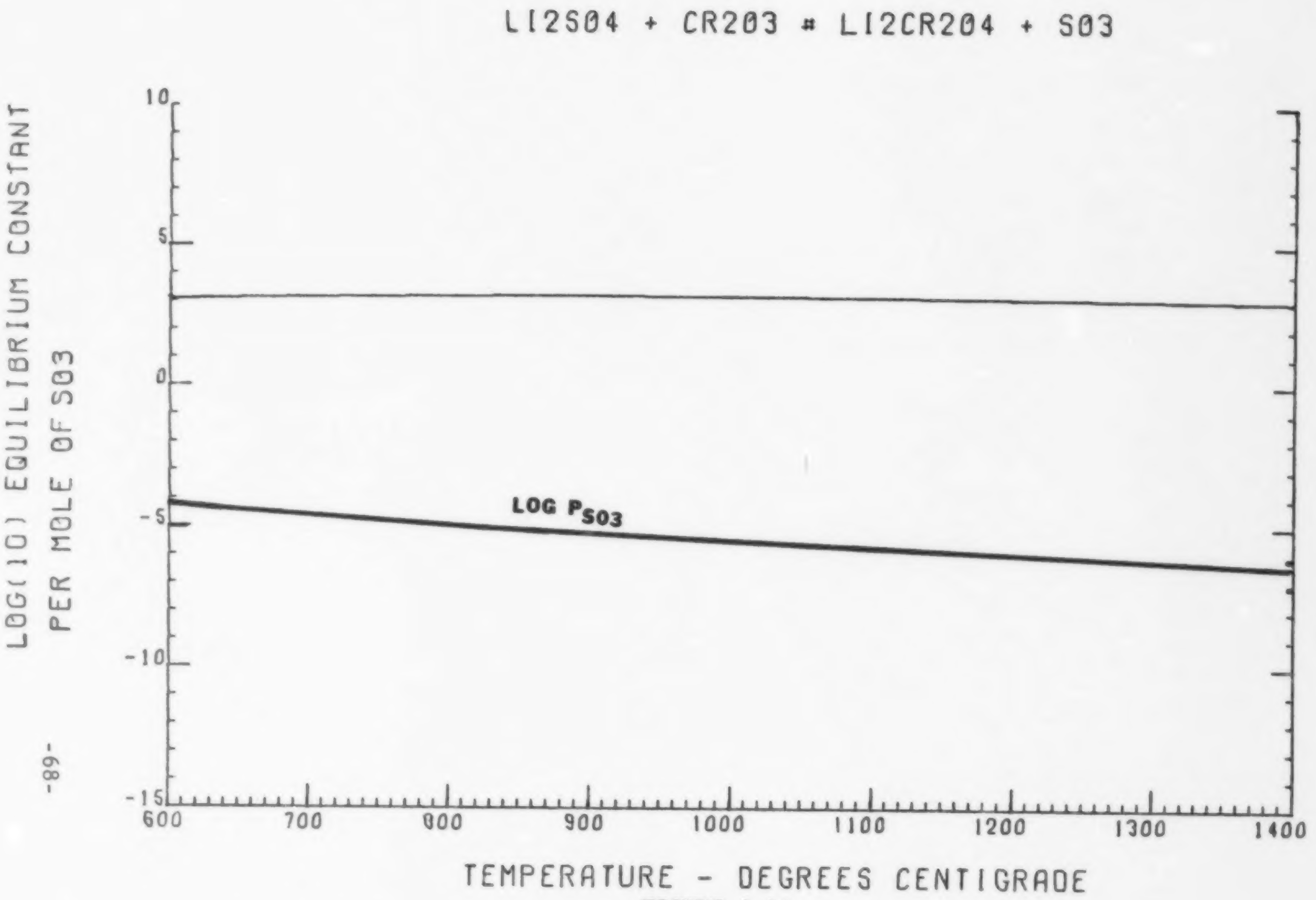

FIGURE A-15

Log K Versus T for the Reaction
$Li_2SO_4 + Cr_2O_3 \rightleftarrows Li_2Cr_2O_4 + SO_3$

07 AUG 74

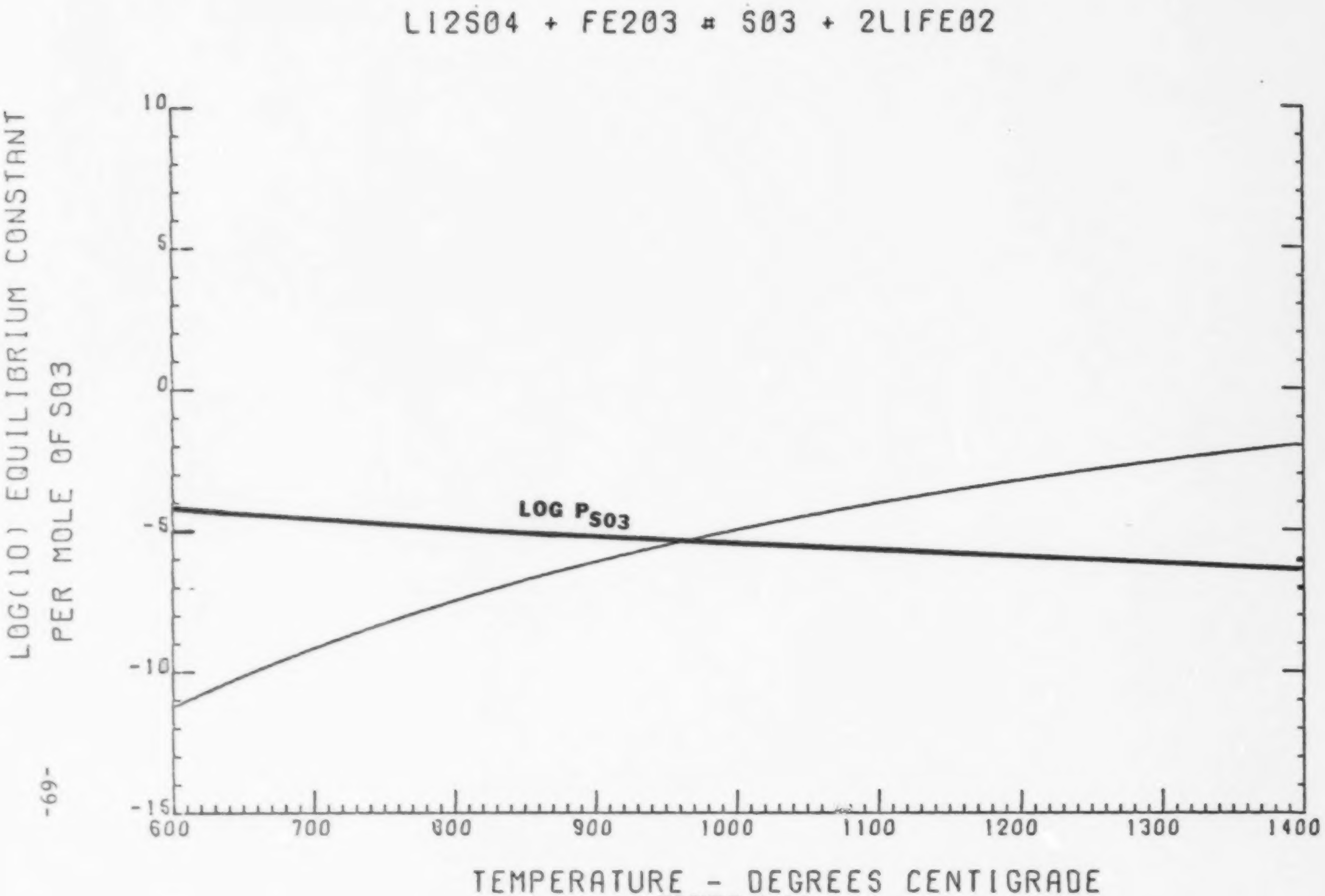

FIGURE A-16

Log K Versus T for the Reaction
$Li_2SO_4 + Fe_2O_3 \rightleftarrows 2LiFeO_2 + SO_3$

08 AUG 74

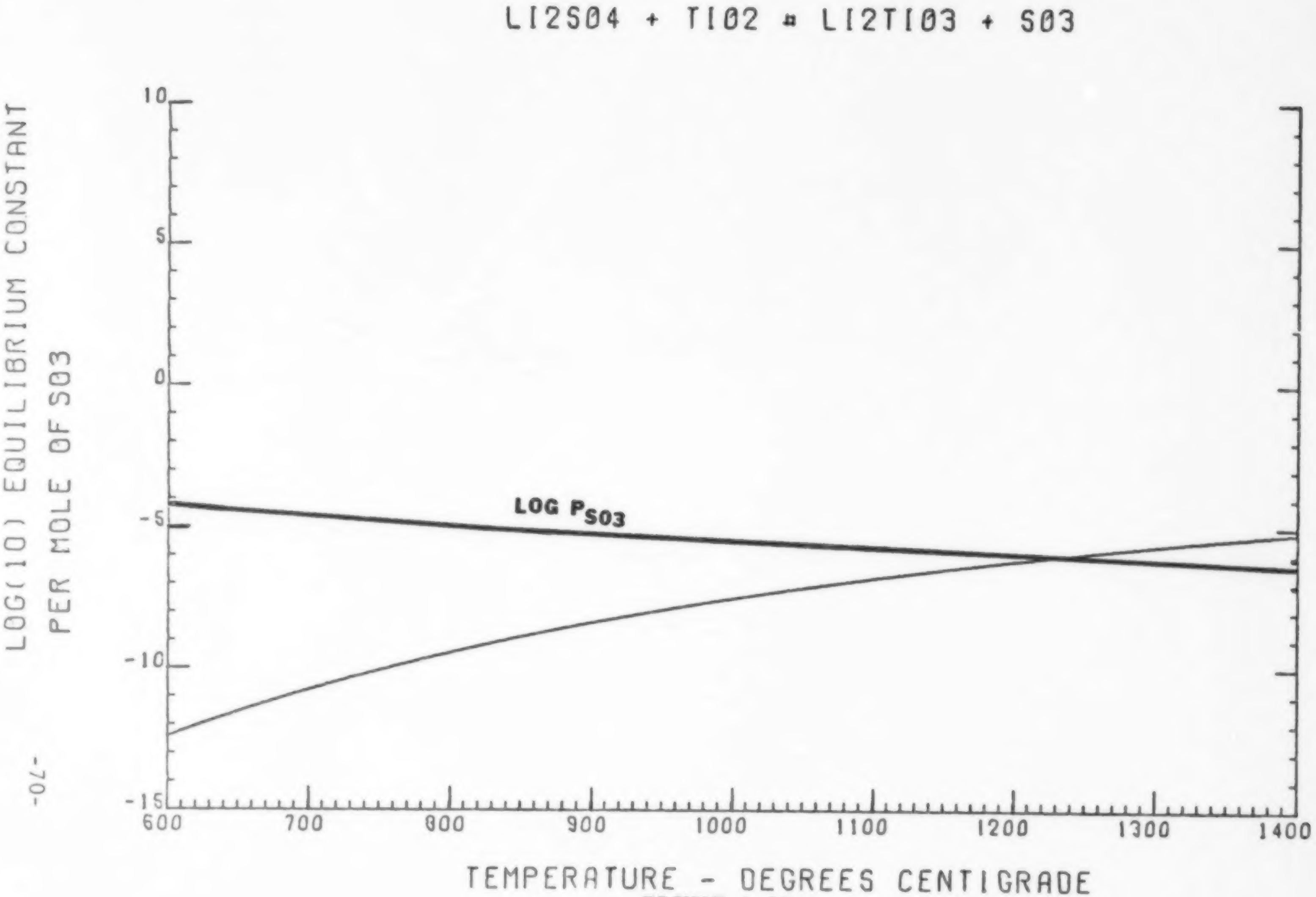

FIGURE A-17

Log K Versus T for the Reaction
$Li_2SO_4 + TiO_2 \rightleftarrows Li_2TiO_3 + SO_3$

08 AUG 74

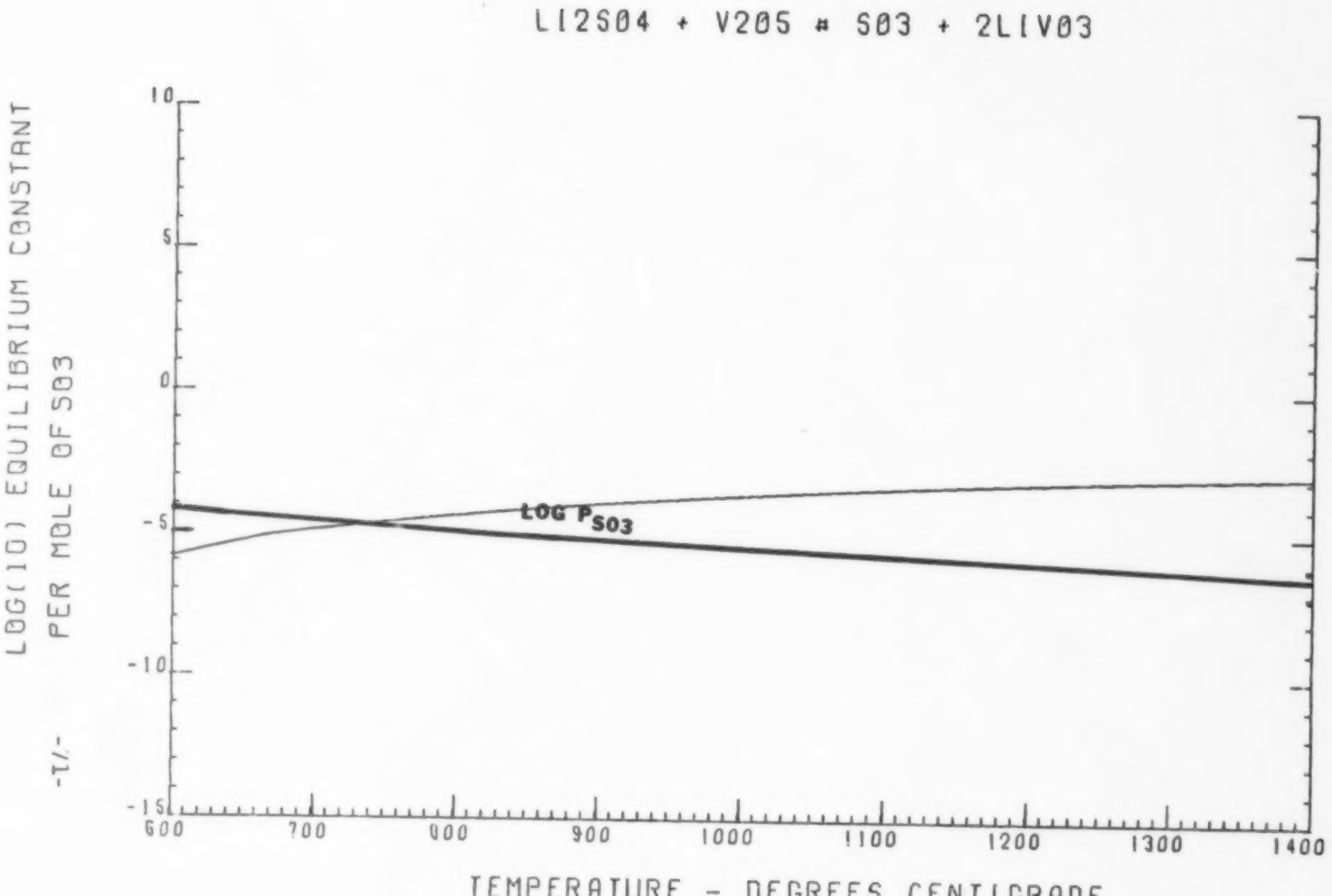

FIGURE A-18

Log K Versus T for the Reaction
$Li_2SO_4 + V_2O_5 \rightleftarrows 2LiVO_3 + SO_3$

08 AUG 74

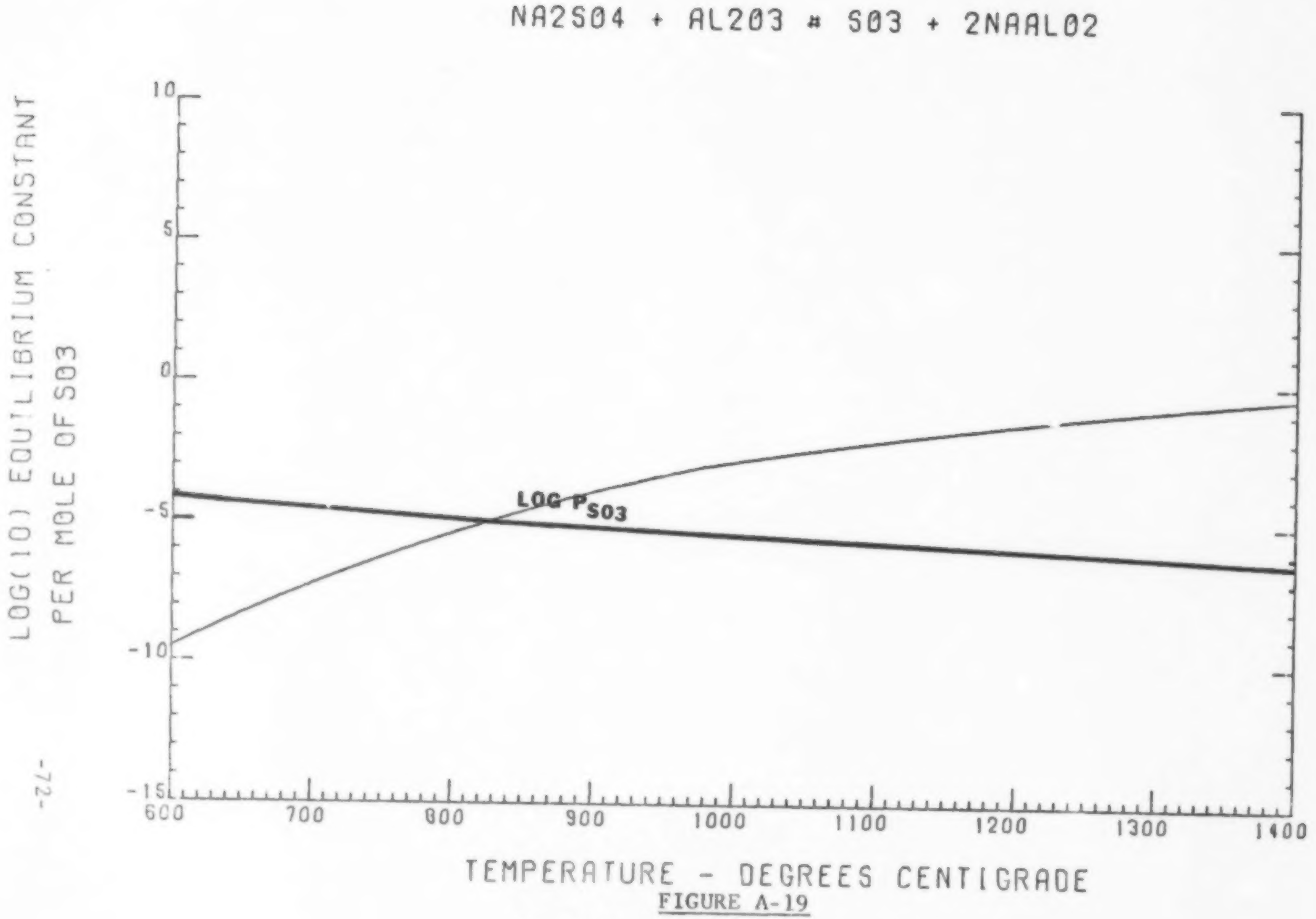

FIGURE A-19

Log K Versus T for the Reaction
$Na_2SO_4 + Al_2O_3 \rightleftarrows 2NaAlO_2 + SO_3$

AUG 74

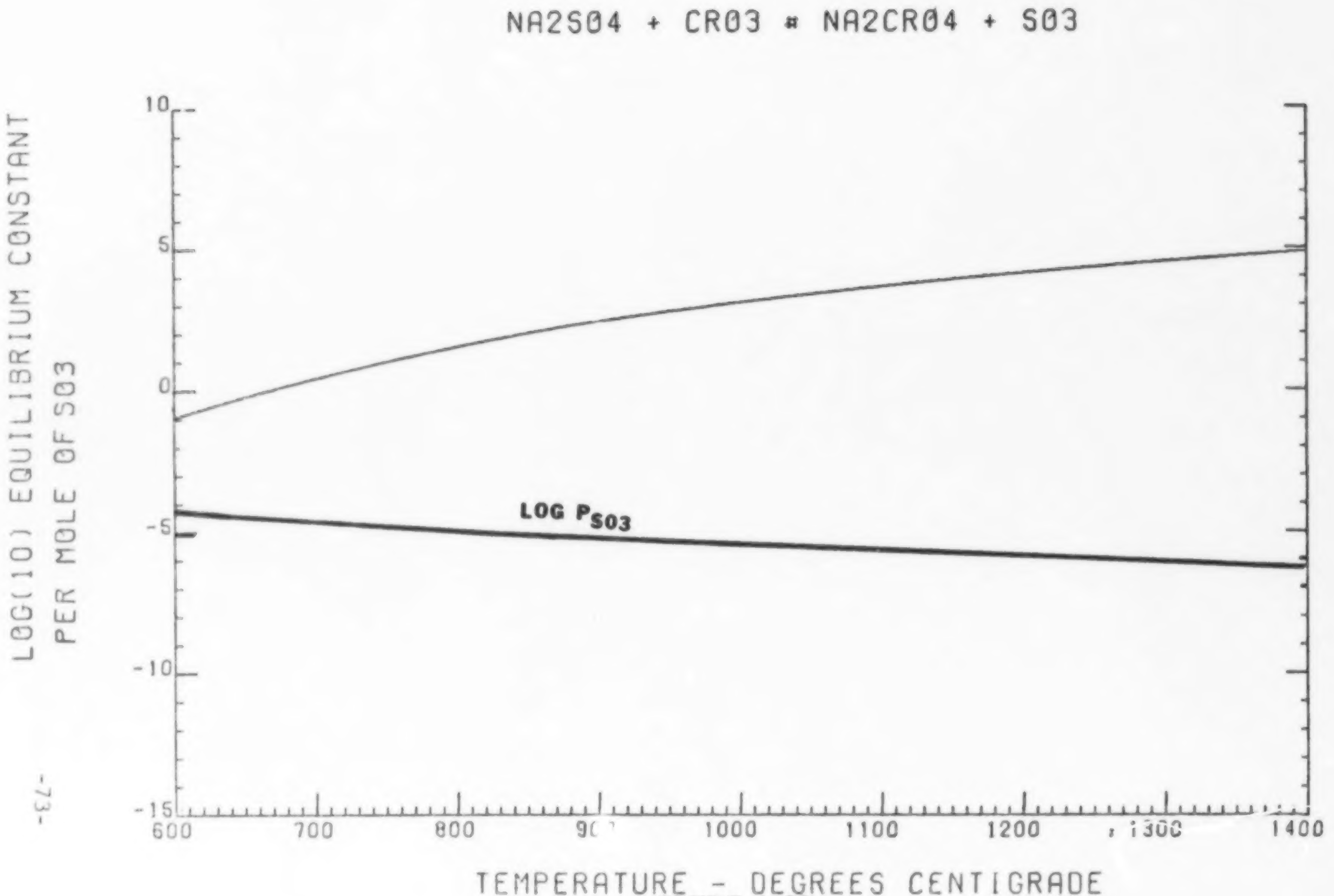

FIGURE A-20

Log K Versus T for the Reaction
$Na_2SO_4 + CrO_3 \rightleftarrows Na_2CrO_4 + SO_3$

08 AUG 74

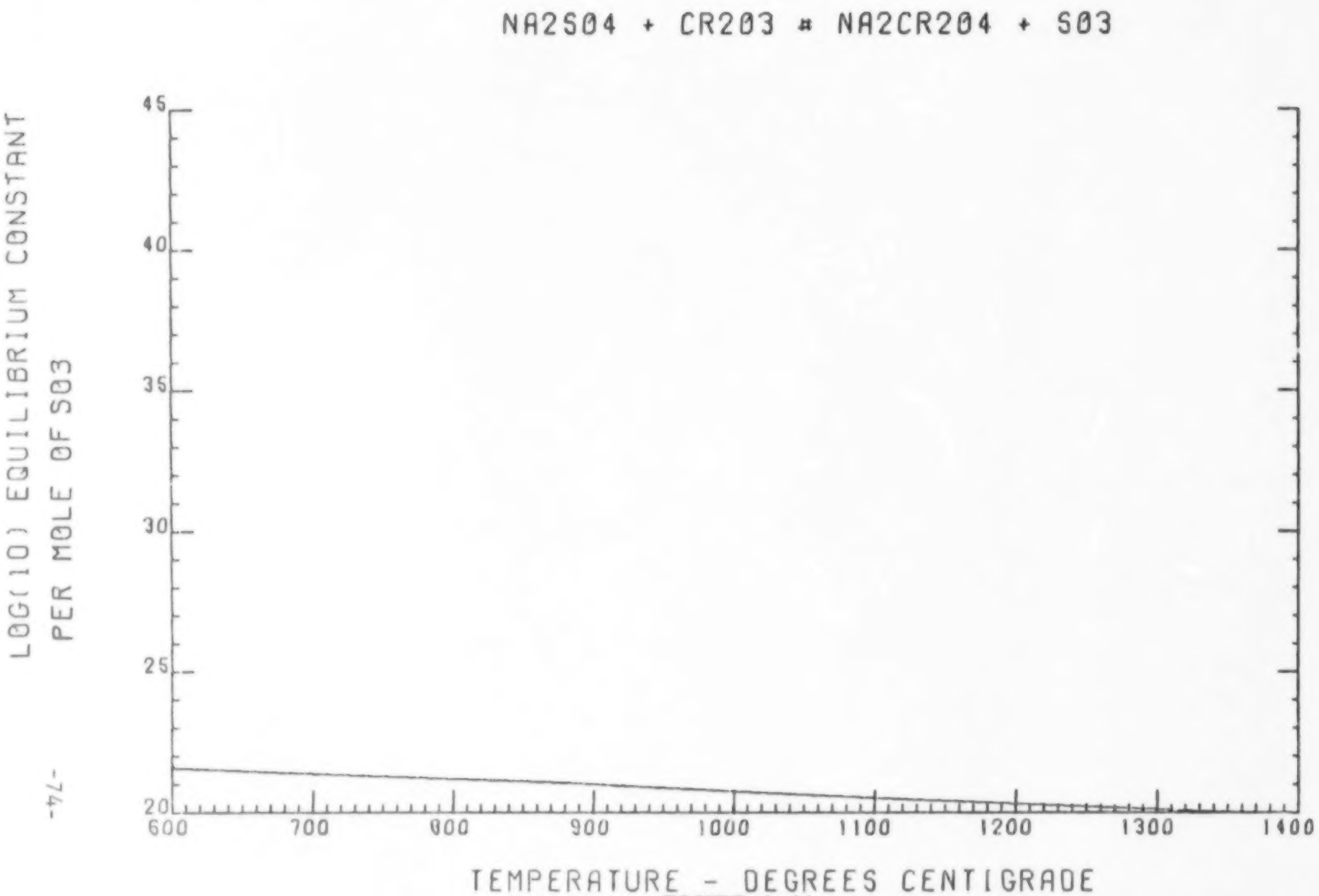

FIGURE A-21

Log K Versus T for the Reaction
$Na_2SO_4 + Cr_2O_3 \rightleftarrows Na_2Cr_2O_4 + SO_3$

08 AUG 74

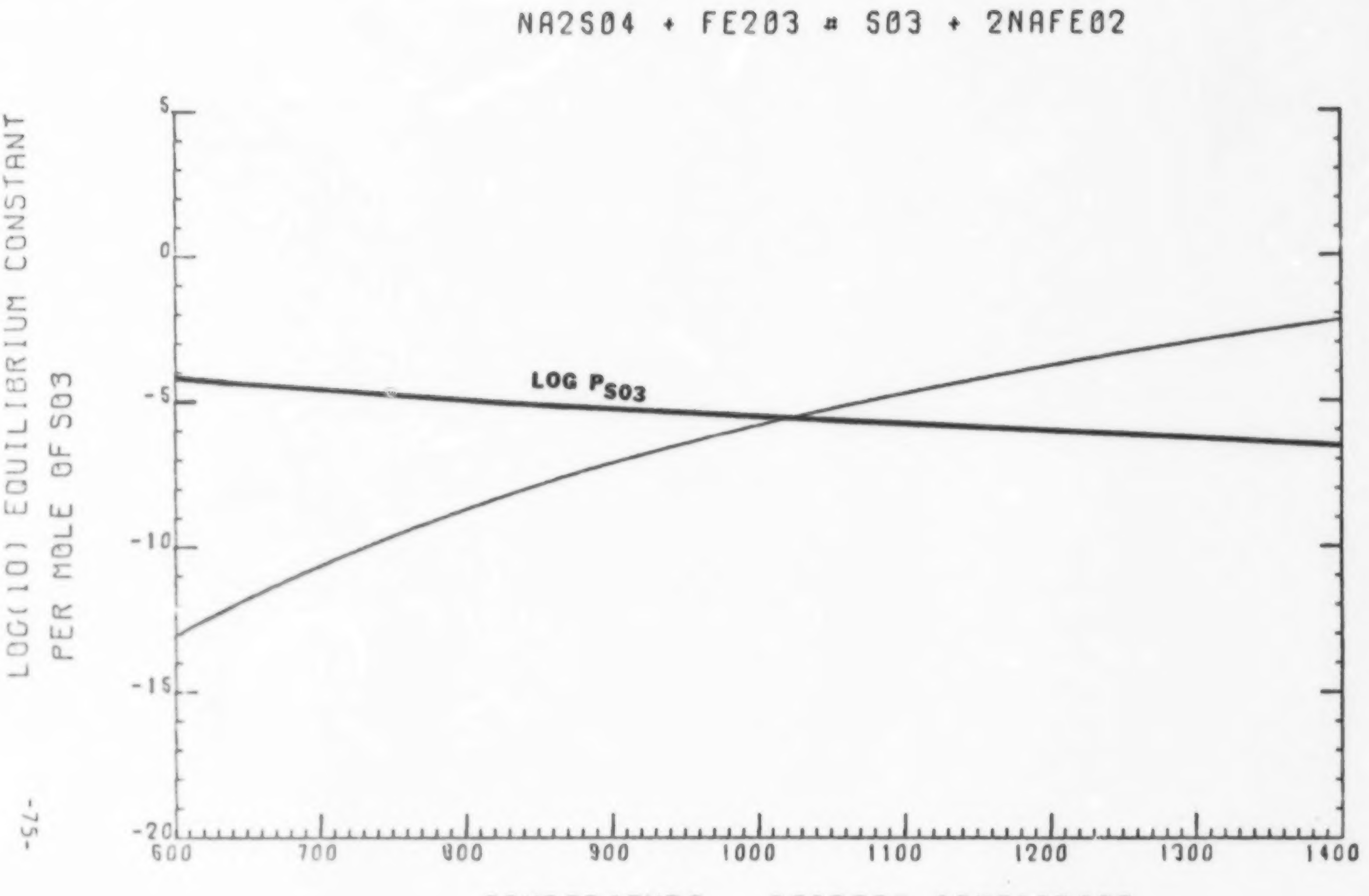

FIGURE A-22

Log K Versus T for the Reaction

$Na_2SO_4 + Fe_2O_3 \rightleftarrows 2NaFeO_2 + SO_3$

08 AUG 74

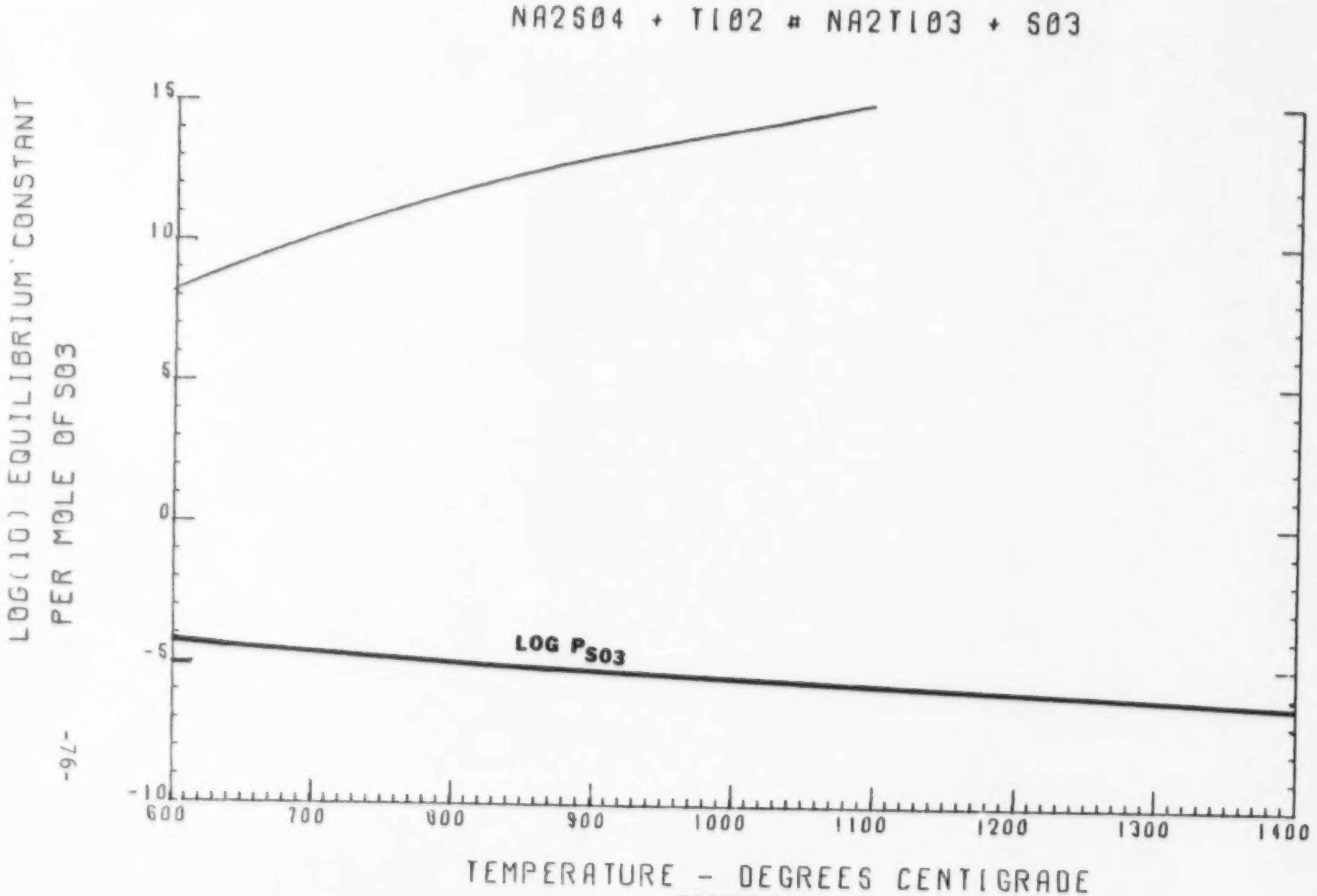

FIGURE A-23

Log K Versus T for the Reaction
$Na_2SO_4 + TiO_2 \rightleftarrows Na_2TiO_3 + SO_3$

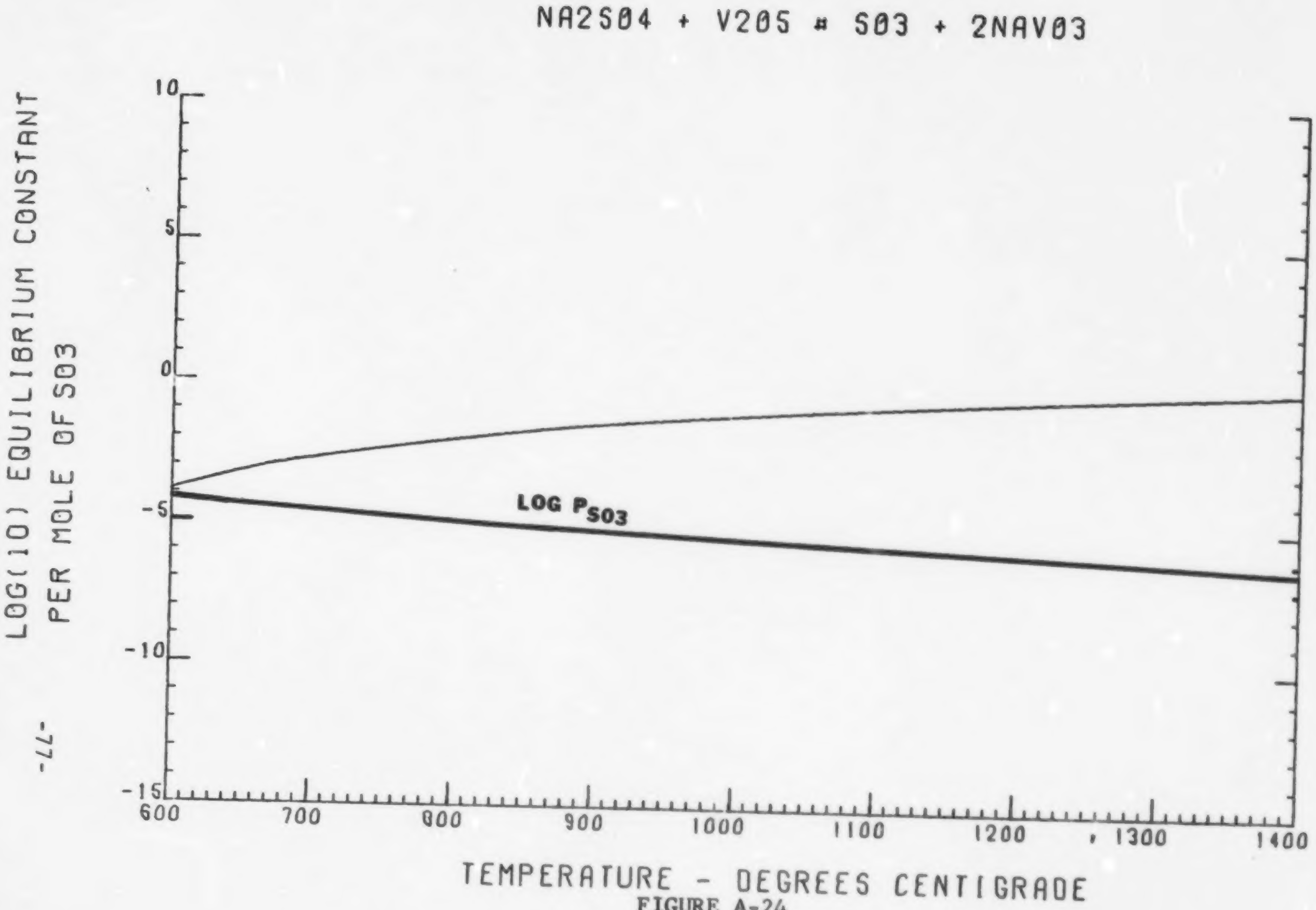

FIGURE A-24

Log K Versus T for the Reaction
$Na_2SO_4 + V_2O_5 \rightleftarrows 2NaVO_3 + SO_3$

08 AUG 74

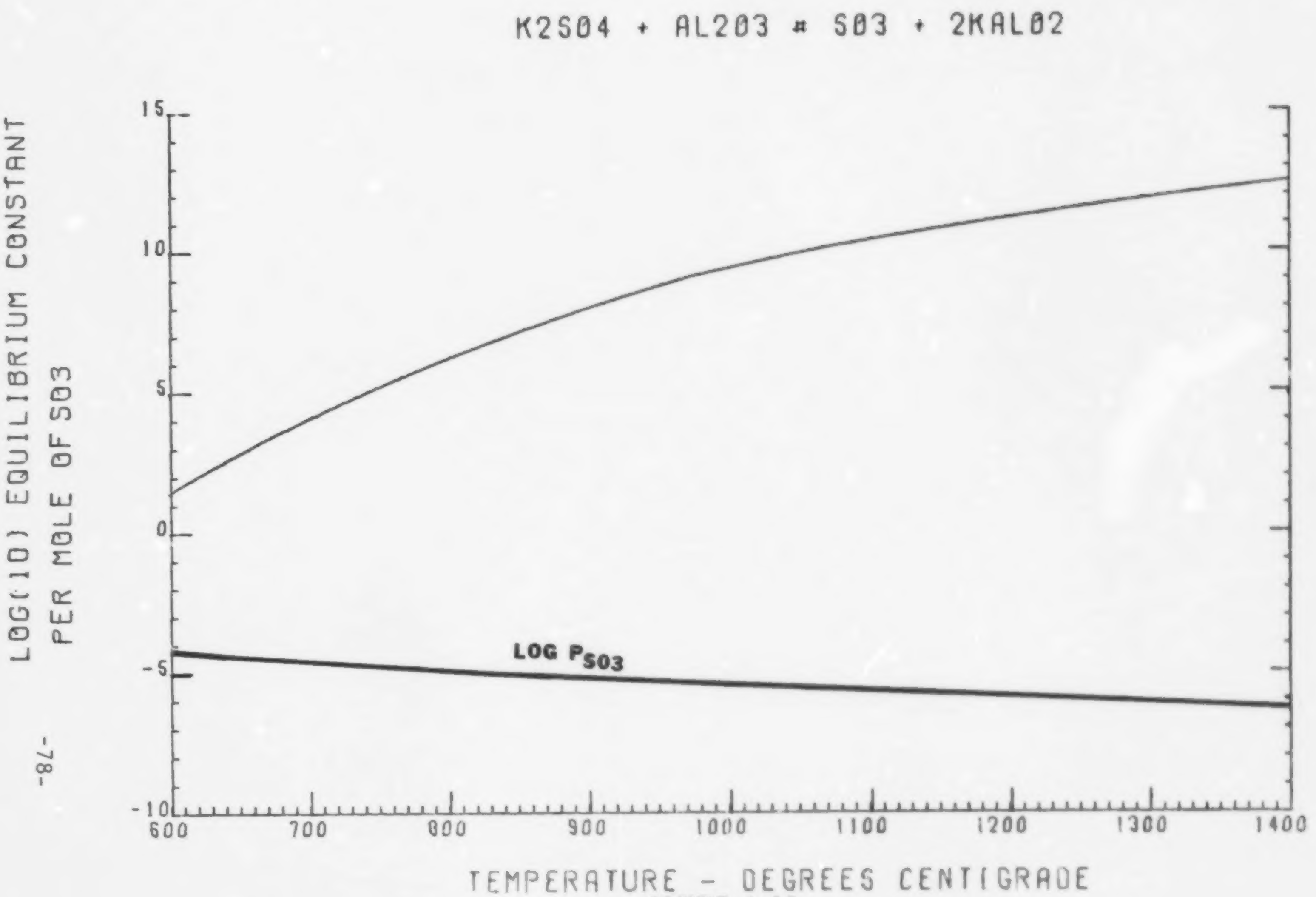

FIGURE A-25

Log K Versus T for the Reaction
$K_2SO_4 + Al_2O_3 \rightleftarrows 2KAlO_2 + SO_3$

AUG 74

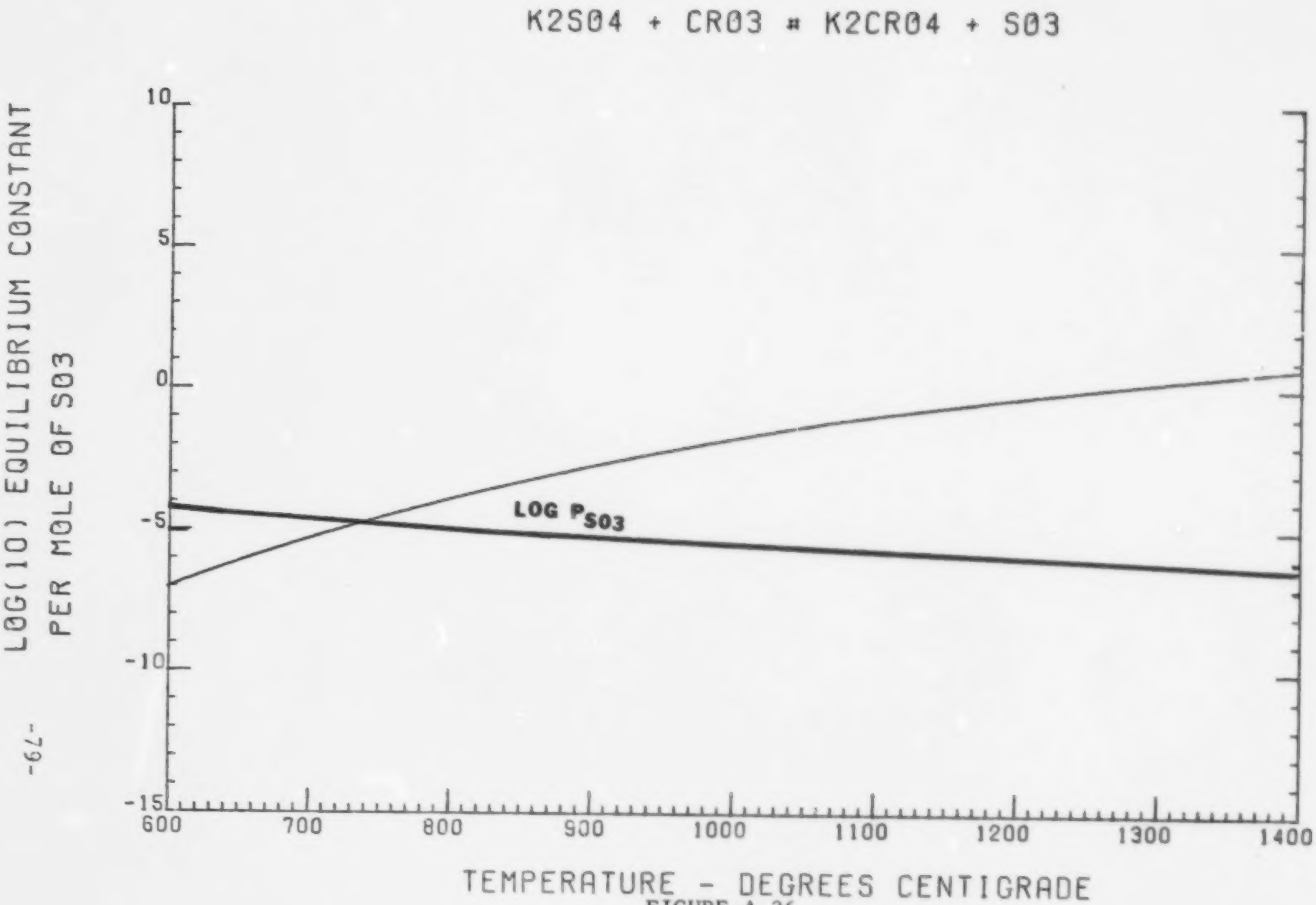

FIGURE A-26

Log K Versus T for the Reaction
$K_2SO_4 + CrO_3 \rightleftarrows K_2CrO_4 + SO_3$

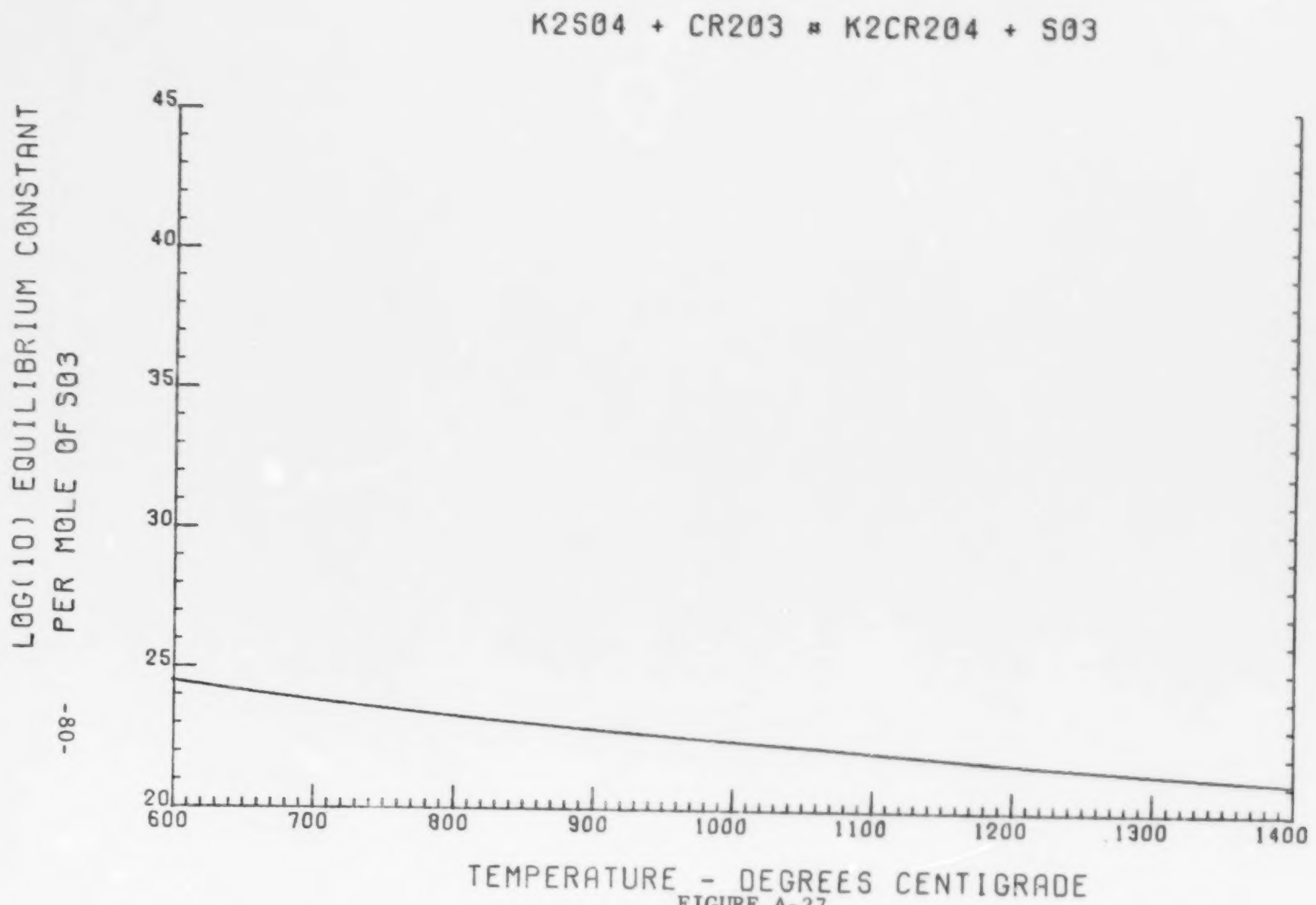

FIGURE A-27

Log K Versus T for the Reaction
$K_2SO_4 + Cr_2O_3 \rightleftarrows K_2Cr_2O_4 + SO_3$

17 AUG 74

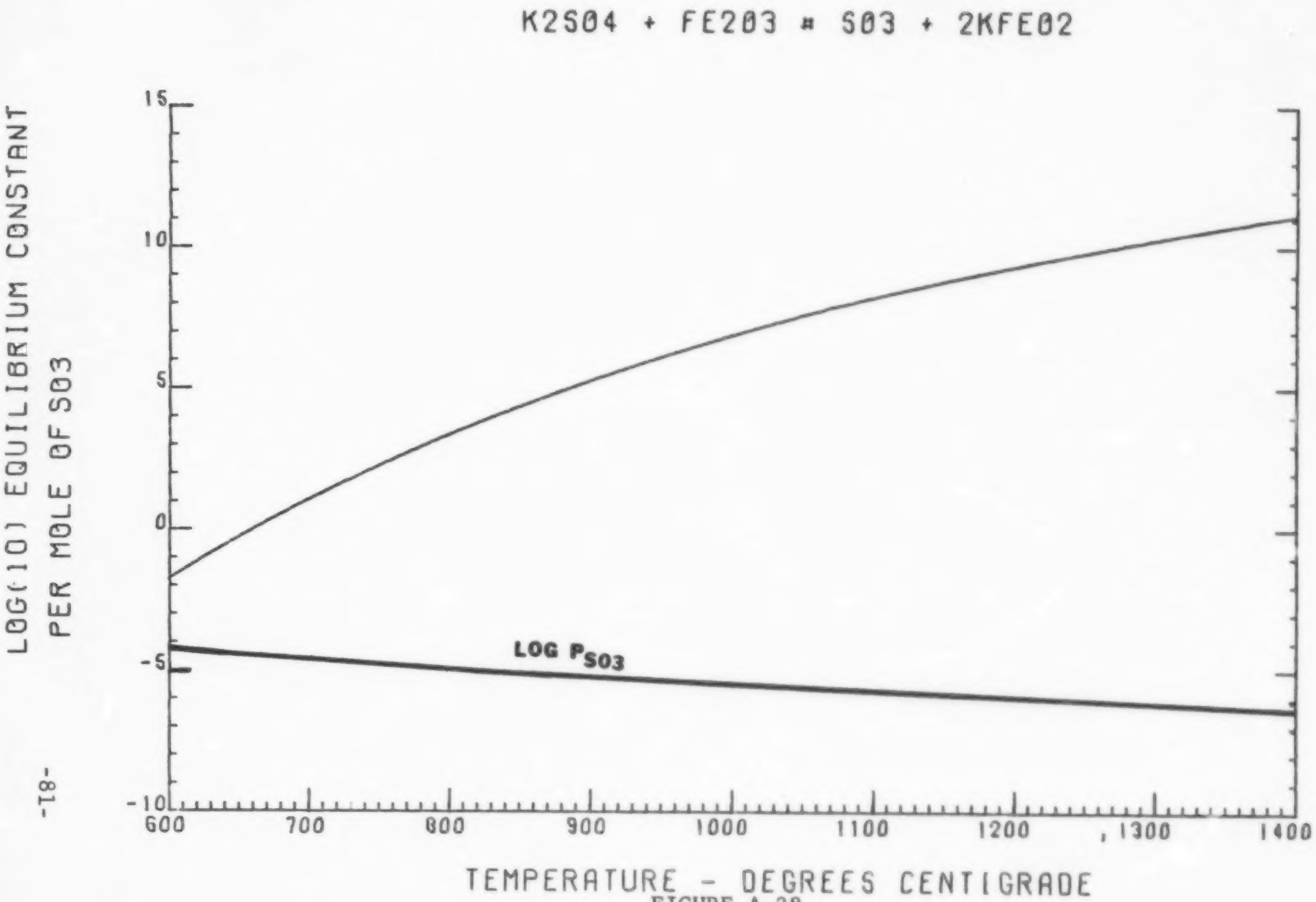

FIGURE A-28

Log K Versus T for the Reaction
$K_2SO_4 + Fe_2O_3 \rightleftharpoons 2KFeO_2 + SO_3$

08 AUG 74

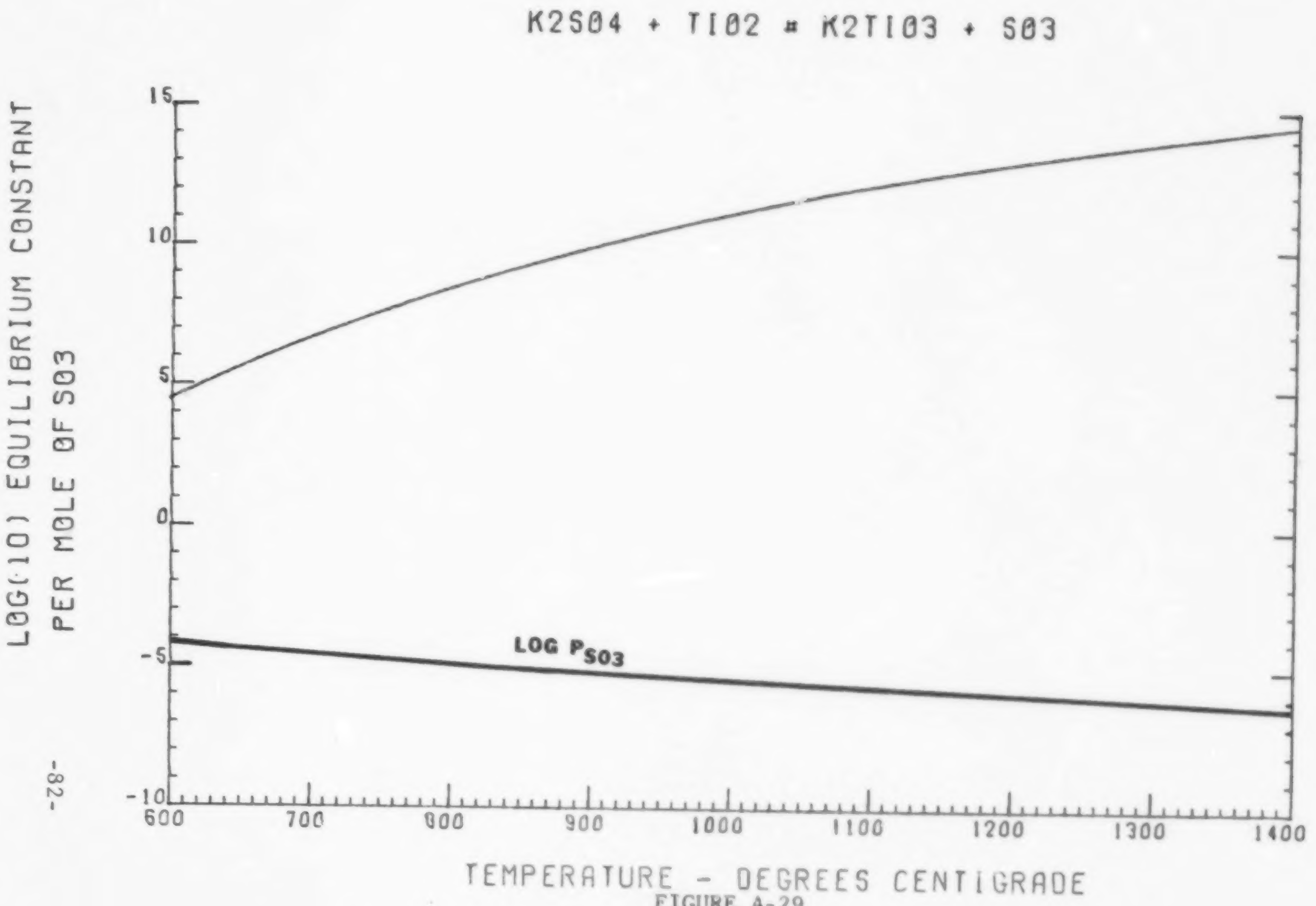

FIGURE A-29

Log K Versus T for the Reaction
$K_2SO_4 + TiO_2 \rightleftarrows K_2TiO_3 + SO_3$

07 AUG 74

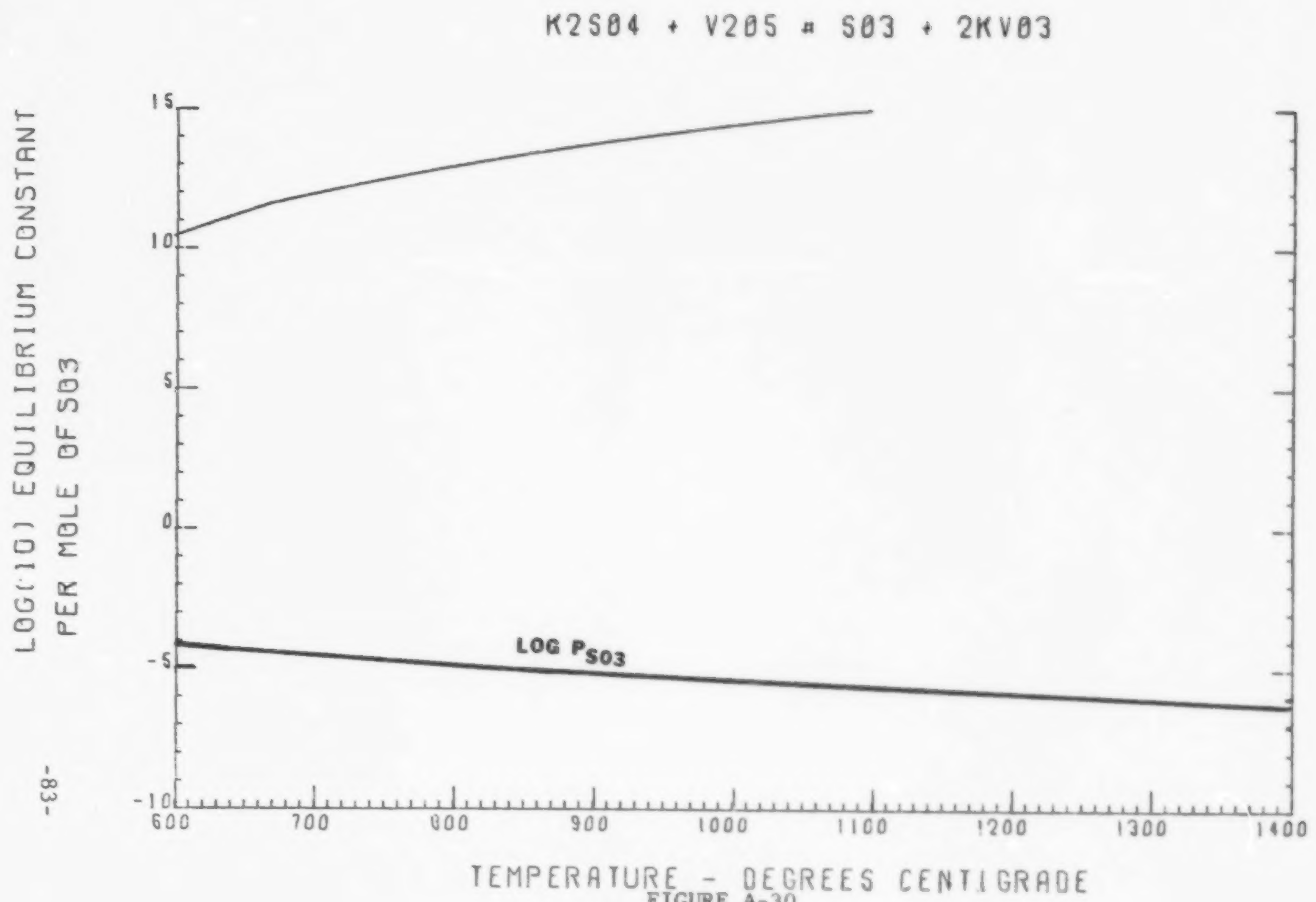

FIGURE A-30

Log K Versus T for the Reaction
$K_2SO_4 + V_2O_5 \rightleftarrows 2KVO_3 + SO_3$

06 AUG 74

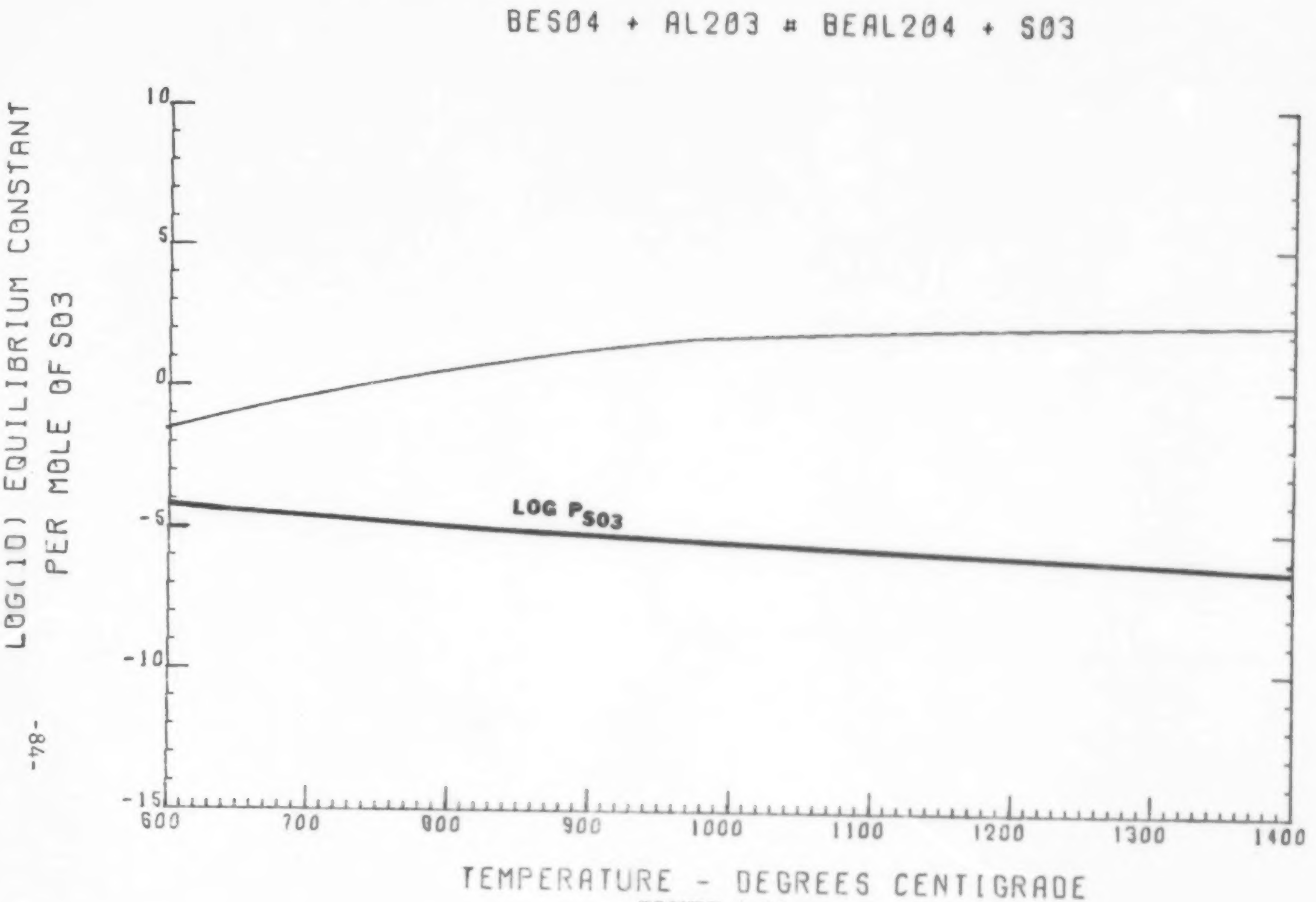

FIGURE A-31

Log K Versus T for the Reaction
$BeSO_4 + Al_2O_3 \rightleftarrows BeAl_2O_4 + SO_3$

07 AUG 74

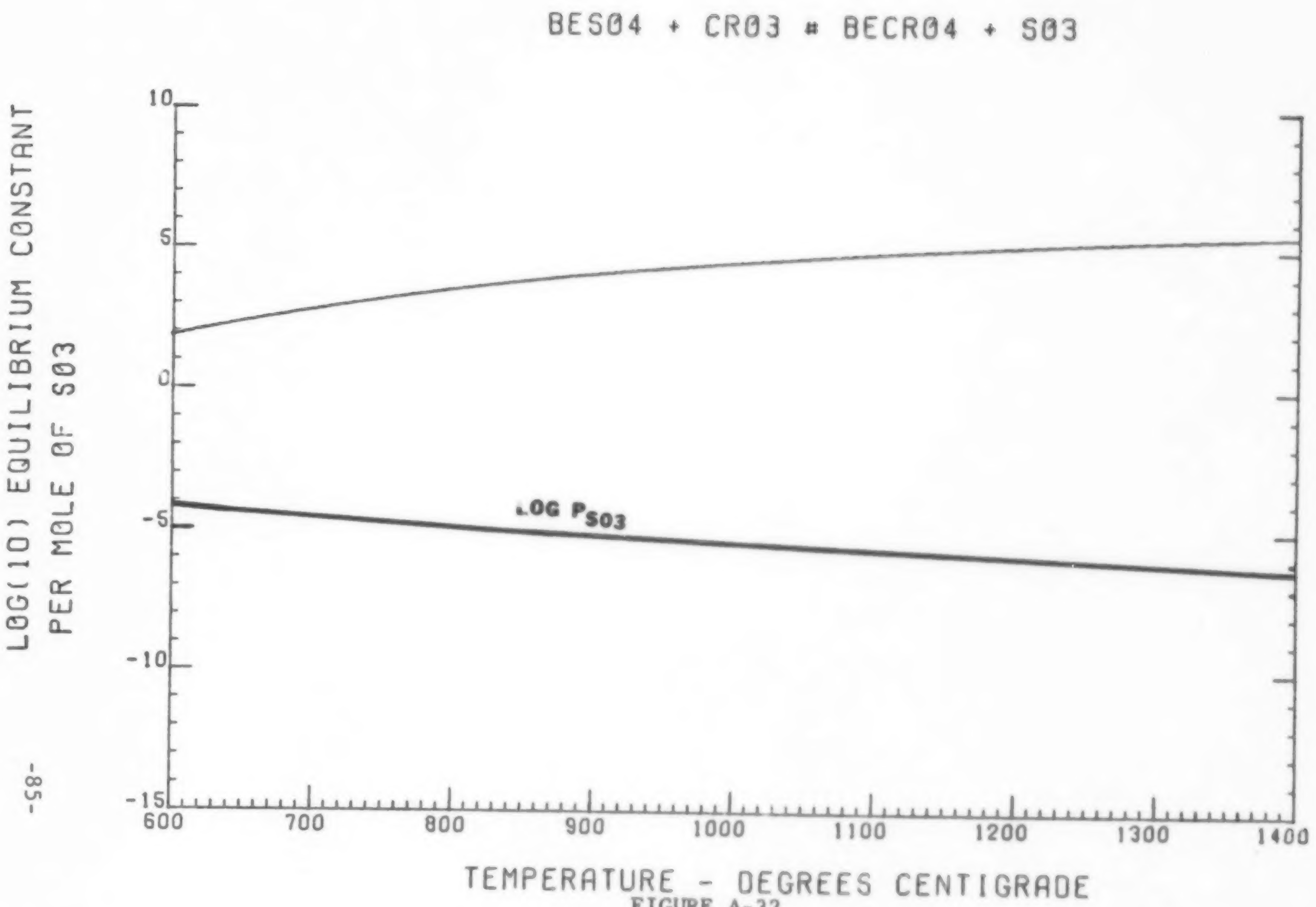

FIGURE A-32

Log K Versus T for the Reaction
$BeSO_4 + CrO_3 \rightleftarrows BeCrO_4 + SO_3$

07 AUG 74

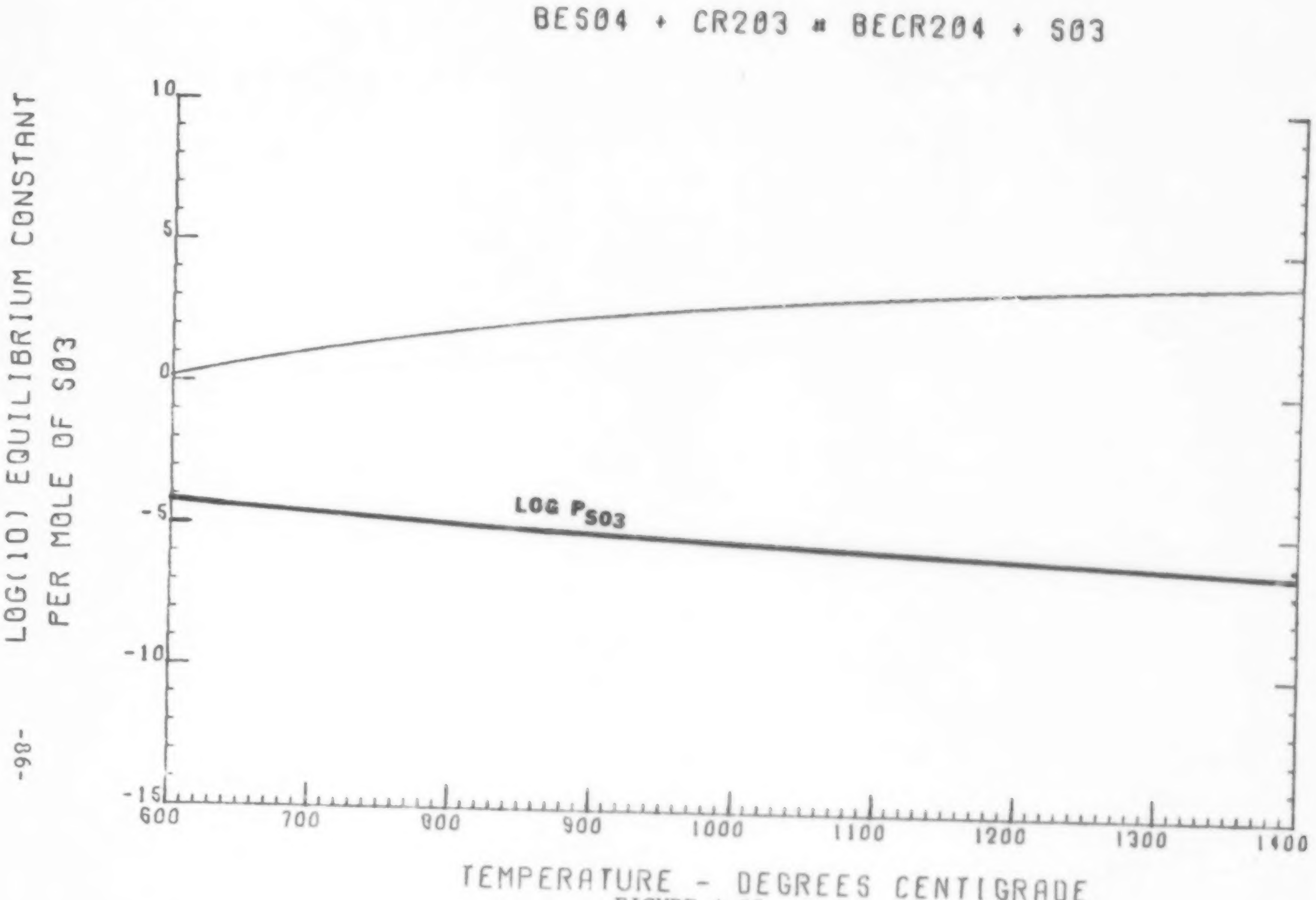

FIGURE A-33

Log K Versus T for the Reaction
$BeSO_4 + Cr_2O_3 \rightleftarrows BeCr_2O_4 + SO_3$

07 AUG 74

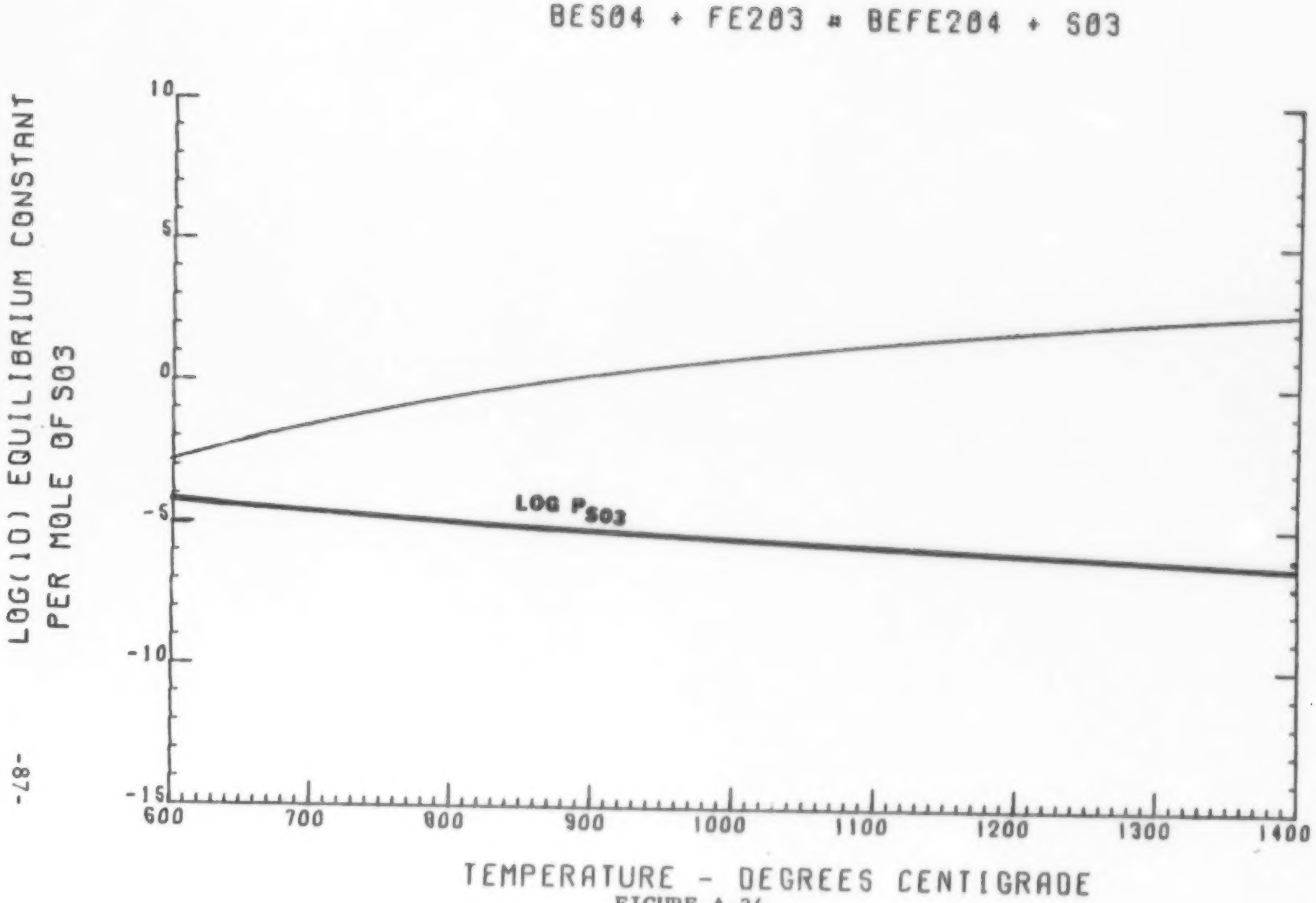

FIGURE A-34

Log K Versus T for the Reaction
$BeSO_4 + Fe_2O_3 \rightleftarrows BeFe_2O_4 + SO_3$

07 AUG 74

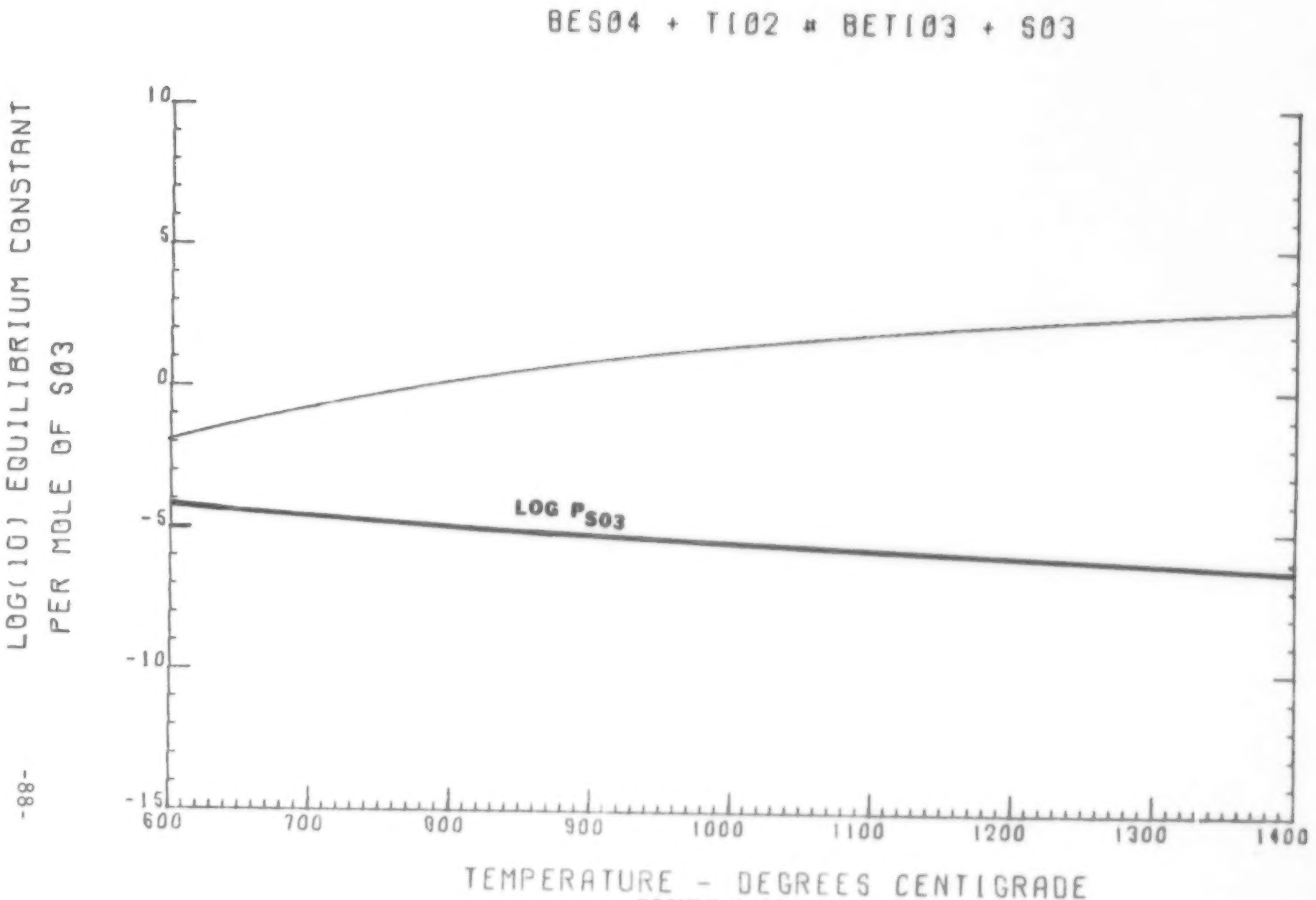

FIGURE A-35

Log K Versus T for the Reaction
$BeSO_4 + TiO_2 \rightleftarrows BeTiO_3 + SO_3$

07 AUG 74

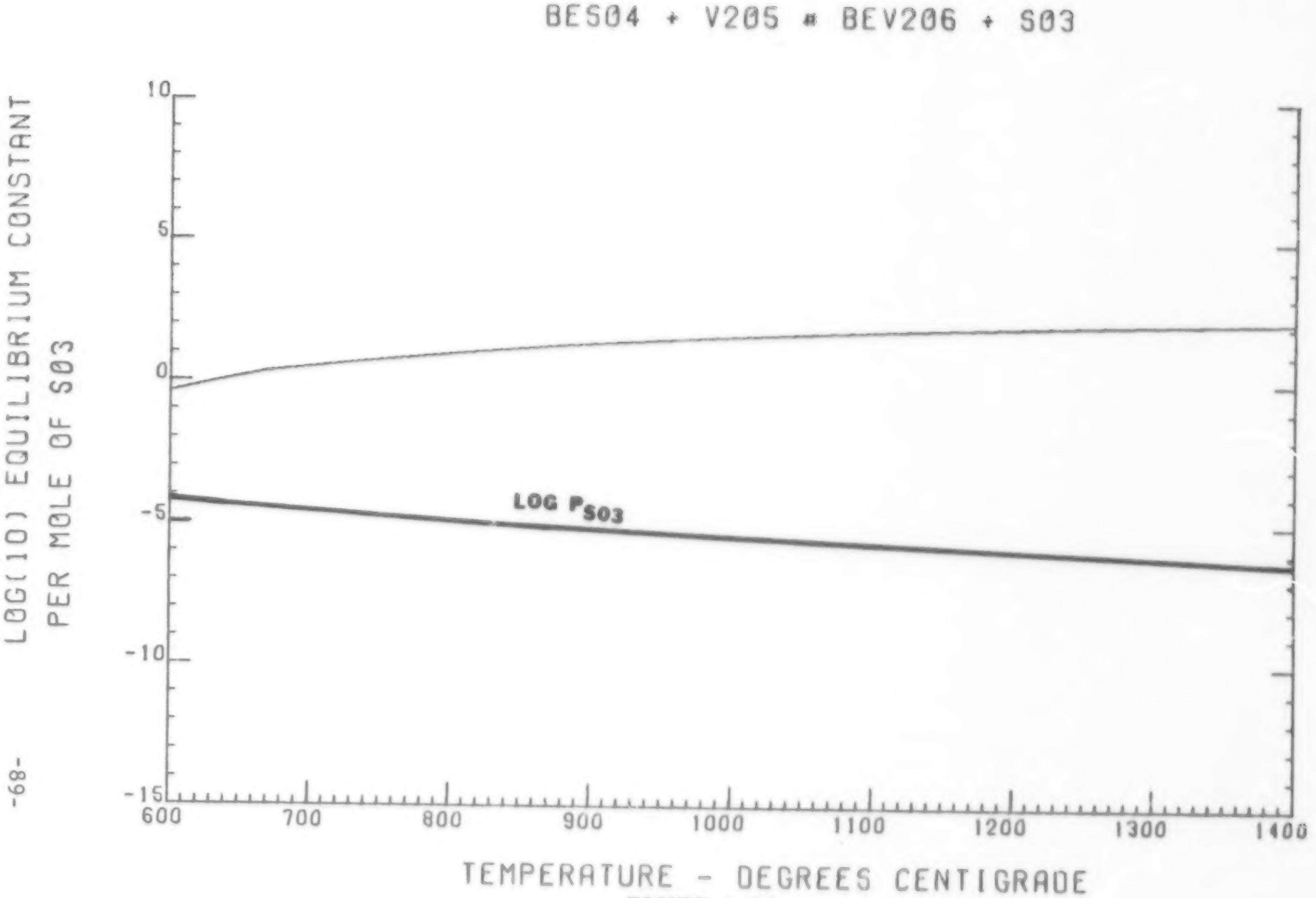

FIGURE A-36

Log K Versus T for the Reaction $BeSO_4 + V_2O_5 \rightleftarrows BeV_2O_6 + SO_3$

07 AUG 74

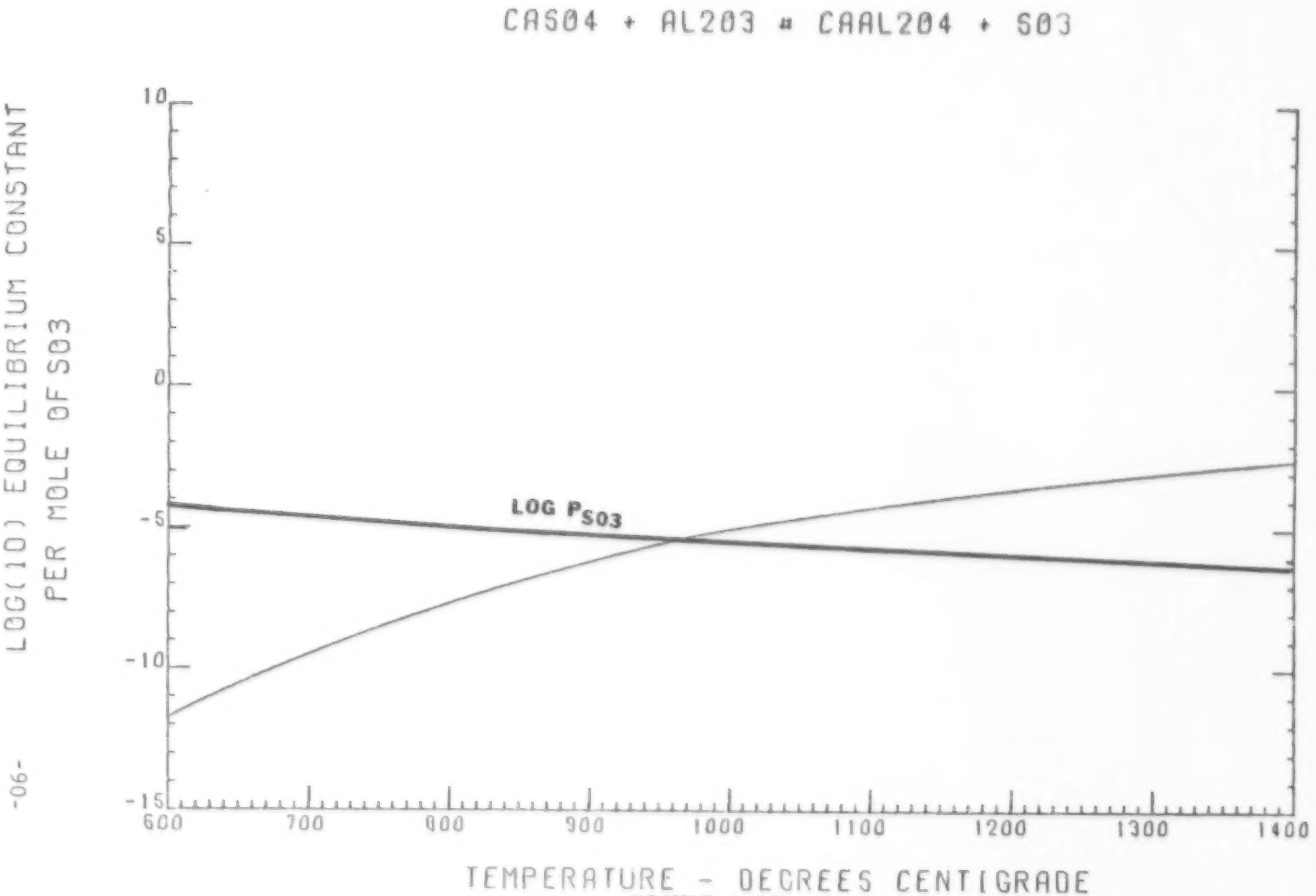

FIGURE A-37

Log K Versus T for the Reaction
$CaSO_4 + Al_2O_3 \rightleftarrows CaAl_2O_4 + SO_3$

17 AUG 74

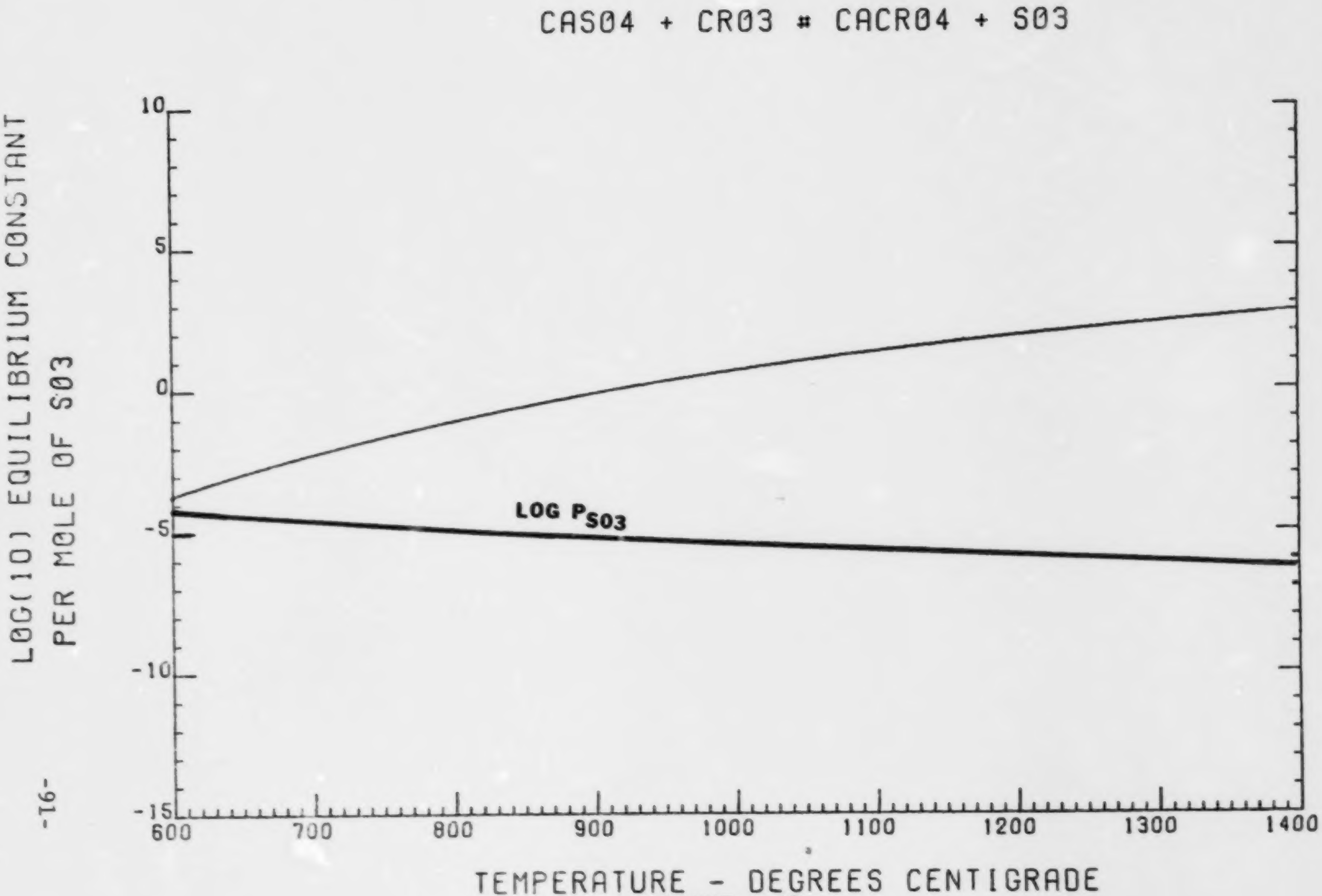

FIGURE A-38

Log K Versus T for the Reaction
$CaSO_4 + CrO_3 \rightleftarrows CaCrO_4 + SO_3$

07 AUG 74

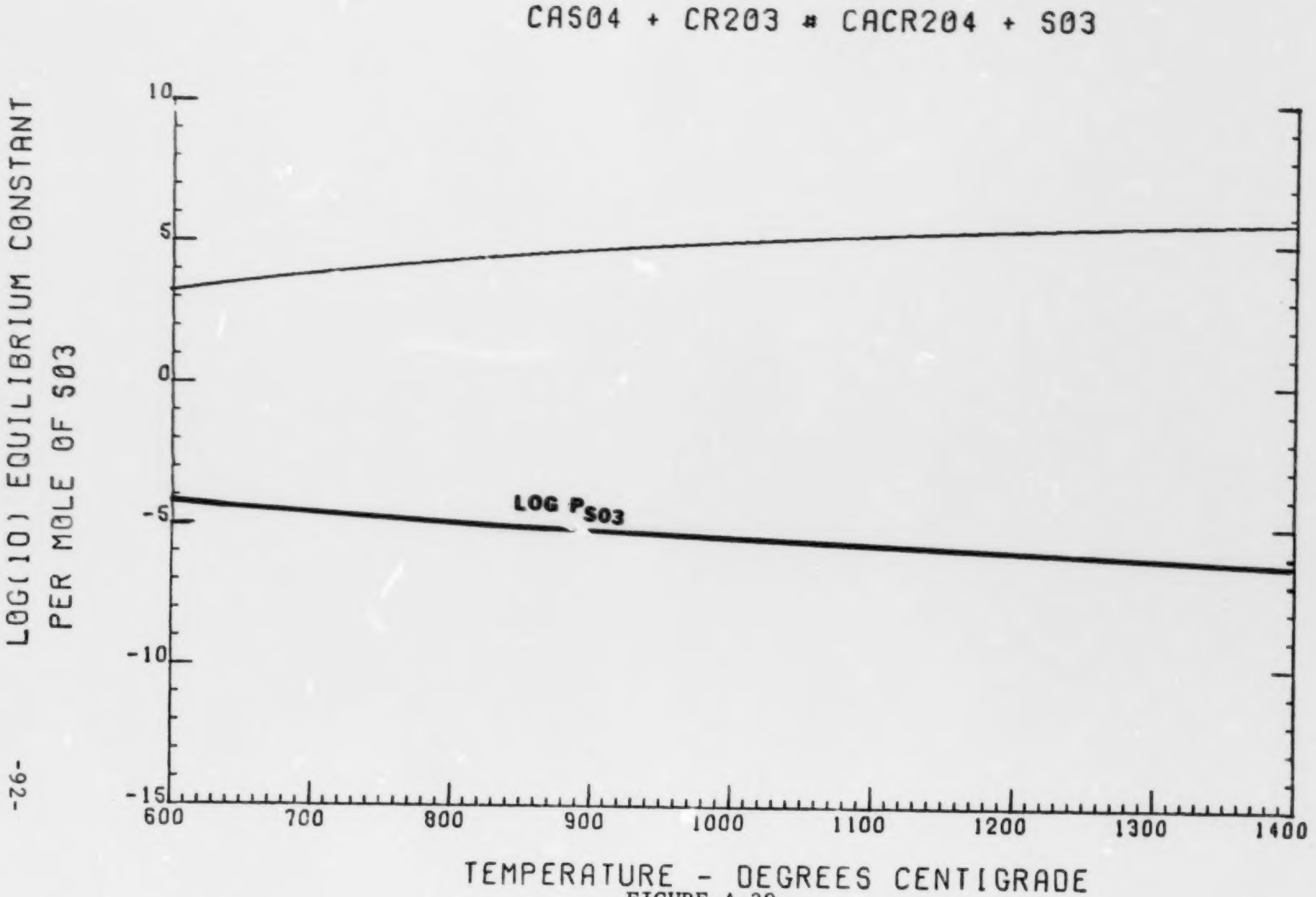

FIGURE A-39

Log K Versus T for the Reaction
$CaSO_4 + Cr_2O_3 \rightleftarrows CaCr_2O_4 + SO_3$

07 AUG 74

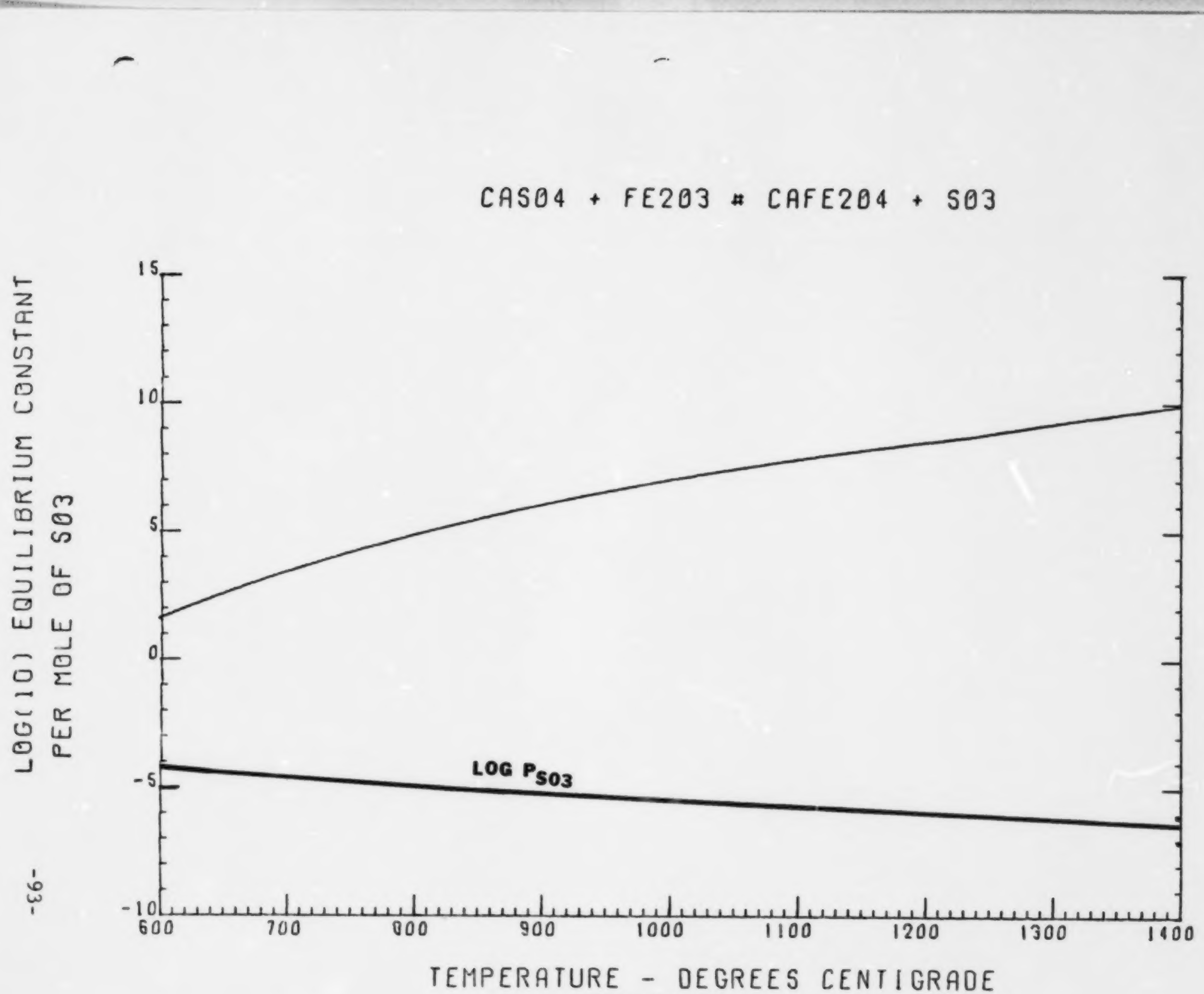

FIGURE A-40

Log K Versus T for the Reaction
$CaSO_4 + Fe_2O_3 \rightleftarrows CaFe_2O_4 + SO_3$

07 AUG 74

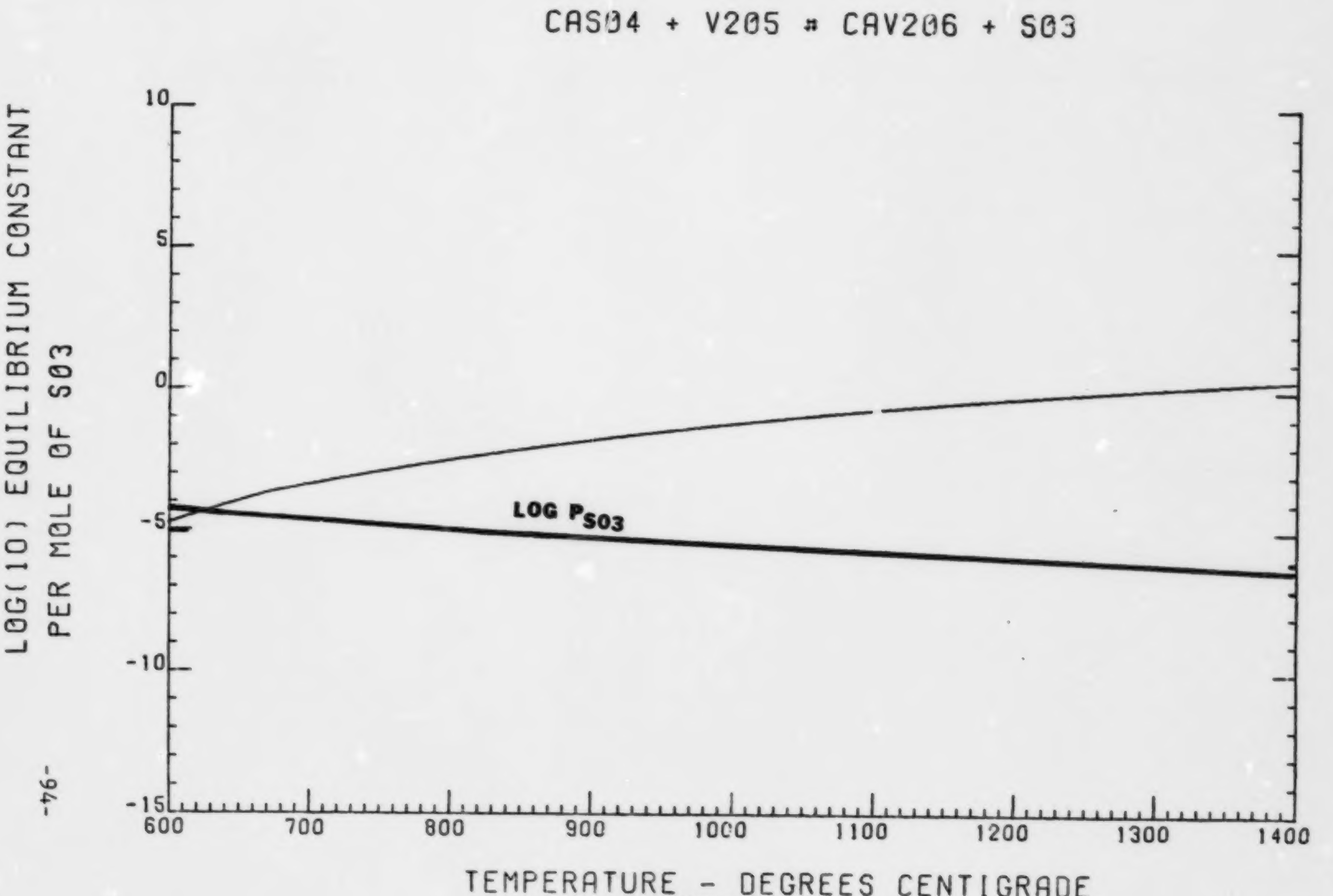

FIGURE A-41

Log K Versus T for the Reaction
$CaSO_4 + V_2O_5 \rightleftarrows CaV_2O_6 + SO_3$

07 AUG 74

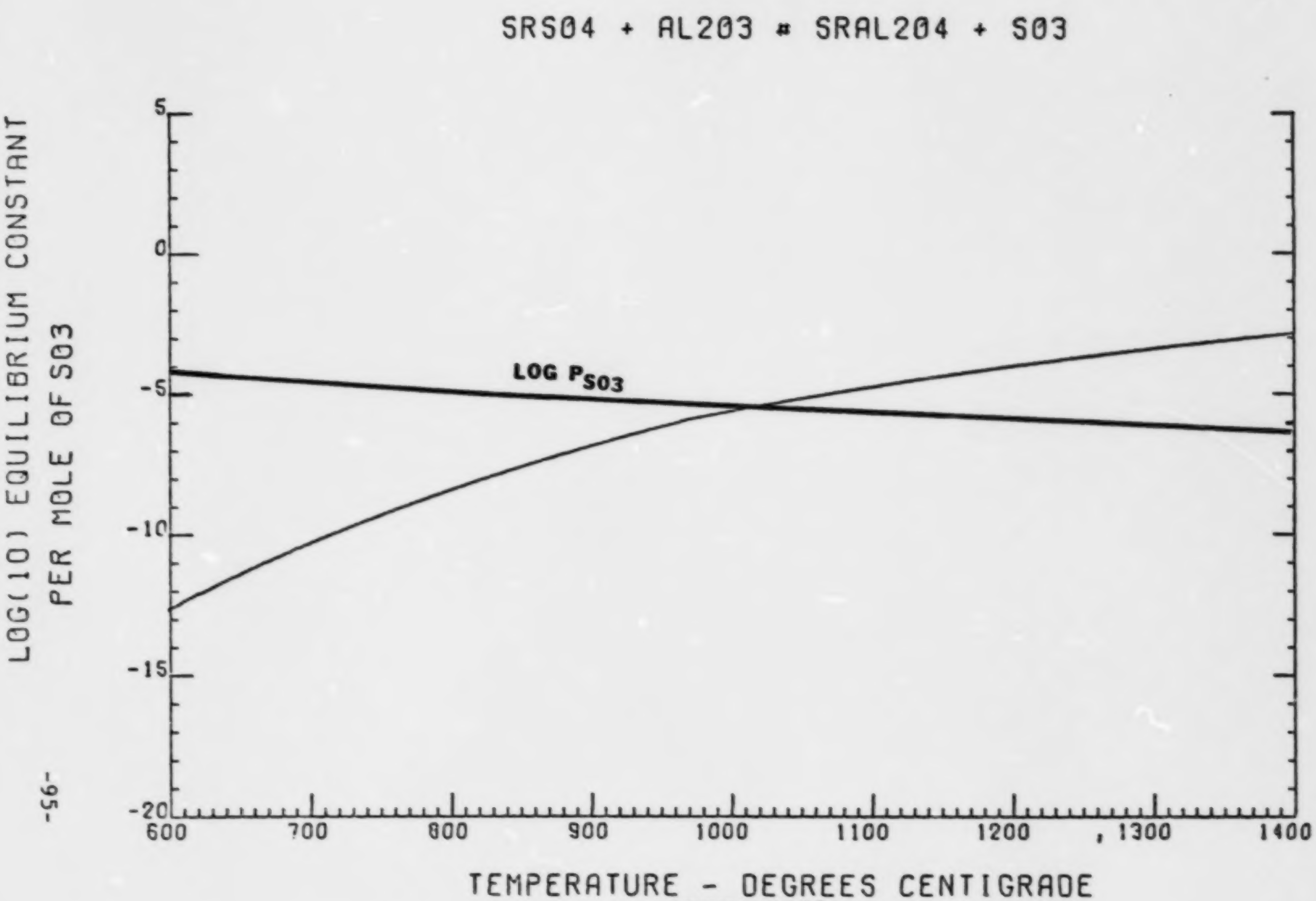

FIGURE A- 42

Log K Versus T for the Reaction
$SrSO_4 + Al_2O_3 \rightleftarrows SrAl_2O_4 + SO_3$

'7 AUG 74

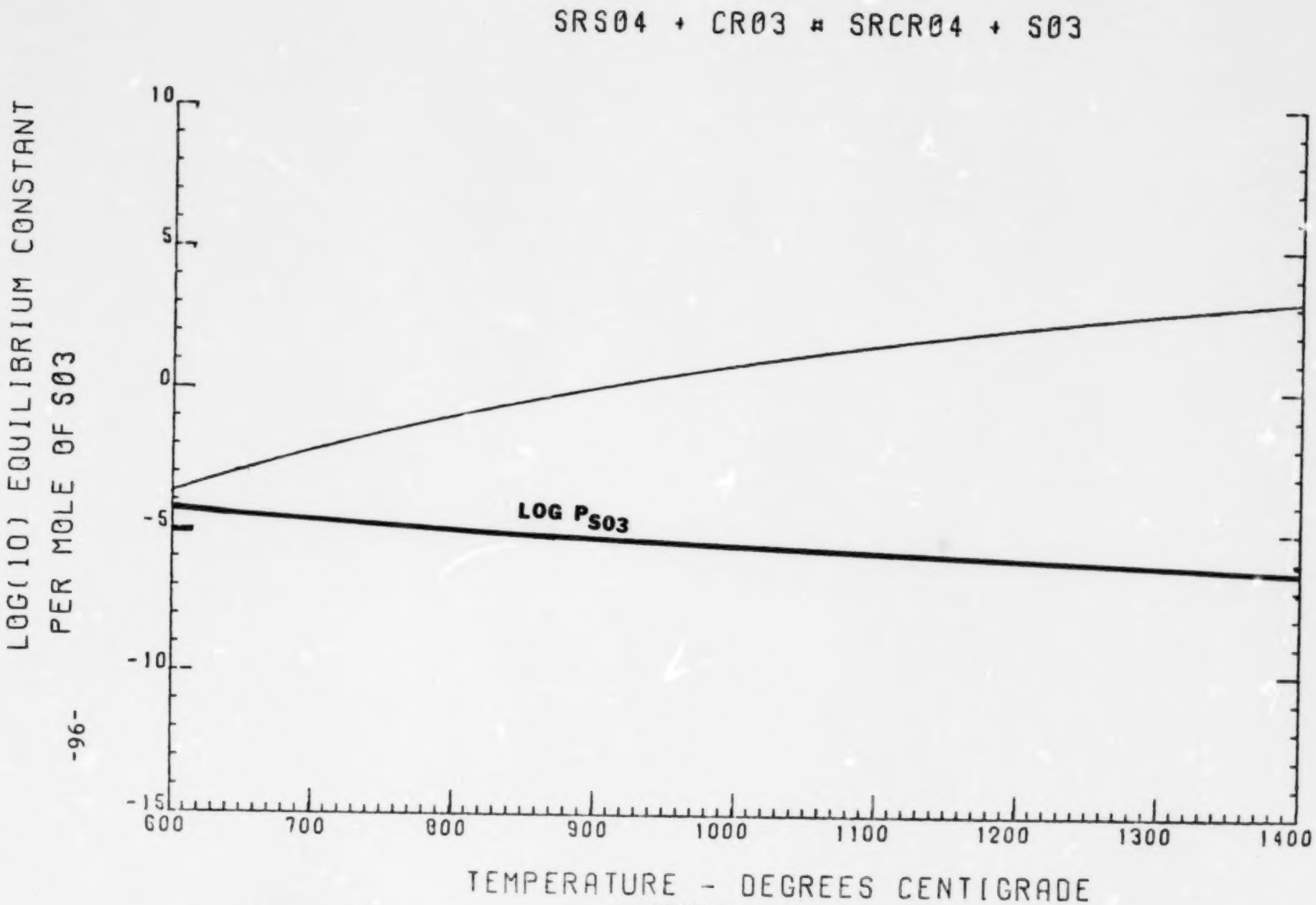

FIGURE A-43

Log K Versus T for the Reaction
$SrSO_4 + CrO_3 \rightleftarrows SrCrO_4 + SO_3$

08 AUG 74

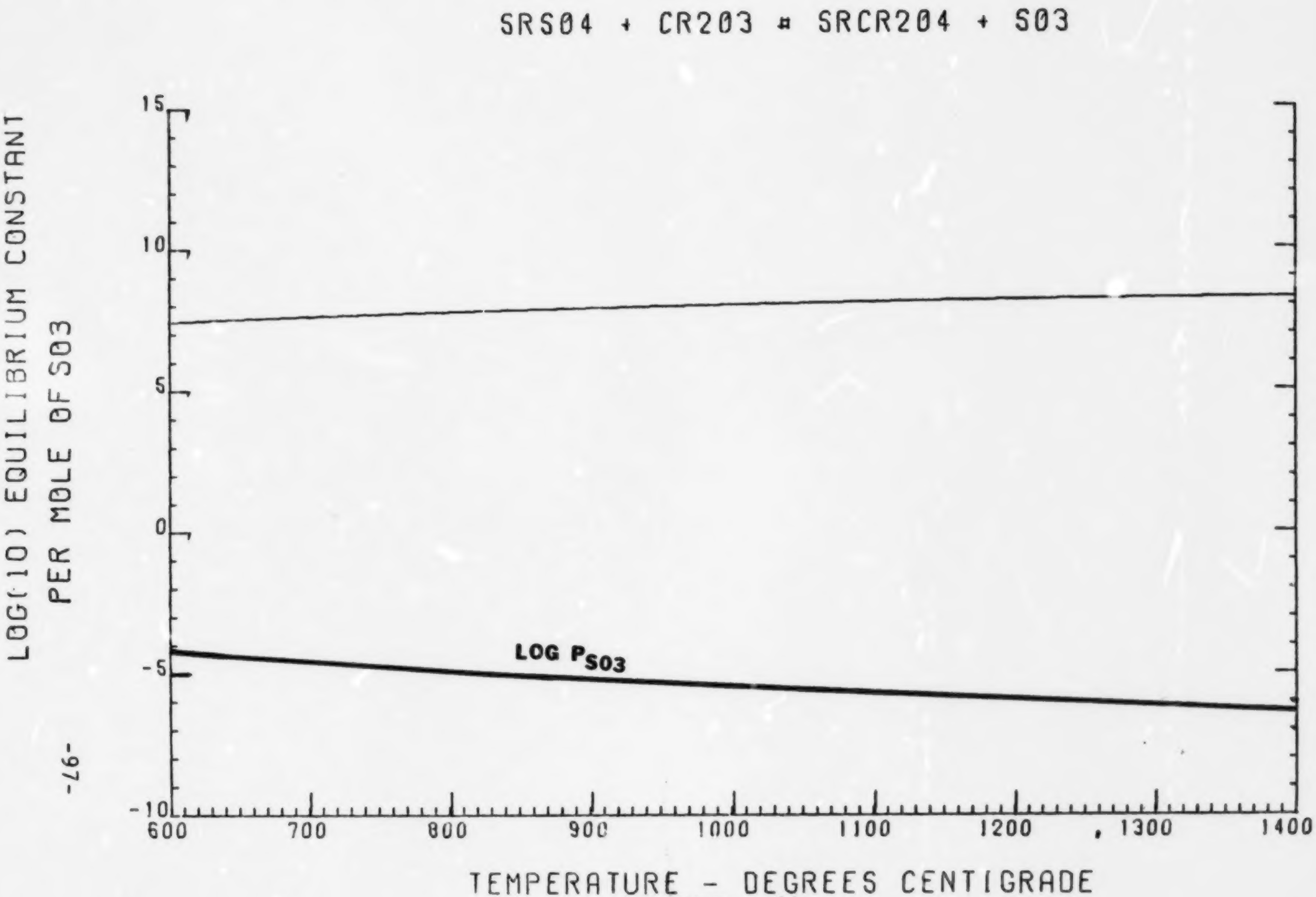

FIGURE A-44

Log K Versus T for the Reaction
$SrSO_4 + Cr_2O_3 \rightleftarrows SrCr_2O_4 + SO_3$

08 AUG 74

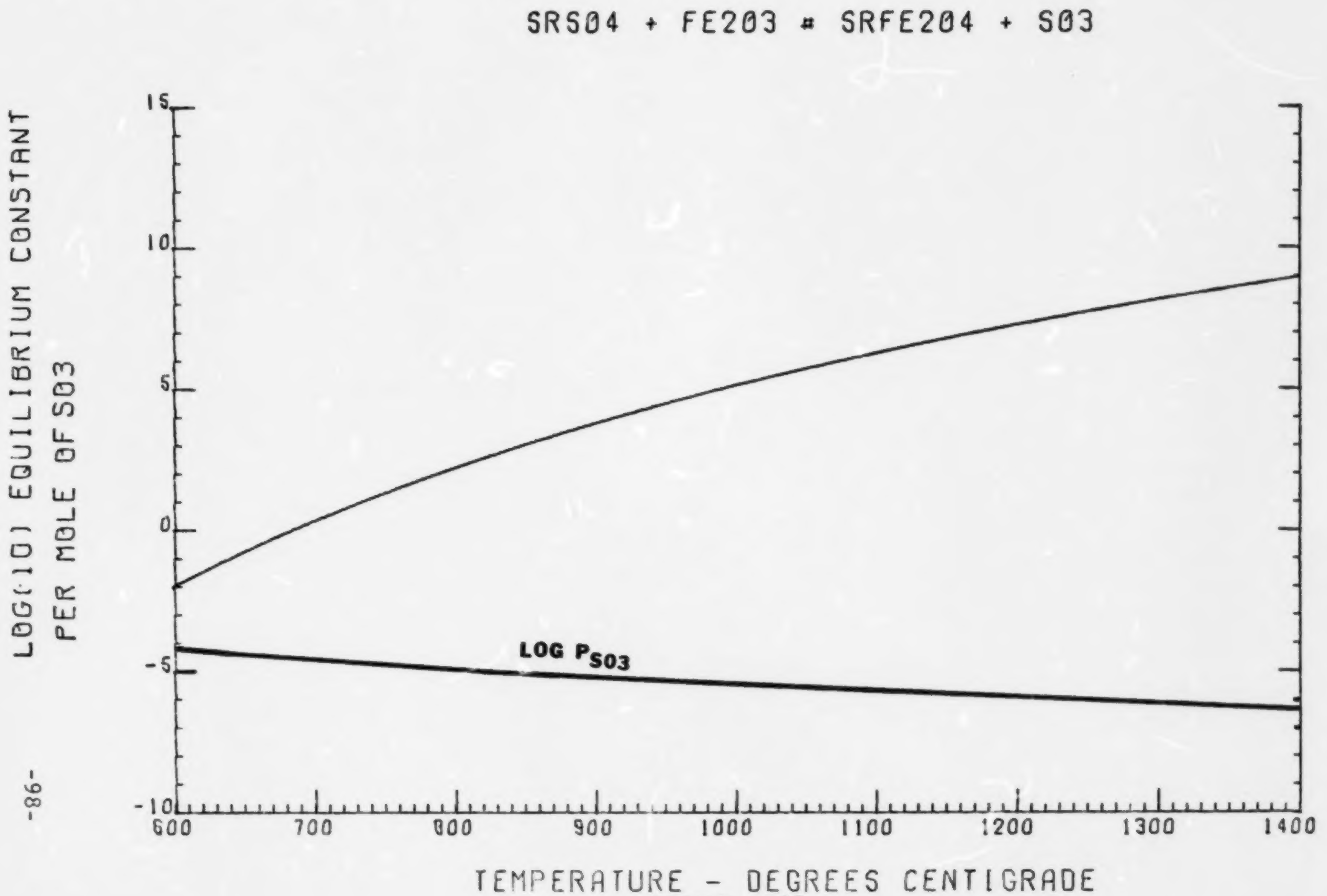

FIGURE A-45

Log K Versus T for the Reaction
$SrSO_4 + Fe_2O_3 \rightleftarrows SrFe_2O_4 + SO_3$

07 AUG 74

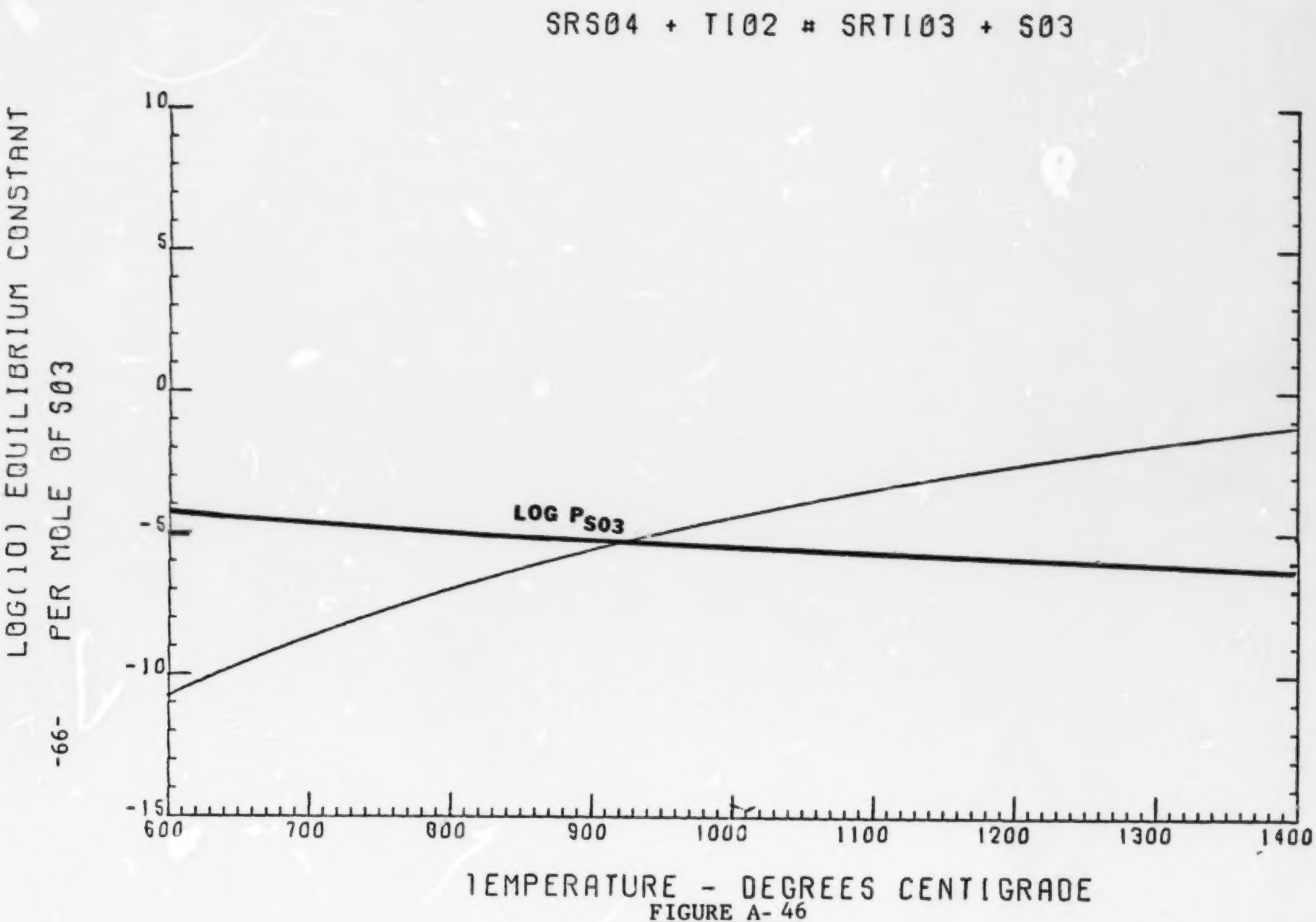

FIGURE A-46

Log K Versus T for the Reaction
$SrSO_4 + TiO_2 \rightleftarrows SrTiO_3 + SO_3$

07 AUG 74

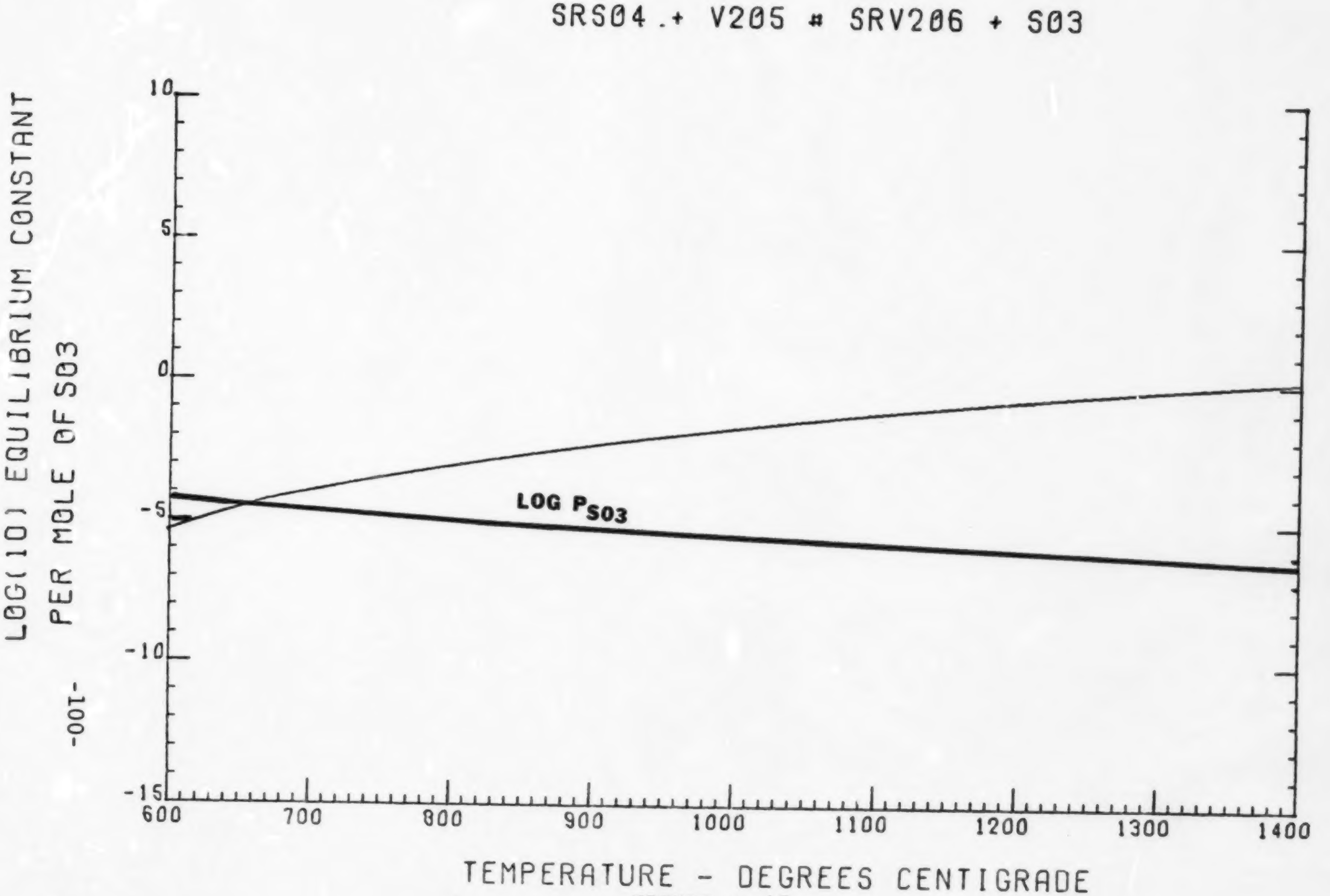

FIGURE A- 47

Log K Versus T for the Reaction
$SrSO_4 + V_2O_5 \rightleftarrows SrV_2O_6 + SO_3$

07 AUG 74

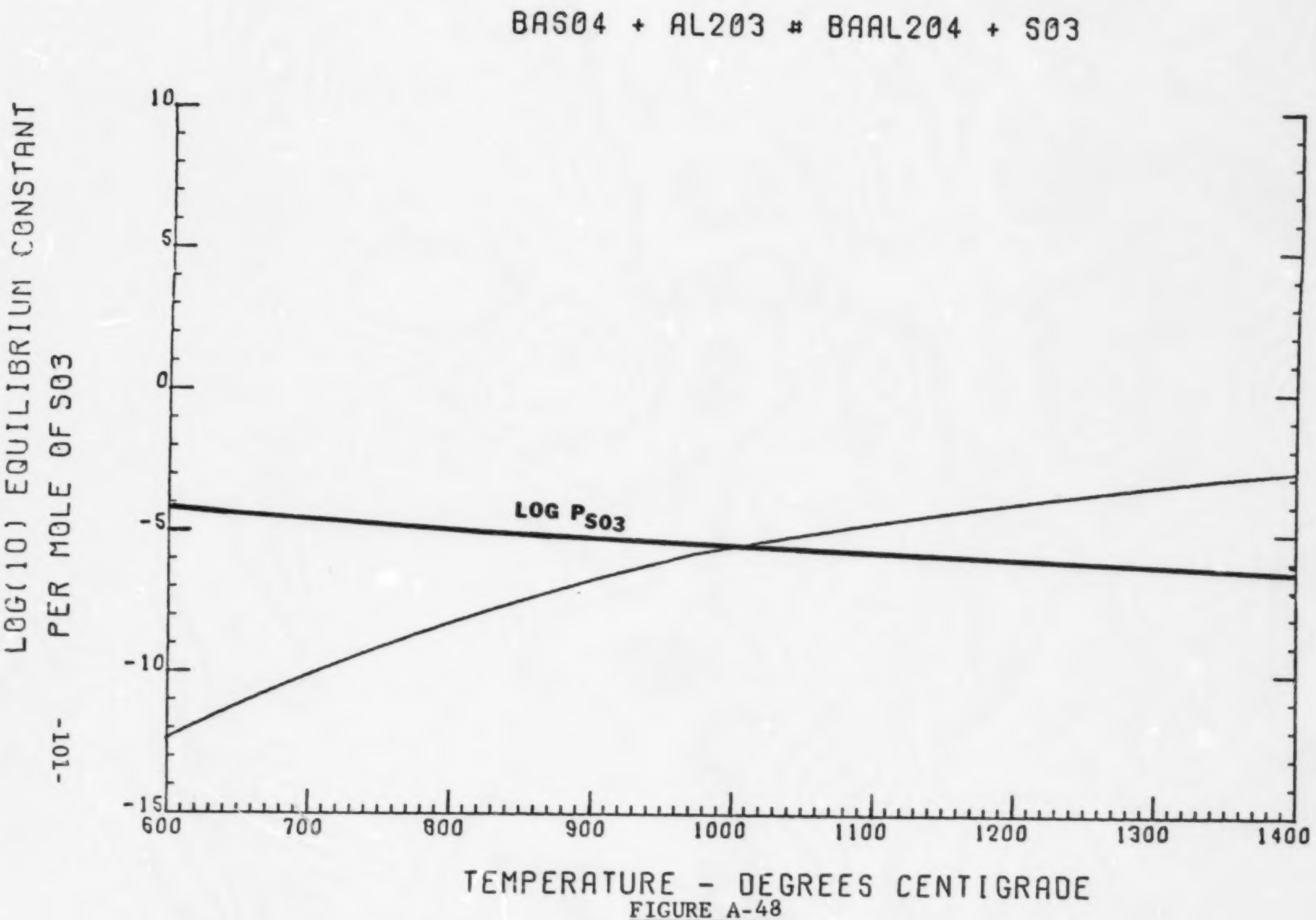

FIGURE A-48

Log K Versus T for the Reaction
$BaSO_4 + Al_2O_3 \rightleftarrows BaAl_2O_4 + SO_3$

07 AUG 74

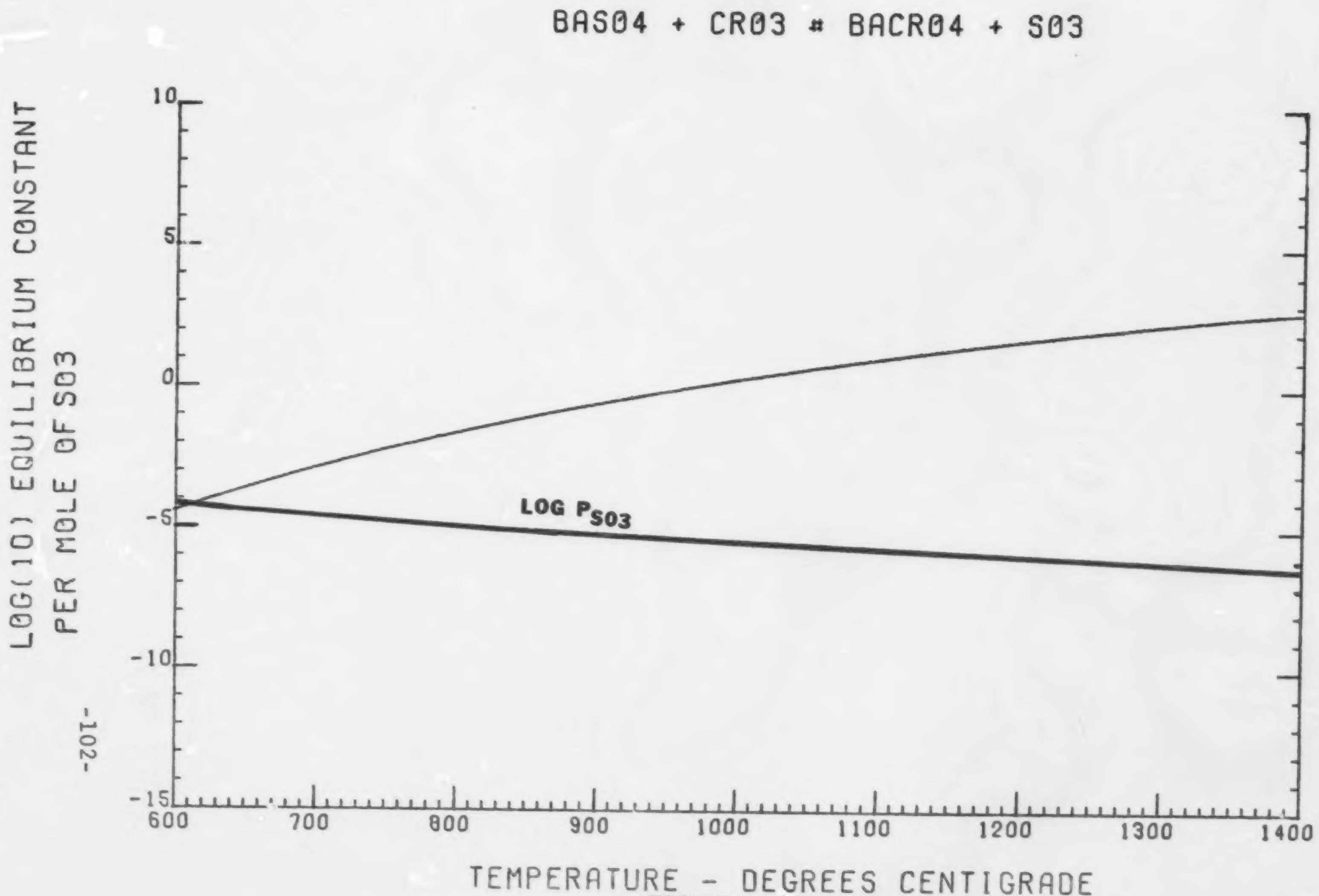

FIGURE A-49

Log K Versus T for the Reaction
$BaSO_4 + CrO_3 \rightleftarrows BaCrO_4 + SO_3$

07 AUG 74

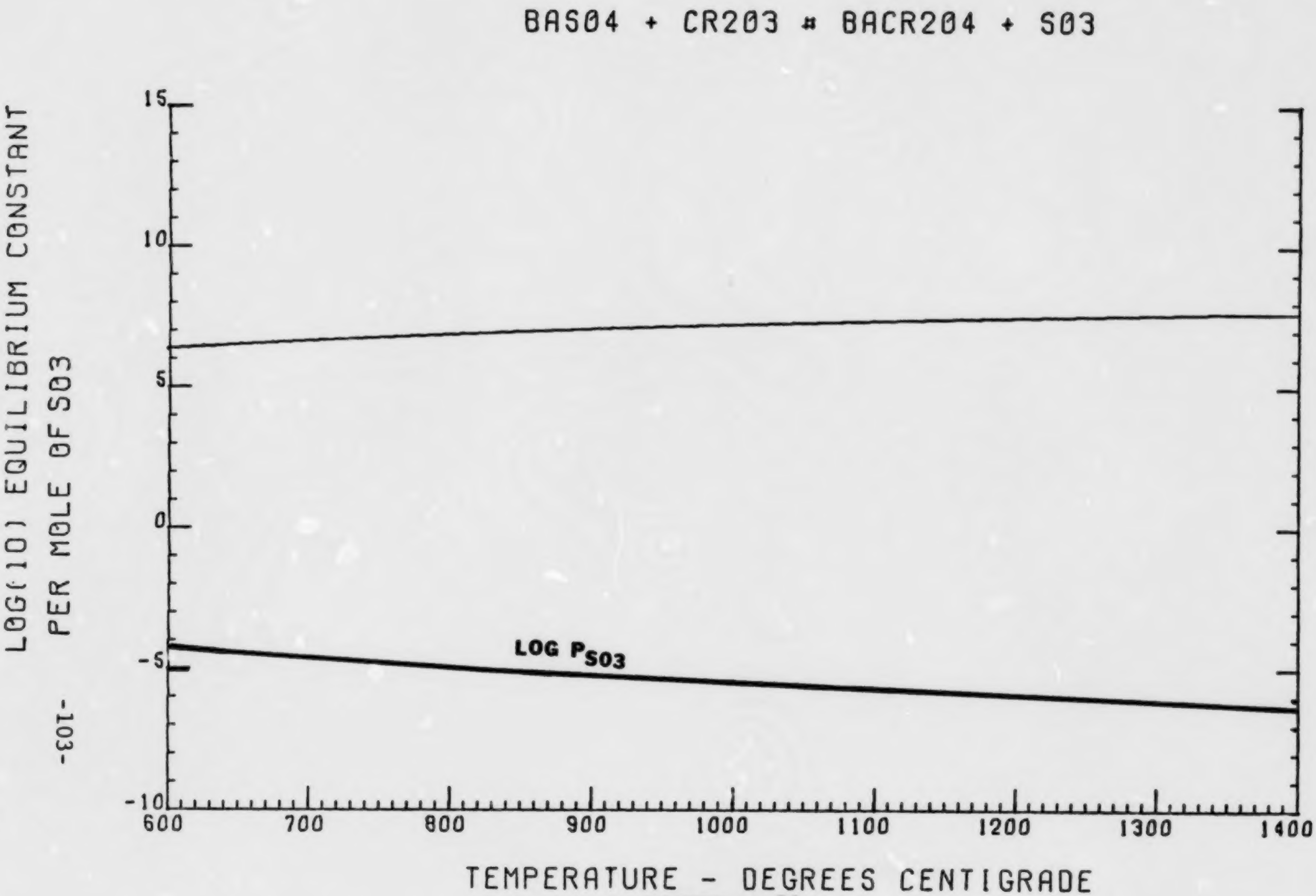

FIGURE A-50

Log K Versus T for the Reaction
$BaSO_4 + Cr_2O_3 \rightleftarrows BaCr_2O_4 + SO_3$

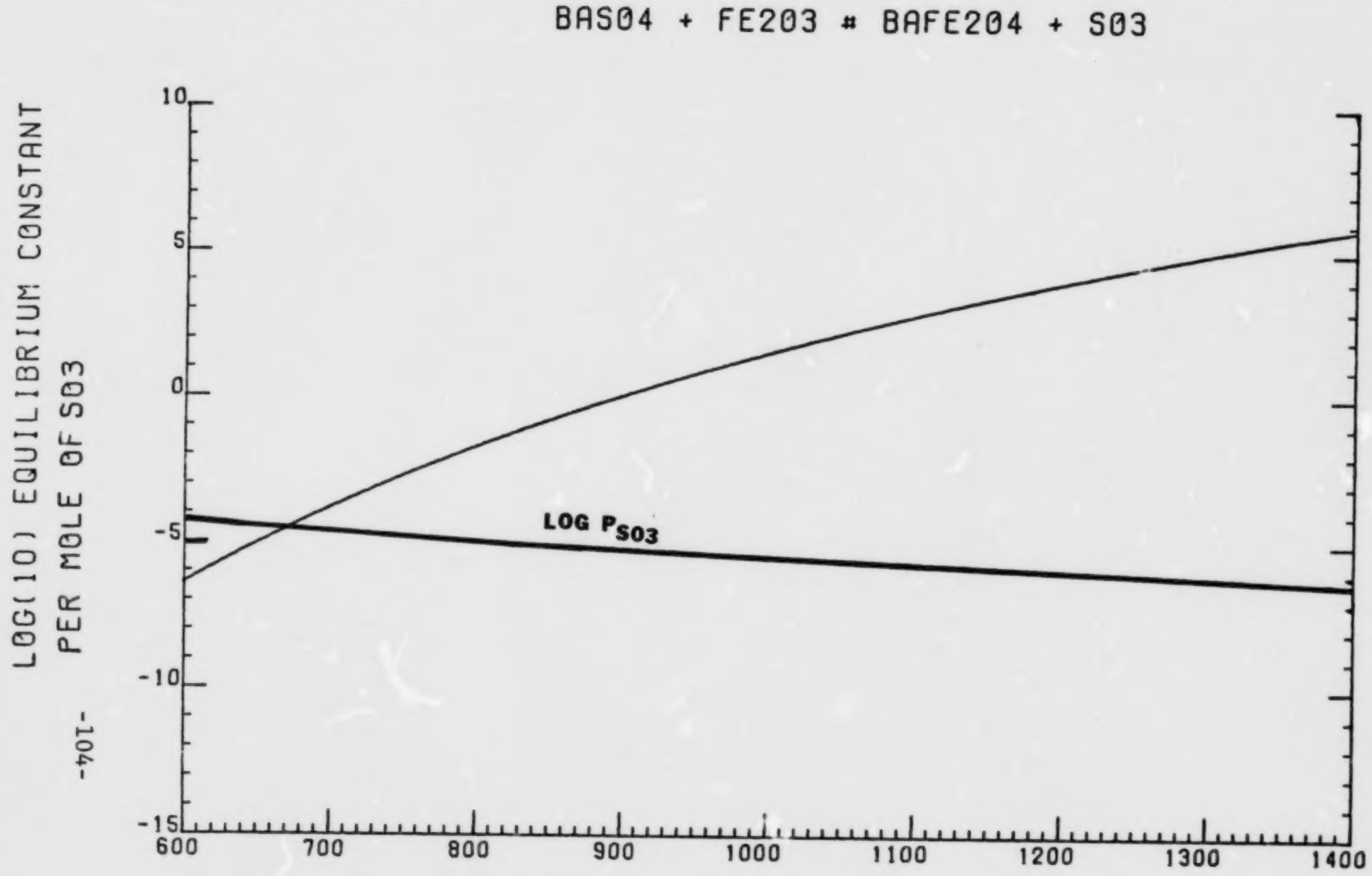

FIGURE A-51

Log K Versus T for the Reaction
$BaSO_4 + Fe_2O_3 \rightleftarrows BaFe_2O_4 + SO_3$

07 AUG 74

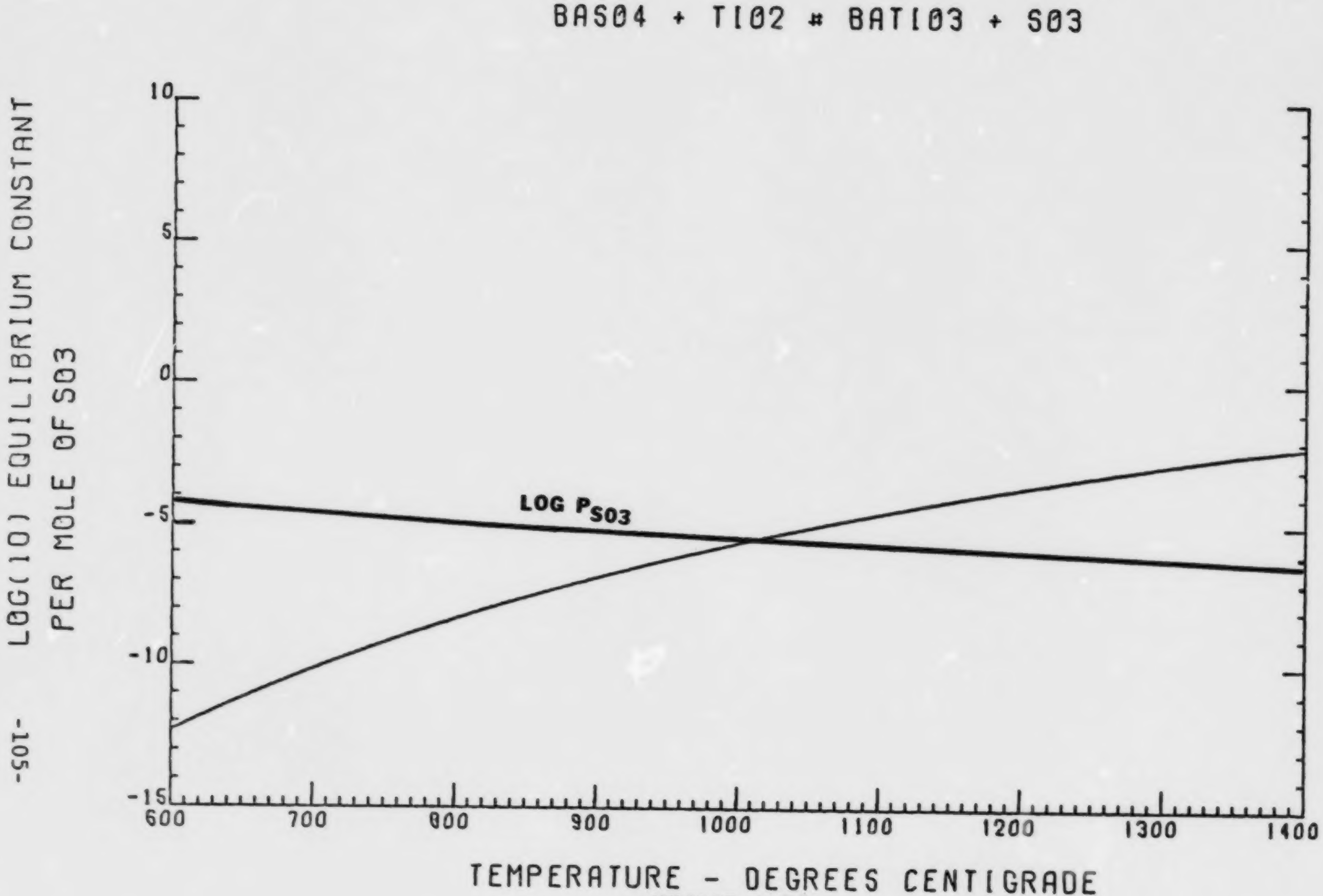

FIGURE A-52

Log K Versus T for the Reaction
$BaSO_4 + TiO_2 \rightleftarrows BaTiO_3 + SO_3$

07 AUG 74

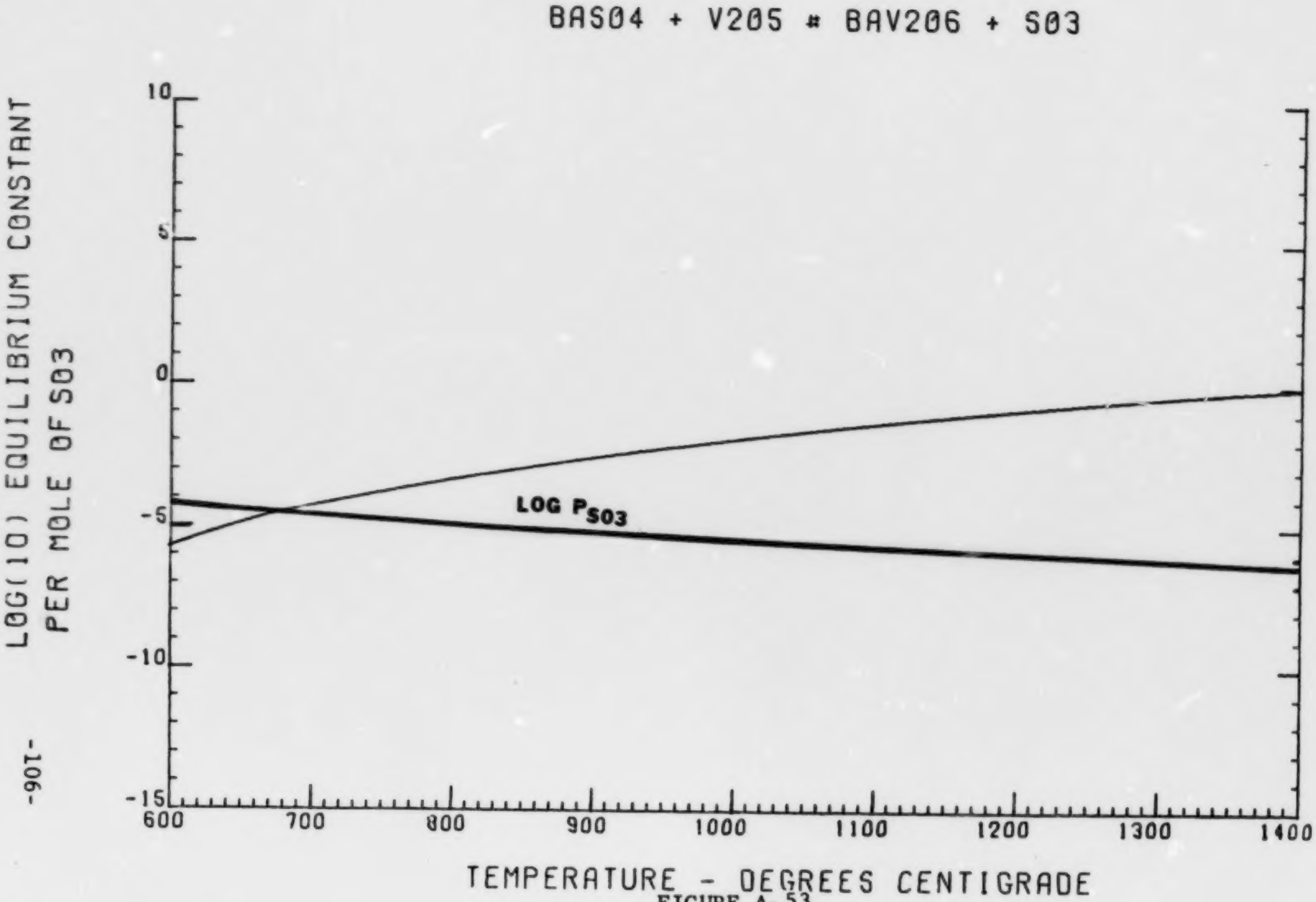

FIGURE A-53

Log K Versus T for the Reaction
$BaSO_4 + V_2O_5 \rightleftarrows BaV_2O_6 + SO_3$

07 AUG 74

RADIAN
CORPORATION

Section 5.2

TECHNICAL NOTE 200-045-10-02a

THE THERMODYNAMICS OF CHEMICAL REGENERATION OF METAL OXIDE SO_2 SORBENTS

25 April 1975

Prepared by:
Philip S. Lowell
Terry B. Parsons

ABSTRACT

This technical note gives the results of an investigation of the thermodynamics of chemical regeneration of spent metal oxide SO_2 sorbents. The goal was to identify conditions under which metal oxides could be regenerated by reductive decomposition of metal sulfate sorption products. Six reducing atmospheres were considered. Three steps were used in thermodynamic analysis of the reaction between reducing agents and metal sulfates. First, the products of reaction between the reducing agent and SO_3 were predicted using an equilibrium model to calculate product stream compositions. Next, the temperature range in which it is thermodynamically feasible to reduce the metal sulfate to the oxide with each reducing agent was predicted. Finally, metal oxides for which there is a tendency to form sulfides during sulfate decomposition were identified. The results are a list of oxide-reducing agent combinations and the temperatures at which the sorption-regeneration processes are predicted to be thermodynamically favored.

TABLE OF CONTENTS

Page

ABSTRACT 108

1.0 INTRODUCTION 110

2.0 REACTIONS OF REDUCING AGENTS WITH SO_3 AND PREDICTION OF EQUILIBRIUM PRODUCT STEAM COMPOSITIONS 114

2.1 Method for Predicting Composition of Product Mixtures 114

2.2 Composition of Product Mixtures at Equilibrium 118

3.0 IDENTIFICATION OF CONDITIONS AT WHICH REDUCTIVE DECOMPOSITION OF METAL SULFATES OCCURS 126

3.1 Methods of Thermodynamic Analysis of Sulfate Reduction Reactions 127

3.2 Results of Thermodynamic Analysis of Sulfate Reduction Reactions 129

4.0 INVESTIGATION OF THE POSSIBILITY OF METAL SULFIDE FORMATION 134

4.1 Method of Thermodynamic Analysis of the Sulfide Formation Reaction 134

4.2 Results of Thermodynamic Analysis of the Sulfide Formation Reaction 137

5.0 RESULTS 142

5.1 Summary of Results for Each Metal Oxide 143

5.2 Conclusions 163

BIBLIOGRAPHY 166

APPENDIX - FIGURES A-1 THROUGH A-30 167

1.0 INTRODUCTION

This technical note gives the results of an investigation of the thermodynamics of chemical regeneration of spent metal oxide SO_2 sorbents. The work was done under EPA Contract No. 68-02-1319. It is part of a study of the feasibility of using metal oxides as SO_2 sorbents in fluidized bed combustion of coal.

Radian Technical Note 200-045-10-01, "Thermodynamic Screening of Dry Metal Oxides for High Temperature SO_2 Removal", describes the identification of metal oxides which are predicted to react with sulfur oxides in combustion gas to form metal sulfates. These candidate sorbents were identified by comparing the vapor pressure of SO_3 over the corresponding metal sulfate with the partial pressure of SO_3 in combustion gas. If the partial pressure of SO_3 in combustion gas is greater than the SO_3 vapor pressure over the metal sulfate, this provides driving force for sorption. Table 1-1 lists both single and binary metal oxides for which the SO_3 vapor pressures over the corresponding sulfate are of the desired magnitude. The high temperature at which sorption can occur for the flue gas condition chosen is also listed. It should be noted that higher pressures, higher mole percent SO_x, or higher O_2 mole fraction would raise the maximum stated temperature.

Further screening of the fourteen candidate SO_2 sorbents listed in Table 1-1 was done in this study. Simple thermal decomposition according to Equation 1-1 would be a desirable method of regenerating the metal oxide.

$$MeSO_4 \underset{\Delta}{\rightarrow} MeO + SO_3 \qquad (1\text{-}1a)$$

$$MeSO_4 \underset{\Delta}{\rightarrow} MeO + SO_2 + \tfrac{1}{2}O_2 \qquad (1\text{-}1b)$$

TABLE 1-1

POTENTIAL SORBENTS FOR SO_2 REMOVAL FROM FLUE GASES

Sorbent*	Maximum Sorption Temperature (°C)
Na_2O	1380
CaO	1090
SrO	1260
BaO	1380
$LiAlO_2$	1200
$LiFeO_2$	950
Li_2TiO_3	1200
$NaAlO_2$	820
$NaFeO_2$	1020
$CaAl_2O_4$	950
$SrAl_2O_4$	1000
$SrTiO_3$	920
$BaAl_2O_4$	1000
$BaTiO_3$	1000

---

* Potential sorbents were selected on the basis of the vapor pressure of SO_3 over the metal sulfate. If the SO_3 vapor pressure was less than the partial pressure of SO_3 in the flue gas, then a driving force for sorption was said to exist. See Technical Note 200-045-10-01 for details. Conditions were 100 ppm SO_x, 5% O_2, and 1 atm total pressure.

Table 1-1 indicates that the sorption temperatures are extremely high. Thus, thermal regeneration temperatures would be prohibitively high (for example, see Vogel, page 11, VO-034).

The goal of this study was to identify the conditions under which these metal oxides could be regenerated by reductive decomposition of the metal sulfate sorption products. The feasibility of chemical regeneration was investigated using the model shown in Equation 1-2.

$$\text{MeSO}_4 + \text{Reducing Agent} \rightarrow \text{MeO} + \begin{array}{l}\text{Products of Reaction}\\ \text{between Reducing Agent}\\ \text{and SO}_3\end{array} \qquad (1\text{-}2)$$

Six reducing agents were considered. The thermodynamics of reactions in the form of Equation 1-2 were considered for each reducing agent-metal sulfate combination. The following individual steps were used.

- The products of reaction between the reducing agent and SO_3 were calculated as a function of temperature assuming Equation 1-2 proceeded as written. The method and results are described in Section 2.
- The temperature range in which it is thermodynamically feasible to reduce the metal sulfate to metal oxide with each reducing agent was predicted. Section 3 describes the method and results of this analysis.

- Metal oxides for which there is a thermodynamic tendency to form sulfides by reaction with SO_3 reduction products were identified. Section 4 gives the method and results in detail.

The results of this study are summarized for each candidate metal oxide sorbent in Section 5.

2.0 REACTIONS OF REDUCING AGENTS WITH SO_3 AND PREDICTION OF EQUILIBRIUM PRODUCT STEAM COMPOSITIONS

One of the objectives of this study was to regenerate the sorbent in one step to the oxide. Production of SO_2, elemental sulfur, etc., would be done with the resulting gas. The six reducing agents considered for this evaluation were hydrogen (H_2), carbon monoxide (CO), synthesis gas ($CO + \frac{1}{2}H_2$), coal (which has a carbon to hydrogen ratio of approximately one), char (C), and methane (CH_4). The reducing agents were evaluated in terms of their tendency to produce an SO_2 product.

$$MeSO_4 + \text{Reducing Agent} \rightarrow MeO + SO_2 + \text{Other Products} \qquad (2\text{-}1)$$

To accomplish this, the reducing agent must remove one gram atom of oxygen from SO_3. This can potentially be accomplished with one gram mole of CO or H_2 (CO_2 or H_2O product) or one-half gram atom of C (one-half CO_2 product). Additional reducing agents will result in a stronger reducing atmosphere. The reducing atmospheres used and their oxygen sorbing potentials are listed in Table 2-1.

The first step was to determine the products of reaction between the reducing agents and SO_3. The method used is described in Section 2.1 and the results are given in Section 2.2.

2.1 Method for Predicting Composition of Product Mixtures

If Equation 1-2 is assumed to proceed as written, the equilibrium mixture for the gas phase may be described by considering Equation 2-2.

$$\text{Reducing Agent} + SO_3 \rightarrow \text{Products} \qquad (2\text{-}2)$$

TABLE 2-1

REDUCING ATMOSPHERES

Name	Composition per Mole of SO_3	Oxygen Sorption Capacity, gram atoms
Hydrogen	H_2	1.0
Carbon Monoxide	CO	1.0
Synthesis Gas	$CO + \frac{1}{2}H_2$	1.5
Char	C	2.
Coal	$C + H$	2.5
Methane	CH_4	4.

Compounds which may exist in the gas phase system containing hydrogen, oxygen, carbon, and sulfur are listed in Table 2-2. The interaction of these compounds may be described by Equations 2-3 through 2-11.

$$H_2O + CO \rightarrow H_2 + CO_2 \qquad (2\text{-}3)$$

$$3H_2 + CO \rightarrow H_2O + CH_4 \qquad (2\text{-}4)$$

$$CO + \tfrac{1}{2}O_2 \rightarrow CO_2 \qquad (2\text{-}5)$$

$$2CO + S_2 \rightarrow CO_2 + CS_2 \qquad (2\text{-}6)$$

$$CO + \tfrac{1}{2}S_2 \rightarrow COS \qquad (2\text{-}7)$$

$$2H_2S + O_2 \rightarrow S_2 + 2H_2O \qquad (2\text{-}8)$$

$$SO_2 + \tfrac{1}{2}O_2 \rightarrow SO_3 \qquad (2\text{-}9)$$

$$2SO_2 \rightarrow S_2 + 2O_2 \qquad (2\text{-}10)$$

$$H_2 + \tfrac{1}{2}O_2 \rightarrow H_2O \qquad (2\text{-}11)$$

In order to predict compositions, a model of the gas phase H-O-C-S system at equilibrium was used. It is based on a set of non-linear equations derived from thermodynamic expressions for equilibrium constant-activity relationships and mass balances for the species and reactions described in Equations 2-3 through 2-11. The solution of this set of non-linear equations yields the mole fraction and activity of each component at equilibrium at a given temperature. Fugacity coefficients were set equal to one.

TABLE 2-2

COMPOUNDS ASSUMED IN THE GAS PHASE

H_2O
H_2
CO
CO_2
CH_4
O_2
S_2
CS_2
COS
H_2S
SO_2
SO_3

2.2 Composition of Product Mixtures at Equilibrium

The gas phase equilibrium model described in Section 2.1 was used to predict the products of reaction between SO_3 and each of the six reducing agents at temperatures of 600, 1000, and 1400°C. The resulting gas phase compositions are given in Tables 2-3 through 2-8. The product compositions indicate which species predominate at the temperatures of interest. For instance, Table 2-3 shows that the products of the reaction between one mole of SO_3 and two gram atoms of hydrogen are approximately 50 mole percent SO_2 and 50 mole percent H_2O. The SO_3 and H_2 react essentially to completion and S_2 and H_2S are not produced in significant quantities. Table 2-9 lists the major products formed at 600 and 1400°C with each reducing agent. Note that SO_2 is the sulfur product formed most frequently. The undesirable products COS and CS_2 are never formed in amounts greater than 0.2%.

Some product distributions vary with a change in temperature; for instance, methane produces a regeneration product of 100% H_2S at 600°C and 86% SO_2 - 14% H_2S at 1400°C. Product distributions also vary with a change in reactant stoichiometry. The amount of various reduced species increases with an increase in reducing agent. The interaction between the products is rather complex. The total pressure was taken as one atmosphere with no diluents. A lower total pressure or addition of diluents would lower the regeneration temperature.

TABLE 2-3

REDUCING AGENT: HYDROGEN (H_2)

GASEOUS PRODUCTS OF THE REACTION BETWEEN ONE MOLE OF SO_3 AND TWO GRAM ATOMS OF HYDROGEN

	COMPOSITION AT EQUILIBRIUM Mole Fraction at 1 Atmosphere		
Component	T = 600°C	T = 1000°C	T = 1400°C
H_2	$0.118396\text{x}10^{-5}$	$0.481968\text{x}10^{-4}$	$0.551022\text{x}10^{-3}$
O_2	$.245294\text{x}10^{-12}$	$.339883\text{x}10^{-6}$	$.199154\text{x}10^{-3}$
H_2O	.499998	.499952	.499349
H_2S	$.326662\text{x}10^{-7}$	$.134609\text{x}10^{-6}$	$.133200\text{x}10^{-5}$
S_2	$.917765\text{x}10^{-11}$	$.192453\text{x}10^{-9}$	$.674711\text{x}10^{-8}$
SO_2	.499998	.499952	.499743
SO_3	$.235055\text{x}10^{-5}$	$.479374\text{x}10^{-4}$	$.156752\text{x}10^{-3}$

TABLE 2-4

REDUCING AGENT: CARBON MONOXIDE (CO)

GASEOUS PRODUCTS OF THE REACTION BETWEEN ONE MOLE OF SO_3 AND ONE MOLE OF CARBON MONOXIDE

COMPOSITION AT EQUILIBRIUM

	Mole Fraction At 1 Atmosphere		
Component	T = 600°C	T = 1000°C	T = 1400°C
CO	$.513035\text{x}10^{-5}$	$.612247\text{x}10^{-4}$	.116270-02
O_2	$.183394\text{x}10^{-14}$	$.535616\text{x}10^{-6}$	.462035-03
CO_2	.499994	.499939	.498606
S_2	$.164187\text{x}10^{-6}$	$.774918\text{x}10^{-10}$	.125249-08
CS_2	$.123942\text{x}10^{-14}$	$.303624\text{x}10^{-19}$	.320641-17
COS	$.499079\text{x}10^{-7}$	$.263125\text{x}10^{-9}$	.276169-08
SO_2	.500000	.499940	.499530
SO_3	$.203246\text{x}10^{-6}$	$.601762\text{x}10^{-4}$	.238655-03

TABLE 2-5

REDUCING AGENT: SYNTHESIS GAS ($CO + \frac{1}{2}H_2$)

GASEOUS PRODUCTS OF THE REACTION BETWEEN ONE MOLE OF SO_3, ONE MOLE OF CARBON MONOXIDE AND ONE GRAM ATOM OF HYDROGEN (H)

COMPOSITION AT EQUILIBRIUM

	Mole Fraction At 1 Atmosphere		
Component	T = 600°C	T = 1000°C	T = 1400°C
H_2O	.153228	.164597	.135788
CO	$.776387\text{x}10^{-4}$	$.734461\text{x}10^{-2}$	$.376903\text{x}10^{-1}$
H_2	$.759325\text{x}10^{-4}$	$.176317\text{x}10^{-2}$	$.436810\text{x}10^{-2}$
CO_2	.427168	.417200	.359935
CH_4	$.107080\text{x}10^{-15}$	$.208966\text{x}10^{-5}$	$.339941\text{x}10^{-1}$
O_2	$.584507\text{x}10^{-17}$	$.259192\text{x}10^{-10}$	$.229132\text{x}10^{-6}$
S_2	$.796167\text{x}10^{-2}$	$.159053\text{x}10^{-1}$	$.354527\text{x}10^{-2}$
CS_2	$.161107\text{x}10^{-7}$	$.107468\text{x}10^{-6}$	$.132114\text{x}10^{-7}$
COS	$.166316\text{x}10^{-3}$	$.452219\text{x}10^{-3}$	$.150616\text{x}10^{-3}$
H_2S	$.604023\text{x}10^{-1}$	$.461350\text{x}10^{-1}$	$.774064\text{x}10^{-2}$
SO_2	.350920	.346600	.416784
SO_3	$.805311\text{x}10^{-8}$	$.290216\text{x}10^{-6}$	$.443430\text{x}10^{-5}$

TABLE 2-6

REDUCING AGENT: CHAR (C)

GASEOUS PRODUCTS OF THE REACTION BETWEEN ONE MOLE OF SO_3 AND ONE MOLE OF CARBON

COMPOSITION AT EQUILIBRIUM

	Mole Fraction at 1 Atmosphere		
Component	T = 600°C	T = 1000°C	T = 1400°C
CO	$.234833\text{x}10^{-3}$	$.178657\text{x}10^{-1}$	.118337
O_2	$.113495\text{x}10^{-17}$	$.756482\text{x}10^{-11}$	$.337866\text{x}10^{-7}$
CO_2	.569342	.548256	.433955
S_2	.141274	.135454	.107185
CS_2	$.196226\text{x}10^{-5}$	$.412089\text{x}10^{-5}$	$.326585\text{x}10^{-5}$
COS	$.211906\text{x}10^{-2}$	$.321014\text{x}10^{-2}$	$.260020\text{x}10^{-2}$
SO_2	.287028	.295210	.337918
SO_3	$.290251\text{x}10^{-8}$	$.133540\text{x}10^{-6}$	$.138056\text{x}10^{-5}$

TABLE 2-7

REDUCING AGENT: COAL (C:H = 1:1)

GASEOUS PRODUCTS OF THE REACTION BETWEEN ONE MOLE OF SO_3, ONE MOLE OF CARBON, AND ONE GRAM ATOM OF HYDROGEN (H)

COMPOSITION AT EQUILIBRIUM

Component	Mole Fraction at 1 Atmosphere		
	T = 600°C	T = 1000°C	T = 1400°C
H_2O	$.761338\text{x}10^{-1}$	.108435	$.469918\text{x}10^{-1}$
CO	$.188428\text{x}10^{-3}$	$.161235\text{x}10^{-1}$	$.777471\text{x}10^{-1}$
H_2	$.799368\text{x}10^{-4}$	$.228384\text{x}10^{-2}$	$.332204\text{x}10^{-2}$
CO_2	.489312	.465814	.337852
CH_4	$.610229\text{x}10^{-15}$	$.151332\text{x}10^{-4}$	$.891323\text{x}10^{-1}$
O_2	$.130206\text{x}10^{-17}$	$.670468\text{x}10^{-11}$	$.474441\text{x}10^{-7}$
S_2	$.562874\text{x}10^{-1}$	$.768056\text{x}10^{-1}$	$.610661\text{x}10^{-1}$
CS_2	$.585686\text{x}10^{-6}$	$.223997\text{x}10^{-5}$	$.103159\text{x}10^{-5}$
COS	$.107325\text{x}10^{-2}$	$.218155\text{x}10^{-2}$	$.128945\text{x}10^{-2}$
H_2S	.169073	.131319	$.244324\text{x}10^{-1}$
SO_2	.207852	.197020	.358164
SO_3	$.225128\text{x}10^{-8}$	$.839037\text{x}10^{-7}$	$.173398\text{x}10^{-5}$

TABLE 2-8

REDUCING AGENT: METHANE (CH_4)

GASEOUS PRODUCTS OF THE REACTION BETWEEN ONE MOLE OF SO_3, ONE MOLE OF CARBON, AND FOUR GRAM ATOMS OF HYDROGEN (H)

COMPOSITION AT EQUILIBRIUM

Component	Mole Fraction at 1 Atmosphere		
	T = 600°C	T = 1000°C	T = 1400°C
H_2O	.332826	.335427	.240288
CO	$.688416x10^{-3}$	$.240621x10^{-1}$	$.208380x10^{-1}$
H_2	$.188172x10^{-2}$	$.163271x10^{-1}$	$.122353x10^{-1}$
CO_2	.331990	.300795	.125719
CH_4	$.665248x10^{-11}$	$.266753x10^{-2}$	.233412
O_2	$.449050x10^{-19}$	$.125529x10^{-11}$	$.914511x10^{-7}$
S_2	$.390023x10^{-3}$	$.784554x10^{-2}$	$.126183x10^{-1}$
CS_2	$.798397x10^{-7}$	$.789156x10^{-6}$	$.411506x10^{-7}$
COS	$.326399x10^{-3}$	$.104053x10^{-2}$	$.157099x10^{-3}$
H_2S	.331301	.300044	$.409046x10^{-1}$
SO_2	$.596700x10^{-3}$	$.117894x10^{-1}$	.313826
SO_3	$.120023x10^{-11}$	$.217244x10^{-8}$	$.210937x10^{-5}$

TABLE 2-9

MAJOR PRODUCTS OF THE REACTION OF SO_3 WITH REDUCING AGENTS

Reactants	Sulfur Bearing Products 600°C	Sulfur Bearing Products 1400°C	Other Products 600°C	Other Products 1400°C
$SO_3 + H_2$	100% SO_2	100% SO_2	100% H_2O	100% H_2O
$SO_3 + CO$	100% SO_2	100% SO_2	100% CO_2	100% CO_2
$SO_3 + CO + H$	83% SO_2 17% H_2S	100% SO_2	75% CO_2 25% H_2O	63% CO_2 24% H_2O 6% CH_4 7% CO
$SO_3 + C + H$	50% SO_2 40% H_2S 10% S_2	86% SO_2 14% S_2	88% CO_2 12% H_2O	66% CO_2 16% CH_4 9% H_2O 14% CO
$SO_3 + C$	66% SO_2 34% S_2	75% SO_2 25% S_2	100% CO_2	80% CO_2 20% CO
$SO_3 + CH_4$	100% H_2S	86% SO_2 14% H_2S	50% CO_2 50% H_2O	20% CO_2 40% CH_4 40% H_2O

3.0 IDENTIFICATION OF CONDITIONS AT WHICH REDUCTIVE DECOMPOSITION OF METAL SULFATES OCCURS

This section describes the use of thermodynamic data to predict the temperatures at which reductive decomposition of metal sulfates can occur with the six reducing agents. Methods of data generation and analysis are described in Section 3.1 and results are given in Section 3.2.

There are several computational schemes by which the answer may be obtained. One is, for a given compound and temperature, to choose a stoichiometry for which the P_{SO_3} of the gas exactly balances that of the solid. This would require an iterative calculation of several stoichiometries at each temperature. Or, by choosing a fixed stoichiometry at three temperatures the actual regeneration temperature may be interpolated.

From a process point of view the temperature conditions correspond to that of the exit gas. Since the activity of solid is unity, this analysis would be applicable to a cocurrent reactor. The reacting gas could be in contact with the last trace of solid sulfate if a stoichiometric amount of solid sorbent were circulated. The gas could be in contact with a considerable amount of excess sulfate if more than stoichiometric sorbent were circulated. This analysis would also be applicable to the exit gas/inlet solid of a countercurrent reactor. As the gas exits after picking up the required amount of sulfur there still must be a slight driving force available.

3.1 Methods of Thermodynamic Analysis of Sulfate Reduction Reactions

The feasibility of reduction of metal sulfates to metal oxides was determined by comparing the equilibrium partial pressure of SO_3 in the six reducing gases to the equilibrium vapor pressure of SO_3 over the metal sulfate. At temperatures where the SO_3 vapor pressure over the sulfate is greater than P_{SO_3} in the reducing gas, there is driving force for the sulfate to give up SO_3, or decompose to the oxide.

The data needed for this analysis were SO_3 partial pressures in the reducing gases as a function of temperature and vapor pressures of SO_3 over metal sulfates as a function of temperature.

Section 2.1 described how the equilibrium compositions of six reducing gases were calculated as a function of temperature. Tables 2-3 through 2-8 gave the detailed composition in mole fraction for each reducing gas at 600, 1000, and 1400°C at one atmosphere total pressure. The mole fraction (activity) of SO_3 is equal to the partial pressure at one atmosphere total pressure. The $\log_{10} P_{SO_3}$ for each reducing gas taken from Tables 2-3 through 2-8 is plotted in Figure 3-1.

Both Radian Technical Note 200-045-10-01a and previous work (PA-016) describe the methods used to calculate metal sulfate SO_3 vapor pressures as a function of temperature. Briefly, the equilibrium constant for metal sulfate decomposition reaction is described in Equation 3-1, where a_n is the activity of the n^{th} product or reactant.

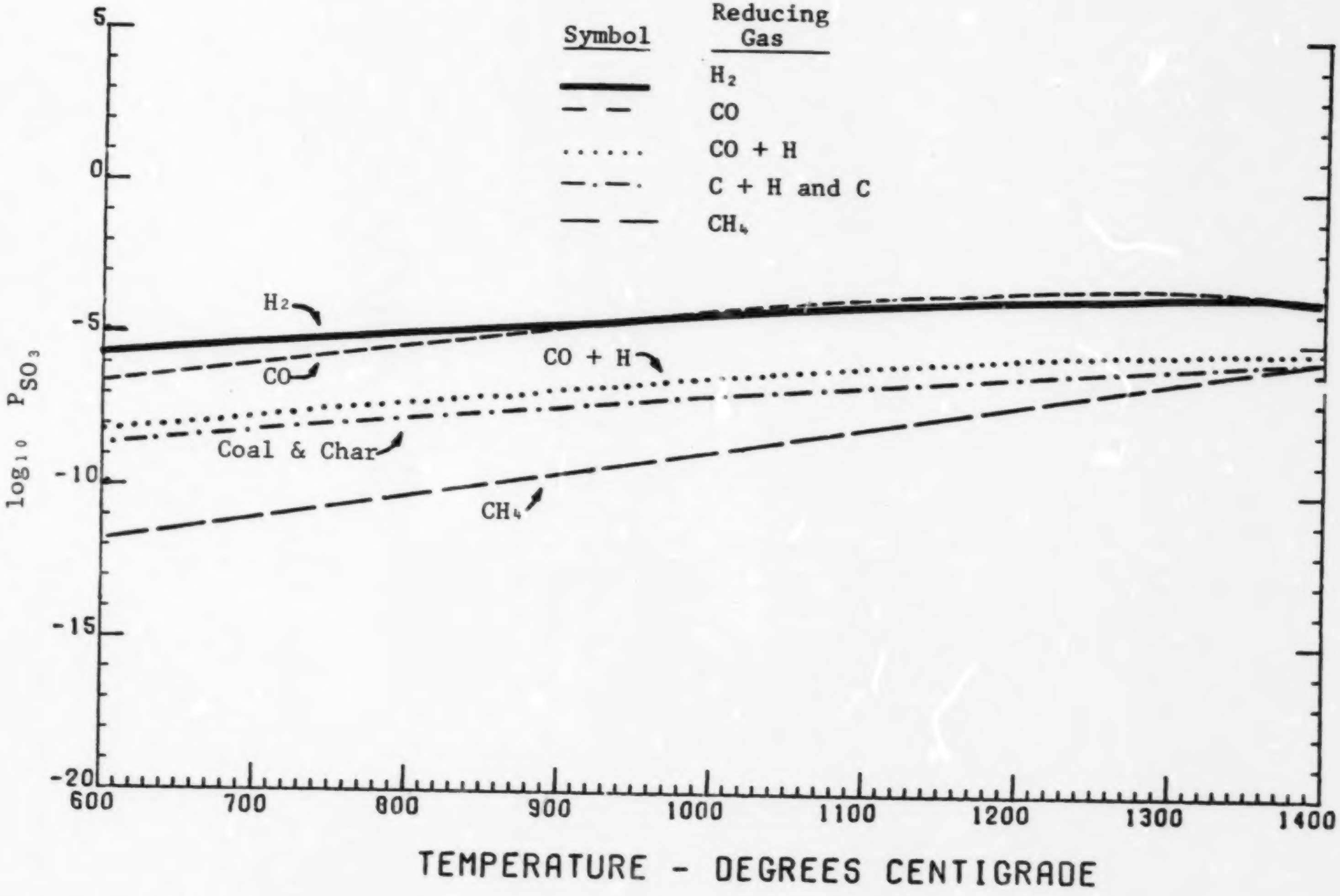

FIGURE 3-1 - LOG$_{10}$P$_{SO_3}$ IN SIX REDUCING GASES AS A FUNCTION OF TEMPERATURE

$$K_{eq} = \frac{a_{MeO}a_{SO_3}}{a_{MeSO_4}} \qquad (3\text{-}1)$$

Since activities of solids are equal to 1, the equilibrium constant is numerically equal to the activity of SO_3 at equilibrium (or the mole fraction at one atmosphere) when the reaction is normalized to one mole of SO_3. Graphs of $\log_{10}K_{eq}$ (equal to $\log_{10}P_{SO_3}$) for metal sulfate decomposition reactions from 600 to 1400°C are given in the Appendix of Technical Note 200-045-10-01a. An example for the calcium sulfate decomposition reaction is shown in Figure 3-2.

3.2 Results of Thermodynamic Analysis of Sulfate Reduction Reactions

Using data such as those shown in Figures 3-1 and 3-2, the vapor pressure of SO_3 over metal sulfates may be compared to the partial pressure of SO_3 in reducing gases in the temperature range from 600 to 1400°C. This comparison is facilitated by plotting both the SO_3 vapor pressure and the reducing gas SO_3 partial pressure data on the same set of coordinates. An example is shown in Figure 3-3 for calcium sulfate. Figure 3-3 shows that the line representing the SO_3 vapor pressure over calcium sulfate intersects the line representing the equilibrium partial pressure of SO_3 in a gas containing a mole of methane and a mole of SO_3 at a temperature of about 730°C. Below 730°C there is driving force for the sulfate to absorb SO_3 from the reducing gas, and above 730°C there is driving force for the sulfate to give up SO_3 to the gas or decompose. Figure 3-3 shows that the corresponding decomposition temperature for a reducing gas produced by coal or char is 960°C. For $CO + \frac{1}{2}H_2$ reducing gas the minimum decomposition temperature is about 1025°C. For one mole

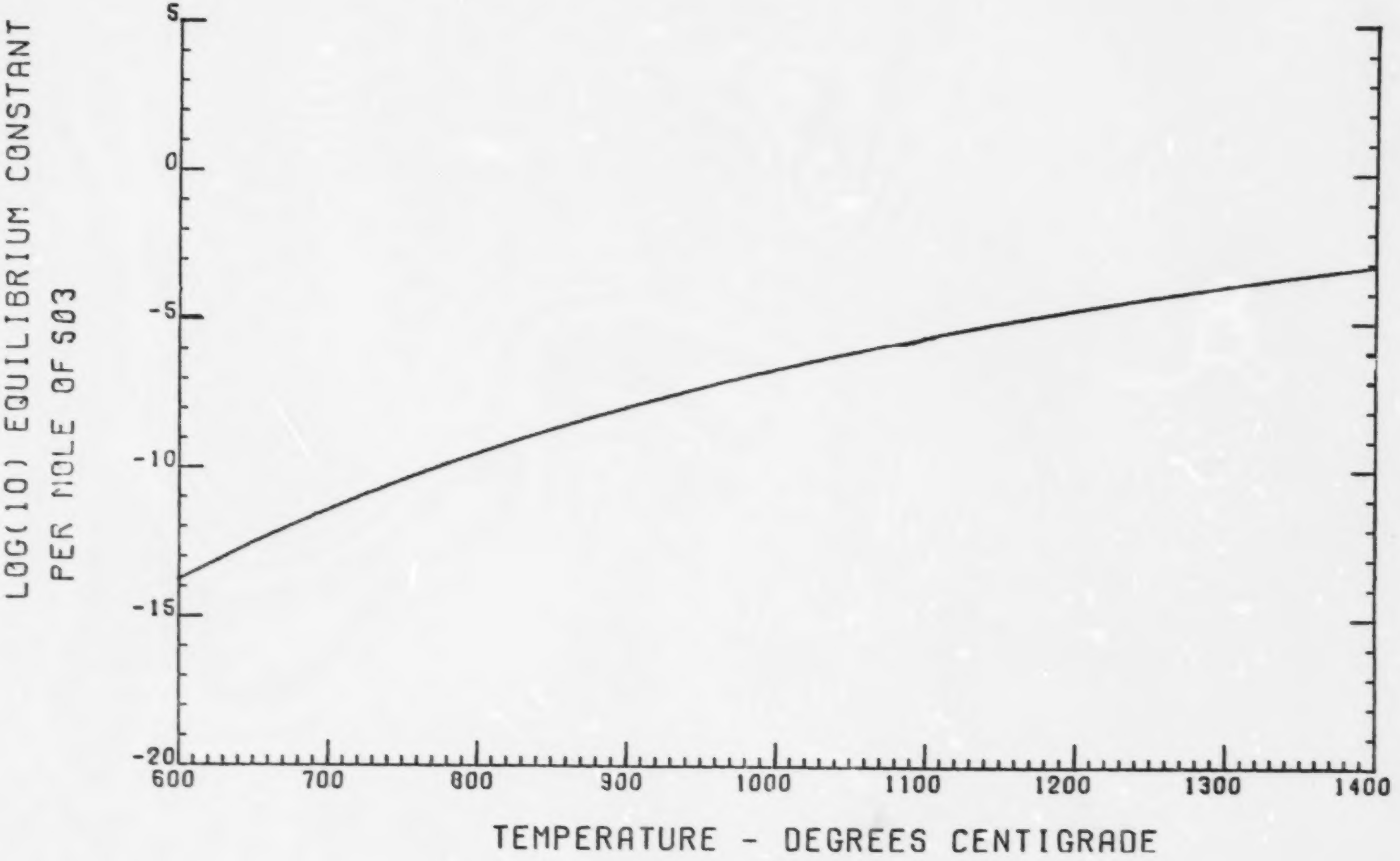

FIGURE 3-2 - LOG K VERSUS T FOR THE REACTION

$CaSO_4 \rightleftarrows CaO + SO_3$

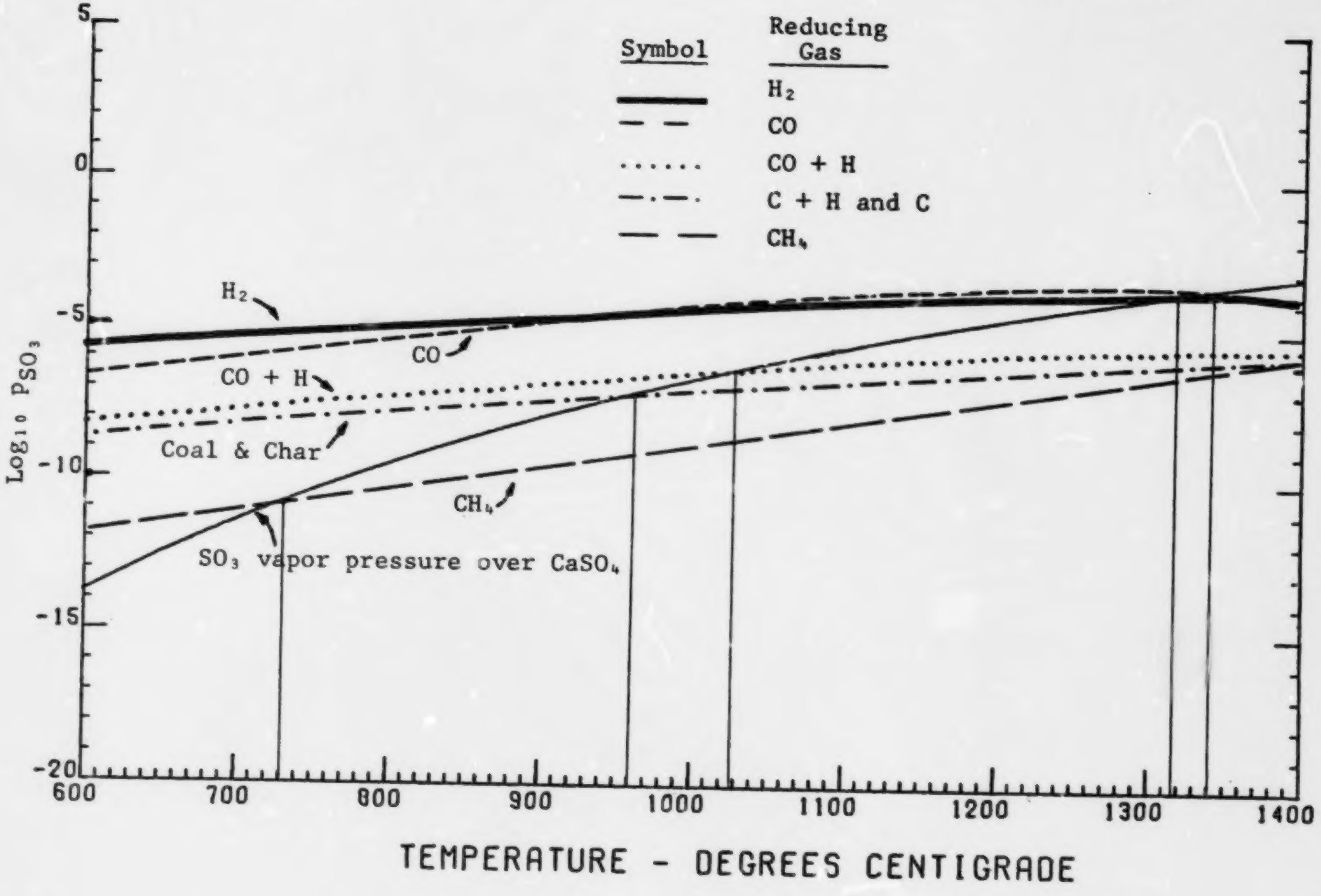

FIGURE 3-3 - COMPARISON OF $CaSO_4$ VAPOR PRESSURE WITH P_{SO_3} IN REGENERATION CASES

of carbon monoxide or one mole of hydrogen (H_2) the minimum temperatures for reductive decomposition of sulfate are approximately 1340 and 1320, respectively. Graphs such as those shown in Figure 3-3 comparing sulfate vapor pressures with reducing gas SO_3 partial pressures were prepared for each potential metal oxide sorbent. They are included in the Appendix. Table 3-1, taken from Figures A-1 through A-14 in the Appendix, lists the minimum temperatures for reductive decomposition at one atmosphere pressure for each metal sulfate listed in Table 1-1 in each reducing gas.

TABLE 3-1

MINIMUM TEMPERATURES AT WHICH METAL SULFATES ARE REDUCED BY SIX REDUCING AGENTS*

	Temperature (°C)					
Reducing Agents / Metal Sulfates	Hydrogen H_2	Carbon Monoxide CO	Synthesis Gas $CO + \frac{1}{2}H_2$	Coal C/H = 1	Char C	Methane CH_4
Na_2SO_4	>1400	>1400	>1400	>1400	>1400	>1400
$CaSO_4$	1320	1340	1025	960	960	730
$SrSO_4$	>1400	>1400	1310	1240	1210	1060
$BaSO_4$	>1400	>1400	>1400	>1400	>1400	>1400
$Li_2SO_4 + Al_2O_3$	>1400	>1400	1400	960	960	
$Li_2SO_4 + Fe_2O_3$	1110	1160	825	775	785	<600
$Li_2SO_4 + TiO_2$	>1400	>1400	1350	1140	1140	660
$Na_2SO_4 + Al_2O_3$	830	800	670	645	655	<600
$Na_2SO_4 + Fe_2O_3$	1220	1245	930	875	890	670
$CaSO_4 + Al_2O_3$	1180	1220	840	790	800	600
$SrSO_4 + Al_2O_3$	1250	1290	900	840	860	640
$SrSO_4 + TiO_2$	1020	1040	775	735	740	<600
$BaSO_4 + Al_2O_3$	1230	1290	890	840	850	630
$BaSO_4 + TiO_2$	1190	1220	910	850	860	630

---

* Minimum temperature for which the vapor pressure of SO_3 over the metal sulfate is greater than the partial pressure of SO_3 in the reducing gas.

4.0 INVESTIGATION OF THE POSSIBILITY OF METAL SULFIDE FORMATION

The model used for thermodynamic analysis of potential SO_2 removal processes includes reactions for SO_2 sorption with metal sulfate formation and regeneration of the metal oxide by reductive decomposition of the metal sulfate. Other possible reactions include reduction of the metal oxide all the way to the elemental state (metal) or the formation of metal sulfide through reaction of the metal oxide with sulfur species present in the reducing gas. Reduction of the sulfate to the metal by the reducing gas has been reported by Shell to occur during reduction of copper oxide SO_2 sorbent by hydrogen (PO-001). This was not a serious problem for Shell since formation of the oxide occurs readily in the oxidizing atmosphere of the combustion gas. Formation of metal sulfide would require an additional processing step of a solid at high temperature. This is to be avoided if possible. Therefore, this study included identification of the conditions under which sulfide formation might be expected during reductive sulfate decomposition. The methods of data generation and analysis for this investigation are given in Section 4.1, and the results are given in Section 4.2.

4.1 Method of Thermodynamic Analysis of the Sulfide Formation Reaction

One reaction which describes formation of metal sulfides from the oxide is given in Equation 4-1.

$$2MeO + S_2 \rightarrow 2MeS + O_2 \qquad (4\text{-}1)$$

Since the gas mixture is an equilibrium mixture the exact reaction path is not important. All reaction paths would give the same results at the same equilibrium temperature. The equilibrium constant for the reaction is described in Equation 4-2, where a_n is the activity of the $n^{\underline{th}}$ product or reactant.

$$K_{eq}(T) = \frac{a^2_{MeS}a_{O_2}}{a^2_{MeO}a_{S_2}} \qquad (4\text{-}2)$$

Since the activities of solid species are equal to one, the equilibrium constant for such a reaction is numerically equal to the ratio of oxygen and sulfur activities at equilibrium for the reaction normalized to one mole of O_2 and S_2. As described in Section 3.0, the equilibrium constant for a reaction may be calculated from standard state thermodynamic properties. As an example, the equilibrium constant for the calcium oxide-sulfide conversion reaction is shown in Figure 4-1.

The ratio of oxygen and sulfur activities for the oxide-sulfide conversion reaction at equilibrium may be compared with the ratio of oxygen and sulfur activities that actually exist in the reducing gases. The temperature at which the a_{O_2}/a_{S_2} in the reducing gas is equal to a_{O_2}/a_{S_2} for the oxide sulfide conversion reaction at equilibrium is the transition temperature. The region where the a_{O_2}/a_{S_2} of the gas is greater is the region of oxide stability. The other region is the sulfide stable range.

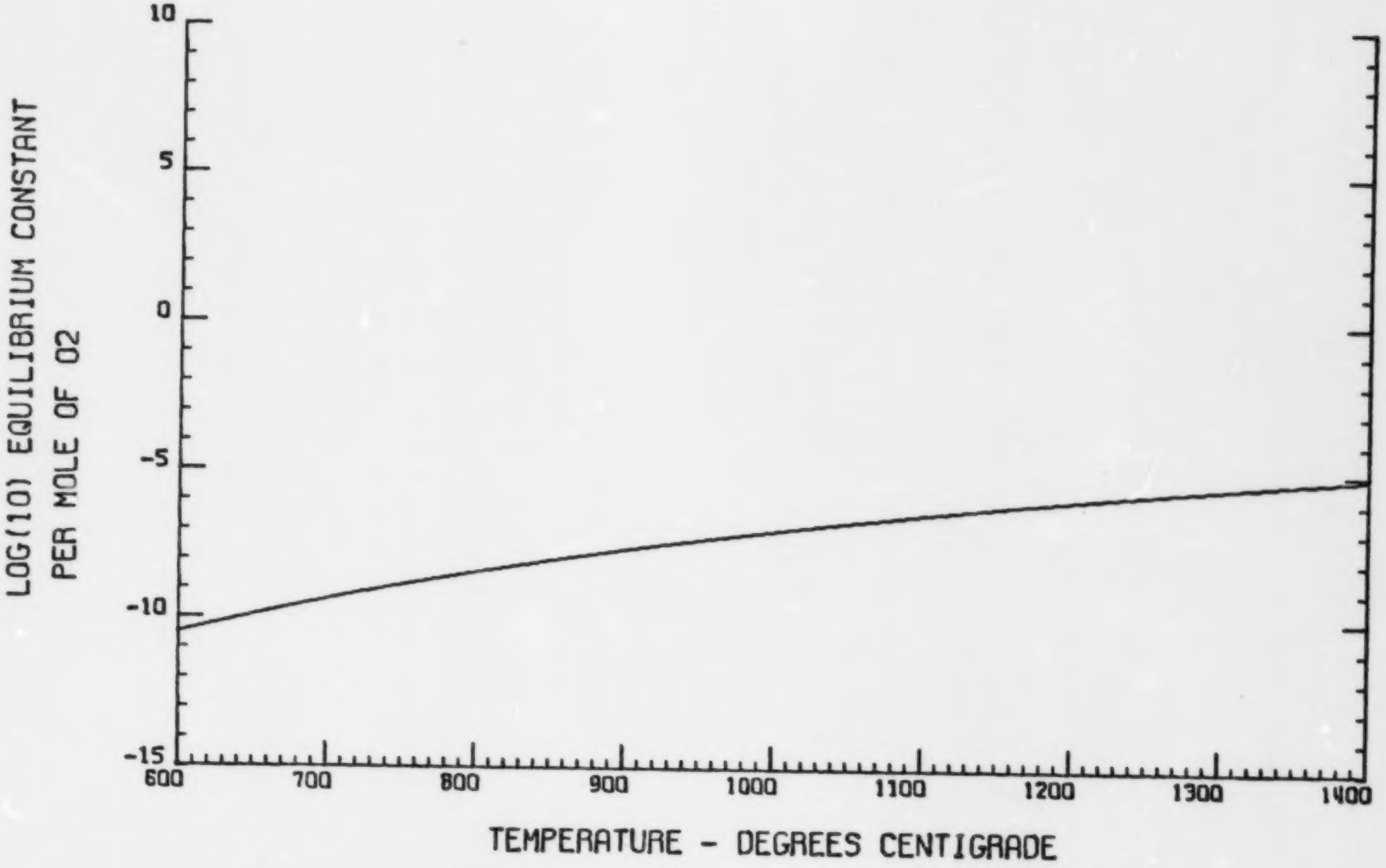

FIGURE 4-1 - LOGARITHM OF THE EQUILIBRIUM CONSTANT FOR THE REACTION $2CaO + S_2 \rightarrow O_2 + 2CaS$

07 NOV 74

Activities of oxygen and sulfur in the reducing gases at 600, 1000 and 1400°C were calculated using the gas phase equilibrium model as described in Section 2.0. Figure 4-2, taken from Tables 2-3 through 2-8 in Section 2.0, shows $\log_{10}$ a_{O_2}/a_{S_2} in the reducing gases from 600 to 1400°C.

4.2 Results of Thermodynamic Analysis of the Sulfide Formation Reaction

Using data such as those shown in Figures 4-1 and 4-2, the oxygen-sulfur activity ratios in reducing gases were compared with the ratios for oxide-sulfur conversion reactions at equilibrium. Again, the comparison was done by plotting both sets of data on one set of coordinates as shown in Figure 4-3 for calcium oxide-sulfide conversion. Figure 4-3 indicates that at 1250°C the line representing $\log_{10}$ a_{O_2}/a_{S_2} over calcium oxide intersects the line representing $\log_{10}$ a_{O_2}/a_{S_2} in a gas composed of one mole of SO_3, a mole of CO and one-half mole of H_2. At temperatures below 1250 there is a driving force for calcium oxide conversion to calcium sulfide. At temperatures above 1250 there would be driving force for the sulfide to oxide conversion. It can be concluded that the minimum temperature for oxide stability with respect to sulfide formation during the reductive decomposition of calcium sulfate by CO + $\frac{1}{2}H_2$ is 1250°C. Figure 4-3 also shows that for calcium sulfate reduction by methane, the minimum temperature for prevention of calcium sulfide formation is 1370°C. For one mole of either carbon monoxide or hydrogen (H_2) alone, calcium oxide is stable throughout the temperature range 600 to 1400°C. The oxide-sulfide conversion temperature

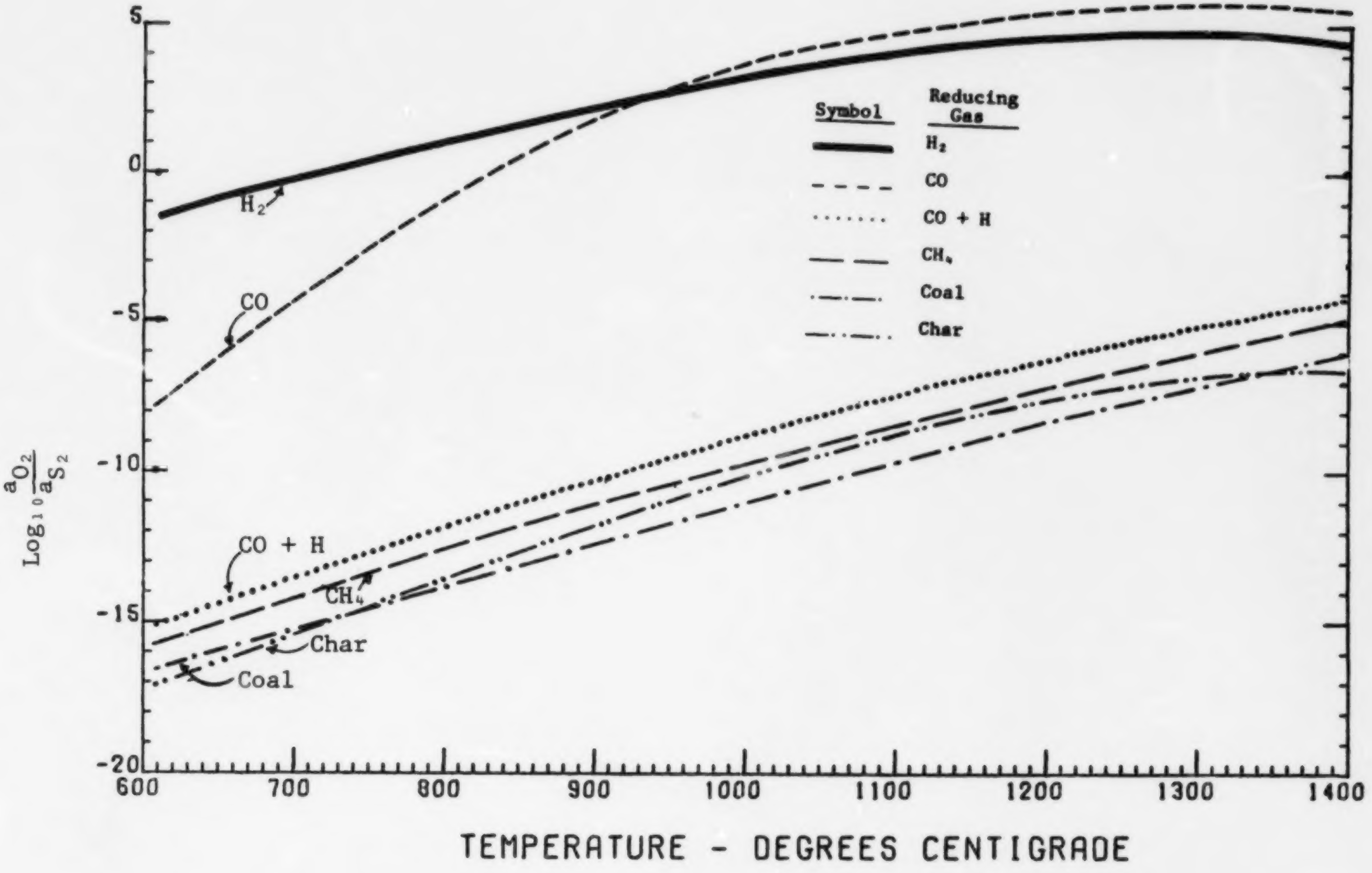

FIGURE 4-2 - VARIATION OF THE LOGARITHM OF THE OXYGEN-SULFUR ACTIVITY RATIO WITH TEMPERATURE IN FIVE REDUCING GASES

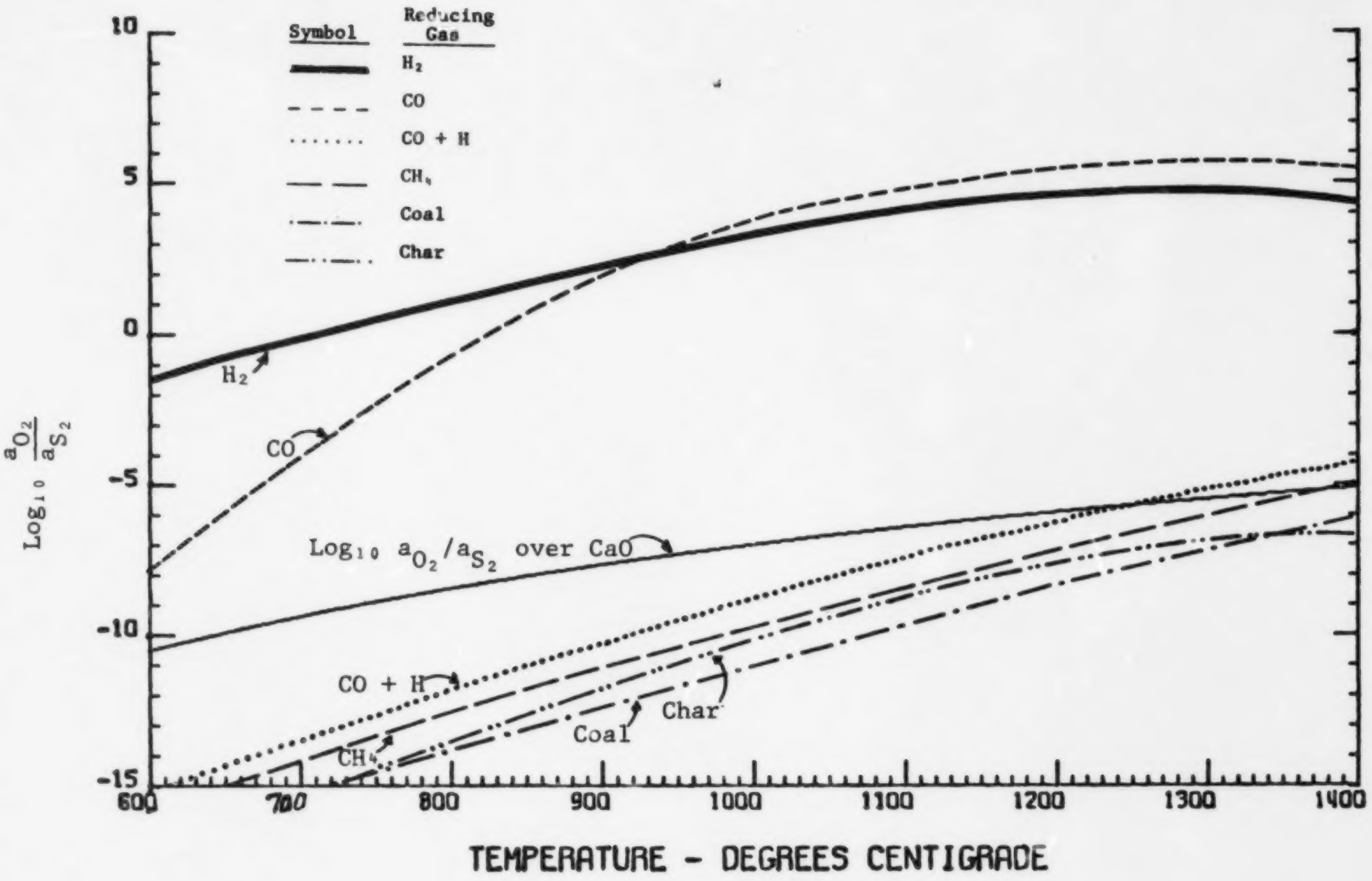

FIGURE 4-3 - COMPARISON OF OXYGEN-SULFUR ACTIVITY RATIOS IN REGENERATION GASES WITH THE RATIO FOR THE REACTION $2CaO + S_2 \rightarrow 2CaS + O_2$

07 NOV 74

is very stoichiometry dependent (see Table 2-2). For coal or char the minimum temperature for calcium oxide stability is greater than 1400°C. Graphs such as the one in Figure 4-3 were prepared for all of the metal oxides considered in this study and are included in the Appendix, Figures A-15 through A-30. Table 4-1 summarizes data from the graphs for the minimum temperature of stability of the metal oxides in each of the six reducing gases.

These calculations correspond to the physical situation in a cocurrent reactor. The gas phase would be in contact with the solid phase of interest, i.e., the solid exiting the regenerator. A counter current reactor does not have the exiting solid in contact with the gas phase composition here. The solid of interest will "see" a stronger reducing atmosphere. It would be expected that sulfide formation would be more of a problem in a counter current than a cocurrent reactor.

Other considerations are that the regeneration pressure is one atmosphere and there are no diluents present. Low pressure operation or diluents could lower the decomposition temperature. An inspection of the log plots can indicate the changes involved.

TABLE 4-1

MINIMUM TEMPERATURE OF STABILITY OF METAL OXIDE WITH RESPECT TO FORMATION OF METAL SULFIDE IN REDUCING GAS*

Reducing Agents / Metal Oxide	Temperature (°C) Hydrogen H_2	Carbon Monoxide CO	Synthesis Gas $CO + \frac{1}{2}H_2$	Coal C/H = 1	Char C	Methane CH_4
Na_2O	970	955	>1400	>1400	>1400	>1400
CaO	<600	<600	1250	>1400	>1400	1370
SrO	<600	590	>1400	>1400	>1400	>1400
BaO	<600	700	>1400	>1400	>1400	>1400
$LiAlO_2$	<600	<600	<600	<600	<600	<600
$LiFeO_2$	<600	<600	750	1100	975	890
Al_2O_3	<600	<600	<600	<600	<600	<600
TiO_2	600-1190	880-1325	>1400	>1400	>1400	>1400
$NaAlO_2$	<600	<600	<600	<600	600	<600
$NaFeO_2$	<600	<600	820	1175	1030	980
$CaAl_2O_4$	<600	<600	740	1360	970-1350	890
$SrAl_2O_4$	<600	<600	<600	<600	<600	<600
$SrTiO_3$	<600	<600	<600	<600	<600	<600
$BaAl_2O_4$	<600	<600	<600	<600	<600	<600
$BaTiO_3$	<600	<600	<600	<600	<600	<600
Li_2TiO_3	<600	<600	<600	<600	<600	<600

---

* Minimum temperature at which the ratio of oxygen activity to sulfur activity in the reducing gas is greater than the ratio of oxygen to sulfur activities at equilibrium for the reaction $2MeO + S_2 \rightarrow 2MeS + O_2$.

5.0 RESULTS

Using thermodynamic analysis, three types of predictions have been made for each candidate metal oxide sorbent:

1. the temperature range in which there is a driving force for SO_2 sorption with sulfate formation,
2. the temperature range in which there is a driving force for reductive decomposition of the sulfate with six reducing agents of varying reduction potentials,
3. the temperature range in which metal oxide formation is favored over metal sulfide formation during sulfate reduction with the six reducing agents.

A temperature range of 600 to 1400°C was selected for this analysis on the bases of the operating temperature of fluidized bed combustion processes and the physical properties of construction materials.

An estimate of the heat of reaction is advisable since heat transfer should be minimized where possible. The heat requirement for regeneration of calcium sulfate with CO may be considered from the following simplified scheme (see Table 2-4).

$$CaSO_4 \rightarrow CaO + SO_3 \qquad (5\text{-}1)$$

$$SO_3 + CO \rightarrow SO_2 + CO_2 \qquad (5\text{-}2)$$

The heats of formation at 25°C may be used to estimate the heat of reaction at other temperatures. Heats of formation are given in Table 5-1.

Reaction 5-1 is endothermic with an enthalpy change of +94.1 Kcal. Reaction 5-2 is exothermic with an enthalpy change of -44.1. The overall reductive decomposition of the sulfate is the sum of these reactions. It is endothermic at +50.0 Kcal.

If hydrogen were the reducing agent, then the gas phase reaction could be approximated by 5-3 (see Table 2-3).

$$SO_3 + H_2 \rightarrow SO_2 + H_2O \qquad (5\text{-}3)$$

Reaction 5-3 is exothermic at -34.3 with the overall reaction being endothermic at +59.8 Kcal. This will have process implications for minimizing heat transfer.

5.1 Summary of Results for Each Metal Oxide

The following paragraphs summarize the results for each candidate metal oxide sorbent. Figures 5-1 through 5-14 show the predicted temperature ranges for sorption with sulfate formation for each metal oxide and the temperature ranges at which sulfate decomposition and oxide stability are predicted for each metal oxide-reducing agent combination. Again the basis for these calculations must be kept in mind. Changes in the design basis would alter the temperature ranges somewhat.

The temperature range in which sorption, regeneration, or oxide stability are predicted is indicated in the figures by cross-hatching. For an example, please see Figure 5-1. Sorption of SO_2 by sodium oxide to form sodium sulfate is predicted to occur from 600 to 1380°C, so the diagram shows cross-hatching on the bottom line from 600 to 1380 on the temperature scale.

TABLE 5-1

HEATS OF FORMATION AT 25°C

Compound	ΔH, Kcal/gmole
CaO	-151.7
$CaSO_4$	-340.2
SO_2	-70.9
SO_3	-94.4
CO	-26.4
CO_2	-94.0
$H_2O(g)$	-57.8

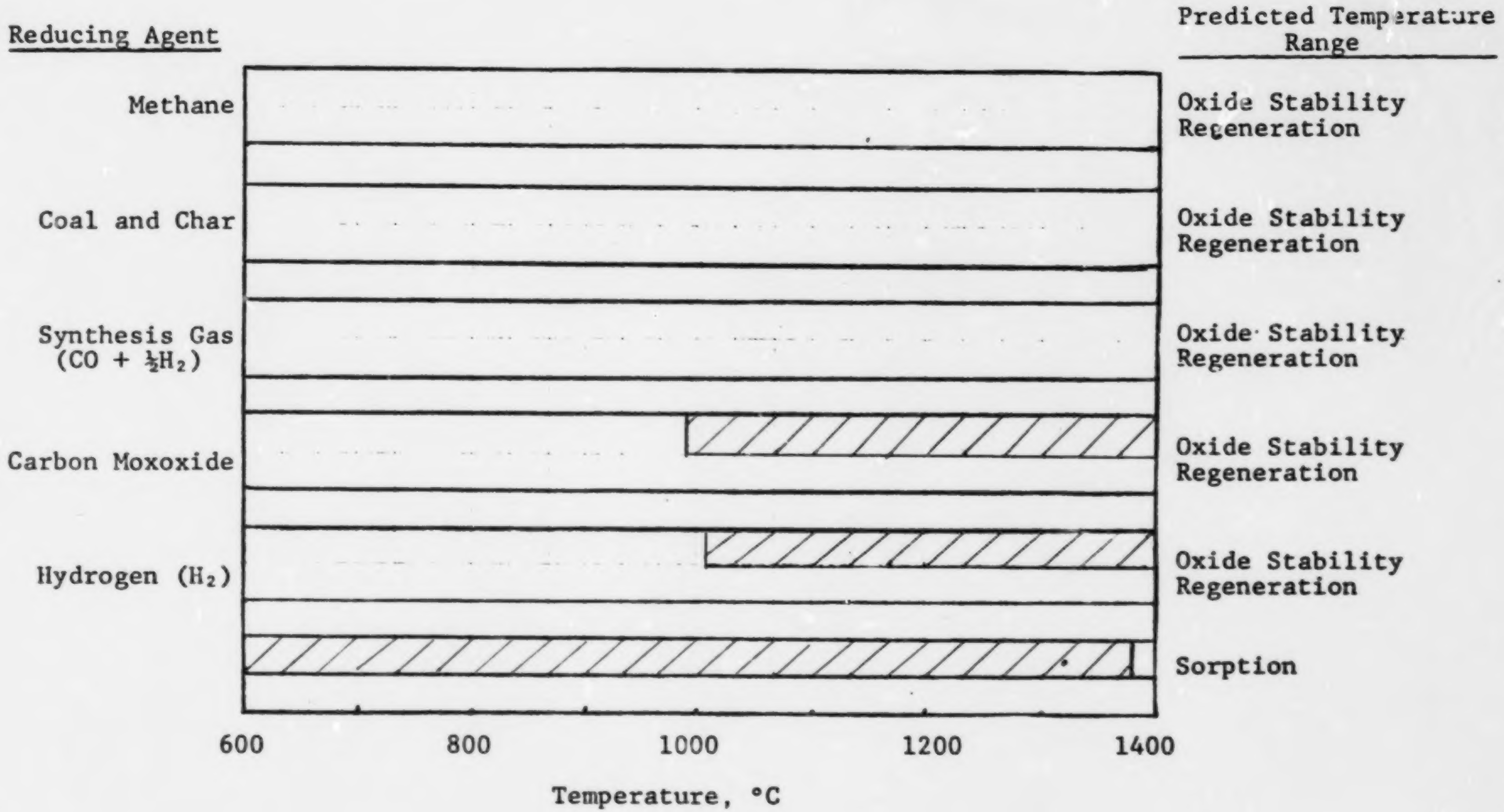

FIGURE 5-1 - TEMPERATURE REGIONS IN WHICH SORPTION, REGENERATION, AND OXIDE STABILITY ARE FAVORED FOR Na_2O

Sodium Oxide

Figure 5-1 summarizes the data for a sodium oxide sorption-regeneration process. The first (lowest) line indicates that sorption to form sodium sulfate occurs up to about 1375°C. The second line indicates that sodium oxide rather than sodium sulfide would be formed at temperatures above 970°C if hydrogen were used as the reducing gas, but that regeneration does not occur with hydrogen up to 1400°C. In fact, Figure 5-1 shows that sodium sulfate is so stable that it cannot be reduced by any of the six reducing agents below 1400°C

Calcium Oxide

Figure 5-2 shows that sorption can occur up to 1100°C. Regeneration is possible with stoichiometric hydrogen above 1320°C. It is possible with stoichiometric CO above 1340°C. The oxide will be formed. Increasing the reducing agent strength to synthesis gas ($CO + \frac{1}{2}H_2$ per mole SO_3) lowers the potential regeneration temperature to about 1020°C. One would expect calcium sulfide formation below 1250°C. Regeneration with the greater stoichiometries will produce the sulfide.

Strontium Oxide

Figure 5-3 shows that there is no temperature between 600 and 1400°C at which regeneration and oxide stability occur simultaneously. For those reducing agents which are predicted to be effective regenerators, strontium sulfide formation can occur. Strontium sulfide formation would not be predicted in stoichiometric carbon monoxide or hydrogen, but sulfate decomposition does not occur at temperatures below 1400°C with these reducing agents. (An increase in the

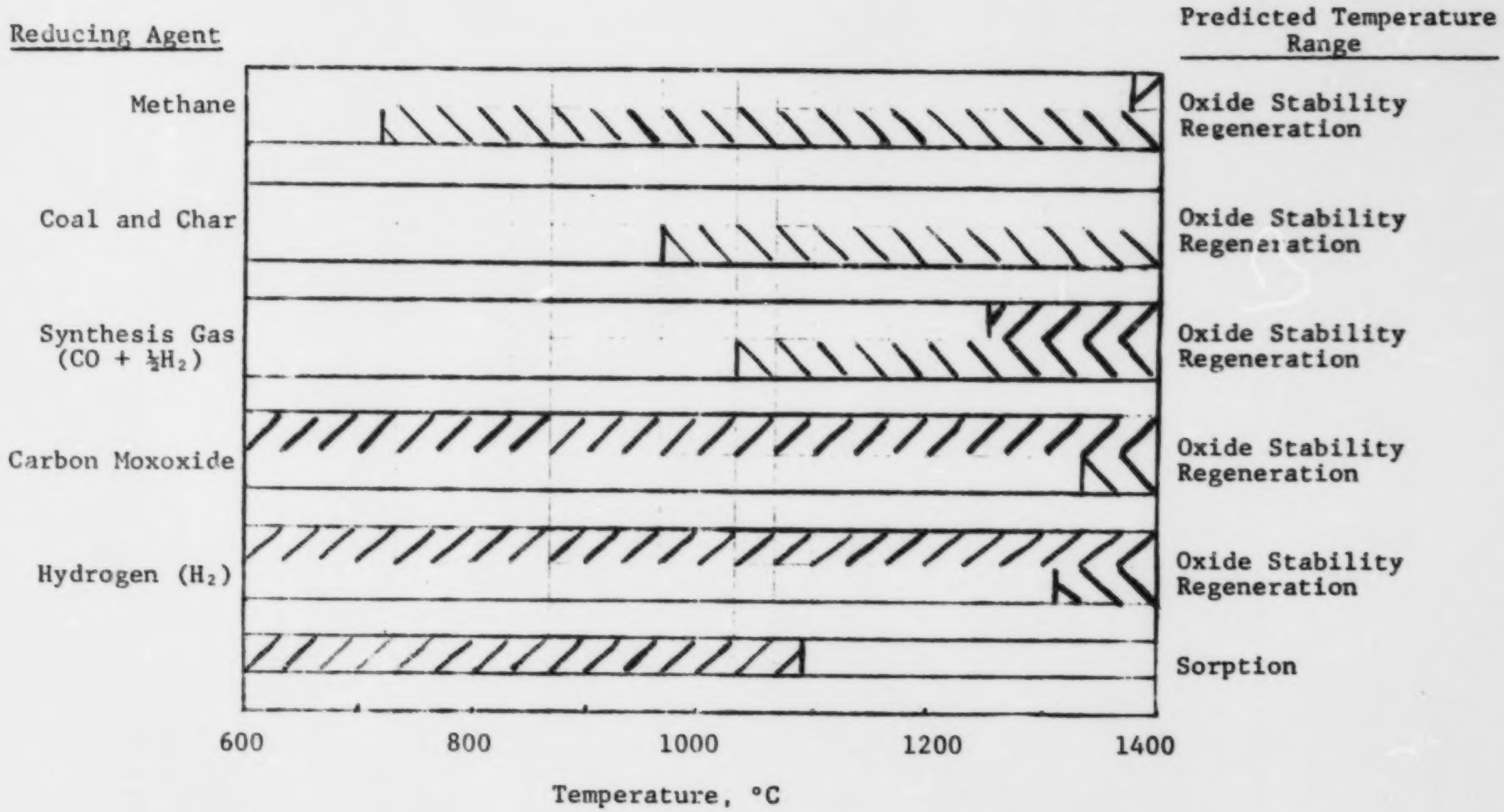

FIGURE 5-2 - TEMPERATURE REGIONS IN WHICH SORPTION, REGENERATION, AND OXIDE STABILITY ARE FAVORED FOR CaO

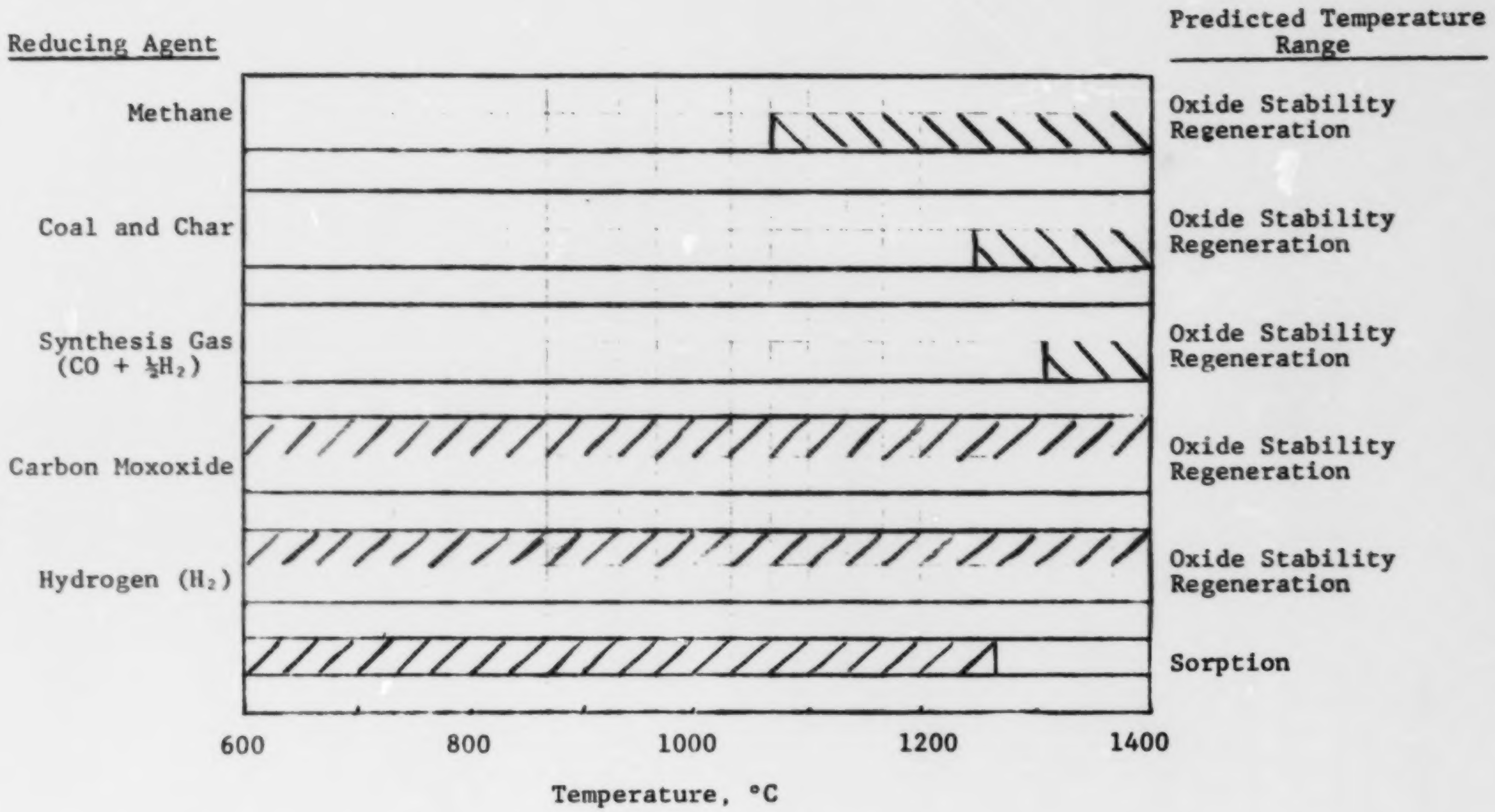

FIGURE 5-3 - TEMPERATURE REGIONS IN WHICH SORPTION, REGENERATION, AND OXIDE STABILITY ARE FAVORED FOR SrO

CO or H_2 stoichiometry or a change in pressure might lower the strontium sulfate reduction temperature and make this process feasible.)

Barium Oxide

Figure 5-4 shows that barium sulfate, like sodium, cannot be reduced by any of the six reducing agents between 600 and 1400°C.

Lithium Aluminum Oxide

Figure 5-5 indicates that the lithium-aluminum binary oxide can be regenerated by the stronger reducing agents. Neither formation of lithium nor aluminum sulfide is predicted. Synthesis gas ($CO + \frac{1}{2}H_2$) could be used as the reducing agent with no sulfide formation in a process in which sorption takes place up to 1200°C and regeneration occurs around 1400°C. Since the regeneration reaction is probably endothermic the lower regeneration temperature may be attractive.

Lithium-Iron(III) Oxide

Figure 5-6 shows that the lithium-iron(III) binary oxide could be regenerated by all of the reducing agents. Formation of lithium sulfide could be a problem. Due to lack of thermodynamic data for iron(III) sulfide no analysis could be made of the possibility of conversion of iron(III) oxide to the sulfide. Coal, char, carbon monoxide or hydrogen could all be used as reducing agents in processes which employ sorption up to about 930°C and a higher temperature for either regeneration or conversion of lithium sulfide to lithium oxide.

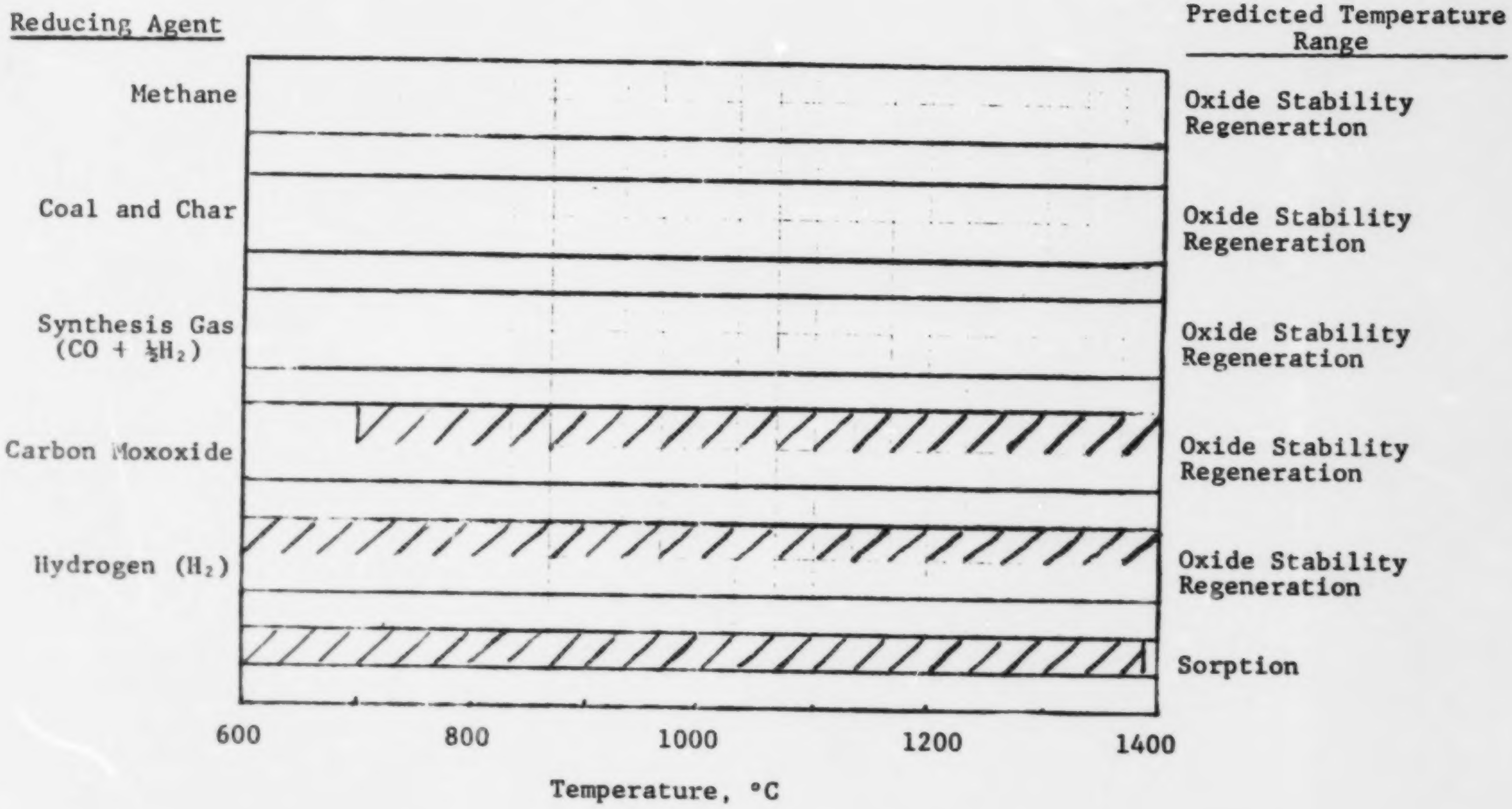

FIGURE 5-4 - TEMPERATURE REGIONS IN WHICH SORPTION, REGENERATION, AND OXIDE STABILITY ARE FAVORED FOR BaO

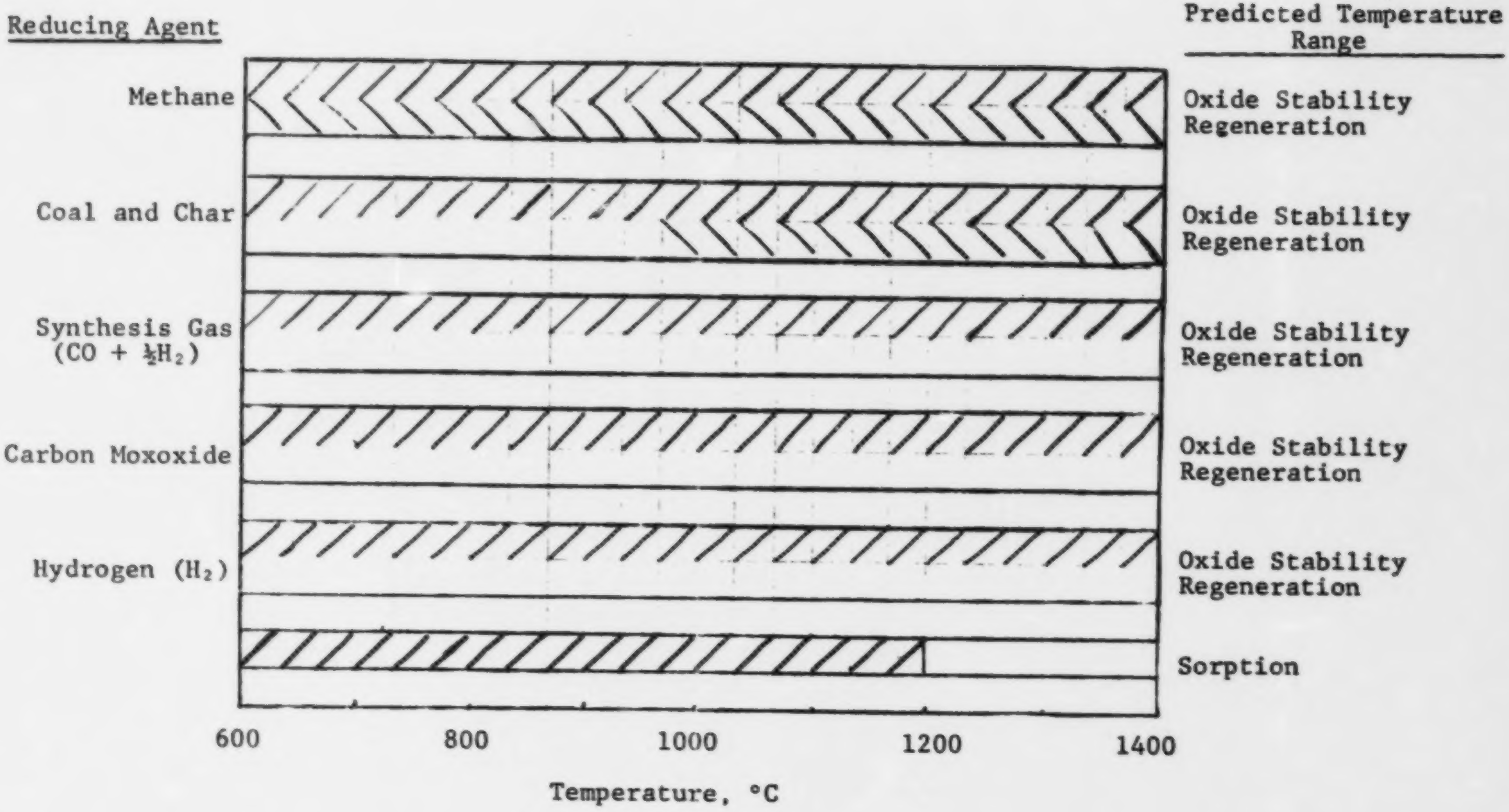

FIGURE 5-5 - TEMPERATURE REGIONS IN WHICH SORPTION, REGENERATION, AND OXIDE STABILITY ARE FAVORED FOR $LiAlO_2$

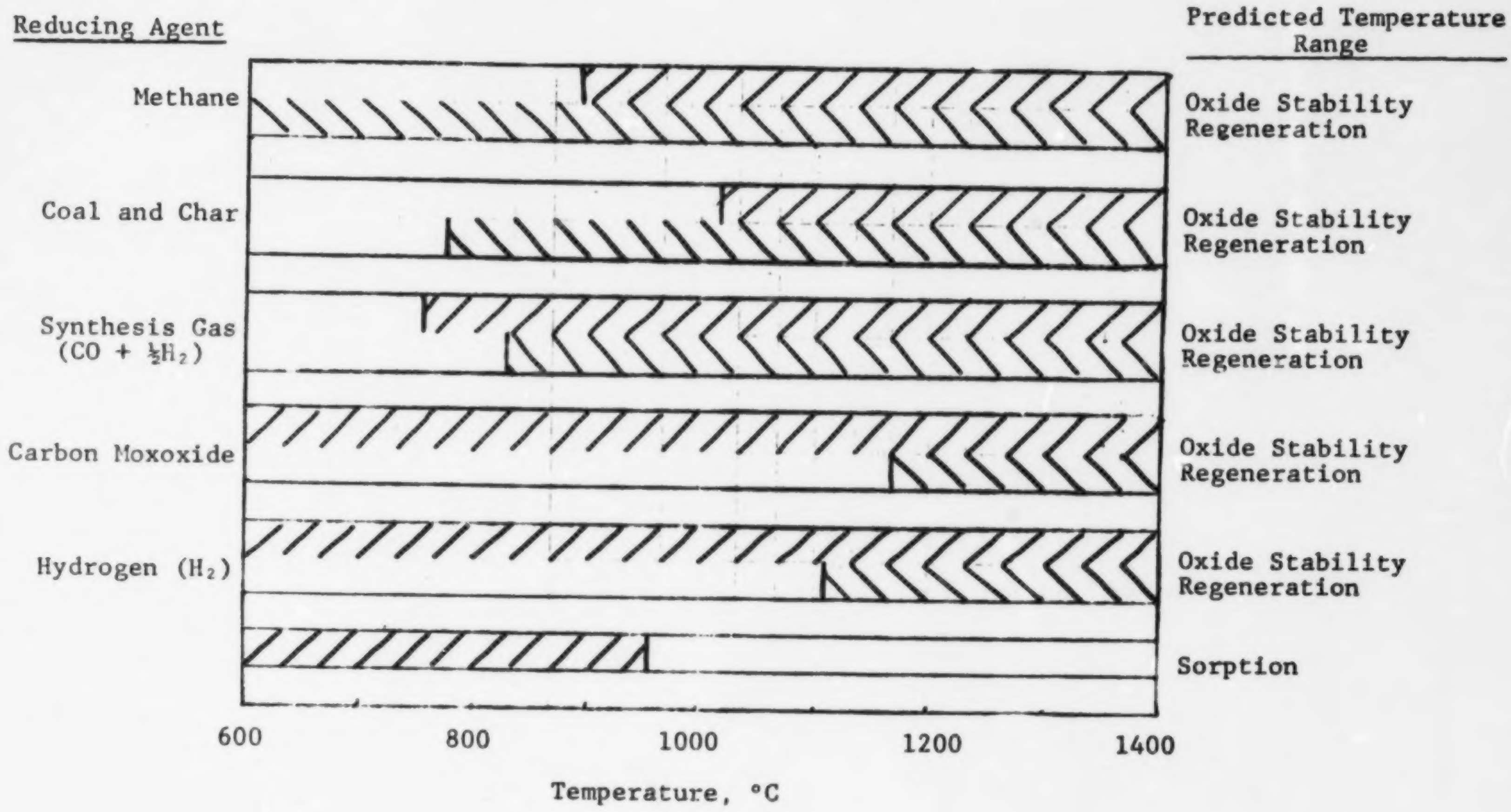

FIGURE 5-6 - TEMPERATURE REGIONS IN WHICH SORPTION, REGENERATION, AND OXIDE STABILITY ARE FAVORED FOR $LiFeO_2$

Sodium Aluminum Oxide

Figure 5-7 shows that sodium aluminate can be regenerated with no formation of sodium or aluminum sulfide using all of the reducing agents.

Sodium-Iron(III) Oxide

Figure 5-8 indicates that all reducing agents have a region of regeneration temperature where no formation of sodium sulfide is predicted. Again, the possibility of iron sulfide formation could not be assessed.

Calcium-Aluminum Oxide

Figure 5-9 shows that calcium aluminate can be regenerated by the four strongest reducing agents with no formation of calcium or aluminum sulfide in the upper temperature regions. Carbon monoxide and hydrogen are also effective reducing agents, but the regeneration step requires a higher temperature than the sorption step.

Strontium Aluminum Oxide

Figure 5-10 indicates that all reducing agents could be used to regenerate strontium aluminate without formation of strontium or aluminum sulfide. The extreme stability of the oxide looks promising.

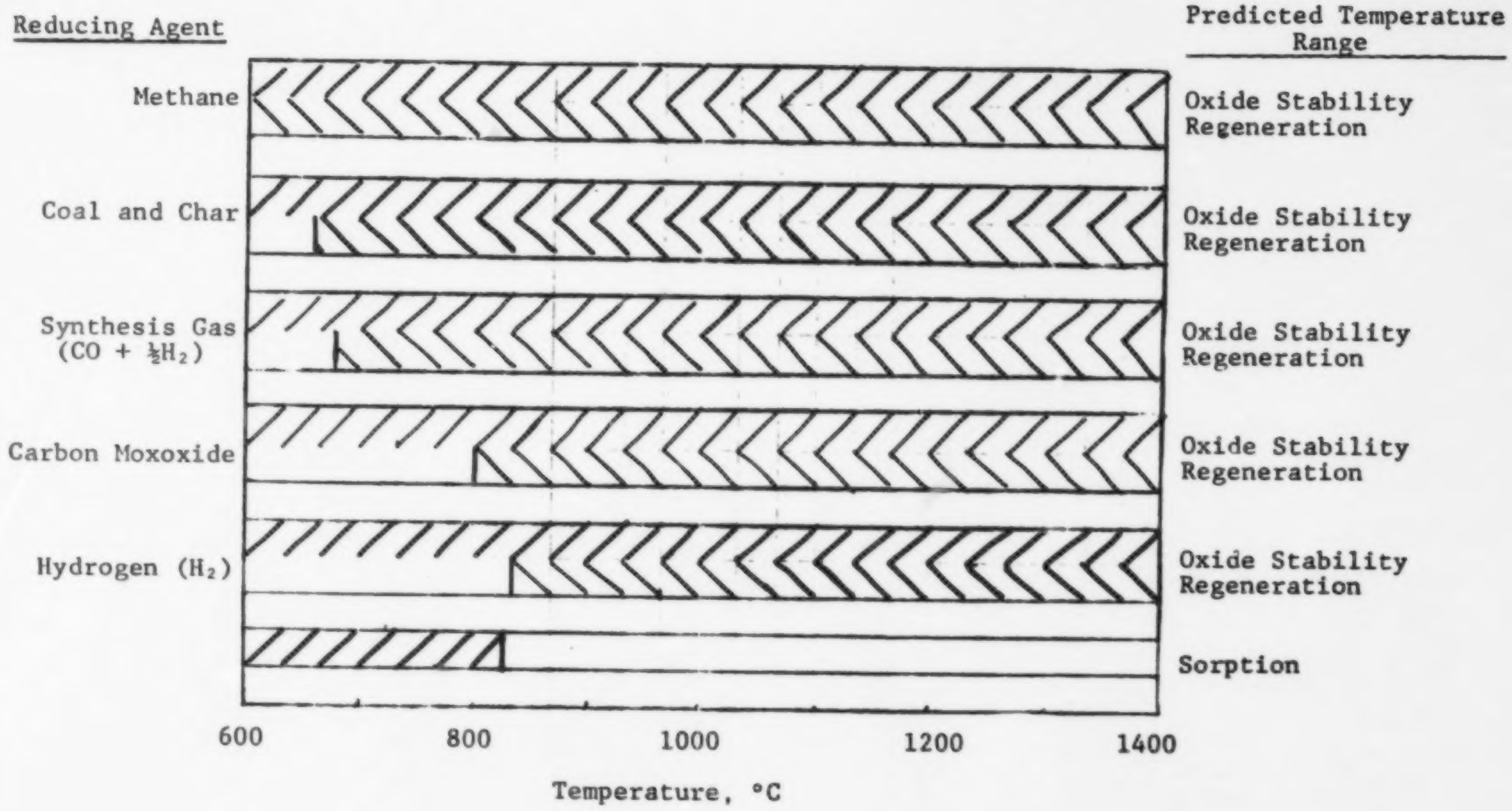

FIGURE 5-7 - TEMPERATURE REGIONS IN WHICH SORPTION, REGENERATION, AND OXIDE STABILITY ARE FAVORED FOR $NaAlO_2$

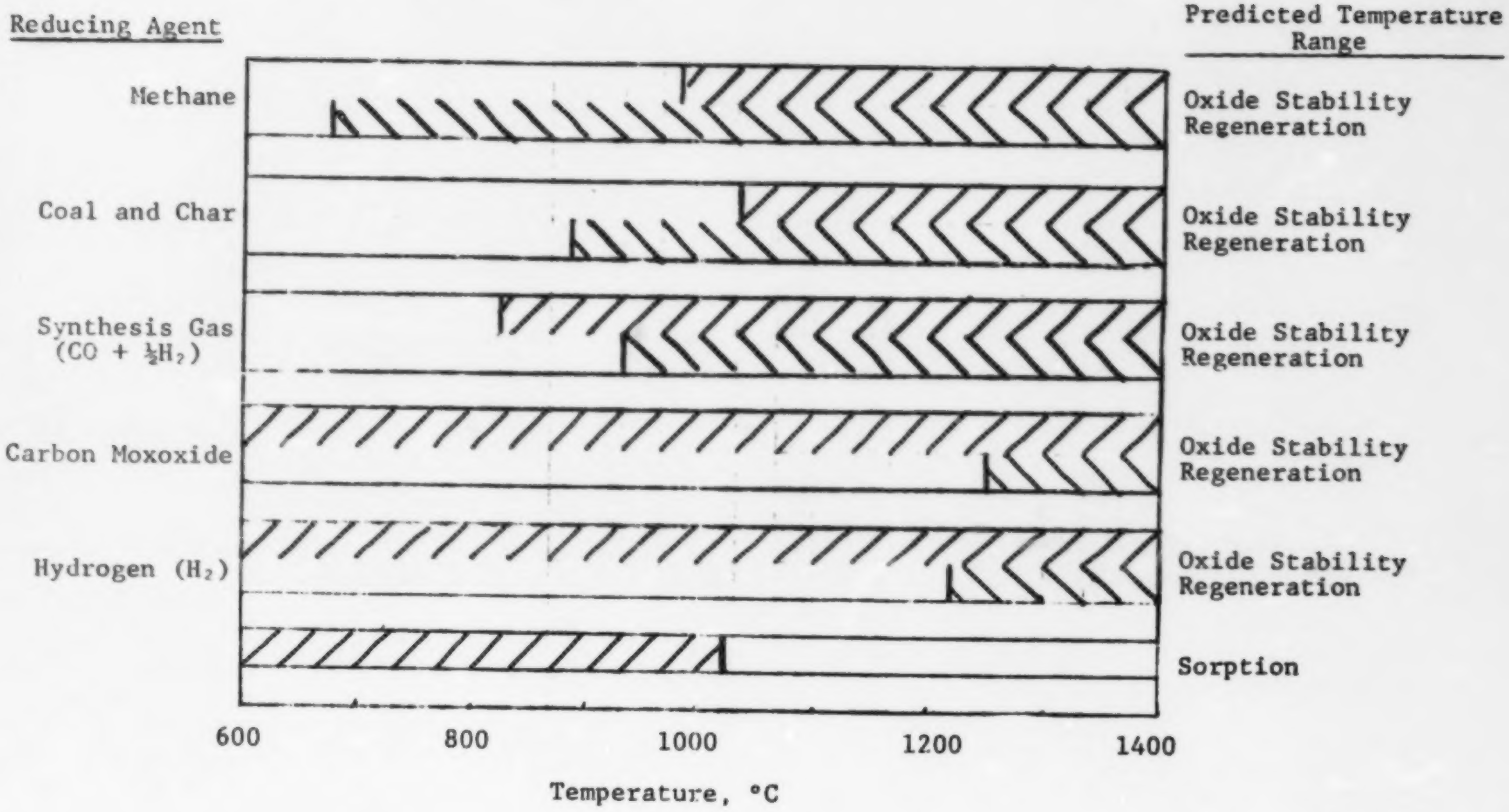

FIGURE 5- 8 - TEMPERATURE REGIONS IN WHICH SORPTION, REGENERATION, AND OXIDE STABILITY ARE FAVORED FOR $NaFeO_2$

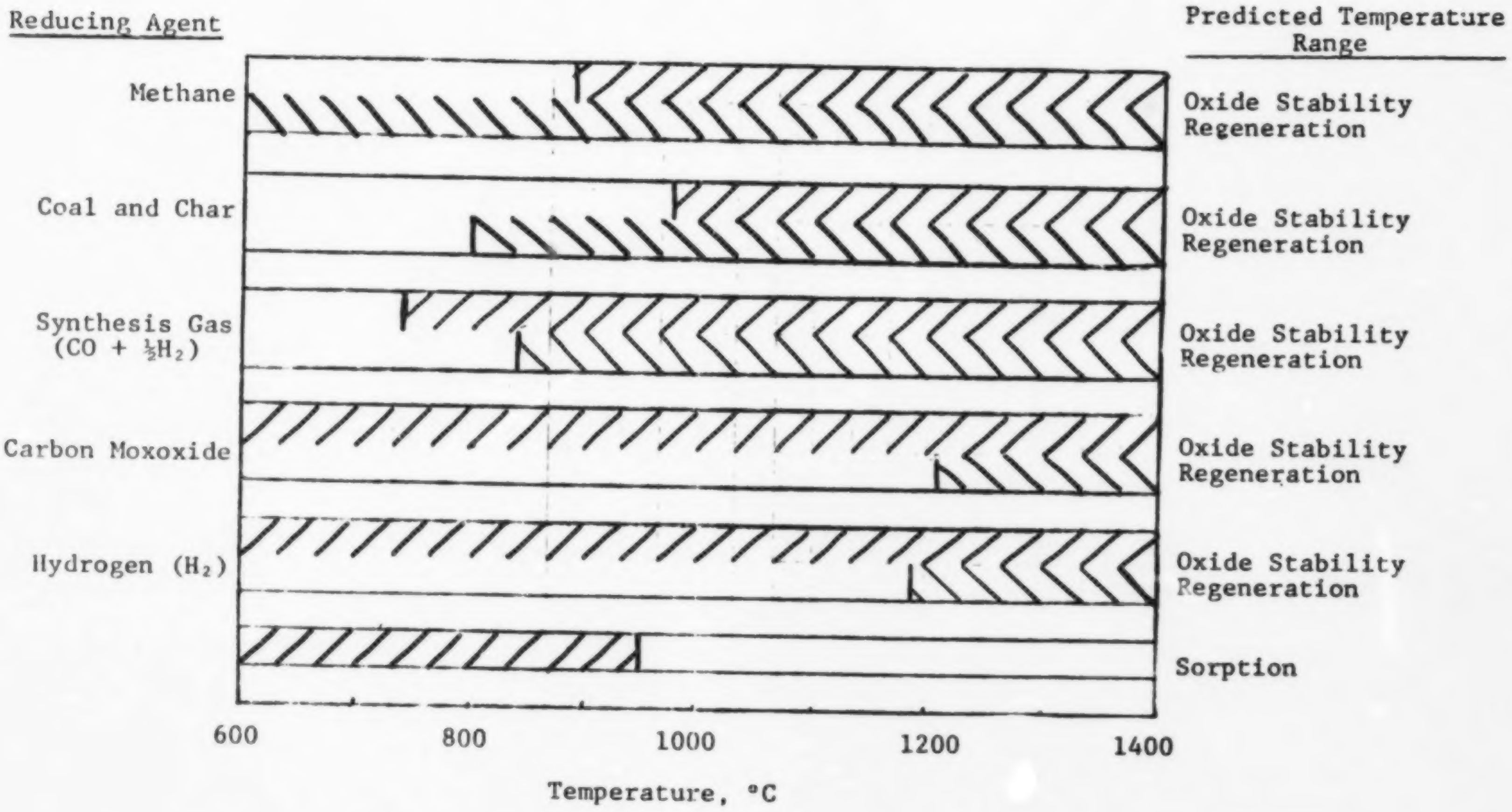

FIGURE 5-9 - TEMPERATURE REGIONS IN WHICH SORPTION, REGENERATION, AND OXIDE STABILITY ARE FAVORED FOR $CaAl_2O_4$

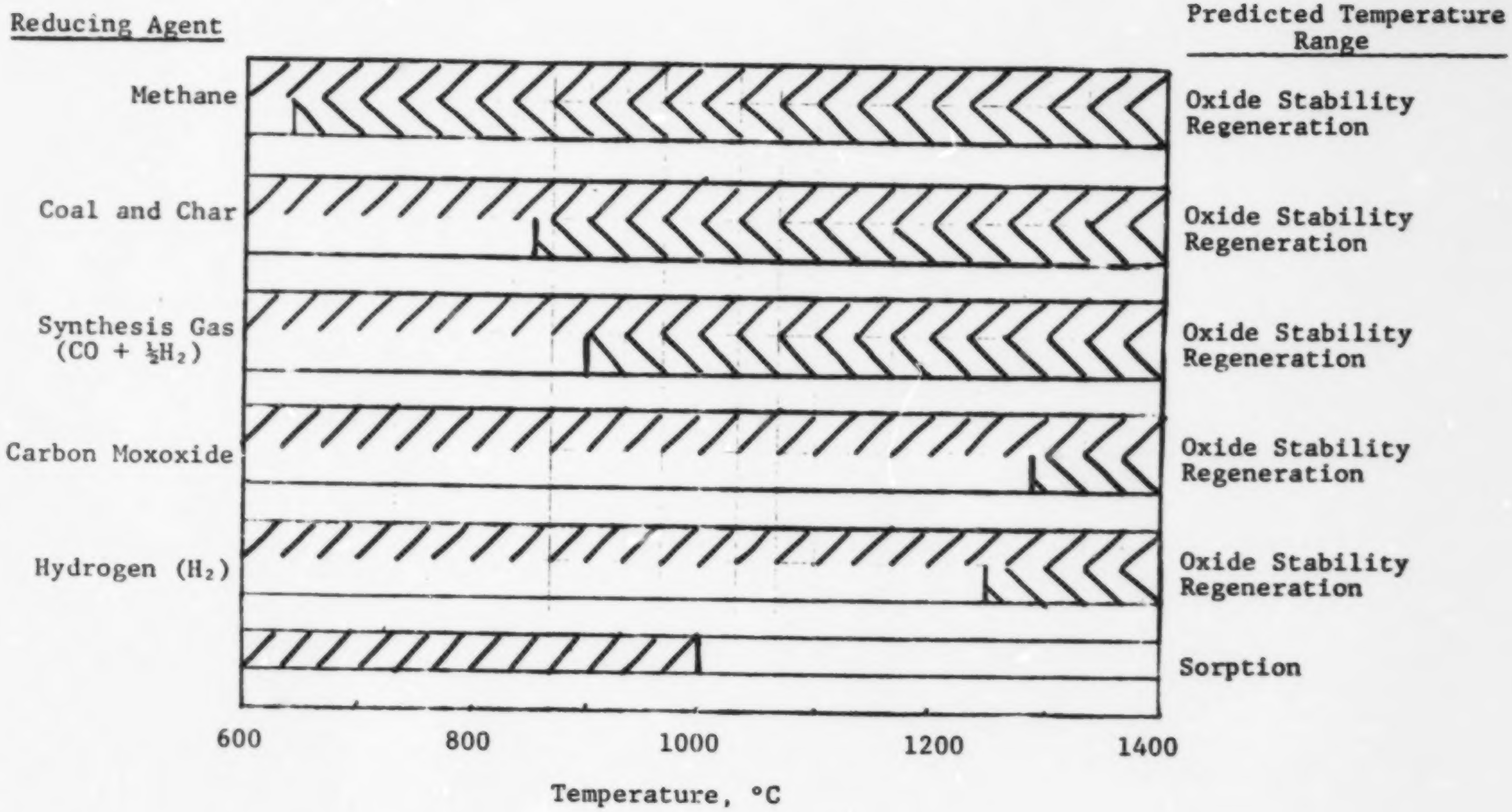

FIGURE 5-10 - TEMPERATURE REGIONS IN WHICH SORPTION, REGENERATION, AND OXIDE STABILITY ARE FAVORED FOR $SrAl_2O_4$

Strontium-Titanium Oxide

Figure 5-11 shows that strontium titanate could be difficult to regenerate without sulfide formation. Sulfide formation would not be predicted in carbon monoxide or hydrogen based decomposition processes above about 1040 or 1020°C, respectively.

Barium Aluminum Oxide

As indicated in Figure 5-12 barium aluminate could be regenerated by a strong reducing agent without sulfide formation.

Barium Titanium Oxide

Figure 5-13 shows that prevention of titanium sulfide formation is possible only with the use of carbon monoxide or hydrogen as reducing agents. A process employing these reductants would involve a sorption step below 1000°C and a higher temperature regeneration step.

Lithium Titanium Oxide

Figure 5-14 shows that lithium titanate cannot be regenerated below 1400°C without sulfide formation.

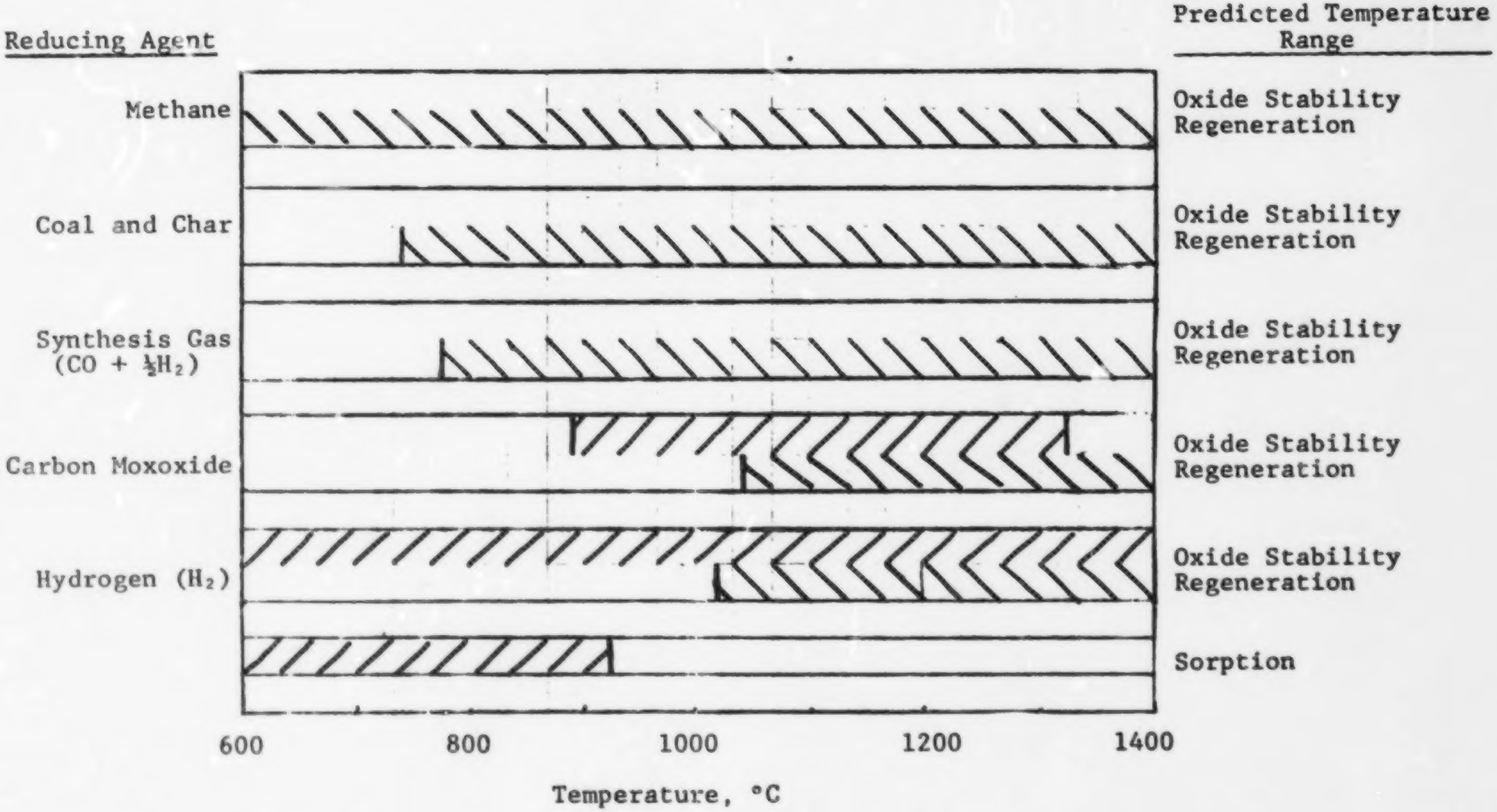

FIGURE 5-11 - TEMPERATURE REGIONS IN WHICH SORPTION, REGENERATION, AND OXIDE STABILITY ARE FAVORED FOR $SrTiO_3$

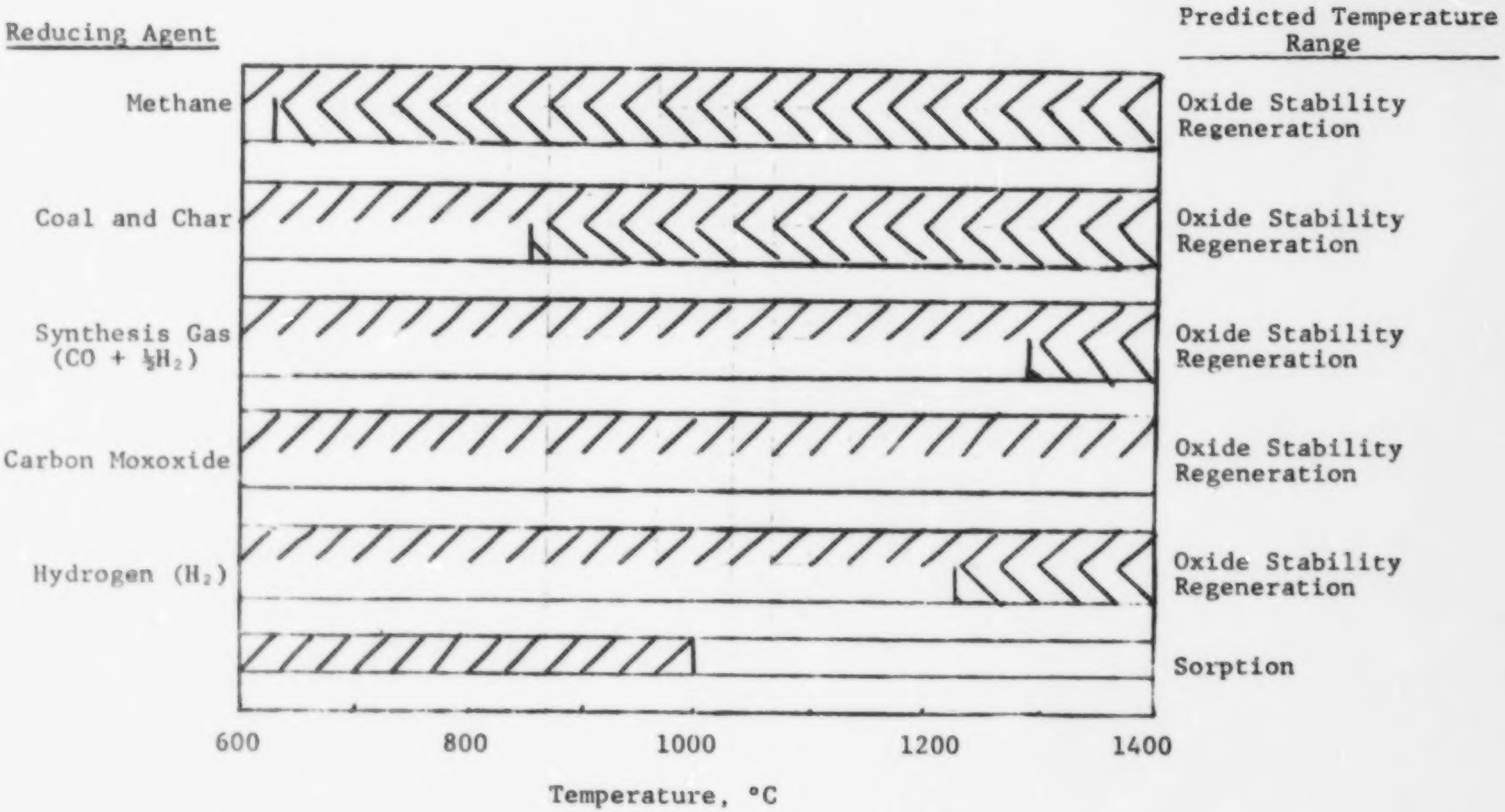

FIGURE 5-12 - TEMPERATURE REGIONS IN WHICH SORPTION, REGENERATION, AND OXIDE STABILITY ARE FAVORED FOR $BaAl_2O_4$

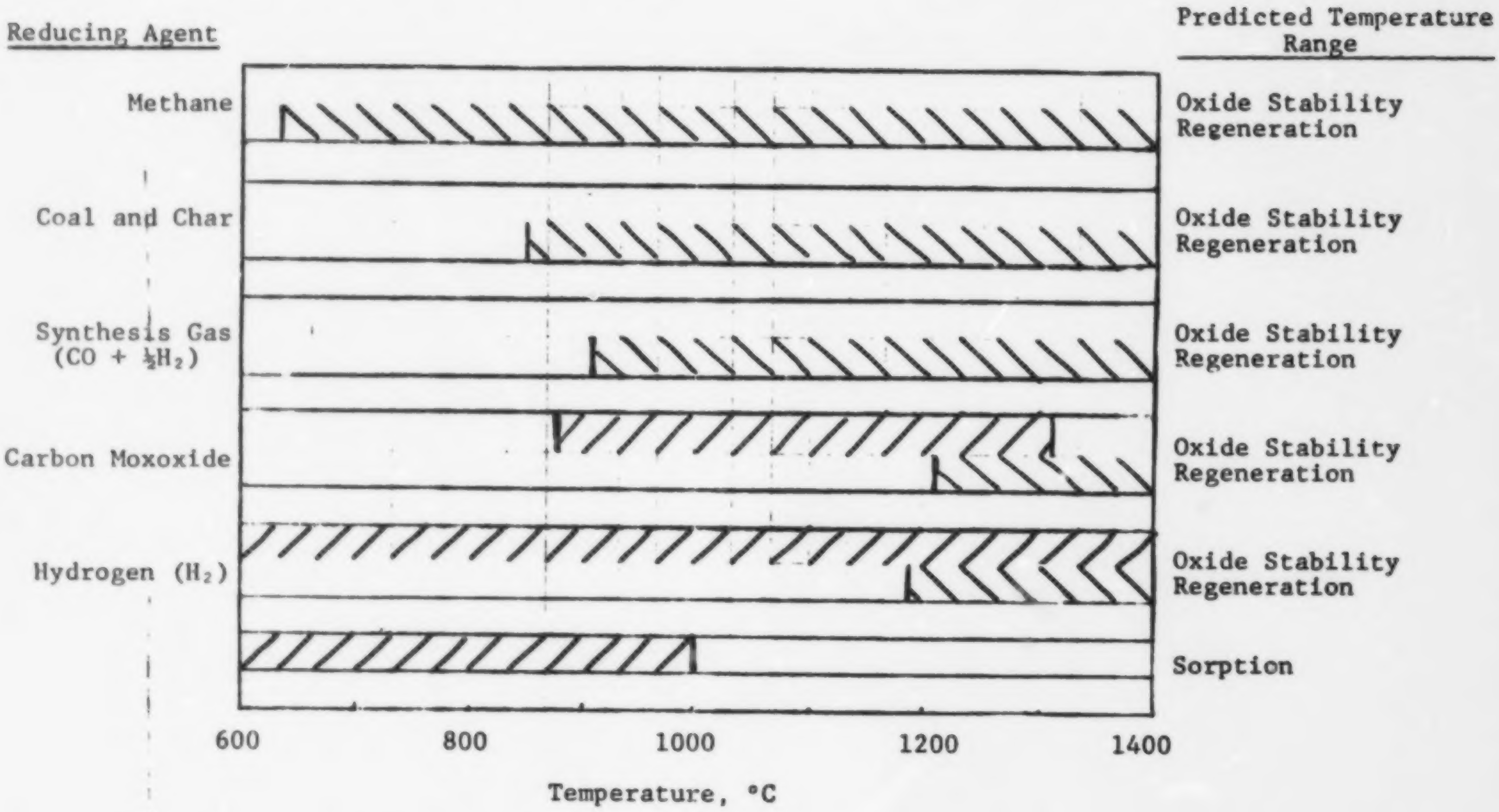

FIGURE 5-13 - TEMPERATURE REGIONS IN WHICH SORPTION, REGENERATION, AND OXIDE STABILITY ARE FAVORED FOR $BaTiO_3$

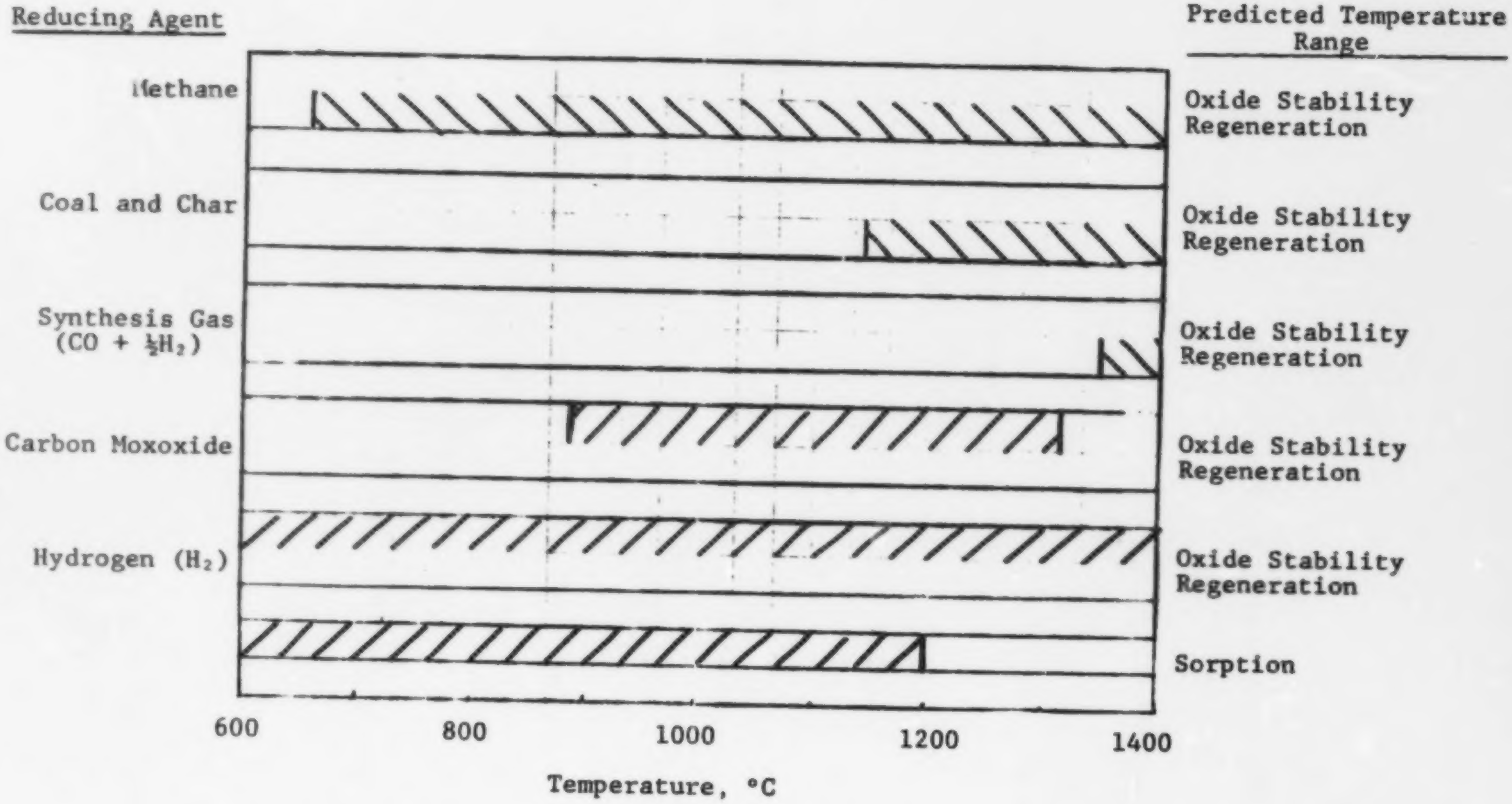

FIGURE 5-14 - TEMPERATURE REGIONS IN WHICH SORPTION, REGENERATION, AND OXIDE STABILITY ARE FAVORED FOR Li_2TiO_3

5.2 Conclusions

The thermodynamic conclusions are of two types. First is the definition of the temperature range in which the sorbent will perform. Second is the regenerability of the sorbent. The most desirable regeneration is one in which the sulfated sorbent is decomposed to yield gaseous products and the original oxide sorbent. A less desirable process is one that yields a sulfide solid, which would require regeneration in a second step to yield the oxide form of the sorbent for recycle.

These results are theoretical calculations to be used as an aid in making decisions. They are based on data that have associated experimental errors. Furthermore, some of the data are estimated. This means that a margin for error should be considered in making decisions based upon these data.

Table 5-2 presents the temperature ranges for processes in which the oxide is the predicted regeneration product. Table 5-3 presents the temperature ranges of applicability of the sulfide producing (two-step) regeneration processes.

Many of the sorbents presented in Table 5-2 look promising. The selection of materials upon which to base a process should begin with these. Factors such as melting and softening point, possibility of flux formation with ash constituents, unusual properties such as the piezoelectric characteristics of $BaTiO_3$, and reaction kinetics must be considered in a process development program.

TABLE 5-2
SORPTION-REGENERATION PROCESSES IN WHICH OXIDE FORMATION IS PREDICTED

Sorbent	Maximum Sorption Temperature (°C)	Reducing Agent[1]	Temperature Range for Regeneration with Oxide Formation (°C)
CaO	1090	H_2	1320-1400
		CO	1340-1400
		$CO + \frac{1}{2}H_2$	1250-1400
		CH_4	1370-1400
$LiAlO_2$	1200	Coal and Char	960-1400
		CH_4	600-1400
$LiFeO_2$[2]	950	H_2	1110-1400
		CO	1160-1400
		$CO + \frac{1}{2}H_2$	825-1400
		Coal	1100-1400
		Char	1020-1400
		Methane	890-1400
$NaAlO_2$	820	H_2	830-1400
		CO	800-1400
		$CO + \frac{1}{2}H_2$	670-1400
		Coal and Char	650-1400
		Methane	600-1400
$NaFeO_2$[2]	1020	H_2	1220-1400
		CO	1245-1400
		$CO + \frac{1}{2}H_2$	930-1400
		Coal	1030-1400
		Char	1175-1400
		Methane	980-1400
$CaAl_2O_4$	950	H_2	1180-1400
		CO	1220-1400
		$CO + \frac{1}{2}H_2$	840-1400
		Char	970-1350
		Coal	1360-1400
		Methane	890-1400
$SrAl_2O_4$	1000	H_2	1250-1400
		CO	1290-1400
		$CO + \frac{1}{2}H_2$	900-1400
		Coal and Char	~850-1400
		Methane	640-1400
$SrTiO_3$	920	H_2	1020-1400
		CO	1040-1320
$BaAl_2O_4$	1000	H_2	1230-1400
		$CO + \frac{1}{2}H_2$	1290-1400
		Coal and Char	850-1400
		Methane	630-1400
$BaTiO_3$	1000	H_2	1190-1400
		CO	1220-1320

---

[1]

Formula	Reducing Agent
CH_4	Methane
$C + \frac{1}{2}H_2$	Coal
C	Char
$CO + \frac{1}{2}H_2$	Synthesis Gas
CO	Carbon Monoxide
H_2	Hydrogen

One mole of reducing agent per mole of SO_2 was assumed.

[2] Possibility of iron sulfide formation not investigated due to lack of thermodynamic data.

TABLE 5-3

SORPTION-REGENERATION PROCESSES IN WHICH SULFIDE FORMATION IS PREDICTED

Sorbent	Maximum Sorption Temperature (°C)	Reducing Agent[1]	Temperature Range for Regeneration with Sulfide Formation (°C)
CaO	1090	$CO + \frac{1}{2}H_2$	1030-1250
		Coal and Char	960-1400
		Methane	725-1370
SrO	1260	$CO + \frac{1}{2}H_2$	1310-1400
		Coal and Char	1240-1400
		Methane	1060-1400
$LiFeO_2$ [2]	950	Coal	775-1100
		Char	775-1020
		Methane	600-890
$NaFeO_2$ [2]	1020	Coal	875-1030
		Char	875-1175
		Methane	670-980
$CaAl_2O_4$	950	Char	800-970
		Coal	800-1360
		Methane	600-890
$SrTiO_3$	920	CO	1320-1400
		$CO + \frac{1}{2}H_2$	775-1400
		Coal and Char	740-1400
		Methane	600-1400
$BaTiO_3$	1000	CO	1320-1400
		$CO + \frac{1}{2}H_2$	910-1400
		Coal and Char	850-1400
		Methane	630-1400
Li_2TiO_3	1200	$CO + \frac{1}{2}H_2$	1350-1400
		Coal and Char	1140-1400
		Methane	660-1400

---

[1]

Formula	Reducing Agent
CH_4	Methane
$C + \frac{1}{2}H_2$	Coal
C	Char
$CO + \frac{1}{2}H_2$	Synthesis Gas
CO	Carbon Monoxide
H_2	Hydrogen

One mole of reducing agent per mole of SO_2 was assumed.

[2] Possibility of iron sulfide formation not investigated due to lack of thermodynamic data.

BIBLIOGRAPHY

PA-016 Parsons, T. B., Gary D. Schroeder, and David DeBerry, Applicability of Metal Oxides to the Development of New Processes for Removing SO_2 from Flue Gases, 2 volumes, Austin, Texas, Tracor, Inc., 1969.

PO-001 Pohlenz, J. B., "The Shell Flue Gas Desulfurization Process", presented at the Environmental Protection Agency Flue Gas Desulfurization Symposium, Atlanta, Georgia, November 4-7, 1974.

APPENDIX

FIGURES A-1 THROUGH A-30

LIST OF FIGURES

Figure

A-1 COMPARISON OF SO_3 PARTIAL PRESSURE IN REDUCING GASES WITH SO_3 VAPOR PRESSURE OVER Na_2SO_4

A-2 COMPARISON OF SO_3 PARTIAL PRESSURE IN REDUCING GASES WITH SO_3 VAPOR PRESSURE OVER $CaSO_4$

A-3 COMPARISON OF SO_3 PARTIAL PRESSURE IN REDUCING GASES WITH SO_3 VAPOR PRESSURE OVER $SrSO_4$

A-4 COMPARISON OF SO_3 PARTIAL PRESSURE IN REDUCING GASES WITH SO_3 VAPOR PRESSURE OVER $BaSO_4$

A-5 COMPARISON OF SO_3 PARTIAL PRESSURE IN REDUCING GASES WITH SO_3 VAPOR PRESSURE OVER $Li_2SO_4 + Al_2O_3$

A-6 COMPARISON OF SO_3 PARTIAL PRESSURE IN REDUCING GASES WITH SO_3 VAPOR PRESSURE OVER $Li_2SO_4 + Fe_2O_3$

A-7 COMPARISON OF SO_3 PARTIAL PRESSURE IN REDUCING GASES WITH SO_3 VAPOR PRESSURE OVER $Na_2SO_4 + Al_2O_3$

A-8 COMPARISON OF SO_3 PARTIAL PRESSURE IN REDUCING GASES WITH SO_3 VAPOR PRESSURE OVER $Na_2SO_4 + Fe_2O_3$

A-9 COMPARISON OF SO_3 PARTIAL PRESSURE IN REDUCING GASES WITH SO_3 VAPOR PRESSURE OVER $CaSO_4 + Al_2O_3$

A-10 COMPARISON OF SO_3 PARTIAL PRESSURE IN REDUCING GASES WITH SO_3 VAPOR PRESSURE OVER $SrSO_4 + Al_2O_3$

A-11 COMPARISON OF SO_3 PARTIAL PRESSURE IN REDUCING GASES WITH SO_3 VAPOR PRESSURE OVER $SrSO_4 + TiO_2$

A-12 COMPARISON OF SO_3 PARTIAL PRESSURE IN REDUCING GASES WITH SO_3 VAPOR PRESSURE OVER $BaSO_4 + Al_2O_3$

A-13 COMPARISON OF SO_3 PARTIAL PRESSURE IN REDUCING GASES WITH SO_3 VAPOR PRESSURE OVER $BaSO_4 + TiO_2$

A-14 COMPARISON OF SO_3 PARTIAL PRESSURE IN REDUCING GASES WITH SO_3 VAPOR PRESSURE OVER $Li_2SO_4 + TiO_2$

LIST OF FIGURES (cont.)

Figure

A-15 COMPARISON OF a_{O_2}/a_{S_2} IN REDUCING GASES WITH a_{O_2}/a_{S_2} FOR THE REACTION: $2Na_2O + S_2 \rightarrow O_2 + Na_2S$

A-16 COMPARISON OF a_{O_2}/a_{S_2} IN REDUCING GASES WITH a_{O_2}/a_{S_2} FOR THE REACTION: $2CaO + S_2 \rightarrow O_2 + 2CaS$

A-17 COMPARISON OF a_{O_2}/a_{S_2} IN REDUCING GASES WITH a_{O_2}/a_{S_2} FOR THE REACTION: $2SrO + S_2 \rightarrow O_2 + 2SrS$

A-18 COMPARISON OF a_{O_2}/a_{S_2} IN REDUCING GASES WITH a_{O_2}/a_{S_2} FOR THE REACTION: $2BaO + S_2 \rightarrow O_2 + 2BaS$

A-19 COMPARISON OF a_{O_2}/a_{S_2} IN REDUCING GASES WITH a_{O_2}/a_{S_2} FOR THE REACTION: $4LiAlO_2 + S_2 \rightarrow O_2 + 2Li_2S + 2Al_2O_3$

A-20 COMPARISON OF a_{O_2}/a_{S_2} IN REDUCING GASES WITH a_{O_2}/a_{S_2} FOR THE REACTION: $4LiFeO_2 + S_2 \rightarrow O_2 + 2Li_2S + 2Fe_2O_3$

A-21 COMPARISON OF a_{O_2}/a_{S_2} IN REDUCING GASES WITH a_{O_2}/a_{S_2} FOR THE REACTION: $2Al_2O_3 + 3S_2 \rightarrow 3O_2 + 2Al_2S_3$

A-22 COMPARISON OF a_{O_2}/a_{S_2} IN REDUCING GASES WITH a_{O_2}/a_{S_2} FOR THE REACTION: $TiO_2 + S_2 \rightarrow O_2 + TiS_2$

A-23 COMPARISON OF a_{O_2}/a_{S_2} IN REDUCING GASES WITH a_{O_2}/a_{S_2} FOR THE REACTION: $4NaAlO_2 + S_2 \rightarrow O_2 + 2Na_2S + 2Al_2O_3$

A-24 COMPARISON OF a_{O_2}/a_{S_2} IN REDUCING GASES WITH a_{O_2}/a_{S_2} FOR THE REACTION: $4NaFeO_2 + S_2 \rightarrow O_2 + 2Na_2S + 2Fe_2O_3$

LIST OF FIGURES (cont.)

Figure

A-25 COMPARISON OF a_{O_2}/a_{S_2} IN REDUCING GASES WITH a_{O_2}/a_{S_2} FOR THE REACTION: $2CaAl_2O_4 + S_2 \rightarrow O_2 + 2CaS + 2Al_2O_3$

A-26 COMPARISON OF a_{O_2}/a_{S_2} IN REDUCING GASES WITH a_{O_2}/a_{S_2} FOR THE REACTION: $2SrAl_2O_4 + S_2 \rightarrow O_2 + 2SrS + 2Al_2O_3$

A-27 COMPARISON OF a_{O_2}/a_{S_2} IN REDUCING GASES WITH a_{O_2}/a_{S_2} FOR THE REACTION: $2SrTiO_3 + S_2 \rightarrow O_2 + 2SrS + 2TiO_2$

A-28 COMPARISON OF a_{O_2}/a_{S_2} IN REDUCING GASES WITH a_{O_2}/a_{S_2} FOR THE REACTION: $2BaAl_2O_4 + S_2 \rightarrow O_2 + 2BaS + 2Al_2O_3$

A-29 COMPARISON OF a_{O_2}/a_{S_2} IN REDUCING GASES WITH a_{O_2}/a_{S_2} FOR THE REACTION: $2BaTiO_3 + S_2 \rightarrow O_2 + 2BaS + 2TiO_2$

A-30 COMPARISON OF a_{O_2}/a_{S_2} IN REDUCING GASES WITH a_{O_2}/a_{S_2} FOR THE REACTION: $2Li_2TiO_3 + S_2 \rightarrow O_2 + 2Li_2S + 2TiO_2$

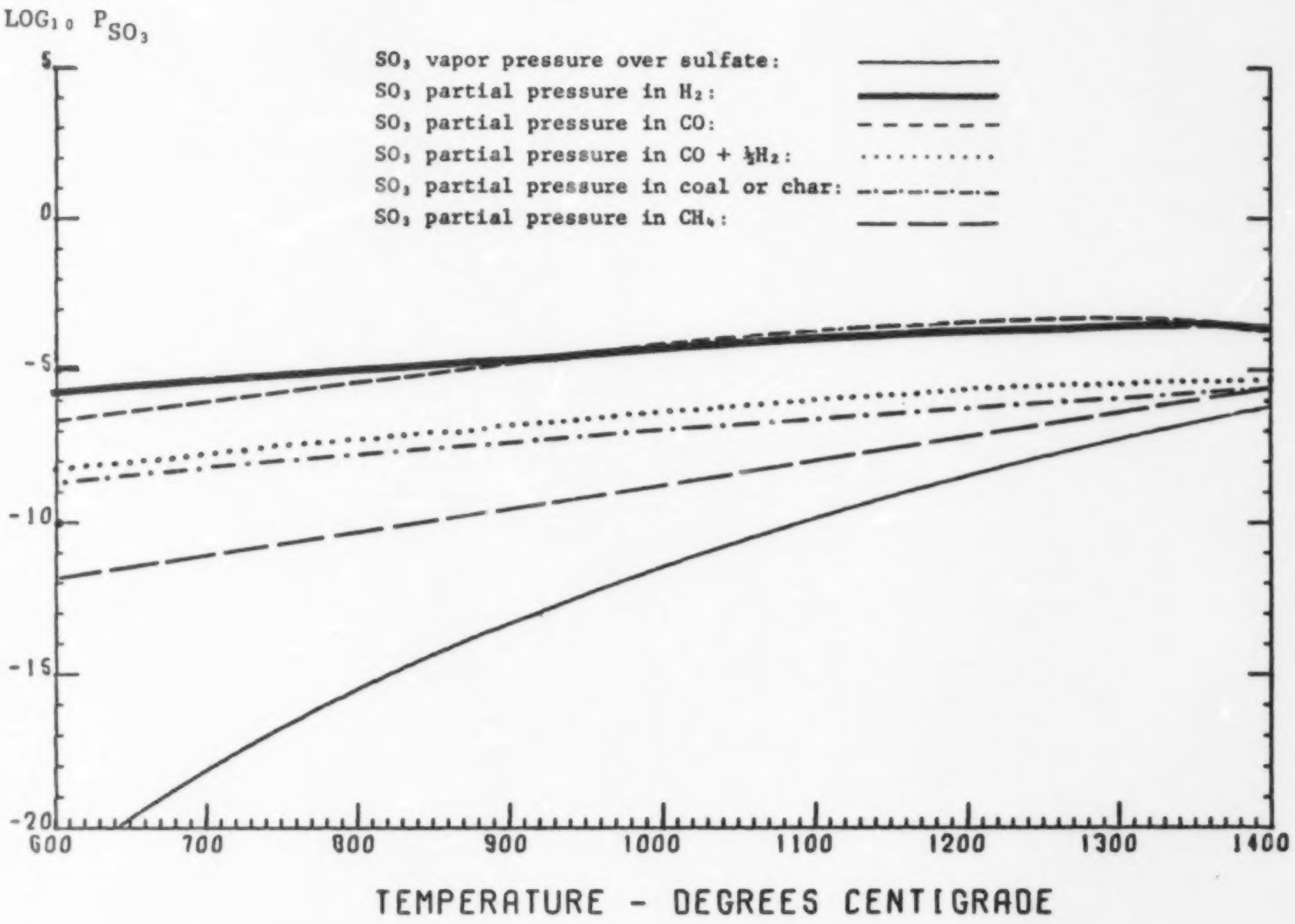

FIGURE A-1 - COMPARISON OF SO_3 PARTIAL PRESSURE IN REDUCING GASES WITH SO_3 VAPOR PRESSURE OVER Na_2SO_4

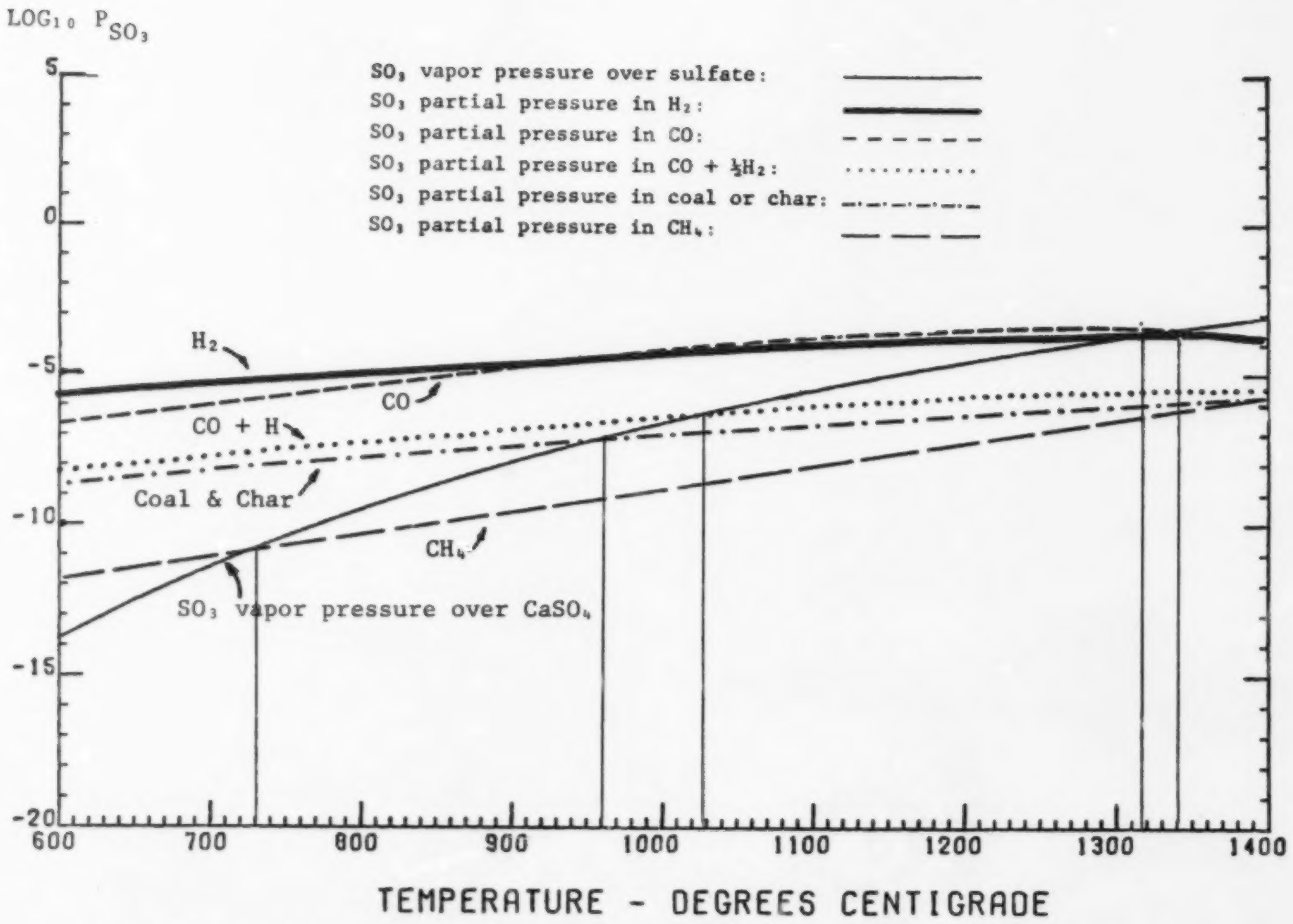

FIGURE A-2 - COMPARISON OF SO_3 PARTIAL PRESSURE IN REDUCING GASES WITH SO_3 VAPOR PRESSURE OVER $CaSO_4$

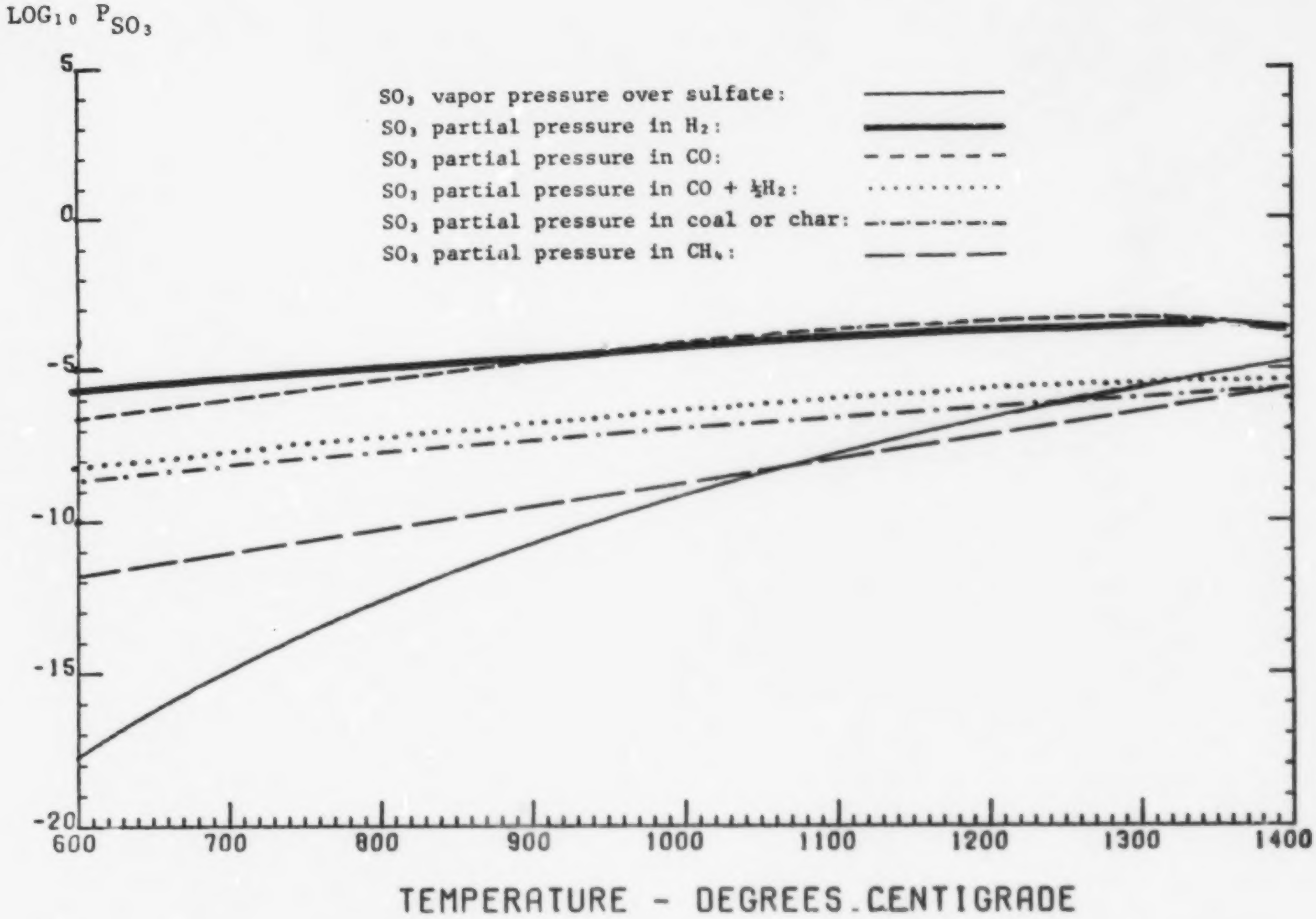

FIGURE A-3 - COMPARISON OF SO_3 PARTIAL PRESSURE IN REDUCING GASES WITH SO_3 VAPOR PRESSURE OVER $SrSO_4$

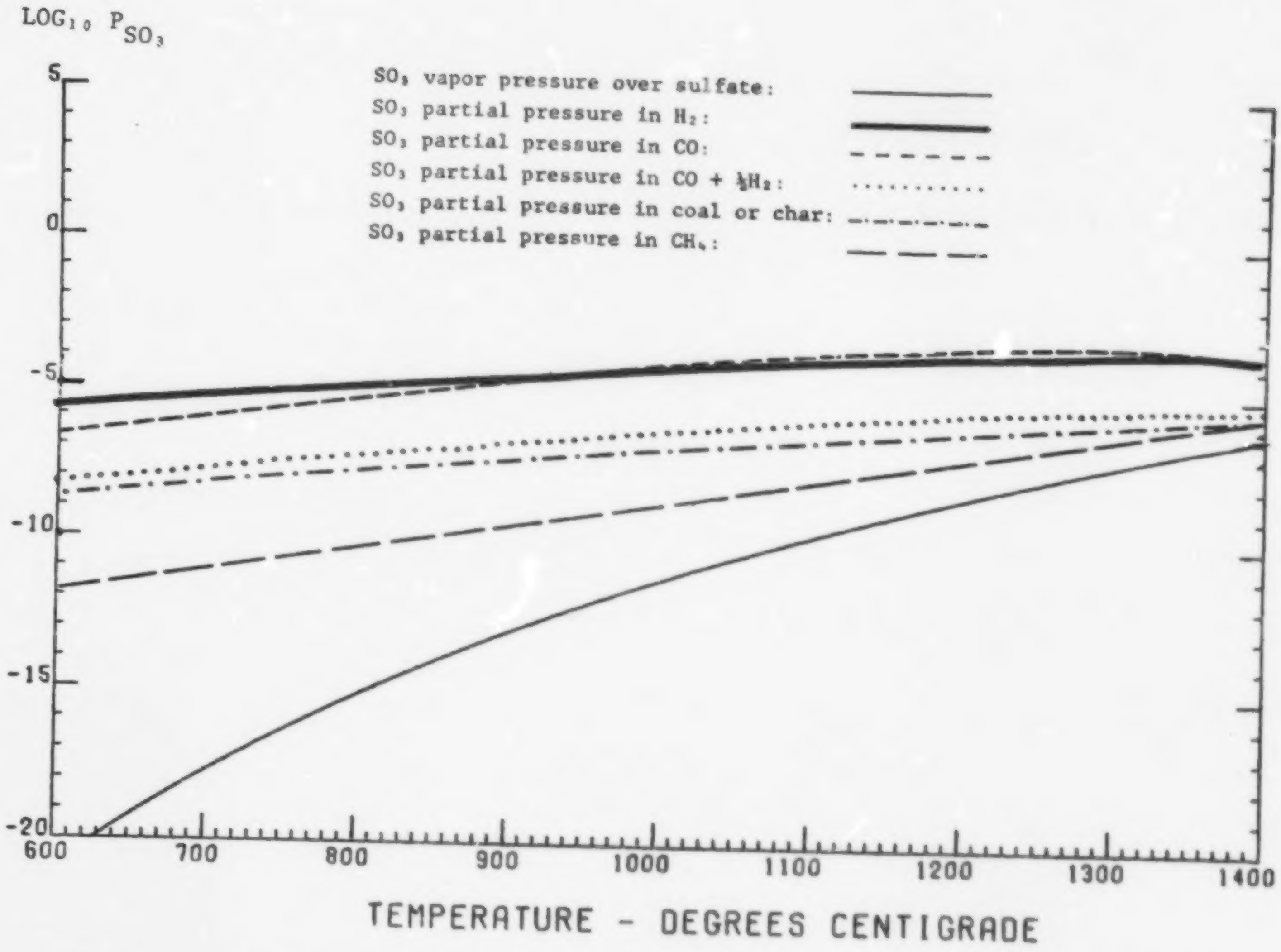

FIGURE A-4 - COMPARISON OF SO_3 PARTIAL PRESSURE IN REDUCING GASES WITH SO_3 VAPOR PRESSURE OVER $BaSO_4$

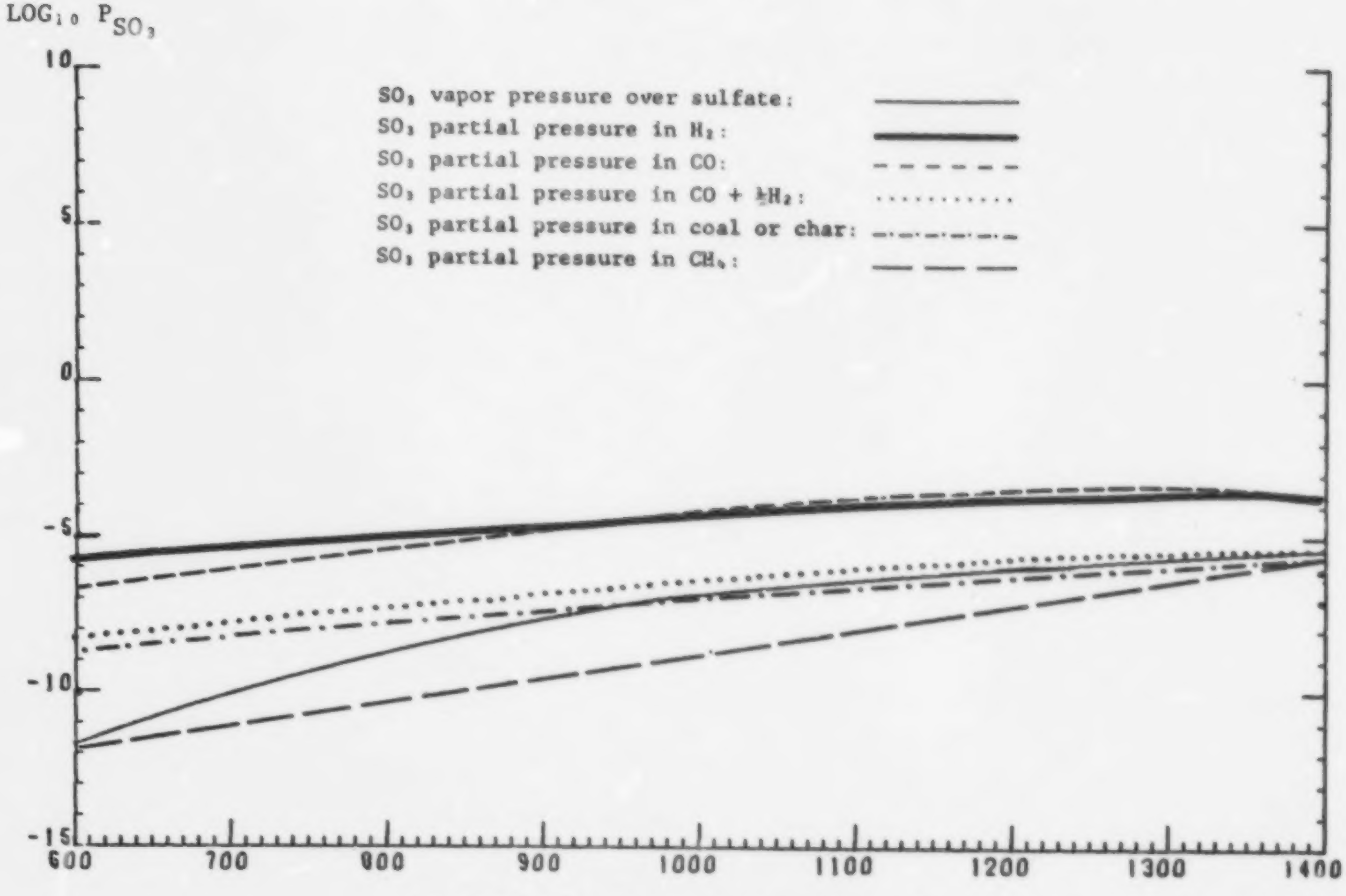

FIGURE A-5 - COMPARISON OF SO_3 PARTIAL PRESSURE IN REDUCING GASES WITH SO_3 VAPOR PRESSURE OVER Li_2SO_4 + Al_2O_3

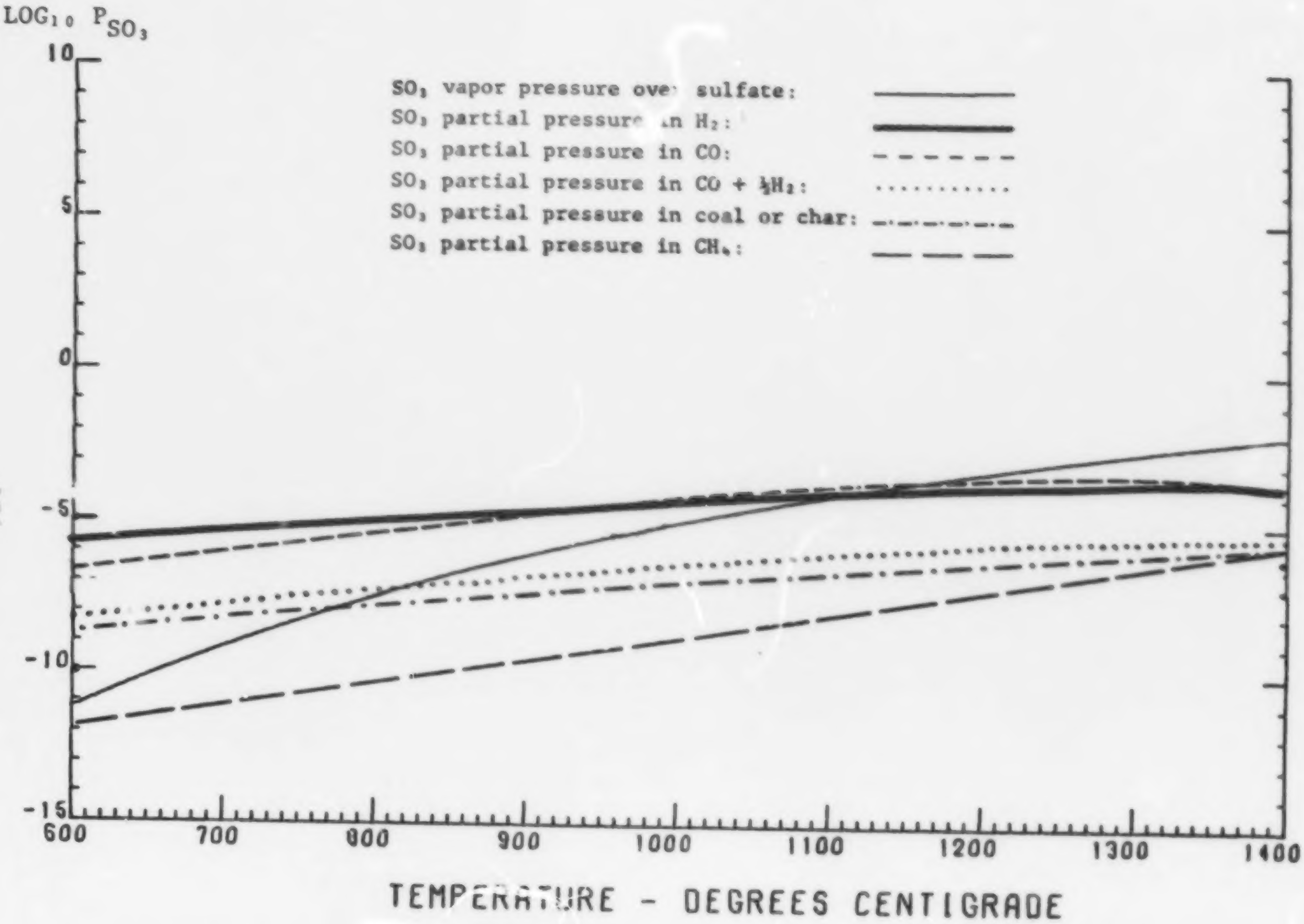

FIGURE A-6 - COMPARISON OF SO_3 PARTIAL PRESSURE IN REDUCING GASES WITH SO_3 VAPOR PRESSURE OVER $Li_2SO_4 + Fe_2O_3$

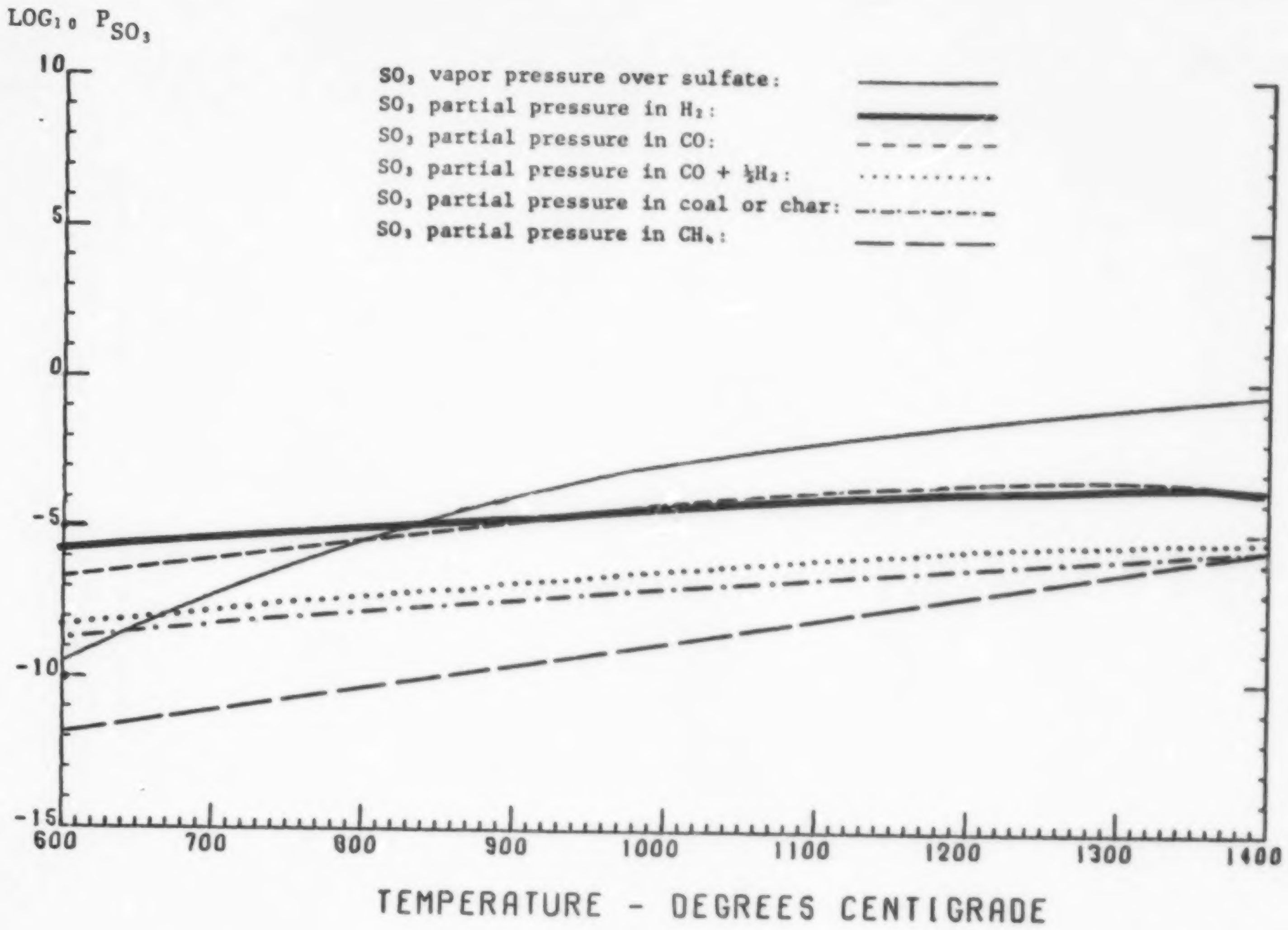

FIGURE A-7 - COMPARISON OF SO_3 PARTIAL PRESSURE IN REDUCING GASES WITH SO_3 VAPOR PRESSURE OVER Na_2SO_4 + Al_2O_3

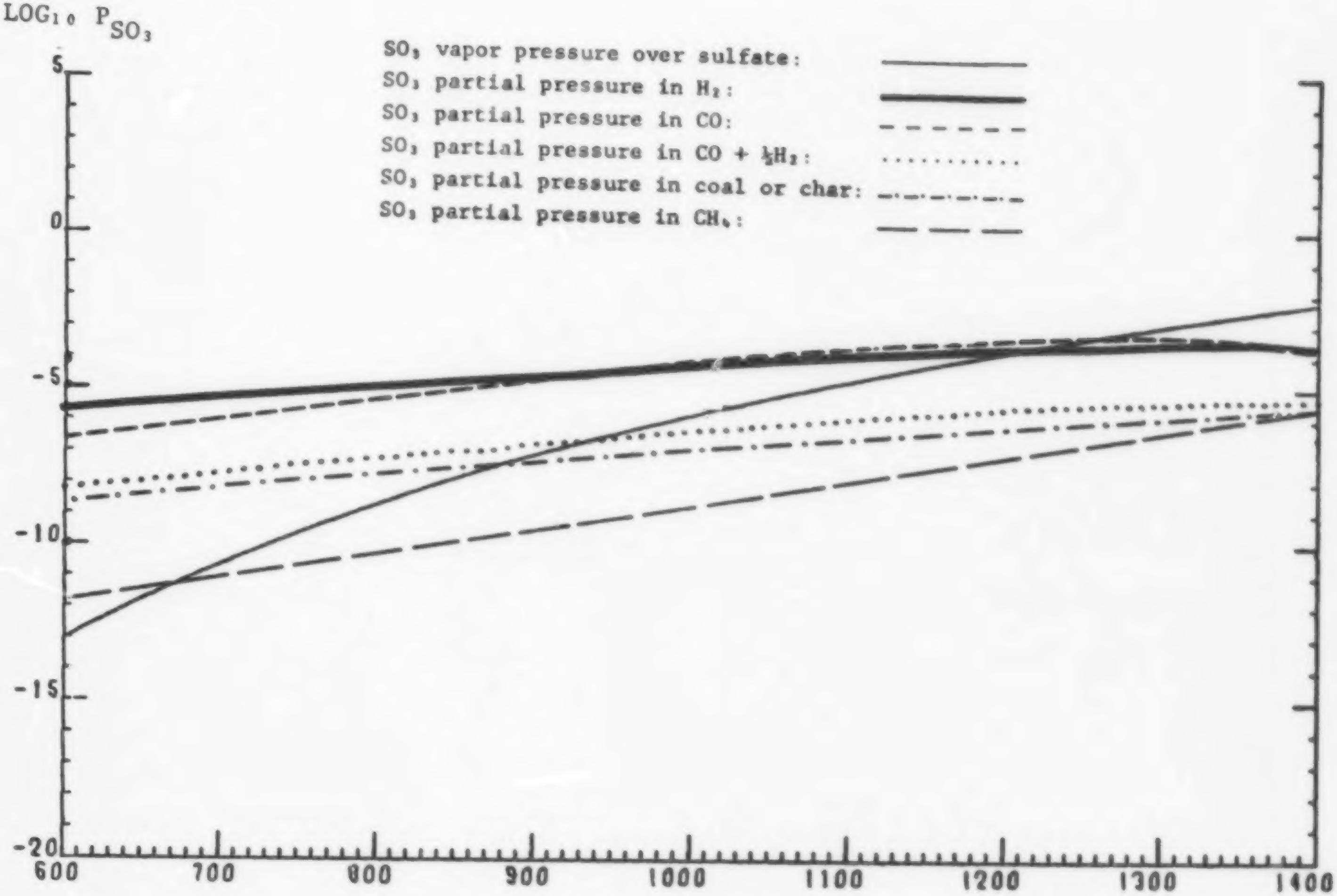

FIGURE A-8 - COMPARISON OF SO_3 PARTIAL PRESSURE IN REDUCING GASES WITH SO_3 VAPOR PRESSURE OVER $Na_2SO_4 + Fe_2O_3$

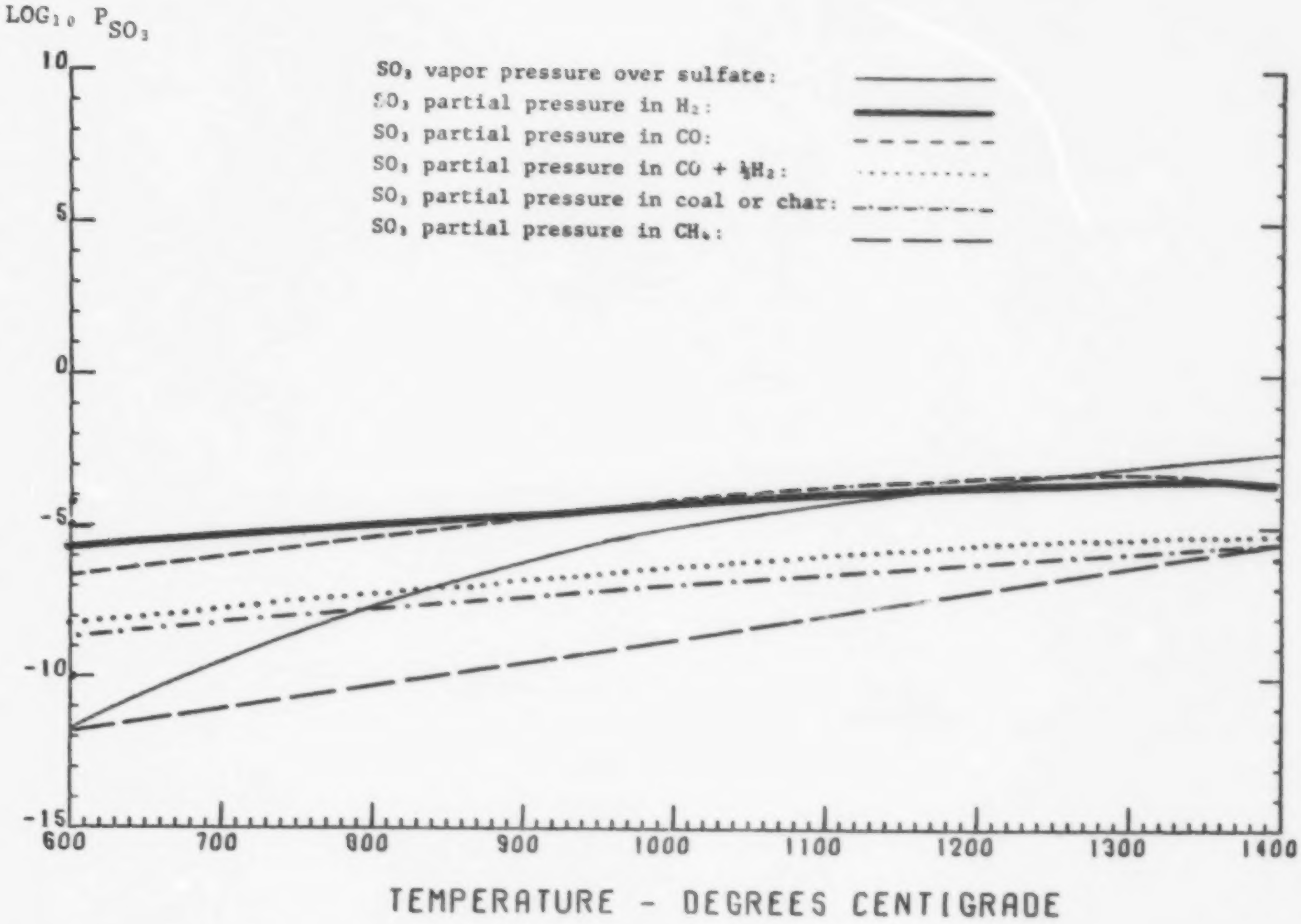

FIGURE A-9 - COMPARISON OF SO_3 PARTIAL PRESSURE IN REDUCING GASES WITH SO_3 VAPOR PRESSURE OVER $CaSO_4 + Al_2O_3$

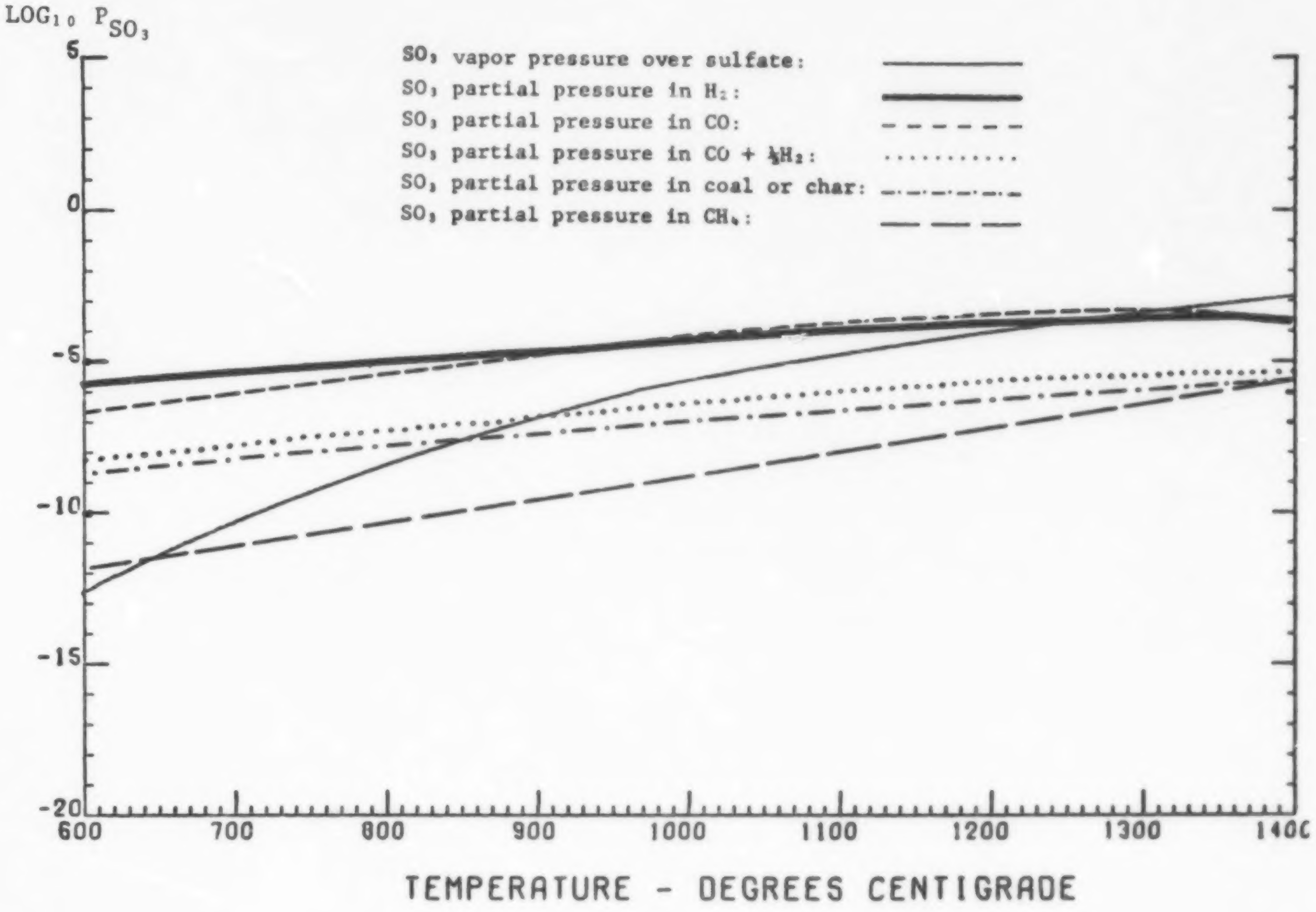

FIGURE A-10 - COMPARISON OF SO_3 PARTIAL PRESSURE IN REDUCING GASES WITH SO_3 VAPOR PRESSURE OVER $SrSO_4 + Al_2O_3$

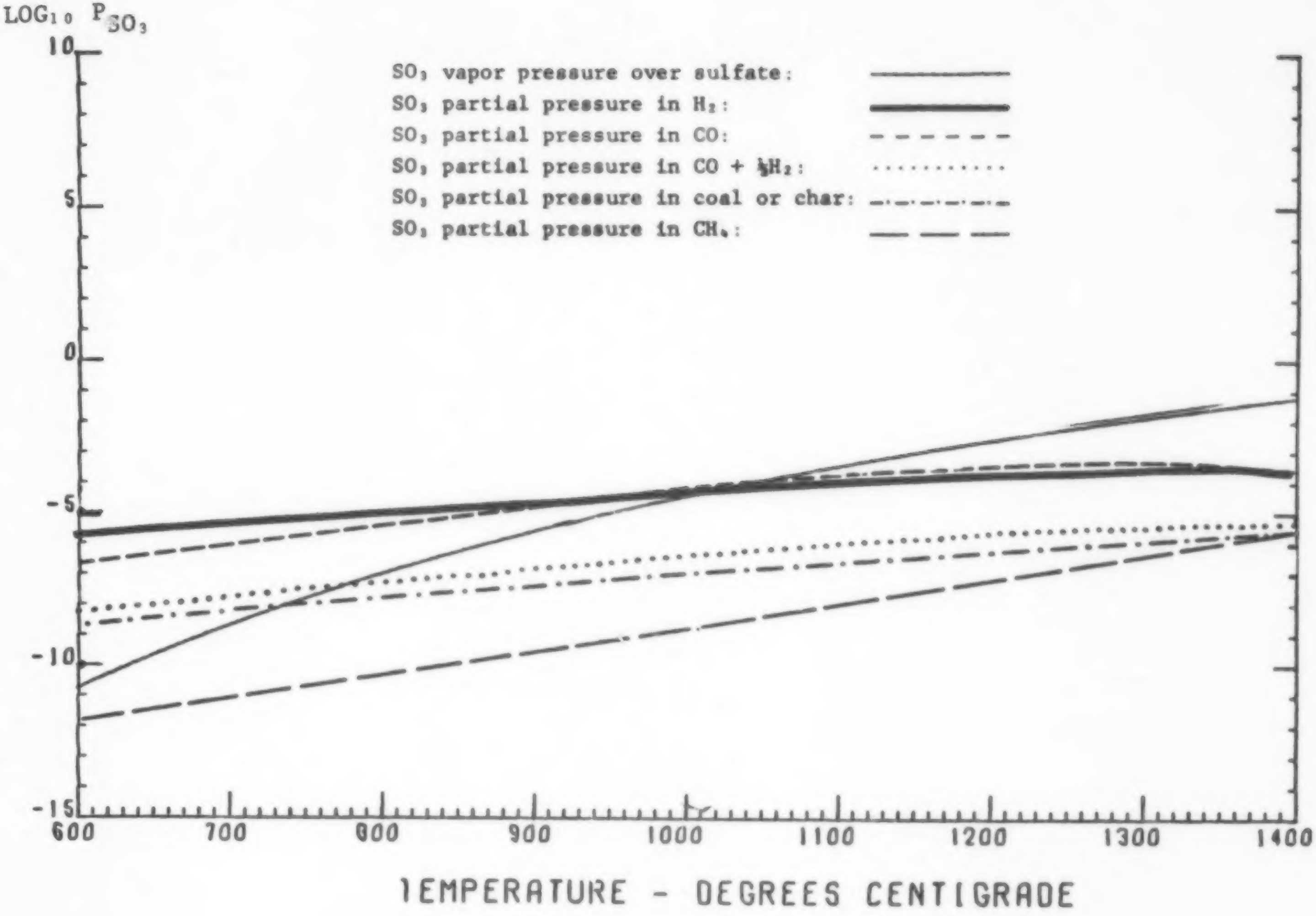

FIGURE A-11 - COMPARISON OF SO_3 PARTIAL PRESSURE IN REDUCING GASES WITH SO_3 VAPOR PRESSURE OVER $SrSO_4$ + TiO_2

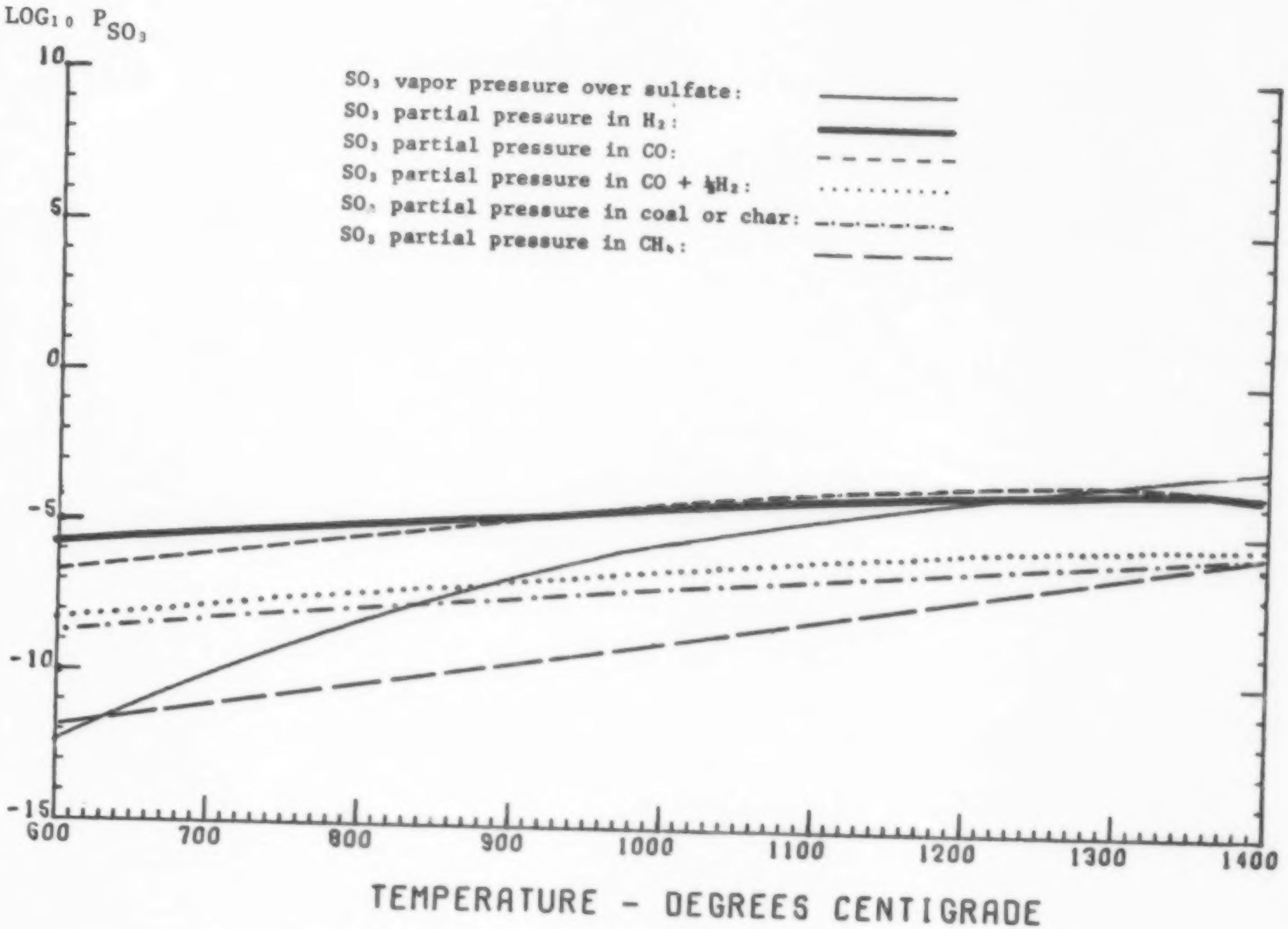

FIGURE A-12 - COMPARISON OF SO_3 PARTIAL PRESSURE IN REDUCING GASES WITH SO_3 VAPOR PRESSURE OVER $BaSO_4 + Al_2O_3$

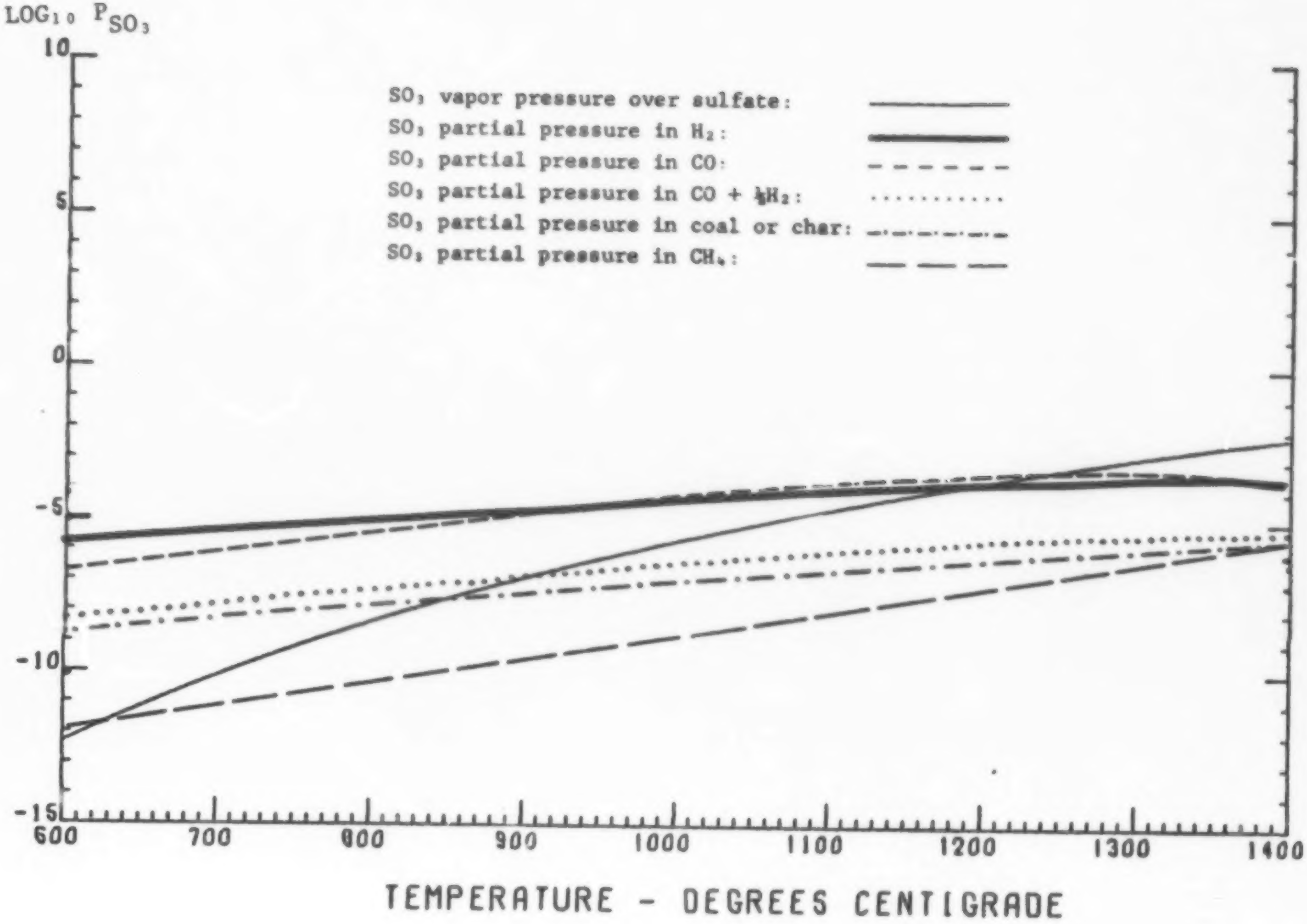

FIGURE A-13 - COMPARISON OF SO$_3$ PARTIAL PRESSURE IN REDUCING GASES WITH SO$_3$ VAPOR PRESSURE OVER BaSO$_4$ + TiO$_2$

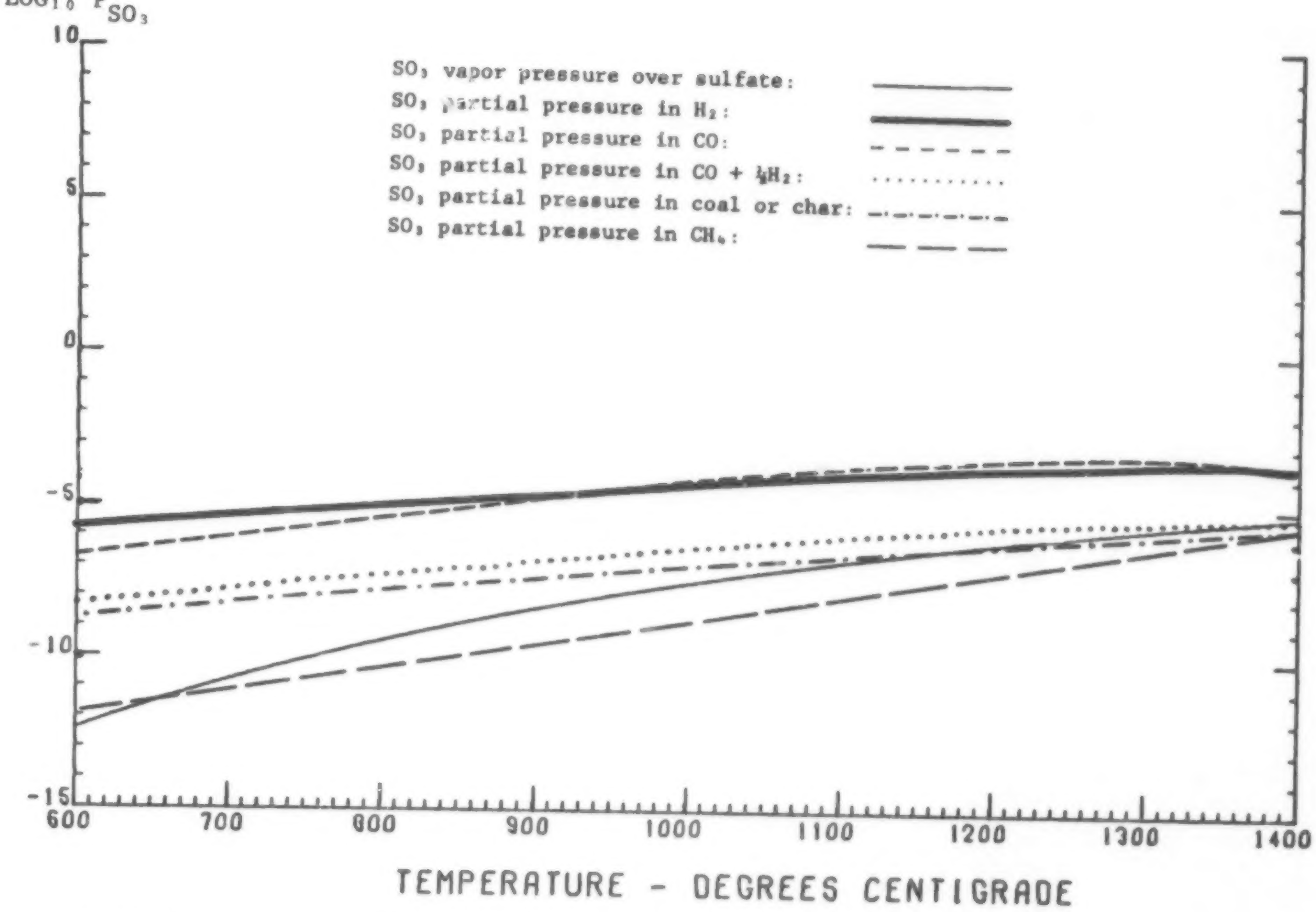

FIGURE A-14 - COMPARISON OF SO$_3$ PARTIAL PRESSURE IN REDUCING GASES WITH SO$_3$ VAPOR PRESSURE OVER Li$_2$SO$_4$ + TiO$_2$

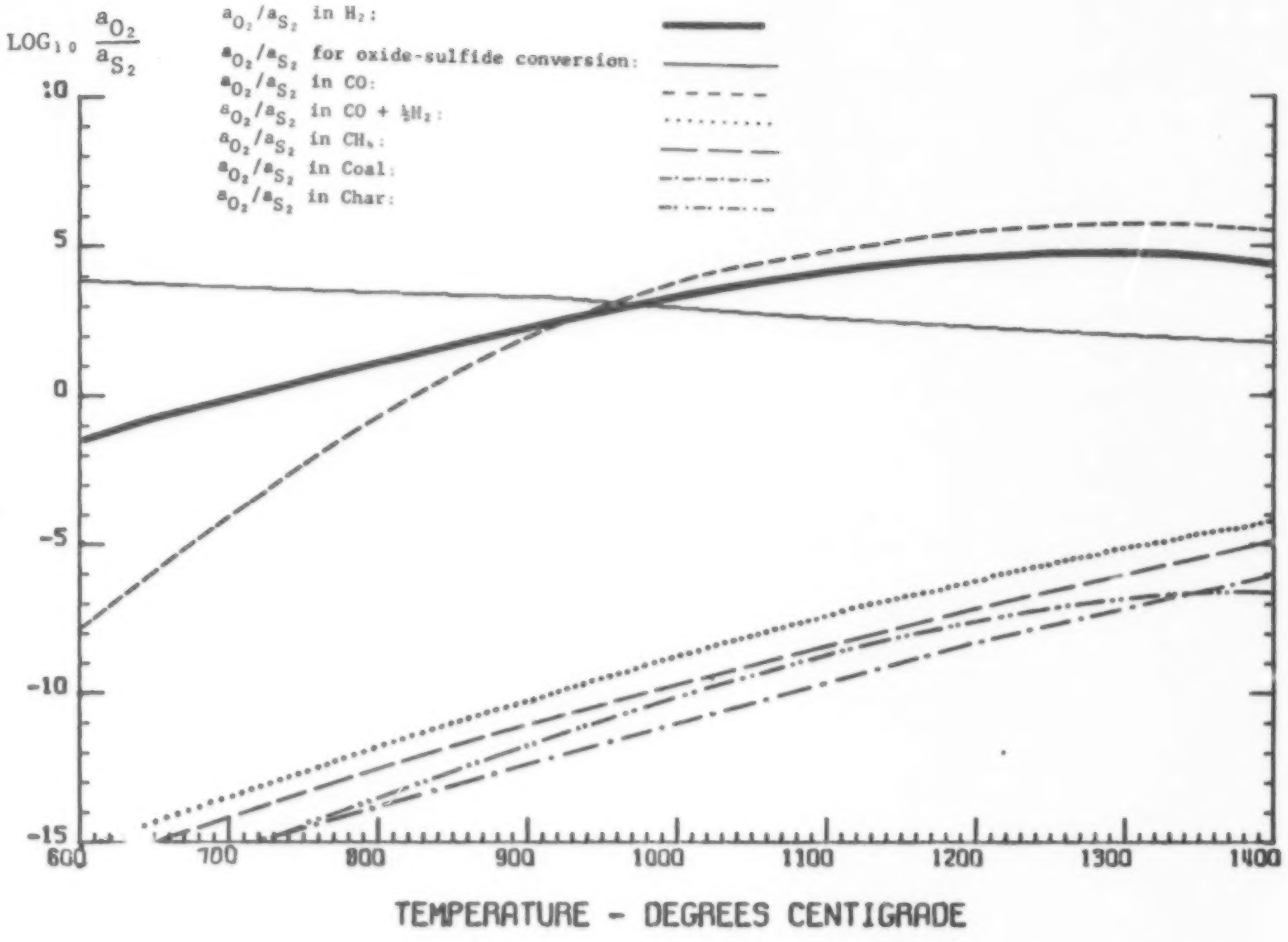

FIGURE A-15 - COMPARISON OF a_{O_2}/a_{S_2} IN REDUCING GASES WITH a_{O_2}/a_{S_2} FOR THE REACTION

$2Na_2O + S_2 \rightarrow O_2 + 2Na_2S$

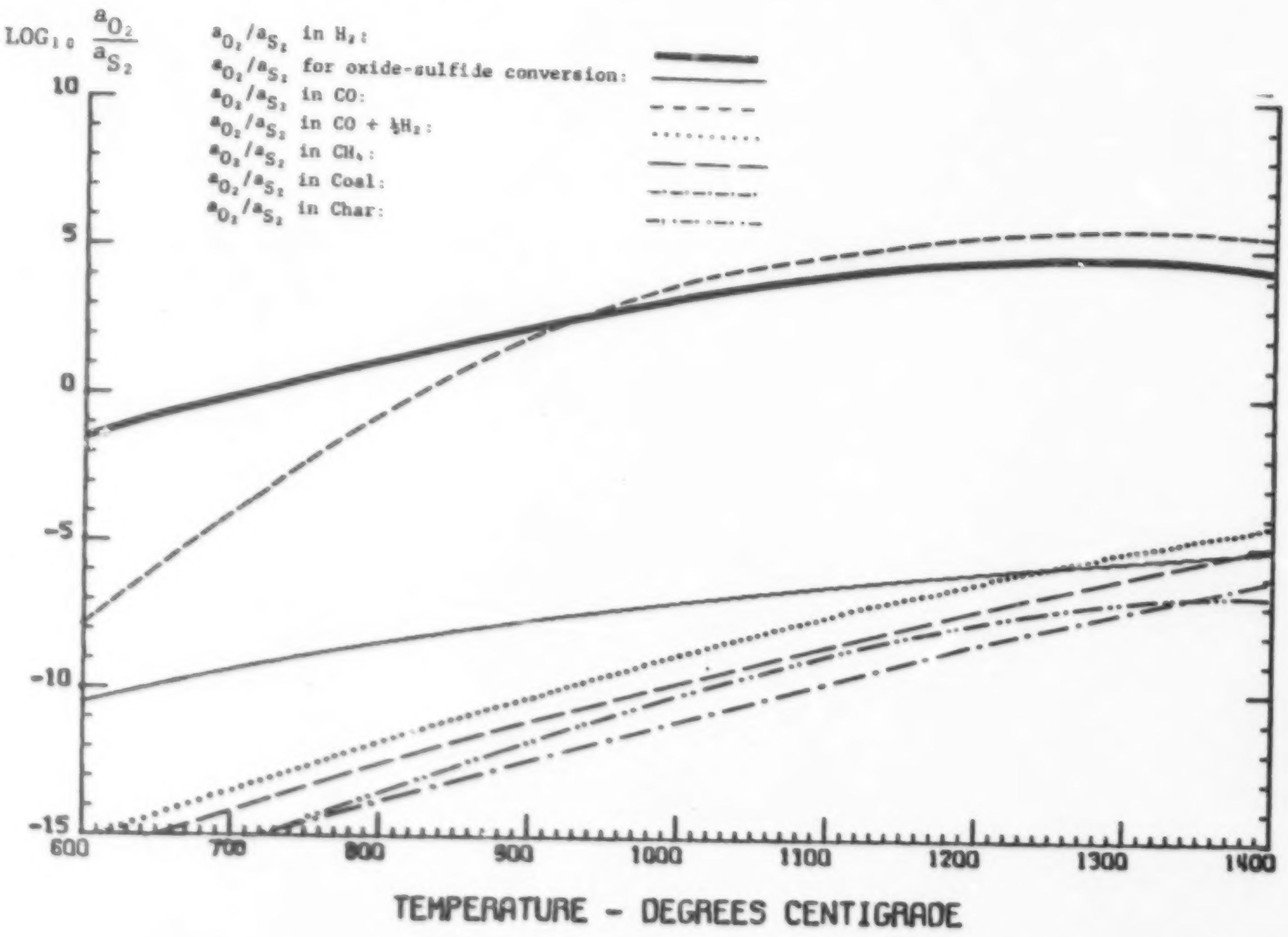

FIGURE A-16 - COMPARISON OF a_{O_2}/a_{S_2} IN REDUCING GASES WITH a_{O_2}/a_{S_2} FOR THE REACTION

$$2CaO + S_2 \rightarrow O_2 + 2CaS$$

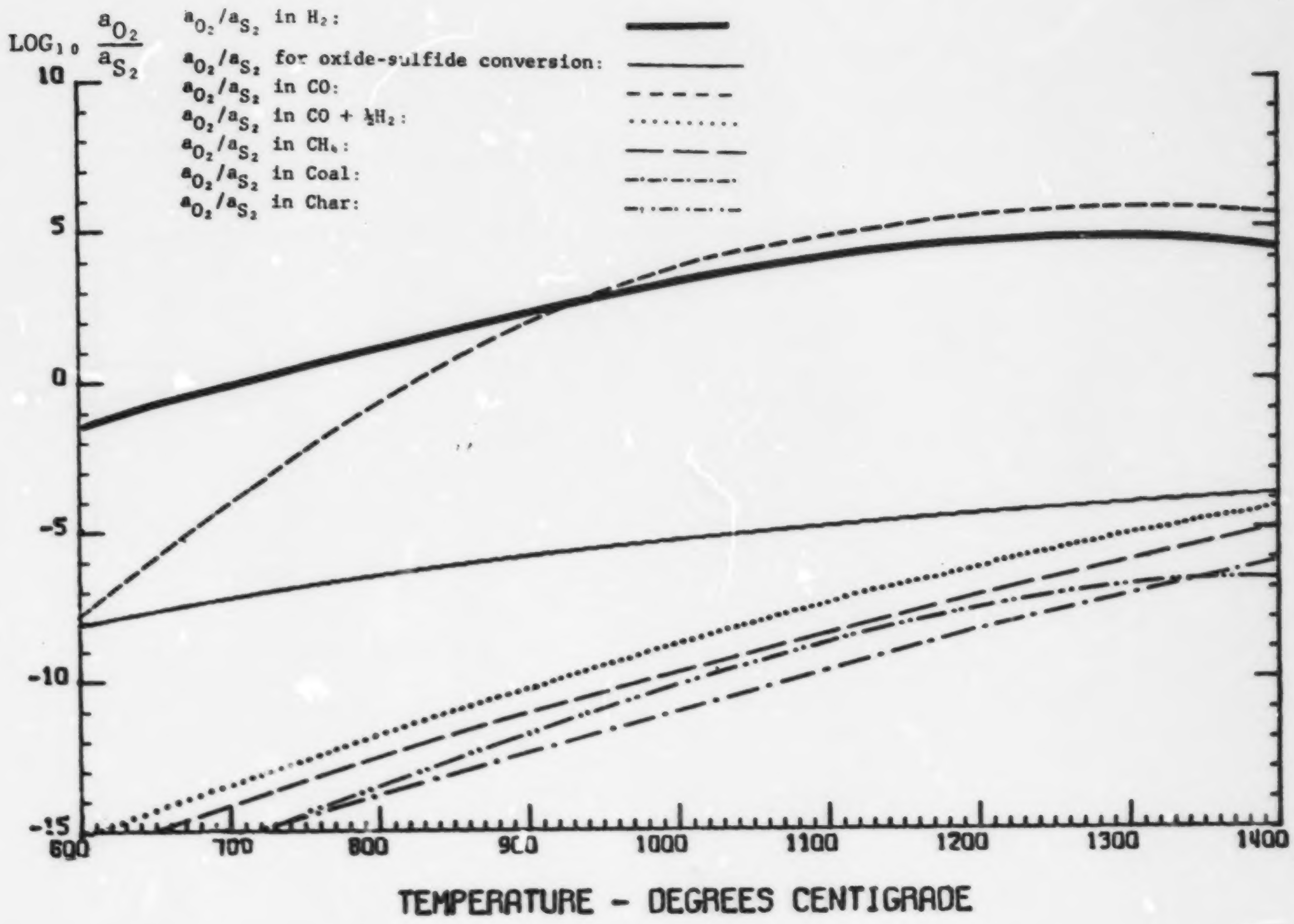

FIGURE A-17 - COMPARISON OF a_{O_2}/a_{S_2} IN REDUCING GASES WITH a_{O_2}/a_{S_2} FOR THE REACTION

$2SrO + S_2 \rightarrow O_2 + 2SrS$

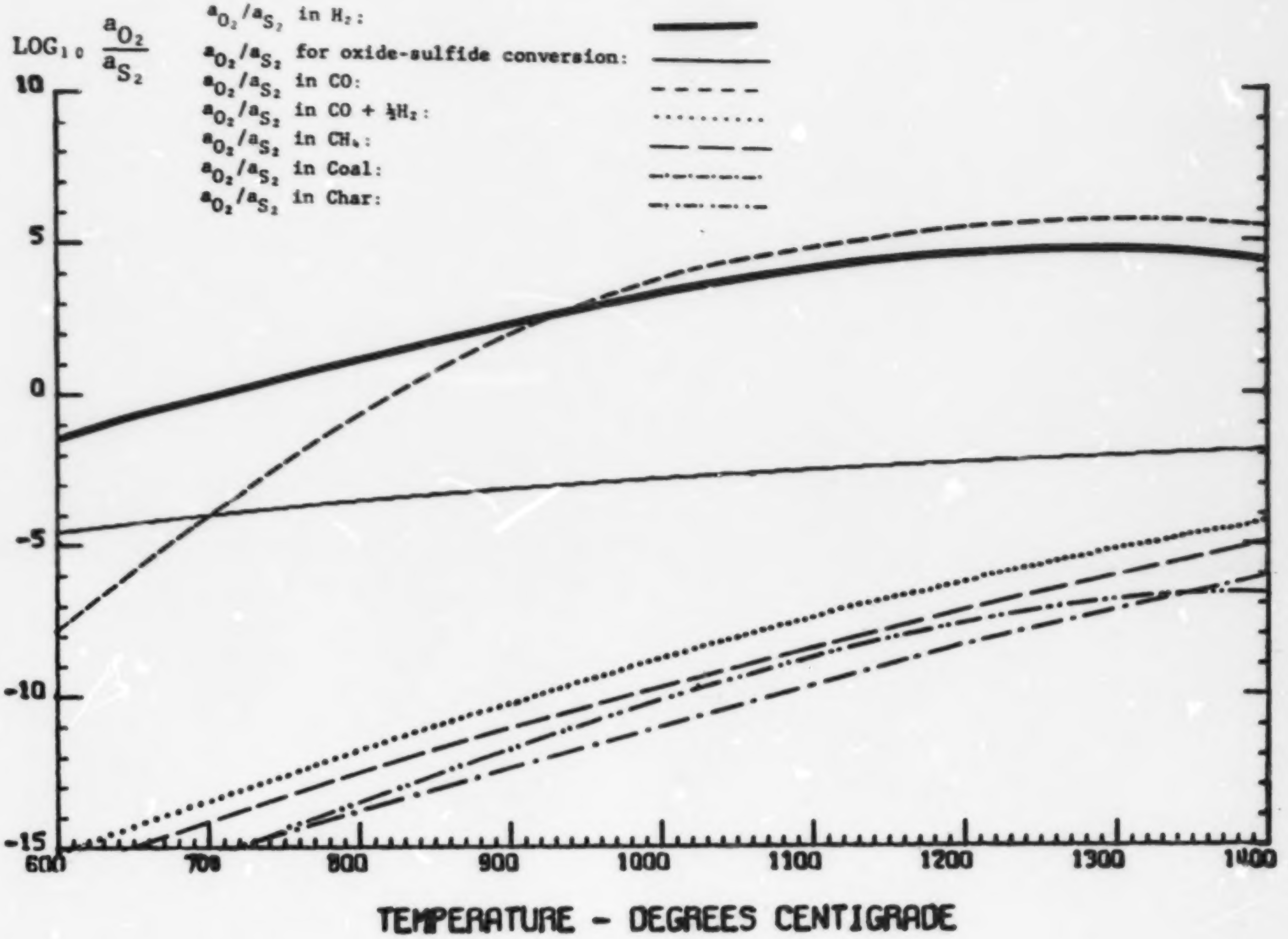

FIGURE A-18 - COMPARISON OF a_{O_2}/a_{S_2} IN REDUCING GASES WITH a_{O_2}/a_{S_2} FOR THE REACTION $2BaO + S_2 \rightarrow O_2 + 2BaS$

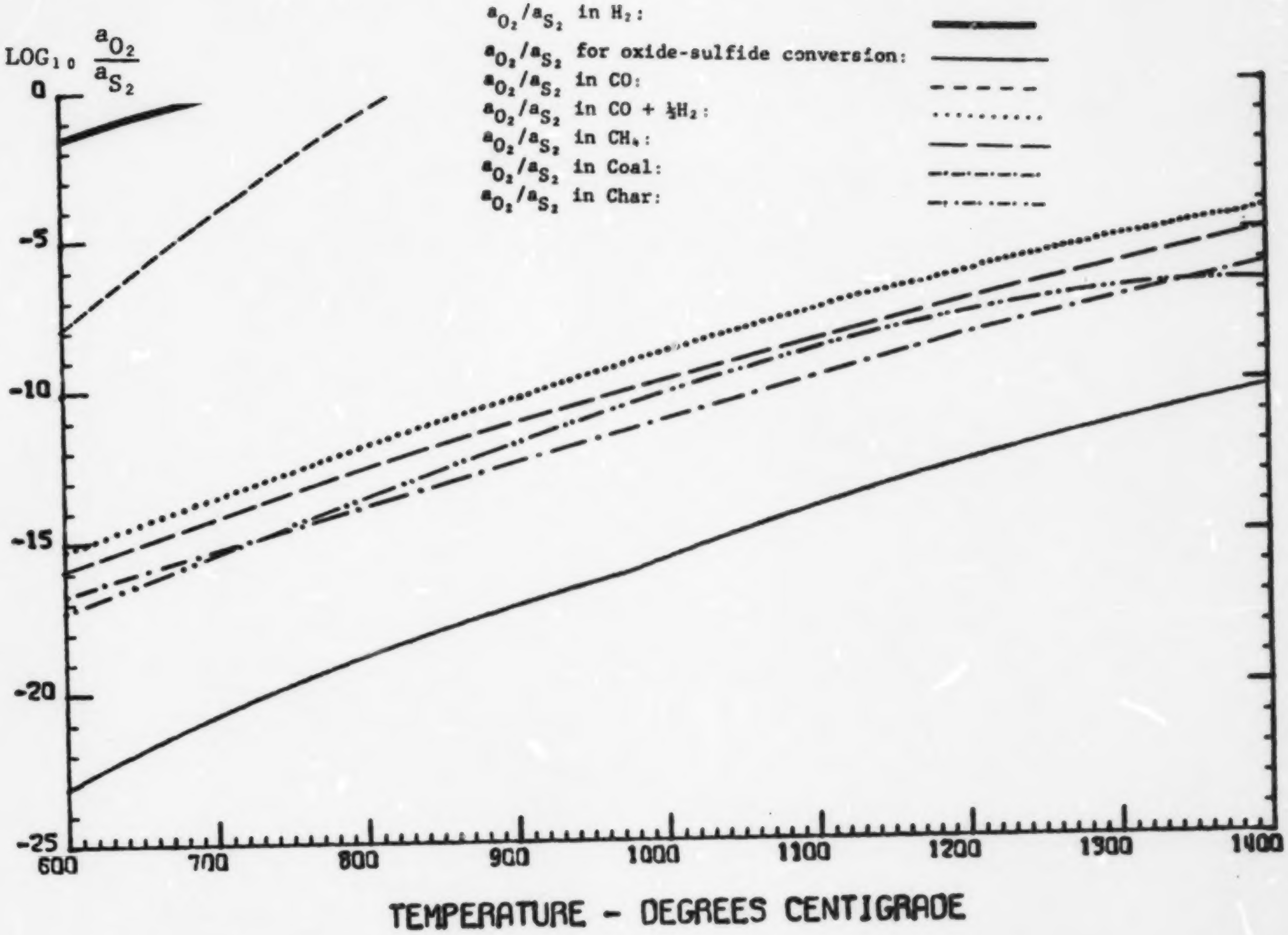

FIGURE A-19 - COMPARISON OF a_{O_2}/a_{S_2} IN REDUCING GASES WITH a_{O_2}/a_{S_2} FOR THE REACTION

$4LiAlO_2 + S_2 \rightarrow O_2 + 2Li_2S + 2Al_2O_3$

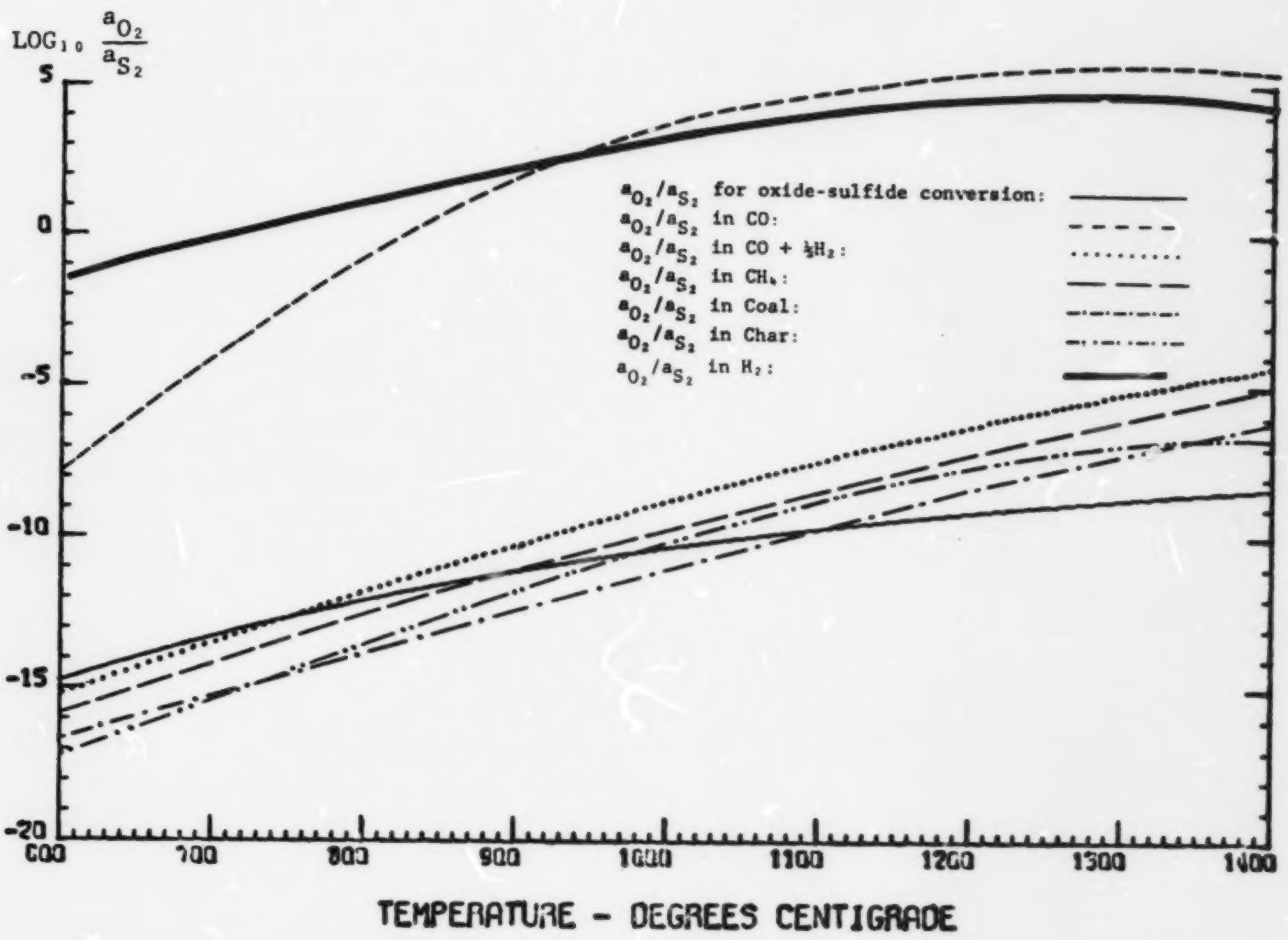

FIGURE A-20 - COMPARISON OF a_{O_2}/a_{S_2} IN REDUCING GASES WITH a_{O_2}/a_{S_2} FOR THE REACTION

$4LiFeO_2 + S_2 \rightarrow O_2 + 2Li_2S + 2Fe_2O_3$

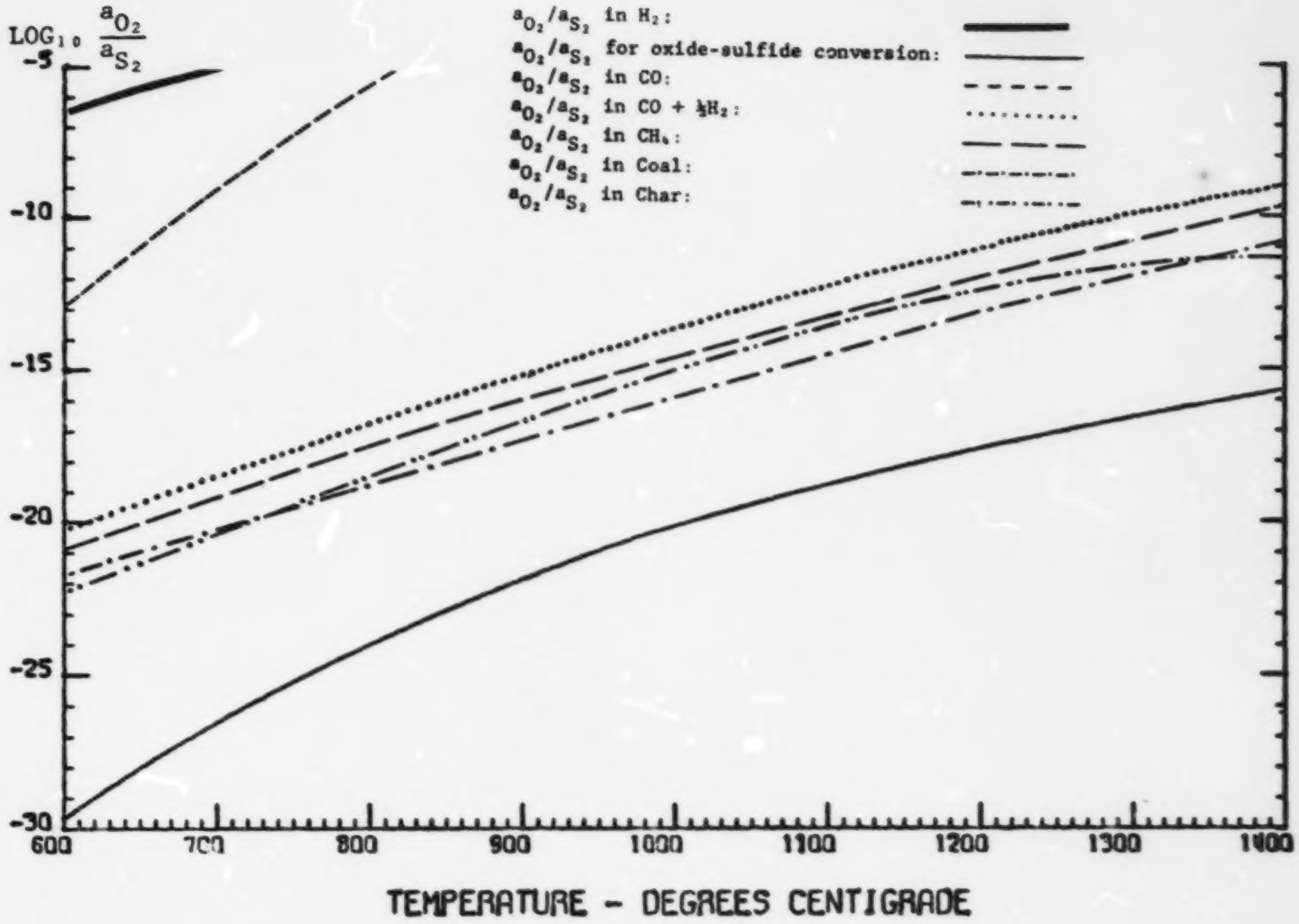

FIGURE A-21 - COMPARISON OF a_{O_2}/a_{S_2} IN REDUCING GASES WITH a_{O_2}/a_{S_2} FOR THE REACTION

$2Al_2O_3 + 3S_2 \rightarrow 3O_2 + 2Al_2S_3$

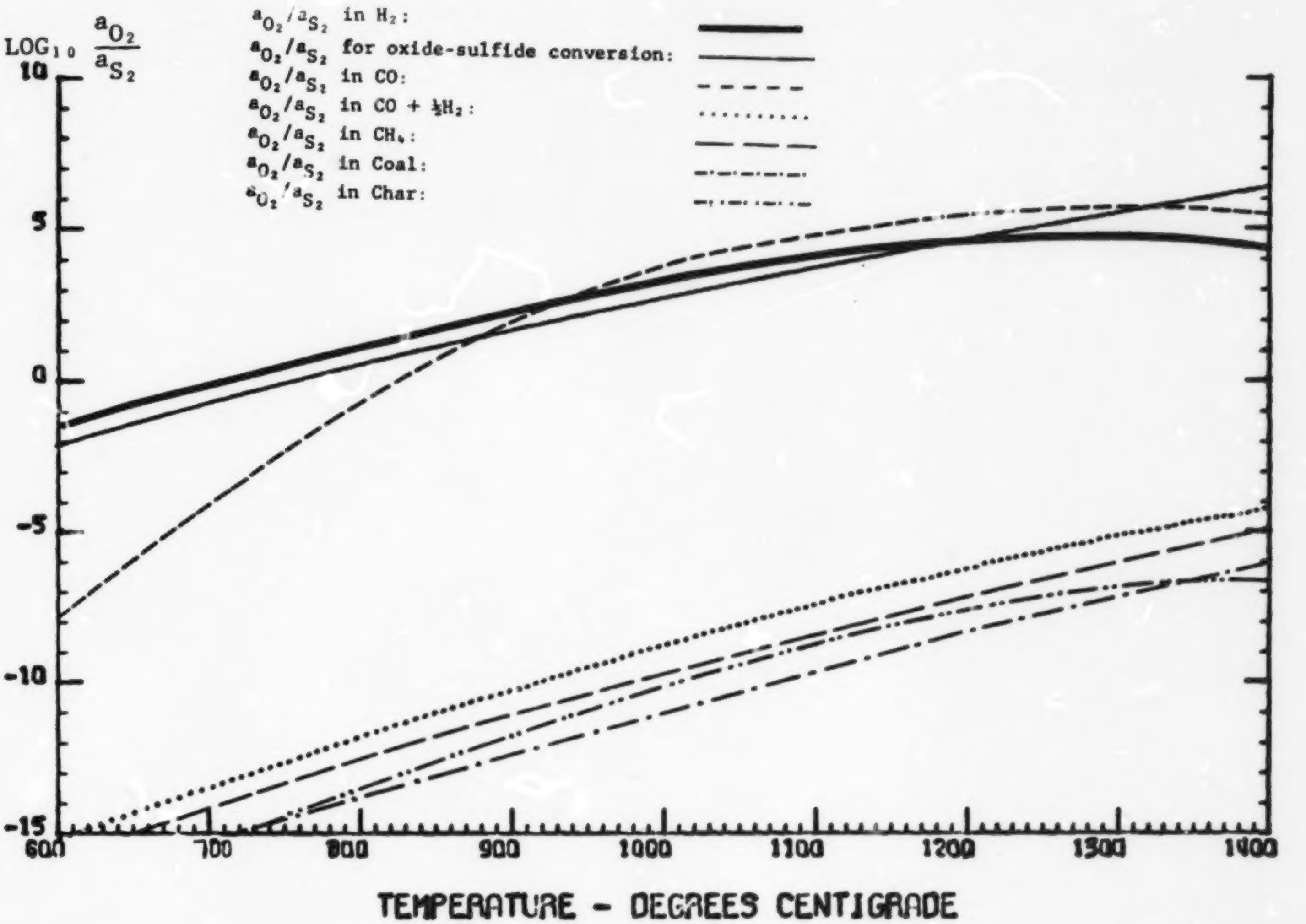

FIGURE A-22 - COMPARISON OF a_{O_2}/a_{S_2} IN REDUCING GASES WITH a_{O_2}/a_{S_2} FOR THE REACTION

$TiO_2 + S_2 \rightarrow O_2 + TiS_2$

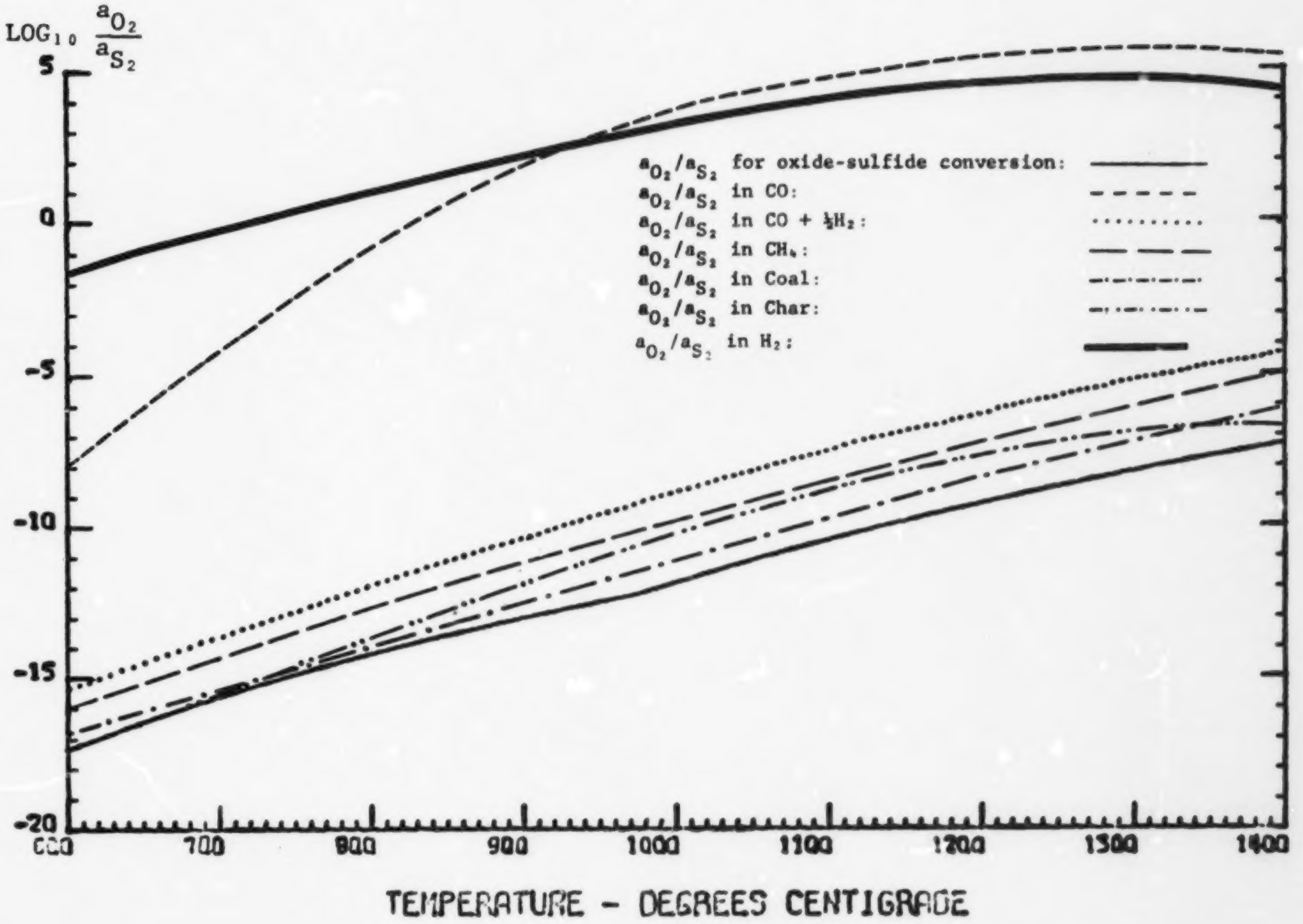

FIGURE A-23 - COMPARISON OF a_{O_2}/a_{S_2} IN REDUCING GASES WITH a_{O_2}/a_{S_2} FOR THE REACTION

$$4NaAlO_2 + S_2 \rightarrow O_2 + 2Na_2S + 2Al_2O_3$$

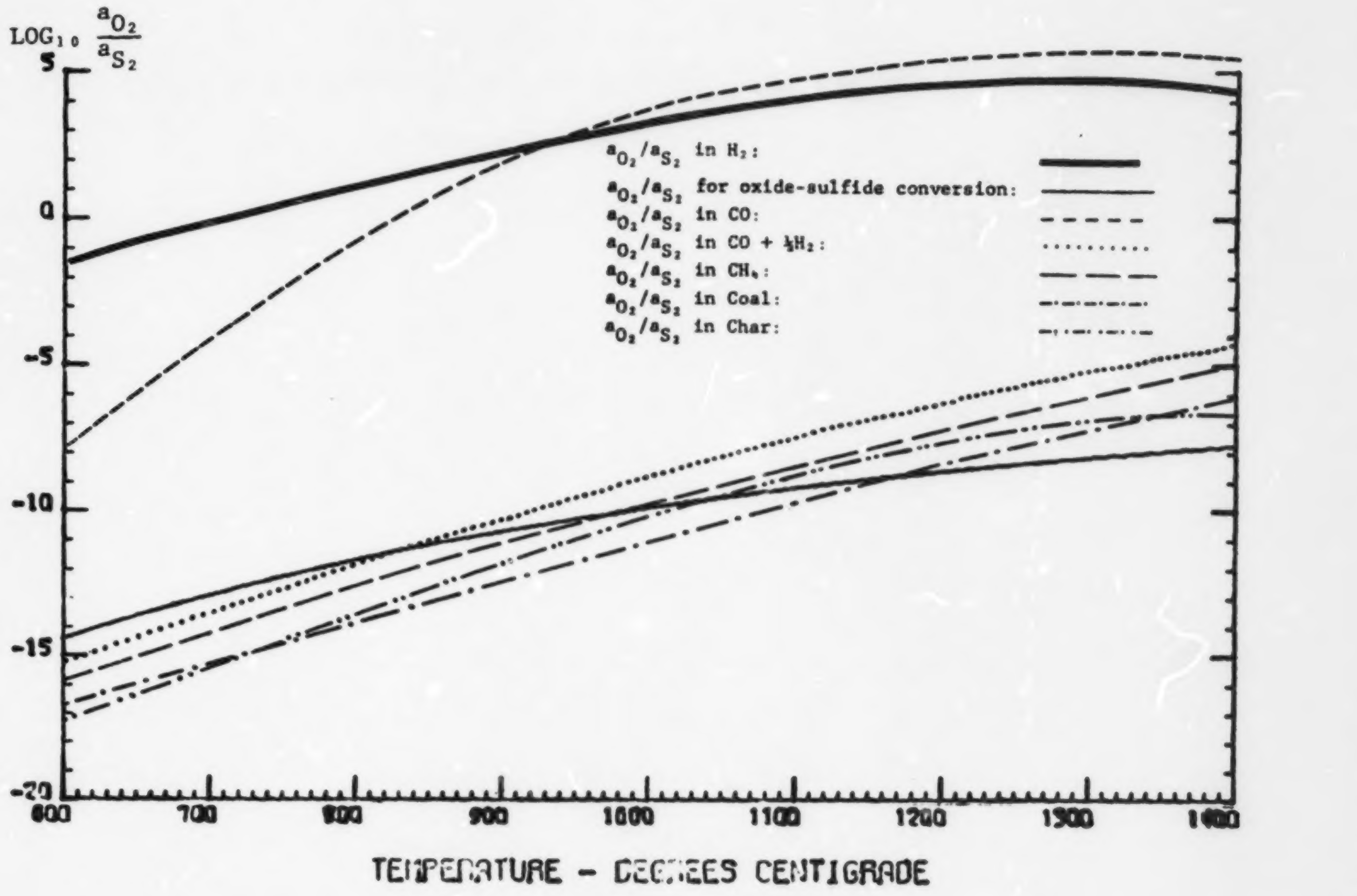

FIGURE A-24 - COMPARISON OF a_{O_2}/a_{S_2} IN REDUCING GASES WITH a_{O_2}/a_{S_2} FOR THE REACTION

$4NaFeO_2 + S_2 \rightarrow O_2 + 2Na_2S + 2Fe_2O_3$

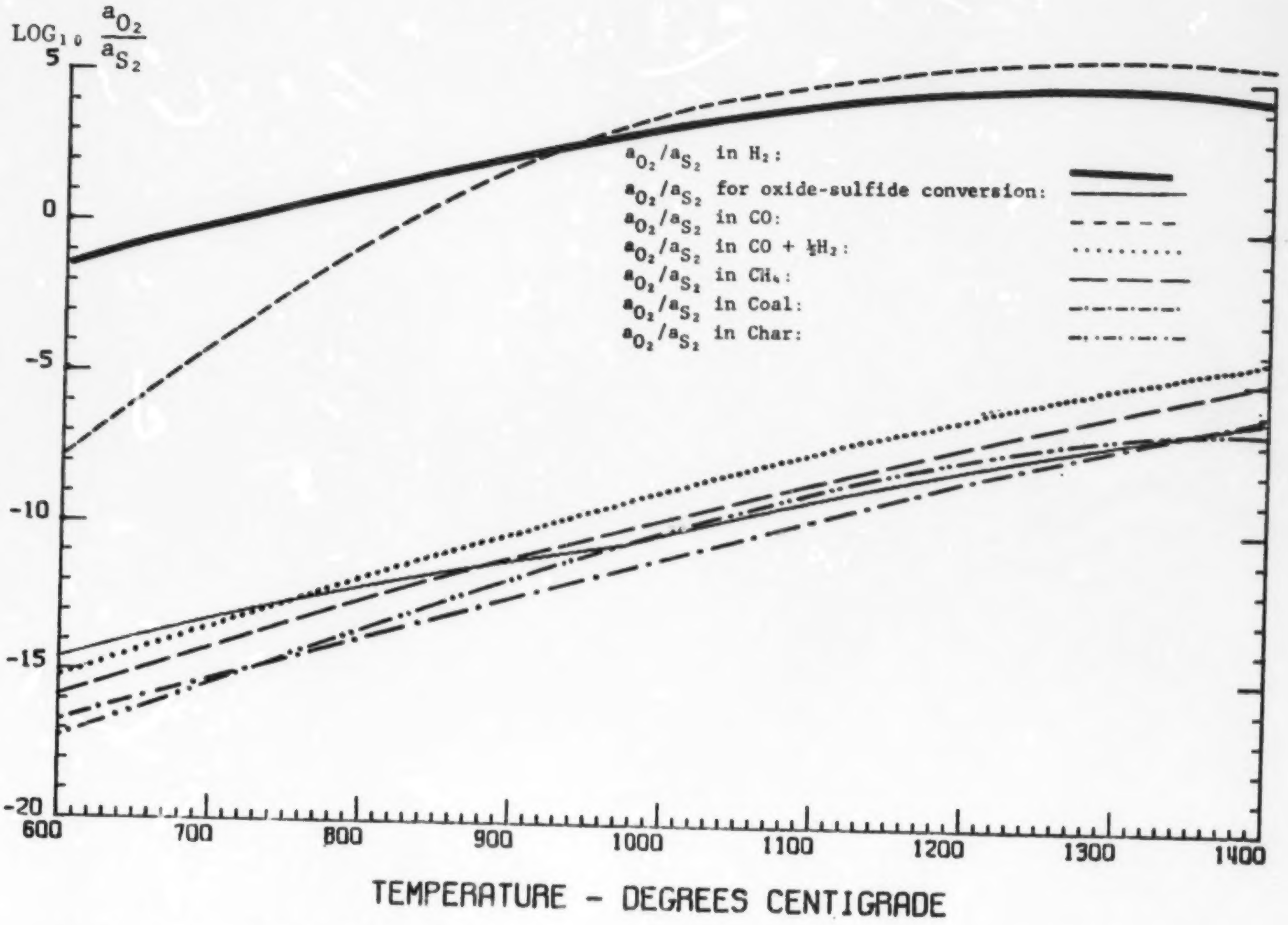

FIGURE A-25 - COMPARISON OF a_{O_2}/a_{S_2} IN REDUCING GASES WITH a_{O_2}/a_{S_2} FOR THE REACTION
$2CaAl_2O_4 + S_2 \rightarrow O_2 + 2CaS + 2Al_2O_3$

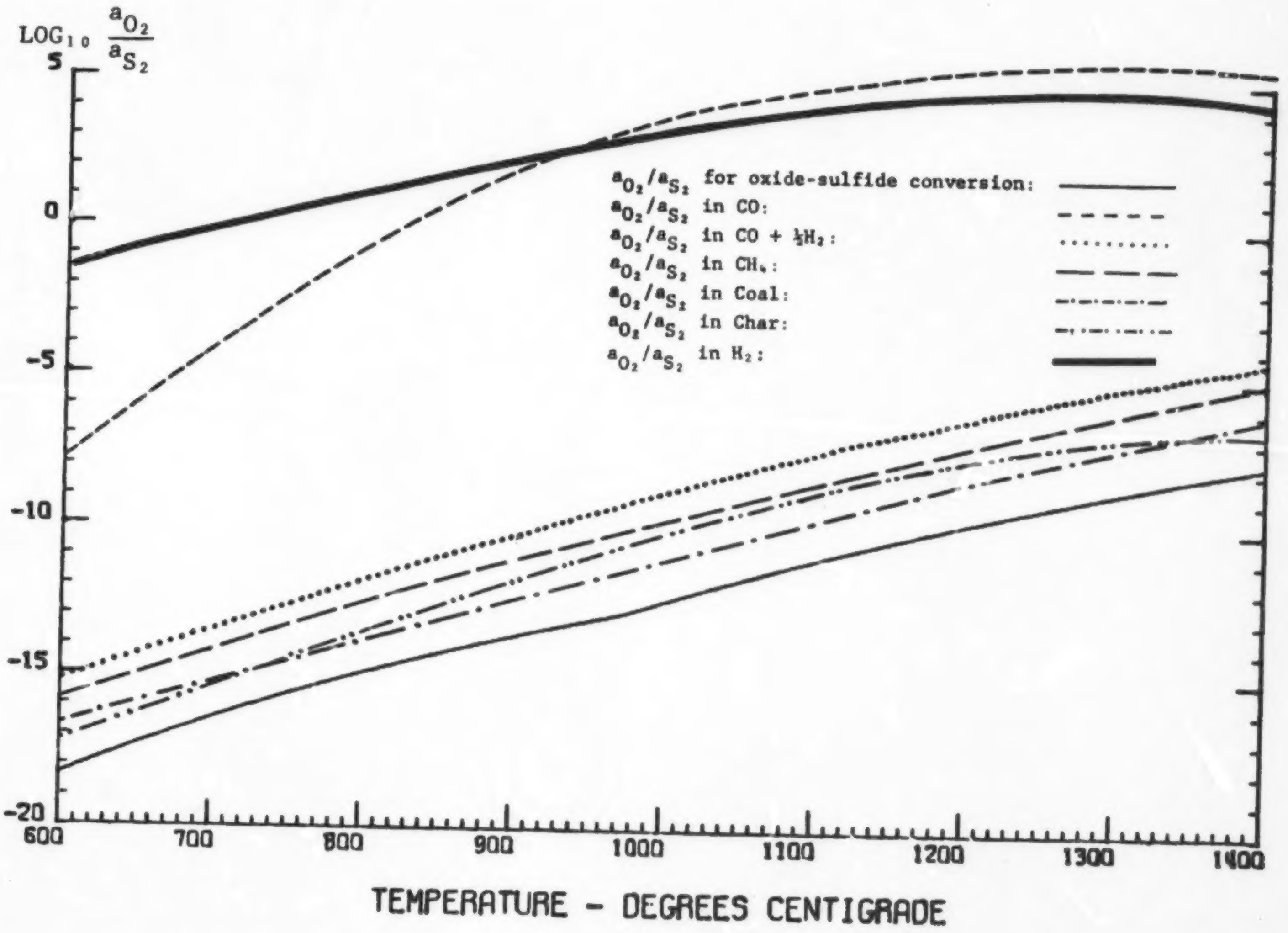

FIGURE A-26 - COMPARISON OF a_{O_2}/a_{S_2} IN REDUCING GASES WITH a_{O_2}/a_{S_2} FOR THE REACTION

$2SrAl_2O_4 + S_2 \rightarrow O_2 + 2SrS + 2Al_2O_3$

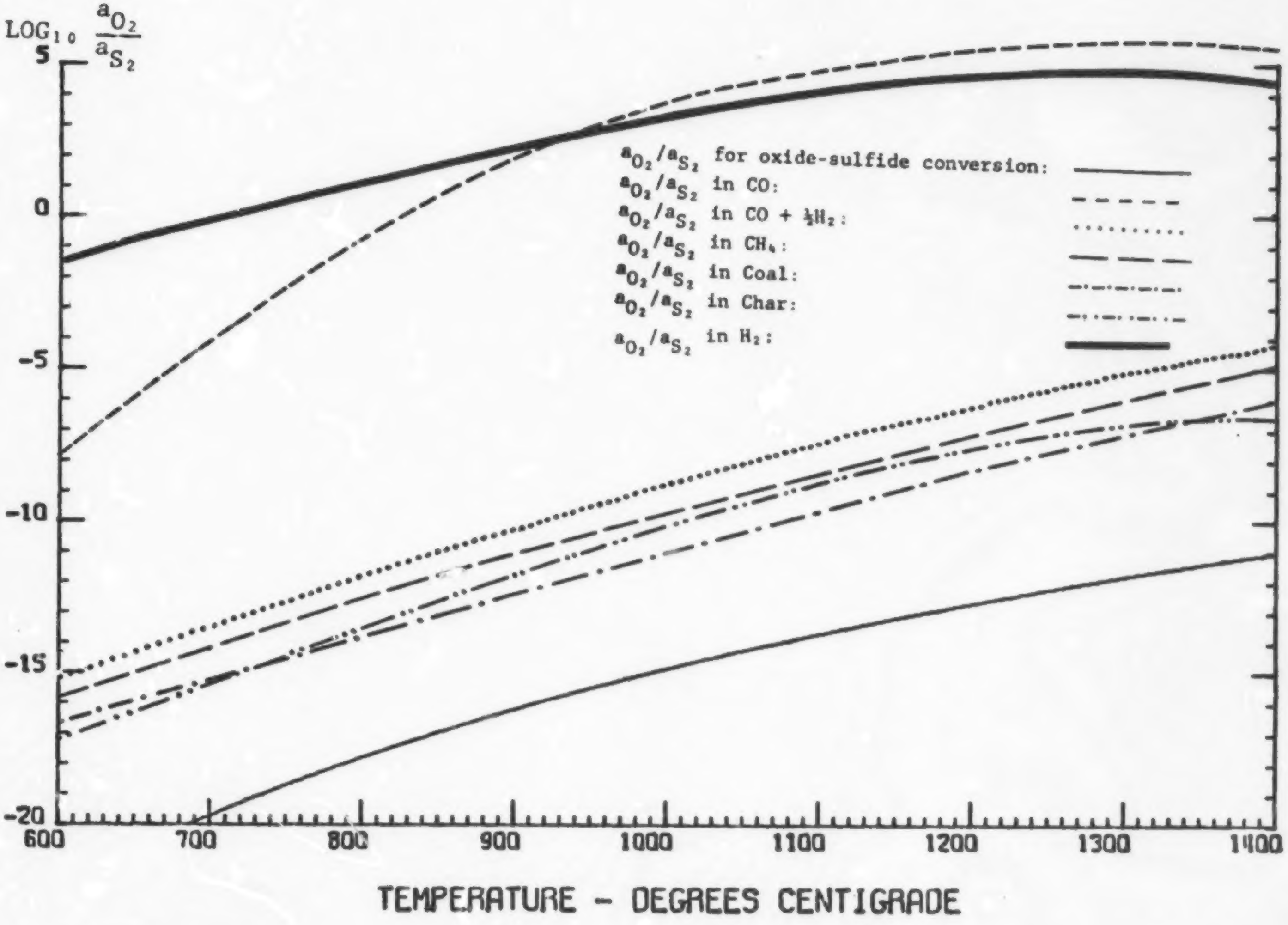

FIGURE A- 27 - COMPARISON OF a_{O_2}/a_{S_2} IN REDUCING GASES WITH a_{O_2}/a_{S_2} FOR THE REACTION

$2SrTiO_3 + S_2 \rightarrow O_2 + 2SrS + 2TiO_2$

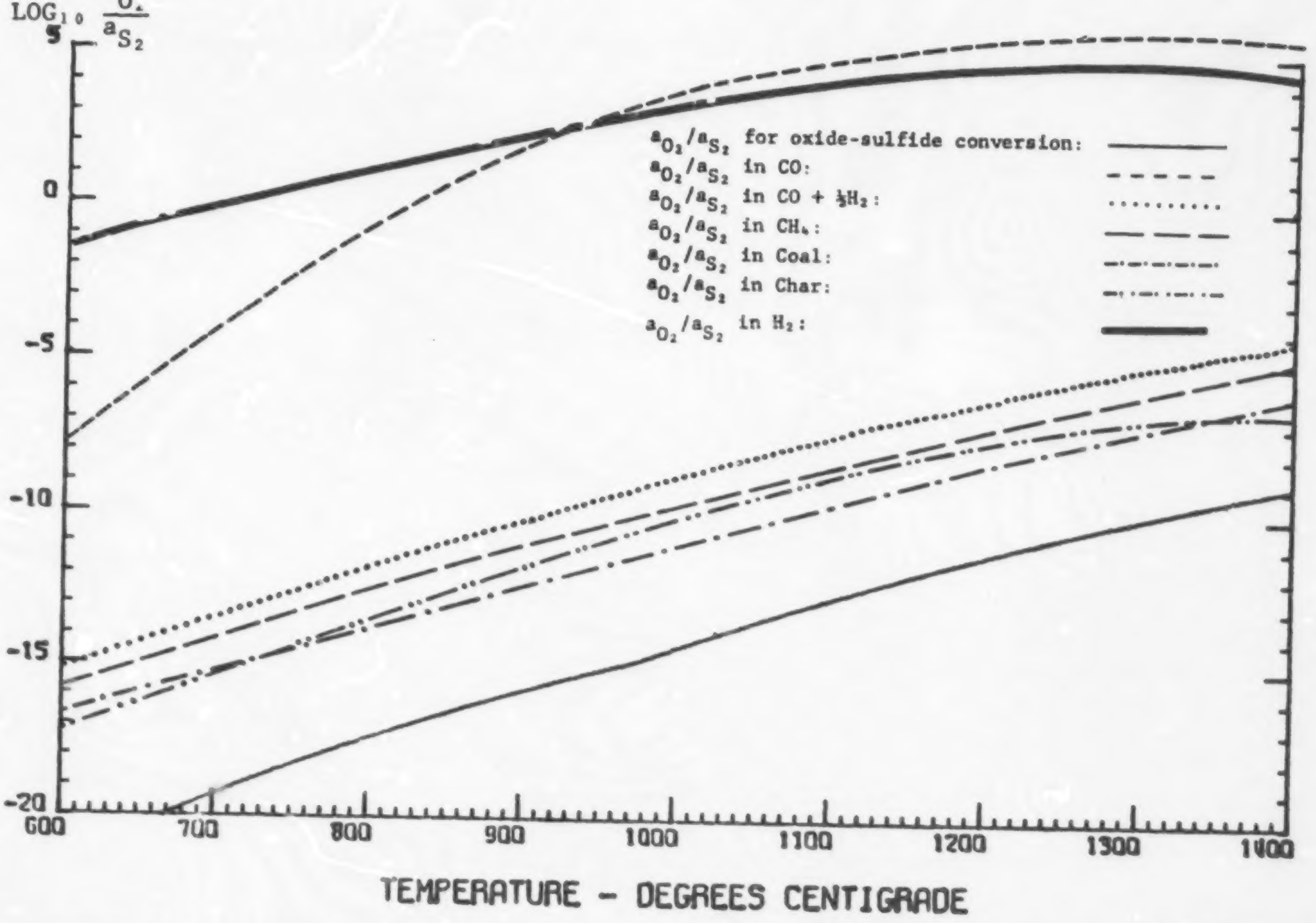

FIGURE A- 28 - COMPARISON OF a_{O_2}/a_{S_2} IN REDUCING GASES WITH a_{O_2}/a_{S_2} FOR THE REACTION

$$2BaAl_2O_4 + S_2 \rightarrow O_2 + 2BaS + 2Al_2O_3$$

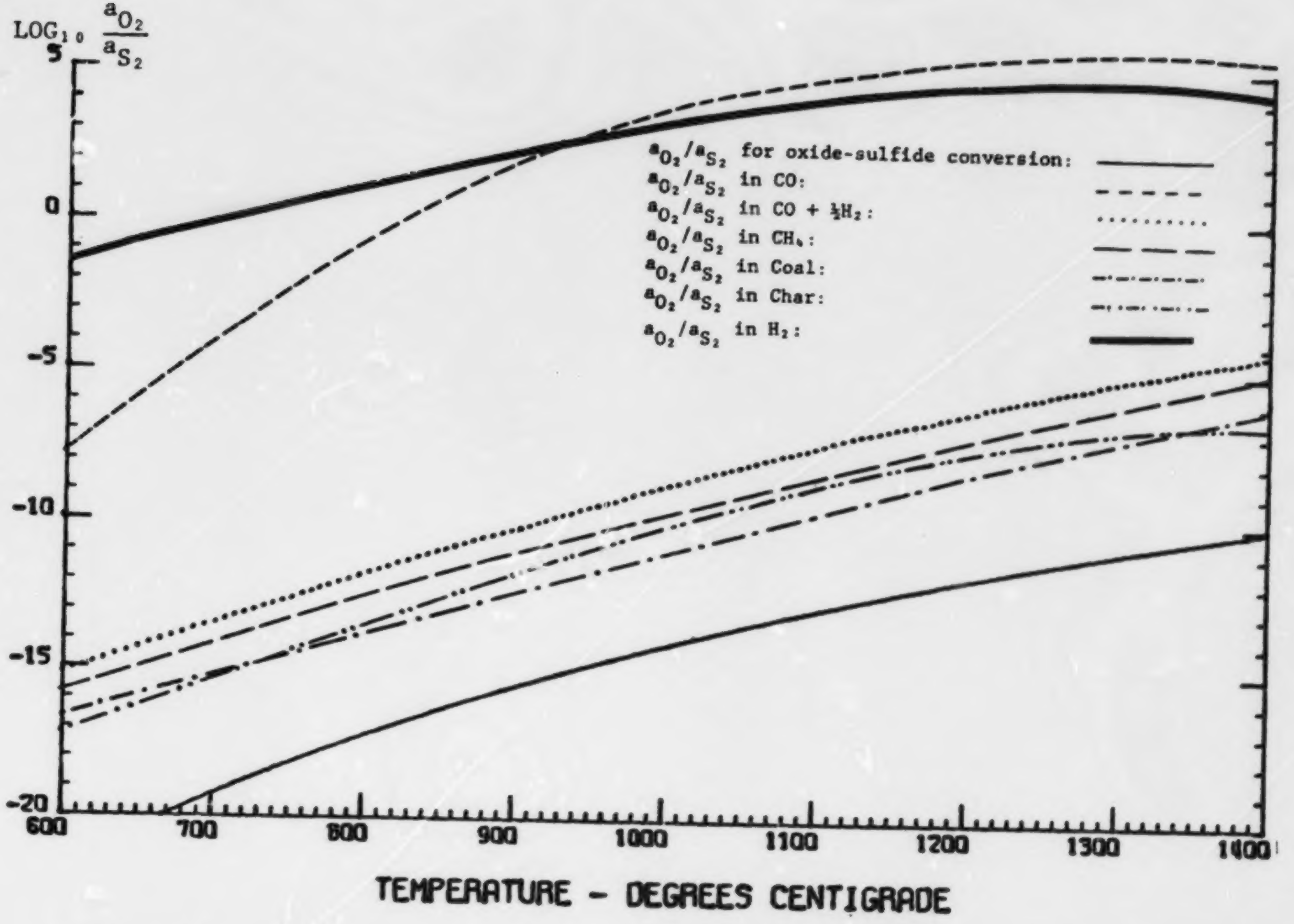

FIGURE A-29 - COMPARISON OF a_{O_2}/a_{S_2} IN REDUCING GASES WITH a_{O_2}/a_{S_2} FOR THE REACTION

$2BaTiO_3 + S_2 \rightarrow O_2 + 2BaS + 2TiO_2$

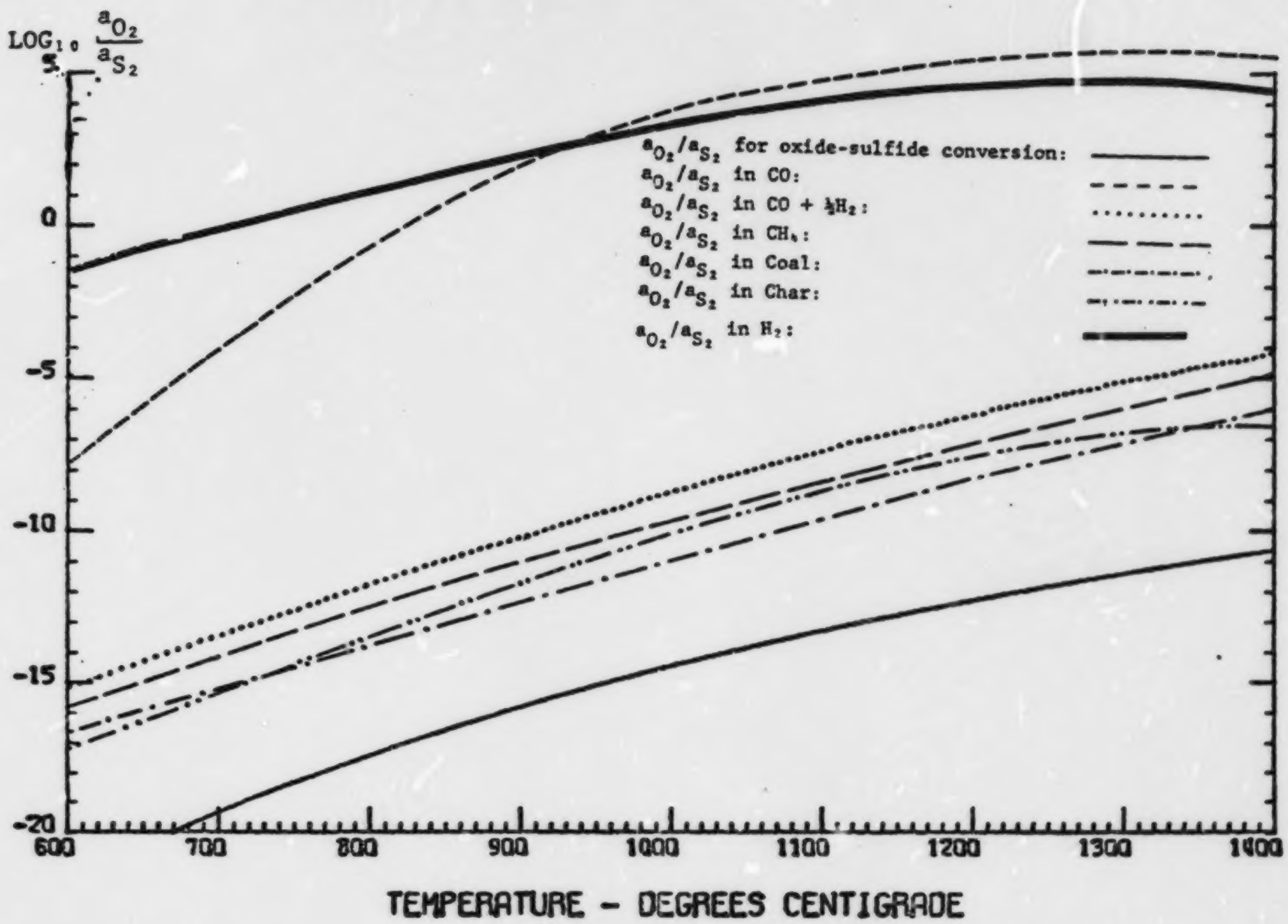

FIGURE A- 30 - COMPARISON OF a_{O_2}/a_{S_2} IN REDUCING GASES WITH a_{O_2}/a_{S_2} FOR THE REACTION

$2Li_2TiO_3 + S_2 \ + \ O_2 + 2Li_2S + 2TiO_2$